UNIVERSITY OF CALGARY

Multimetal Resistance and Tolerance in Microbial Biofilms

by

Joe J. Harrison

A THESIS

SUBMITTED TO THE FACULTY OF GRADUATE STUDIES

IN PARTIAL FULFILMENT OF THE REQUIREMENTS FOR THE

DEGREE OF DOCTOR OF PHILOSOPHY

DEPARTMENT OF BIOLOGICAL SCIENCES

CALGARY, ALBERTA

JULY, 2008

Abstract

Geochemical cycling and industrial pollution have made toxic metals a pervasive environmental pressure throughout the world. Growth in a biofilm, which is the attachment and proliferation of microorganisms at a surface, is a strategy which microbes may use to survive a toxic flux in these inorganic compounds. This research has focused on identifying the reasons why biofilms are less susceptible to metal toxicity than free-swimming planktonic microbes.

During this research, I have developed a simple, high-throughput technology for metal susceptibility testing, *in situ* microscopy and three-dimensional visualization of microbial biofilms using the Calgary Biofilm Device. By using this technique, it was possible to perform combinatorial experiments to examine the effects of exposure times, growth conditions and gene deletion on the susceptibility of bacterial and fungal biofilms to arrays of toxic metals and other antimicrobial agents. This approach identified several genetic, cellular and biochemical processes that may contribute to biofilm "multimetal resistance" and "multimetal tolerance." In conjunction with evidence from the literature, I have assembled these processes into a multifactorial model that I have split into seven components based on mechanism:

1. Chemical and metabolic gradation in the biofilm introduced by structured population growth.
2. Cell-cell signaling events (via small "messenger" molecules) that contribute to the biofilm lifestyle.
3. Metal-ion immobilization by adsorption to biomass.
4. Bioinorganic reactions of metal ions with microbial metabolites.
5. Adaptive responses of the biofilm that may change the physiology of some cells to a metal resistant or tolerant state.
6. Metabolically quiescent cells, termed persister cells, which do not grow, yet do not die on exposure to metal ions.
7. Genetic rearrangements or mutations that produce variant phenotypes in the population.

My assessment of the available evidence suggests that the reduced susceptibility of biofilms to toxic metals is linked to a natural process of cellular diversification that is

ongoing within the microbial population. This model is a conceptual step towards understanding biofilms as a population strategy for microbial survival during exposure to toxic stressors in a diverse range of natural, industrial and clinical settings.

Acknowledgements

I would like to acknowledge the many skilled and aspiring scientists who have worked on aspects of this project over the years. I have met with success because of their contributions, big and small:

Undergraduate students:
Sarah A. Akierman
Erin A. Badry
Daniel A. Joo
Nicole J. Roper
Kimberley M. Sproule
Michelle A. Stan
Pernilla U. Stenroos

Graduate students:
Catherine S. Chan
Ginevra R. Foglia
William D. Wade
Matthew L. Workentine
Jerome Yerly

Post-doctoral fellows:
Maryam Rabiei
Helen A. Vrionis

Experts and collaborators:
Nick D. Allan
Dr. James A. Davies
Andrew Edmundson
Dr. Darran Edmundson
Dr. Belinda Heyne
Dr. Yaoping Hu
Dr. Michael Hynes
Dr. Lyriam Marques
Dr. Robert Martinuzzi
Dr. Merle E. Olson
Liz Middlemiss
Dr. David Schriemer
Carol A. Stremick
Dr. Kerry L. Tomlin
Dr. Aaron Yamniuk
Dr. Christopher Yost

My gratitude also goes to the excellent researchers and to the friends I have made along the way who have taken the extra time to teach me about what they know – Denise Bay, Catherine S. Chan, Carol L. Ladner, Andrew Edmundson, Carol A. Stremick, Valentina Tremaroli, Tara L. Winstone, Matthew L. Workentine, and Jerome Yerly. I have also had several mentors who have had a tremendously positive impact on my time at the University of Calgary. First, my thanks to Dr. Michael Hynes, Dr. Dave Schriemer and Dr. Michael Surette for teaching and organizing the best three courses I have ever taken as a student: Environmental Microbiology (CMMB 543), Mass Spectrometry and Proteomics (MDSC 751.04) and Gene expression in Bacteria (MDSC 613.05). Your guidance over the years has changed my way of thinking. I also owe a debt of thanks to my supervisory committee members (Dr. Elke Lohmeier-Vogel, Dr. Michael Surette, Dr. Raymond J. Turner and Dr. Howard Ceri), internal (Dr. Glen Armstrong, Dr. Gerritt Voordouw) and external examiners (Dr. Paul Stoodley) for their work on my behalf. Last

of all, my most heart felt thanks go to Dr. Raymond J. Turner and Dr. Howard Ceri who have been my supervisors and teachers – you have provided me with one of the best multidisciplinary research environments for biochemistry and microbiology in the world and I would not have been successful without you.

Funding on this research has come from many public sources, including the Natural Sciences and Engineering Research Council (NSERC) of Canada, the Alberta Heritage Foundation for Medical Research (AHFMR), the AHFMR Forefront program, the Canadian Institute for Health Research (CIHR), the Canadian Foundation for Innovation (CFI) Bone and Joint Disease Network, and the Alberta Science and Research Investments Program (ASRIP). Corporate support has been provided by Innovotech Incorporated, Fef Chemicals Incorporated and by EDM Studio Incorporated. My personal thanks go to NSERC for a Canada Graduate Scholarship (CGSD2) and an Industrial Postgraduate Scholarship (IPS1), as well as to AHFMR for a PhD Studentship/Incentive Award. The Department of Biological Sciences has also supported my time as a graduate student with numerous Graduate Teaching Assistantships. Without the professional and personal financial support of these organizations, the research in this Thesis would not have been possible.

Dedication

This thesis is dedicated to the strong and amazing women in my life – my mom, Jane Harrison, my sister, Kate Harrison, my significant other, Kyra Page and to my daughter, Mykayla Page.

Table of Contents

List of Tables

List of Figures and Illustrations

List of Symbols, Abbreviations and Nomenclature

Symbol	Definition
2D	two-dimensional
3D	three-dimensional
AHSL	acyl-homoserine lactone
ANOVA	analysis of variance
AO	acridine orange
AOAC	Association of Official Analytical Chemists
AOBS	acoustic optical beam splitter
ASM	American Society for Microbiology
ASTDR	Agency for Toxic Substances and Disease Registry (USA)
ATCC	American Tissue Culture Collection
ATP	adenosine triphosphate
CA-MHB	cation adjusted-Mueller Hinton broth
carboxy-H_2DCFDA	5-(and 6)-carboxy-2',7'-difluorodihydrofluorescein diacetate
CBD	Calgary Biofilm Device
CDC	Center for Disease Control
c-di-GMP	3'-5'-cyclic-dimeric guanosine monophosphate
CERCLA	Comprehensive Environmental Response, Compensation, and Liability Act (USA)
CFU	colony forming unit
CLSI	Clinical Laboratory Standard Institute
CLSM	confocal laser scanning microscopy
ConA	concanavalin A
DAPA	diaminopimelic acid
DCF	2,7- dichlorofluorescein
ddH_2O	double distilled water
DF	dilution factor
DNA	deoxyribonucleic acid
dsDNA	double stranded deoxyribonucleic acid
ΔE_o	standard reduction potential
ECM	extracellular matrix
G6P	glucose-6-phosphate
GFP	green fluorescent protein
GSH	glutathione
HTP	high-throughput
KB	King's broth
KBA	King's broth agar
LB	Luria-Bertani
LBA	Luria-Bertani agar
LCS	Leica® confocal software
LK	log-killing

MBC_b	biofilm minimum bactericidal concentration
MBC_p	planktonic minimum bactericidal concentration
MDR	multidrug resistance
MDT	multidrug tolerance
MFC	minimum fungicidal concentration
MIC	minimum inhibitory concentration
MLK	mean log-killing
MMR	multimetal resistance
MMT	multimetal tolerance
MOPS	3-*N*-morpholinopropanesulfonic acid
MRLK	mean relative log-killing
MSD	minimum salts dextrose
MSVG	minimum salts vitamins glucose
MSVP	minimum salts vitamins pyruvate
MVCC	mean viable cell count
$MVCC_i$	mean viable cell count of the initial growth controls
Na_2DDTC	sodium diethyldithiocarbamate
$NADP^+$ (NADPH)	nicotinamide adenine dinucleotide phosphate
NBF	*N*-methyl-4-amino-7-nitrobenzofurazan
NBFhd	4[*N*-methyl-*N*(4-hydroxyphenyl)amino]-7-nitrobenzofurazan
PBS	phosphate buffered saline
PCR	polymerase chain reaction
PI	propidium iodide
pK_{SP}	solubility product of the metal-sulfide complex
PMF	proton motive force
PNA	peanut agglutinin
RNA	ribonucleic acid
QS	quorum-sensing
RLK	relative log-killing
ROS	reactive oxygen species
RPMI	Roswell Park Memorial Institute
RQMB	RPMI 1640® glutamine MOPS bicarbonate
SCV	small colony variant
SD	standard deviation
SEM	scanning electron microscopy
ssDNA	single stranded deoxyribonucleic acid
ssRNA	single stranded ribonucleic acid
TA	toxin-antitoxin
TCA	trichloroacetic acid
TIFF	tagged image file format
TRITC	tetramethylrhodamine isothiocyanate
TSA	trypticase soy agar

TSB	trypticase soy broth
VCC	viable cell count
WS	wrinkly spreader
YC	yeast extract casamino acids

Epigraph

"There is probably no chemotherapeutic drug to which in suitable circumstances the bacteria cannot react by in some way acquiring 'fastness' [resistance]."

- Andrew Fleming, 1946

Chapter One: Microbial biofilms and antimicrobial susceptibility

1.1 An introduction to biofilms

Over the past 40 years, an increased understanding of microbial biofilms has driven a revolution that now more than ever is transforming the science of microbiology (15, 92, 108). In contrast to the long-accepted belief that microbes live as solitary entities, biofilms are now regarded as a prominent mode of microbial life in nature and in disease (92). Biofilm[1] formation is a part of the ecological cycle for the vast majority of microbes and is generally thought to involve a series of coordinated developmental (242) and/or social behaviours[2] (184) (Figure 1.1). The salient features of this microbiological process are briefly summarized here.

Biofilm formation begins when microbes attach to a surface, an event that sets in motion a series of temporal and spatial shifts in cellular gene expression that continue as the surface-adherent organisms proliferate (215, 228, 242, 275) (Figure 1.1). This continuum of phenotypic changes results in a heterogeneous microbial consortium that is physiologically and genetically diverse (237). A mature biofilm is highly structured, irregularly organized, and intermingled with a network of fluid-filled channels (92). The microscopic architecture of a biofilm may include cell layers, clumps and ridges, or even more complex microcolonies that are arranged into stalks or mushroom-like formations. The residents in a biofilm may be a single species or a diverse group of microorganisms distributed in various microniches. A prominent characteristic of biofilms is a hydrated

---

[1] A biofilm is conventionally defined as a surface-adherent assemblage of microorganisms that is encased in a self-produced matrix of extracellular polymers. In the literature, the term "biofilm" has been used to describe surface-adherent cells, pellicles, microbial mats, flocs, and colony growth on agar plates, which are processes that undoubtedly produce distinct physiologies as these occur at different physical interfaces. Furthermore, illustrations of the bacterial ecological cycle that describe biofilm growth, including the one in this thesis, generally fail to consider the diverse range of complex, coordinated cellular behaviours in which bacteria engage on surfaces, including swimming, swarming and twitching motilities. Although beyond the scope of the present work, I would suggest that an expanded definition of "biofilm" should be introduced and sub-divided into categories to distinguish between these different microbial behaviours.

[2] At the present time, it is not possible to distinguish between developmental microbiology and sociomicrobiology, as the field of microbiology does not have an adequate conceptual framework to differentiate these ideas.

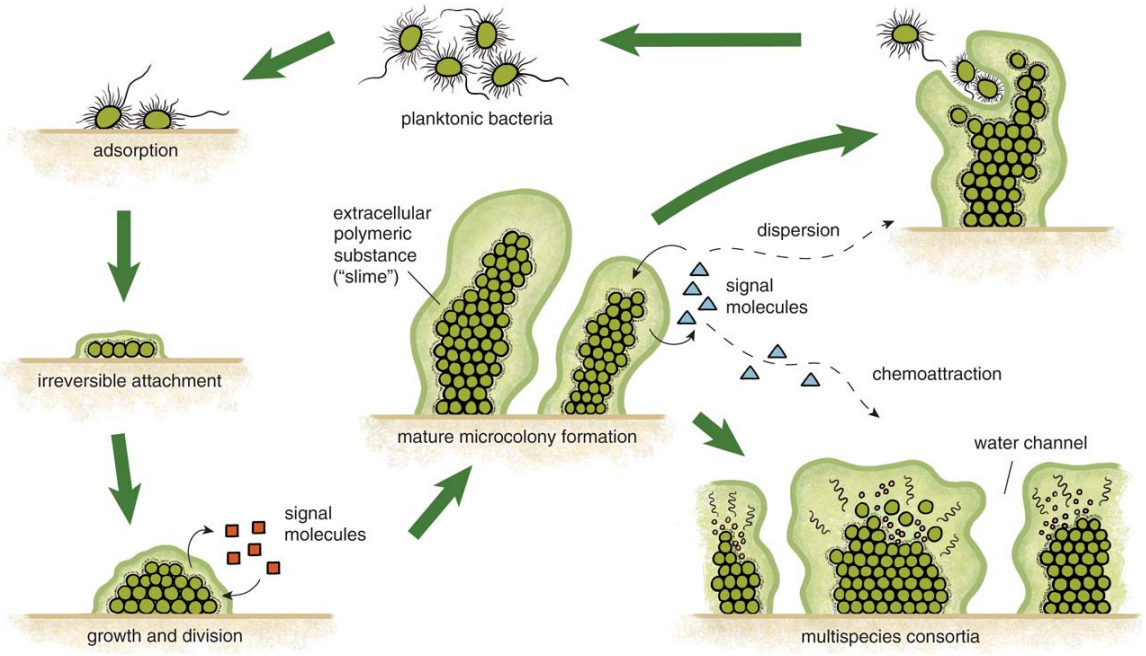

Figure 1.1. Biofilms and planktonic cells are integrated parts of the microbial ecological cycle. Formation of a biofilm may be viewed as a step-wise process that is functionally analogous to the development of multicellular organisms. 1) Planktonic cells may adsorb to surfaces. 2) This event triggers a physiological change in which the bacteria become irreversibly attached to the substratum, usually through the production of an extracellular matrix. 3) These surface-adherent bacteria grow and divide to form 4) mature microcolony structures. The behaviours, and therefore physiology, of cells in a biofilm is controlled, in part, by the cell-to-cell signals that are part of quorum sensing systems. 5) Various other small molecule signals may also cause dispersion of the bacteria (i.e. shedding of planktonic cells from the biofilm into the environment) or 6) may assist in recruiting different microbial species into the consortium. (This figure has been reproduced by permission from Harrison *et al.* (2005) Am. Sci. 93, 508-515).

extracellular matrix (ECM) made of polysaccharides (34, 150, 210, 245), nucleic acids (233, 274) and proteins (33, 34), which may also function to trap additional particulate matter from the surrounding environment (92). It's becoming increasingly clear that the communal life offers microorganisms considerable advantages.

Mounting evidence indicates that biofilm microbes may undergo a process of cell specialization that is functionally analogous to differentiation[3] in multicellular organisms (90, 152, 199, 228); therefore, microbial biofilm populations have emergent functions that their counterparts – single planktonic-cells[4] – lack. For instance, the physical proximity of other cells favours synergistic interactions, even between members of different species. These include the enhanced horizontal transfer of genetic material between microbes (164), the sharing of metabolic by-products, shelter from changes in the environment, active dispersal processes and protection from the immune system of an infected host or from grazing predators (108). Most importantly, growth in a biofilm modulates the susceptibility[5] of microbes to antibiotics, hard-surface disinfectants and toxic metal ions (26, 103, 105, 230, 250), a well known phenomenon that lies at the heart of this thesis.

1.2 Biofilms are sanctuaries that protect microbes from antimicrobial agents

The decreased susceptibility of biofilms to antimicrobials — which occurs in the absence of mobile genetic-resistance determinants (such as integrons, transposons and plasmids) — depends on the nature of the biofilm organisms as well as the antimicrobial agent and the environment, and thus is very complicated. Unsurprisingly, biofilm antibiotic susceptibility has been the subject of intense research and lies at the heart of several excellent reviews (80, 152, 203, 235, 236). By contrast, at the time this thesis

---

[3] Differentiation is a developmental process whereby a cell acquires a specialized gene expression profile that produces a cellular morphology or function that is distinct from the original cell type. This process may occur, to some extent, independently of exogenous input once initiated; however, in biofilm microbiology, it is experimentally difficult to distinguish this from a response of cells to a heterogeneous environment.

[4] Planktonic cells are microorganisms that grow primarily as free-floating, single cells in a liquid suspension that is under constant mixing.

research was initiated, the study of biofilm metal susceptibility had received relatively little attention. Incredibly, this thesis research began with the question "*Are biofilms less susceptible to metal toxicity than planktonic bacteria?*" Although the focus of this thesis eventually shifted to "*How are biofilms more resistant and tolerant to toxic metal ions than planktonic bacteria*?" the study of biofilms in metal-microbe interactions remains an important area for research. Toxic metals present problems to biofilm communities that are distinct from antibiotics because different metal species possess distinct chemistries and function through diverse biochemical routes of toxicity. It is because of these challenges that biofilm research involving metals is providing important clues to understanding the altered susceptibility of biofilms to all types of toxic stressors. In fact, biofilm formation might be a mode for co-selection of drug and metal resistance[6] or tolerance[7].

There is now some recognition that antibiotic resistant bacteria may be maintained in the environment through co- or cross-resistance to toxic metals or through co-regulation of resistance pathways (11, 279). Biofilm induction might involve regulatory processes that indirectly activate genetic and biochemical pathways that are shared in the response of microbes to antibiotic and metal exposure (11). This may imply that microbes exposed to metals in the environment or in clinical settings may form biofilms that are simultaneously drug resistant and tolerant (11). As research involving metals progresses, it is possible to elucidate mechanisms that might reduce the susceptibility of biofilms to antibiotics. Conversely, this allows us to pull on the wealth of information available for biofilm antibiotic susceptibility to provide insights into biofilm metal resistance and tolerance. Thus, this thesis will begin where my research did: looking to the literature for clues about the cellular and molecular mechanisms likely responsible for the decreased susceptibility of biofilms to antibiotics.

---

[5] Susceptibility is the sensitivity of an organism to a toxic environmental stressor.
[6] Resistance is the ability of an organism to continue growing in the presence of an antimicrobial agent.
[7] Tolerance is the ability of an organism to survive, but not grow, in the presence of an antimicrobial agent.

1.3 The antibiotic resistance and tolerance of microbes in biofilms

Stewart and Costerton (236) were the first to propose that biofilms may rely on a multicellular strategy to survive antibiotic exposure and pointed out several factors that may contribute to biofilm drug resistance: metabolic heterogeneity resulting from micronutrient and oxygen restriction, a biofilm-specific gene expression pattern (i.e. distinct biofilm physiology), and restricted penetration of the antibiotic into the biofilm matrix. By contrast, Spoering and Lewis (230) first proposed that the recalcitrance of infectious biofilms to antibiotic therapy was due to the production of a specialized sub-population of survivor cells termed 'persisters.' Lastly, Drenkard and Ausubel (69) demonstrated that antibiotic resistance and biofilm formation were linked to phenotypic variation[8]. Collectively, these reports suggested that the reduced susceptibility of biofilms to antibiotics is a multifactorial process with many interacting components. Below follows a brief elaboration on each of these components in the recalcitrance of bacterial biofilms to antibiotic treatments, and these reports have served as the starting point for the multifactorial model presented in the final chapter of this thesis describing biofilm susceptibility to toxic metal ions.

1.3.1 Metabolic and chemical gradients in biofilms

There are many elegant studies showing metabolic gradients within solid-surface-attached biofilms, a stratification that is correlated to the restricted diffusion of nutrients, O_2 and metabolites throughout the community (121, 273, 281). This results in non-uniform distributions in extracellular pH and redox poise (123, 198) and also restricts microbial growth rates in certain portions of the biofilm (204); therefore, biofilm microbes can possess very different physiological states, even when separated by as little as 10 μm (280). In *Pseudomonas aeruginosa* biofilms that are >100 μm thick, the cells

[8] Phenotypic variation is a process in which the colony morphology of a microbial strain grown on agar medium is somehow changed in comparison to a reference strain independently of genetic change. This should be distinguished from genotypic variation, where a phenotypic change might result from site-specific genetic rearrangement or random mutation.

nearest to the substratum are in anoxic zones and are slow-growing, which itself leads to an intrinsic tolerance to killing by antibiotics relative to the aerobic fast-growers in the outer biofilm layers (31, 270). It is also possible that changes in pH or accumulation of metabolic wastes in certain regions of the biofilm may antagonise the action of antibiotics. In the case of the latter, inhibitive waste metabolites may cause bacteria to enter non-growing states that are not susceptible to killing (236). However, it is important to note that mature biofilm structure is likely only one contributing factor to biofilm antibiotic susceptibility.

Immature biofilms that consist of little more than adherent layers of cells as well as those in the early stages of growth possess elevated resistance to antibiotics relative to planktonic cells. For example, biofilms of *Candida albicans* and *Candida tropicalis* form thin layers of cells (scantily clad with extracellular polymers) in microtitre plates as well as on the polystyrene surface of the Calgary Biofilm Device (CBD) (101, 103, 147). However, *C. tropicalis* and *C. albicans* biofilms are highly resistant and/or tolerant to antifungals (103, 106, 147). Consistent with these observations, Lafleur *et al*. (147) have suggested that surface attachment may trigger the physiological transition to a multidrug and resistant and/or tolerant state for *Candida* spp. Myself and others have made similar observations for the antibiotic susceptibility of bacterial biofilm systems, including *P. aeruginosa* (59) and *Escherichia coli* (96).

To summarize, microbial biofilms that lack complex three-dimensional structures still have reduced susceptibility to antibiotics, indicating that population structure (and the associated metabolic heterogeneity) is only one contributing factor to reducing susceptibility to antimicrobials. Another set of processes required for structured biofilm growth are the extracellular signalling pathways used by biofilm microorganisms.

1.3.2 Distinct patterns of gene expression in biofilm cells

We are just beginning to appreciate the importance of signalling processes in biofilm development (136, 184). One prominent signal system that probably has a role in biofilm susceptibility to antimicrobial toxicity is extracellular signalling via quorum sensing (QS) systems. There have been many recent studies examining the role of QS in

bacterial biofilms, and there remains little doubt that under certain conditions it is a contributing factor to the mature biofilm lifestyle (52, 146, 272, 283). QS signals may also accumulate in certain regions of biofilms, which means that these intercellular cues may affect cells in different regions of the biofilm in different ways (117, 135). Biofilms of QS-deficient mutants of *P. aeruginosa* are hypersensitive to killing by aminoglycosides and hydrogen peroxide (H_2O_2) (26). In both biofilm and planktonic cultures, QS-systems cause sweeping changes in global gene expression (18, 220, 269); however, in relation to biofilm antimicrobial tolerance, it is important to note that cellular defence machinery may be upregulated by these systems. For example, three known QS-regulated genes upregulated during *P. aeruginosa* biofilm formation are manganese-cofactored superoxide dismutase (*sodA*), iron-cofactored superoxide dismutase (*sodB*) and catalase (*katA*) (109). Hypothetically, since many bactericidal antibiotics that target different cellular pathways kill cells by a common mechanism – through the production of reactive oxygen species (ROS) (72) – it may be that heightened expression of these enzymes in biofilms may play a role in abrogating cell death. One of the other ways signalling events might contribute to drug resistance and tolerance is by regulating synthesis of ECM components (136) that facilitate biosorption.

1.3.3 Restricted diffusion of antibiotics into biofilms

Certain antibiotics, as well as other antimicrobials, fail to penetrate beyond the surface layers of the biofilm (145, 223). For example, the positively charged aminoglycosides, such as tobramycin and gentamicin, bind to negatively charged ECM constituents, and thus do not penetrate *P. aeruginosa* biofilms (145, 223). Similarly, secreted catalase and β-lactamase protect biofilm cells by breaking down hydrogen peroxide (239) and β-lactam antibiotics (6), respectively, thereby preventing full penetration of these agents into the biofilm. Other components of biofilm matrices are extracellular membrane vesicles, which may also bind to and sequester aminoglycosides (218).

More recently, it has been suggested that changes in the fluid viscosity experienced by bacteria, which would result from growth in an ECM, may also contribute

to population physiological changes that increase antibiotic tolerance (141). In addition to sequestration in the ECM, it is also possible that antibiotics may be sequestered in the bacterial periplasm. Mah et *al*. (161) have identified that the *P. aeruginosa* gene *ndvB*, which does not affect mature biofilm structure when inactivated by mutation, is required for the synthesis of periplasmic glucans that are involved in the high level resistance of biofilms to multiple classes of antibiotics. Periplasmic glucans may directly interact with antibiotics thereby preventing these compounds from reaching their sites of action.

In the field of biofilm research, there has been intense interest in intracellular signalling by the bacterial second messenger bis-(3'–5')cyclic dimeric guanosine monophosphate (c-di-GMP). Recent studies suggest that c-di-GMP is ubiquitously produced in bacterial taxa and that it regulates physiology and many coordinated activities of microbial communities, such as virulence-factor expression and biofilm formation (208). The GGDEF and EAL protein domains (which correspond to diguanylate cyclases and phosphodiesterases, respectively) are responsible for the synthesis and degradation of c-di-GMP, respectively. There is a correlation between antibiotic resistance, phenotypic variation and c-di-GMP signalling (mediated by the EAL-domain protein PvrR) that has been recently established for *P. aeruginosa* PA14 (69). Although there are several different proteins in *P. aeruginosa* that mediate c-di-GMP signalling, this second messenger is likely involved in drug resistance through regulation of extracellular polymer production, which would likely alter the adsorption properties of the ECM. It is important to note that colony morphology variants, which are frequently recovered after microbial growth in biofilms (30), produce extracellular polymers of different quantity and character than the original inoculating strain (110, 134) (discussed in Section *1.3.5*).

Here I will emphasize that restricted diffusion cannot solely account for the reduced susceptibility of biofilms to antibiotics. Measurements of antibiotic penetration into biofilms *in vitro* have shown that the β-lactam antibiotics piperacillin and imipenem rapidly penetrate *P. aeruginosa* biofilms that are otherwise highly tolerant to killing by these drugs. Similarly, *P. aeruginosa* biofilms that are relatively thin (10-20 μm) are also highly tolerant to killing by ciprofloxacin, a fluoroquinolone antibiotic that also rapidly

penetrates the biofilm ECM. Furthermore, colistin, a cyclic cationic antimicrobial peptide, as well as the anionic detergent sodium dodecyl sulphate (90), kill established *P. aeruginosa* biofilm cells in the interior regions of microcolonies before those in the outer layers (128). It is also interesting to note that cells in *C. tropicalis* biofilms surviving exposure to the antifungal amphotericin B seem to be randomly interspersed in the population (103, 106). The spatial patterns of killing deduced from these studies indicate that, although restricted penetration of antimicrobials by biosorption is an important component to reduced biofilm susceptibility to toxic stressors, this phenomenon is not the only mechanism of resistance — otherwise biofilms would always die from the outside in, and not from the inside out. Collectively, the killing kinetics of microbial populations by agents that rapidly penetrate biofilms as well as the spatial patterns of biofilm killing discussed here indicate that there may be specific cell types that may withstand the action of antimicrobials.

1.3.4 Persister cells

Single species populations that consist of Gram-positive and Gram-negative bacteria, as well as *C. albicans* (97, 105, 147, 152), produce subpopulations of specialized cells, termed persister cells, that may survive exposure to high concentrations of bactericidal antibiotics (25, 130, 153, 230, 235). Typically, persister cell subpopulations represent 0.1% or less of the bacterial population (168, 230), although in biofilms it has been estimated to be as high as 10% (230); therefore, this might account for the remarkable antimicrobial tolerance of bacteria growing on a surface (130, 153, 230). Although first reported in the literature during the 1940's (25), this particular mechanism of antimicrobial tolerance is currently subject to much controversy and has generated appreciable attention over the past several years. At the molecular level, persister cells have only begun to be characterized for *E. coli*, and this topic is briefly reviewed here.

E. coli persister cells are associated with a slow-growth, metabolically quiescent phenotype that may be identified using microscopy prior to antibiotic exposure (12). This suggests that persister cells pre-exist in a population and that they are not produced

in response to antibiotics (12, 130). At the population level, persister cells give rise to hallmark biphasic population killing kinetics that are either time-dependent (12, 130, 243) or concentration-dependent (35). Furthermore, persister cells may seed a new bacterial culture with normal susceptibility once the antibiotic is removed (105, 130). This latter observation may account for the recalcitrant nature of biofilm diseases encountered in medicine, where acute infections may return once chemotherapy is ceased (56, 67, 80, 92, 194).

There are now numerous reports that have demonstrated a genetic basis for bacterial persistence (28, 29, 131, 139, 154, 167, 168, 216). In *E. coli*, the proportion of persisters in the bacterial population is controlled by the high persistence (*hip*) operon (28, 29, 139, 167, 168) as well as by other toxin-antitoxin (TA) modules (J. J. Harrison, S. A. Aikerman, W. D. Wade, H. Ceri and R. J. Turner, unpublished data). There is some controversy surrounding the TA model of persister cell formation, as unrelated proteins expressed at toxic levels, such as PmrC and DnaJ, also lead to an increased proportion of persisters in *E. coli* populations (265). By contrast, recent evidence suggests that PhoU (154), a negative regulator of phosphate metabolism, as well as *glpABC*, *glpD* and *plsB* (231), which are involved in glycerol-3-phosphate metabolism, may also play a role in persister cell formation. In contrast to these findings, it is also important to note that a recent mathematical model has predicted that persisters may accumulate in regions of substrate limitation within the biofilm (207). Furthermore, Klapper *et al*. (137) have recently proposed that cellular senescence – the deterioration of a microorganism that is associated with advanced age and whereby it loses the ability to divide – may also explain bacterial persistence. Nonetheless, since the majority of research has examined the TA model of persistence, the research described in this thesis will focus on TA mediated mechanisms.

In *E. coli*, the *hip* operon encodes two genes (*hipBA*) that are postulated to comprise a TA module; this is based on the homology of *hipBA* with a plasmid addiction system harbored by the symibiotic *Rhizobium* plasmid pNGR234a (74). In this system, *hipA* encodes a toxic serine kinase (54), whereas *hipB* encodes a DNA binding protein that autoregulates expression of the *hip* operon. HipB also binds to HipA to nullify its

toxicity, which is a characteristic of all known TA modules (139). The *hipA7* allele is a gain-of-function mutation known to mediate up to a 1000-fold increase in the number of persisters produced by *E. coli* (139, 167, 168). Since the *hipA7* mediated high persistence phenotype is abolished in a Δ*relA* Δ*spoT* background, Korch and colleagues (139) postulated that (p)ppGpp synthesis may govern the 'persistent' physiological state.

It is well known that the bacterial stringent response is also governed by (p)ppGpp synthesis. To date, the stringent response plays an unidentified role in the production of persisters. However, it is known that stringent response regulated genes play an important role in *E. coli* biofilm formation (13), entry into stationary phase, and bacterial adaptation to nutrient limitation and oxidative stress (45). The persistent response of *hip* mutants not only reduces cell death due to antibiotic exposure, but also reduces the lethality of heat shock (216) and metabolic block (i.e. starvation for diaminopimelic acid) (168).

Interestingly, deletion of the *hipBA* operon does not have an effect on the ability of *E. coli* to form persisters in logarithmic-growing planktonic cultures (28). However, Δ*hipBA* mutants produce a smaller portion of persisters in stationary-phase cultures (131), which are also more tolerant to antibiotics than logarithmically growing cultures (230). Overexpression of *hipA* is correlated to joint tolerance of *E. coli* to β-lactam and fluoroquinolone antibiotics (73). Interestingly, MazF and another unrelated toxin, RelE, may also act as attenuators of the stringent response (50, 188). Keren et *al*. (131) have recently demonstrated that *relE* is overexpressed in populations of *E. coli* cells that have been enriched for persisters (131). RelE functions by cleaving mRNA on ribosomes, thereby stalling translation (189). Ectopic overexpression of *relE* also results in an increase in the number of persister cells in a bacterial population (131). Thus, toxin modules, which reversibly block translation, may shut down potential antibiotic targets, resulting in the persistent phenotype that is responsible for multidrug tolerance (131). However, it still is possible to isolate other types of phenotypic variants from biofilm populations, and as persister cells can only explain drug tolerance, there might be other cell types that mediate biofilm resistance.

1.3.5 Phenotypic variation is linked to biofilm formation and antibiotic resistance

It is frequently possible to recover colony morphology variants from biofilm populations, many of which have altered phenotypic traits relative to the colonizing strain (30, 59). For example, small colony variant (SCV) cells, which are typically superior at forming biofilms and less motile than their progenitors, are often recovered from aged biofilms of clinical and/or rhizosphere *Pseudomonas* spp. (110, 134, 263). In laboratory-grown biofilms of *P. aeruginosa*, *P. chlororaphis* and *P. fluorescens*, SCVs occur at a frequency in the population that is increased by exposure to certain antibiotics and H_2O_2 (59, 69). Drenkard and Ausubel (69) were the first to describe that the varying abilities of colony morphology variants to form biofilms is linked to antibiotic resistance; furthermore, these researchers established a link between this process and intracellular signalling by c-di-GMP. Boles *et al.* (30) have shown that genotypic and phenotypic diversity may be introduced into *P. aeruginosa* biofilm populations in a *recA* dependent fashion. In their study, the phenotypic variants recovered from biofilms also showed varying levels of resistance to H_2O_2. Although these ideas do not provide direct experimental evidence for the insurance hypothesis[9] (30), ecologists have long thought that random mutations or site-specific genetic rearrangements might ensures population survival, as some phenotypes or genotypes may be poised to survive environmental insults that others may not.

1.3.6 A multifactorial model of biofilm multidrug resistance and tolerance

It is possible to bring these different mechanisms of antibiotic resistance and tolerance together to qualitatively describe the reduced susceptibility of biofilms to antibiotics using a multifactorial model (Figure 1.2). Collectively, the literature reviewed here suggests that the extraordinary resilience of biofilms is linked to the remarkable

---

[9] In ecology, the insurance hypothesis states that biodiversity insures ecosystems against declines in their functioning because many species provide greater guarantees that some will maintain functioning even if others fail. Although the experiments of Boles et al. (30) may be flawed in their test of the insurance hypothesis, this idea is a notable reference for future research.

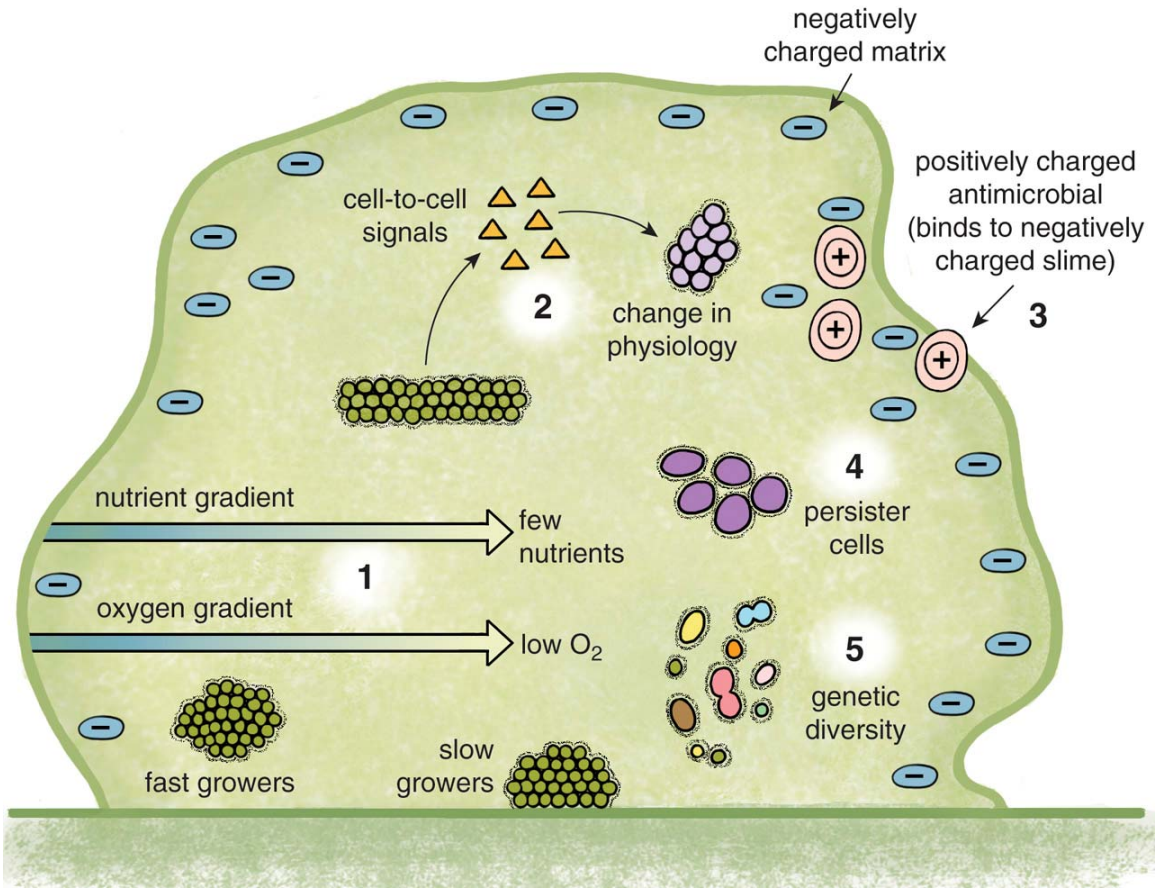

Figure 1.2. A multifactorial model of multidrug resistance and tolerance in microbial biofilms. Biofilms derive their extraordinary resilience from several factors. 1) Bacteria near the center of a microcolony grow very slowly because they are exposed to lower concentrations of oxygen and nutrients. They are thus spared the effects of antibiotic drugs, which are much more effective against fast-growing cells. 2) Intercellular signals can alter the physiology of the biofilm cells, causing members to produce enzymes that are important for defence against toxic stresses. 3) The biofilm matrix is negatively charged and so binds to positively charged antimicrobials, preventing them from reaching the cells within the microcolony. 4) Specialized populations of persister cells (4) do not grow in the presence of an antibiotic, but neither do they die. 5) Finally, population diversity (5), genetic as well as physiological, acts as an "insurance policy," improving the chance that some cells will survive any challenge. (This figure has been reproduced by permission from Harrison et al. (2005) Am. Sci. 93, 508-515).

heterogeneity of microbes growing in these communities. Microbial biofilm populations, therefore, may be poised to survive fluxes in bactericidal antibiotics because there are diverse cell types in biofilms that might additionally function to protect each other. It is the specific hypothesis of this thesis that many of the cellular, chemical and biological mechanisms at work in this model may also explain the recalcitrance of biofilms towards toxic metal species (discussed in Section 1.6 of this thesis).

1.4 Biofilms and metal-microbe interactions

In this thesis I will use the collective term 'metal' to denote inorganic ions containing elements from the alkali earth metals, transition metals, semi-metals and metalloids, as well as the lanthanides and actinides. Biofilm multimetal resistance (MMR) and multimetal tolerance (MMT) — which I have named after the corresponding terms used in clinical antibiotic-susceptibility testing for multidrug resistance (MDR) and multidrug tolerance (MDT), respectively — are rapidly gaining interest in the scientific community. This is in part due to the renewed use of metals such as Cu, Ag, Bi, and Ga as anti-infectives in clinical settings, but above all, the United States government has made a recent $100 billion pledge to support remediation of the >30000 sites contaminated by metals from American industrial activity. According to the United States Agency for Toxic Substances and Disease Registry (ASTDR), the Comprehensive Environmental Response, Compensation, and Liability Act (CERCLA) 2005 Priority List names As, Pb, Hg and Cd as four of the 'Top 10' most prevalent environmental toxins hazardous to public health (http://www.atsdr.cdc.gov/cercla/05list.html). A European Commission on heavy metals in waste similarly identified these compounds but highlighted Cr as the most widespread toxic heavy-metal pollutant in the European Union (116). Microbial biofilms, natural or engineered, may be used to remediate heavy-metal pollution through biochemical modification and/or accumulation of toxic metal ions (46, 64, 172, 226), which notably include the radioactive actinides as well as other radionuclides (7). An understanding of metal toxicity in biofilms is crucial to the successful design of bioreactors used for biomining (205), as well as those reactors used for biodegrading organic contaminants that are frequently intermingled with metals

(226). Moreover, this type of research may provide insights into the observed vulnerabilities, physiological shifts and species changes of natural aquatic biofilm communities exposed to toxic heavy metals (149, 268).

1.5 Biochemical mechanisms of metal toxicity

A necessary first step towards understanding the susceptibility of biofilms to metals is to understand the mechanisms through which metals are toxic to microbial cells. Many metal ions may exert toxicity on biological systems through multiple biochemical pathways simultaneously; here, I have broken these reactions into five mechanistic categories (Figure 1.3). First is substitutive metal-ligand binding, in which one metal ion may replace another at the binding site of a specific biomolecule, thereby altering or destroying the biological function of the target molecule (175). Second is covalent and ionic reduction–oxidation (redox) reactions of metal ions with cellular thiols (R-SH) (241, 284), in particular glutathione (GSH) (257). It is worth noting that the Painter-type reaction of thiols with metal oxyanions, such as Se and Te oxyanions (SeO_4^{2-}, SeO_3^{2-}, TeO_4^{2-} and TeO_3^{2-}), may liberate the toxic reactive oxygen species (ROS) superoxide ($O_2^{\bullet-}$) as a by-product of reduction (132, 255). The third category involves the participation of transition metals (such as Cu and Fe) in Fenton-type reactions to produce ROS, such as hydrogen peroxide (H_2O_2), hydroxyl radicals ($OH^{\bullet-}$), and $O_2^{\bullet-}$ (82, 124, 241). In general, ROS are transient and highly reactive compounds that can damage all biological macromolecules (191). The fourth category involves interference with membrane-transport processes, in which a toxic metal species may competitively inhibit a specific membrane transporter by occupying binding sites or by using and/or interfering with membrane potential that is normally reserved for an essential substrate (77). The fifth category involves the indirect siphoning of electrons from the respiratory chain through thiol-disulfide oxidoreductases (32), thereby destroying the proton motive force of the cell membrane (157).

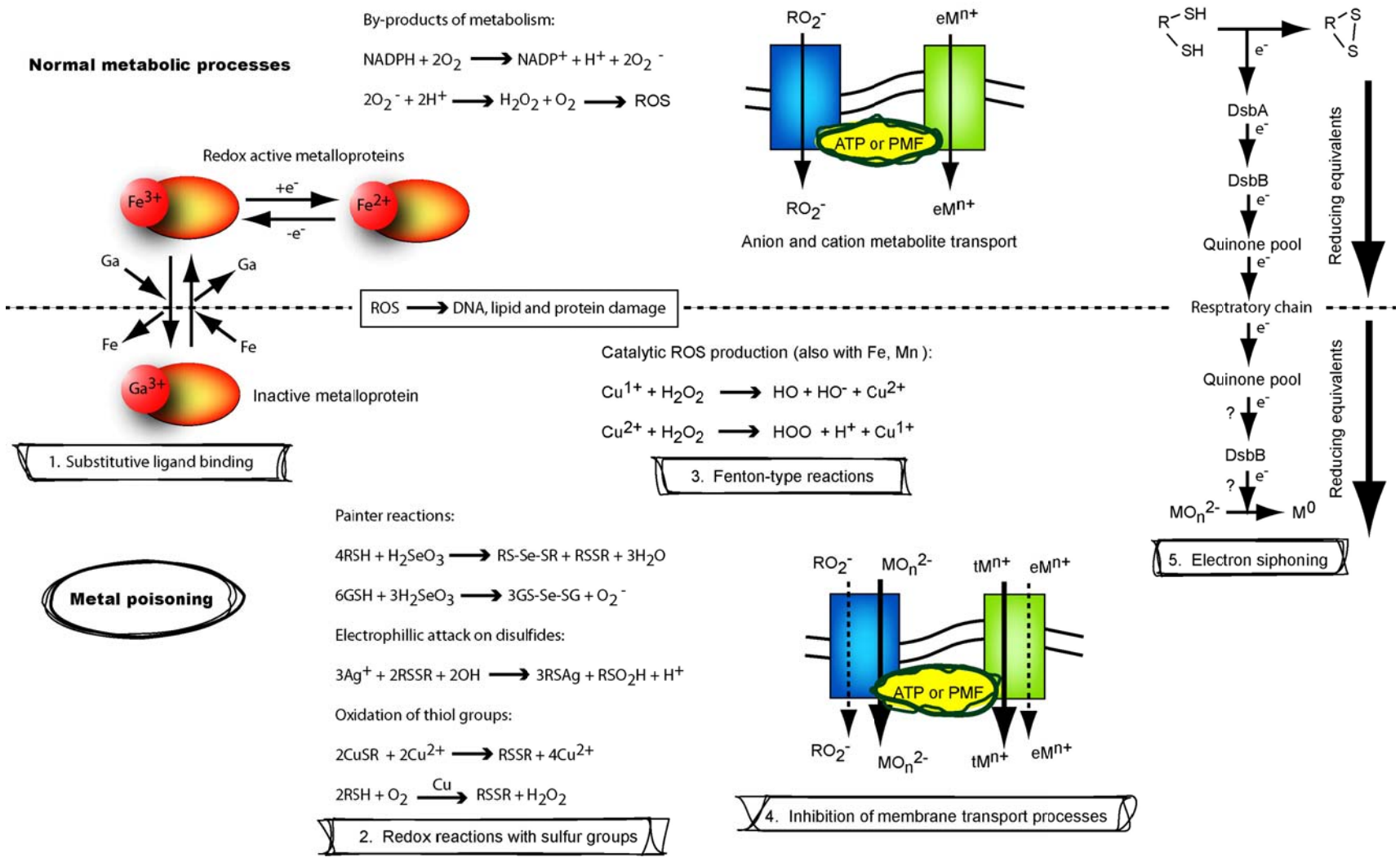
Normal metabolic processes
By-products of metabolism:
NADPH + 2O2 → NADP+ + H+ + 2O2 -
2O2 - + 2H+ → H2O2 + O2 → ROS
Redox active metalloproteins
Fe3+
+e-
-e-
Fe2+
Ga
Ga
Fe
Fe
Ga3+
Inactive metalloprotein
1. Substitutive ligand binding
ROS → DNA, lipid and protein damage
Metal poisoning
Painter reactions:
4RSH + H2SeO3 → RS-Se-SR + RSSR + 3H2O
6GSH + 3H2SeO3 → 3GS-Se-SG + O2 -
Electrophillic attack on disulfides:
3Ag+ + 2RSSR + 2OH → 3RSAg + RSO2H + H+
Oxidation of thiol groups:
2CuSR + 2Cu2+ → RSSR + 4Cu2+
2RSH + O2 Cu→ RSSR + H2O2
2. Redox reactions with sulfur groups
RO2-
eMn+
ATP or PMF
RO2-
eMn+
Anion and cation metabolite transport
Catalytic ROS production (also with Fe, Mn):
Cu1+ + H2O2 → HO + HO- + Cu2+
Cu2+ + H2O2 → HOO + H+ + Cu1+
3. Fenton-type reactions
RO2-
MOn2-
tMn+
eMn+
ATP or PMF
RO2-
MOn2-
tMn+
eMn+
4. Inhibition of membrane transport processes
R SH
SH
e-
R S
S
DsbA
e-
DsbB
e-
Quinone pool
e-
Resptratory chain
e-
Quinone pool
?
e-
DsbB
?
e-
MOn2-
M0
Reducing equivalents
Reducing equivalents
5. Electron siphoning

Figure 1.3. Biochemical mechanisms of microbiological metal toxicity. Metal species exert toxicity through numerous biochemical pathways that may be broken into five mechanistic categories. Examples and/or general mechanisms of biological metal toxicity have been illustrated here, and this is not intended to be an exhaustive list. 1) Toxic metal species may bind to proteins in lieu of essential inorganic ions, altering the biological function of the target molecule. An example is the replacement of Ni for Mg in some redox active metalloproteins or in DNA, which destroys their function and/or may lead to DNA damage, respectively (175). 2) Toxic metal species may participate in an array of reactions with thiols and disulfides, destroying the biological function of proteins containing sensitive sulfur groups (241, 284). These reactions frequently require and produce reactive oxygen species (ROS), which are by-products of normal metabolism (241). Thiol groups are often involved in the binding of substrates to specific carriers and this transport mechanism may be impaired by toxic metal species. Destruction of sensitive thiol groups on nascent proteins by metal species may also impair protein folding or the binding of apoenzymes by cofactors, thereby destroying the normal biological activity of the protein (175). 3) Certain transition metals may participate in catalytic reactions, known as Fenton-type reactions, that produce ROS (241). Collectively, these reactions place the cell in a state of oxidative stress, and increased levels of ROS damage DNA, lipids and proteins through a variety of biochemical routes (82). 4) Toxic metal species must gain entry into cells through transporters or by binding lipophilic carriers, as cell membranes are otherwise non-permeable to these compounds (77). Transporter-mediated uptake of toxic metal species might interfere with normal transport of essential substrates through competitive inhibition; furthermore, this transport process is associated with an energetic cost from the proton motive force (PMF) or ATP pool (77). 5) Recent evidence suggests that some metal oxyanions may be reduced by the oxidoreductase DsbB, which draws electrons from the bacterial transport chain through the quinone pool (32). In effect, certain toxic metal species may starve microbial cells by indirectly siphoning electrons from the respiratory chain (157). The reactions illustrated above and below the dotted line occur through normal metabolic processes and in cases of metal poisoning, respectively. The

formation of ROS that damage DNA, proteins and lipids occur in both circumstances; however, the production of ROS is enhanced during metal poisoning which may mediate additional cellular damage. (This figure has been reproduced by permission from Harrison *et al.* (2007) Nat. Rev. Microbiol. 5:928-938).

The susceptibility of microbes to toxic metal species may be linked to several metal-ion-specific physicochemical parameters; these include standard reduction potential[10] (ΔE_0), electronegativity[11], the solubility product of the metal-sulfide complex[12] (pK_{SP}), the Pearson softness index[13], electron density[14] and the covalent index[15] (177, 277) (Figure 1.4). Since the correlations are different for biofilms and planktonic cells, these trends indicate that the chemical mechanisms of toxicity may be different between the two modes of growth (277). In other words, this suggests that biofilms may reduce metal toxicity by altering their physiology to protect the sensitive chemical targets of the reactive metal species. So how is it that biofilms are less susceptible to metal toxicity than exponentially growing planktonic cell populations, and what are the biofilm cellular and biochemical factors that specifically counter the toxic effects of certain metal-ion physicochemical parameters?

1.6 Scope of this thesis

It is specifically hypothesized that, similar to the case of biofilm antibiotic susceptibility, the mechanism of multimetal resistance and tolerance in microbial biofilms is multifactorial and may be linked to the distinct physiologies of multiple cell types in biofilm populations. That is to say that no single molecular or genetic mechanism is responsible for the reduced susceptibility of biofilms to toxic metal ions, but rather that it is a combination of several factors, or components, that protect the surface-adherent population. To test this hypothesis, this thesis research was carried out according to a list of specific goals (Section 1.6.1). By integrating reports available in the

---

[10] Standard reduction potential (ΔE_0) is the tendency of a chemical species to acquire electrons from a standard hydrogen electrode at 25 °C, 1 atm, and at a concentration of 1 M (measured in Volts, V).
[11] Electronegativity (χ) is the ability of an atom, as part of a molecule, to attract electrons towards itself.
[12] In a biological context, the solubility product of the metal-sulfide complex (pK_{SP}) is the measure of a metal ion's affinity for sulfur.
[13] A scale based on the theory of hard and soft acids and bases. From the viewpoint of biological donor sites, hard ions prefer to bind O or N, soft ions prefer S and borderline ions will bind to O, N or S.
[14] Electron density is the probability of an electron being present in a specific location in an atom or molecule.
[15] The covalent index reflects the ability of an atom to participate in covalent as opposed to ionic bonds.

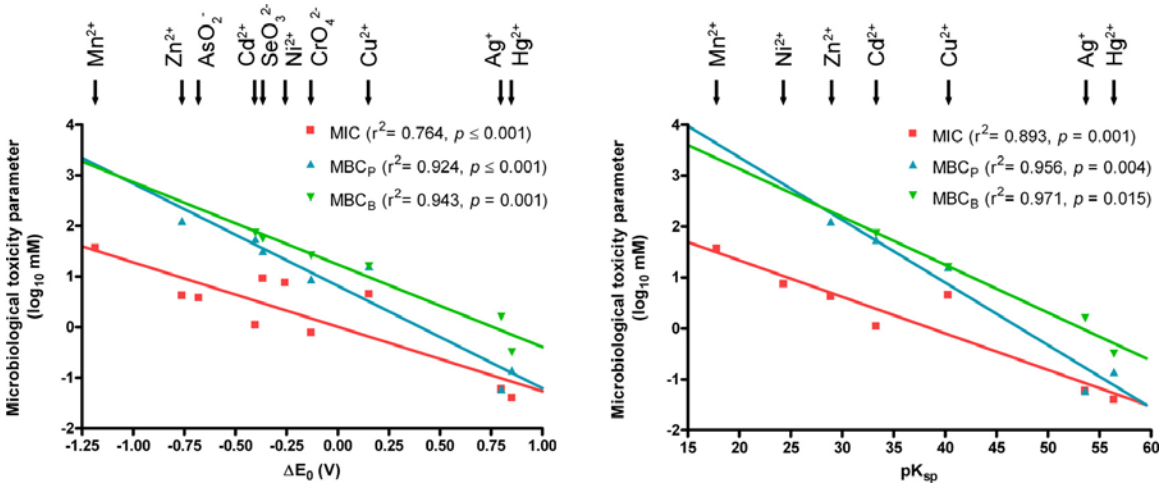

Figure 1.4. Correlation of metal-ion physicochemistry to planktonic-cell and biofilm susceptibility. Nies (177) was the first to describe that bacterial metal cation minimum inhibitory concentration (MIC) values are correlated with solubility constants of the corresponding metal–sulphide complexes (pK_{SP}). A similar correlation may be made for other ion-specific physicochemical parameters as well as for minimum bactericidal concentrations for planktonic-cells (MBC_p) and biofilms (MBC_b) (277). Here, I have taken previously published *Escherichia coli* JM109 biofilm and planktonic-cell susceptibility data (from two-hour exposures using the Calgary Biofilm Device, which was data generated during this thesis research) (97, 104) and plotted these values against standard reduction potential (ΔE_0) (A) and pK_{SP} (B). An important trend that emerges from linear-regression analysis is the increased slope and decreased y-intercept values of MIC and MBC_p values relative to MBC_b values; in other words, the line that best fits biofilm killing trends is up to 100-fold above the best-fit line that describes planktonic-cell growth inhibition and survival. This implies that biofilms have a capacity to protect the cellular targets of metal-ion toxicity, in this case shielding cells from redox reactions involved in planktonic-cell killing. (This figure has been reproduced by permission from Harrison *et al.* (2007) Nature Reviews Microbiology 5:928-938).

scientific literature with the data collected during this thesis research, I have assembled the known cellular and biochemical processes that may contribute to biofilm MMR and MMT into a single, qualitative, multifactorial model. These processes include metabolic heterogeneity introduced by structured population growth, extracellular signalling events that contribute to the biofilm lifestyle, metal-ion immobilization by biosorption, bioinorganic reactions of metal ions with microbial metabolites, adaptive stress responses, persister cells, and genetic rearrangements or mutations that produce variants. My assessment of the available evidence suggests that the reduced susceptibility of biofilms to toxic metals is linked to a natural process of physiological diversification that is ongoing within the biofilm population. The model that I propose in the final chapter of this thesis is a conceptual step towards understanding biofilms as a population strategy for survival during exposure to toxic stressors in a diverse range of natural, industrial and clinical settings.

1.6.1 Specific goals of this research

- To develop a high-throughput (HTP) technique for determining the susceptibility of biofilms to toxic metal species using the Calgary Biofilm Device (CBD). The aim is to develop a method that will allow for the quantitative determination of cell survival rates and killing kinetics of microbial populations exposed to metal ions (Chapter Two).
- To develop techniques for microscopy and three-dimensional visualization of microbial biofilms cultivated in the CBD (Chapter Two).
- To determine if persister cells may contribute to multimetal tolerance in *P. aeruginosa* (Chapter Three) and to test if this might be linked to chromosomal toxin-antitoxin genes in *E. coli* (Chapter Four).
- To determine if phenotypic variation is linked to multimetal resistance (or tolerance) and biofilm formation (Chapter Five).

- To compare the planktonic and biofilm susceptibility of *Candida tropicalis* and *Candida albicans* to metal toxicity and to establish links between metal exposure and cellular differentiation (Chapter Six).
- To evaluate the biochemical mechanisms of metal toxicity to bacterial cells, particularly as it pertains to redox reactions (Chapter Seven).
- To determine if cellular enzymes responsible for defence against oxidative stress might protect bacterial planktonic and biofilm populations from metal toxicity (Chapter Seven).
- To conduct a literature review to build a conceptual model of biofilm multimetal resistance and tolerance (Chapter Eight).

1.7 Contributions

1.7.1 Author's contributions to this work and personal acknowledgements

I would like to extend my gratitude to Dr. Howard Ceri and Dr. Raymond J. Turner for the privilege of a wonderful work environment in which these ideas could be developed. My additional thanks go to Matthew L. Workentine and Dr. Michael F. Hynes for providing many ideas, comments and constructive criticisms that have been incorporated into my work over the years.

1.7.2 Relevant publications

Excerpts from this Chapter have been taken from Harrison *et al*. (2005) American Scientist 93:508-515 and from Harrison *et al.* (2007) Nature Reviews Microbiology 5:928-938.

Chapter Two: The Calgary Biofilm Device (CBD) - A simple technology for high-throughput susceptibility assays and microscopy of microbial biofilms

2.1 Introduction

Determinations of the minimum inhibitory concentration (MIC) and the minimum bactericidal concentration (MBC) – which are based on the ability of an antimicrobial agent to inhibit planktonic population growth and to kill planktonic cells, respectively – are the standard assays used by microbiologists for susceptibility testing[16]. Although the decreased susceptibility of biofilms to antibiotics has been well established, when this thesis research was initiated, only a single study had shown that biofilms may withstand concentrations of toxic metal ions that are 2- to 600-times greater than the planktonic MIC[17] (250). Susceptibility comparisons of this sort have relied on the development of new methods for biofilm cultivation, which include, for example, drip-flow systems, the Center for Disease Control (CDC) biofilm reactor and the modified Robbin's device – as well as others. However, a common drawback to using these systems is the inability to produce more than a few biofilm samples at one time. Furthermore, these continuous culture systems are somewhat prone to contamination and leakage. It is likely because of these reasons that very few studies have comparatively examined biofilm susceptibility to metal ions relative to planktonic cell populations. This technological limitation is an important matter to resolve.

---

[16] The MIC is a measure of resistance and is defined as the lowest concentration of an antimicrobial required to arrest the growth of a planktonic cell population in broth growth medium. By contrast, the minimum bactericidal concentration (MBC) is a measure of tolerance. The Clinical Laboratory Standards Institute (CLSI) defines the MBC as the concentration of a bactericidal agent required to kill 99.9% (or 3 $\log_{10}$) of the cells in the bacterial population. The CLSI definition of the MBC may be inadequate for examining the antimicrobial tolerance of bacterial populations, as it is frequently the case that an antibiotic or toxic metal ion will rapidly kill >99.9% of the population and <0.1% of the bacteria will withstand the same antimicrobial at very high concentrations. This will be discussed in later chapters of this thesis in the context of persister cells.

[17] In the literature, these comparisons are frequently made between biofilm MBC values (a measure of cell death) and planktonic MIC values (a measure of growth inhibition), which undoubtedly exaggerates the differences in susceptibility between these two modes of growth. It is worth noting that there is no commonly accepted measure of biofilm resistance that directly correlates to the planktonic MIC.

A recently developed, high-throughput technology for biofilm cultivation is the Calgary Biofilm Device (CBD, commercially available as the MBEC™ assay, Innovotech Inc., Edmonton, Alberta, Canada, http://www.innovotech.ca) (40). This batch culture method of biofilm cultivation can be used for biofilm and planktonic cell susceptibility testing and may provide three internally consistent, comparative measurements from a single apparatus: 1) the planktonic MIC, 2) the minimum bactericidal concentration for planktonic cells (MBC_p), and 3) the minimum bactericidal concentration (MBC_b) for biofilms. The CBD is not prone to contamination, since it is manipulated in a laminar flow hood, and it is not prone to leakage, since it is sealed in a fashion similar to a Petri dish.

In addition to evaluations of antimicrobial susceptibility, the microscopic features of biofilm structure might also be important for understanding the physiology of these systems, particularly in response to metal ions. For example, the three-dimensional (3D) features of surface-adherent microbial communities may contribute to population heterogeneity and consequently to emergent cellular phenotypes, such as the slow and fast growing cell types arranged in metabolically stratified layers of thick *P. aeruginosa* biofilms (281), the motile and wall cell phenotypes involved in the active dispersal of biofilms (199), as well as yeast and hyphal cell morphotypes in biofilms of *Candida* spp. (101, 144). Therefore, it may be invaluable to determine biofilm susceptibility to metal toxicity while at the same time examining 3D biofilm structures. The specific aim of the research described in this chapter is to develop the CBD technology so that it can be used in such a fashion.

Here, I will detail several of the standard protocols that I have helped to develop for high-throughput antibiotic and metal susceptibility testing, scanning electron microscopy (SEM) and confocal laser scanning microscopy (CLSM) of biofilms grown in the CBD. Furthermore, I will describe a procedure for the image processing of CLSM data stacks using amira™, a virtual reality tool, to create surface and/or volume rendered 3D visualizations of biofilm microorganisms. The combination of microscopy with microbial cultivation in the CBD – an apparatus that was designed for high-throughput antimicrobial susceptibility testing – has allowed for the structure-function analysis of

biofilms under multivariate growth and exposure conditions throughout this thesis. In this chapter I will show sample data and workflow schematics that illustrate key experimental design concepts that have helped to position the CBD as a core technology to study biofilm multimetal resistance and tolerance. Note that many of the examples presented here are for illustrative purposes outside the scope of metal-microbe interactions and it is my goal that this chapter may also serve as a "How to Guide" for incoming students into the Biofilm Research Group.

2.2 Materials and methods

2.2.1 Microbial strains and culture media

Bacterial and fungal strains used in this chapter are summarized in Table 2.1. All strains were stored in Micobank™ vials at -70°C as described by the manufacturer (ProLab Diagnostics, Richmond Hill, ON, Canada). The following growth media were used to culture these microorganisms as indicated throughout this thesis: trypticase soy agar (TSA) and trypticase soy broth (TSB) (EMD Chemicals Inc., Gibbstown, NJ, USA); Miller Luria-Bertani broth (LB, EMD Chemicals Inc.) or LB that was amended with 1.5% w/v granulated agar (LBA); King's Broth (KB) that was prepared as previously described (133) or KB that was amended with 1.5% w/v agar (KBA); minimal salts vitamins glucose (MSVG) or pyruvate (MSVP) broth (250) and minimal salts dextrose (MSD) broth (96), which were also prepared as previously described. MSD plus yeast extract and casamino acids (MSD-YC) broth was prepared by enriching MSD with 2.0 g L^{-1} yeast extract and 1.0 g L^{-1} casamino acids (Sigma-Aldrich, St. Louis, MO, USA). Lastly, Roswell Park Memorial Institue (RPMI) medium 1640 with 5 mM L-glutamine (Sigma-Aldrich, Oakville, ON, Canada) supplemented with 0.165 M 3-*N*-morpholinopropanesulfonic acid (MOPS) and 2.0 g L^{-1} sodium bicarbonate (RQMB) were used to grow *Candida* spp. as indicated (pH of 7.2 ± 0.1). The incubation temperatures required for microbial cultures varied from strain to strain and are indicated in Table 1. All rinse steps were performed by using either 0.9% saline or phosphate buffered saline (PBS; pH 7.4, 8.0 g NaCl, 200 mg KCl, 1.44 g Na_2HPO_4, and 240 mg KH_2PO_4 per liter of double distilled water, ddH_2O).

Table 2.1. Bacteria and fungal strains used in Chapter Two.

Genus and species	Strain	Genotype or description	Growth Medium[1]	Temperature (°C)/Format[2]	Source
Burkholderia cenocepacia	K56-2	Environmental isolate	MSD-YC/TSA	35/S	(252)
Candida albicans	3153A	Clinical isolate	RQMB/TSA	35/S	(147)
Candida tropicalis	99916	Clinical isolate, Foothills Hospital, Calgary, AB	TSB/RQMB/TSA	35/S	(103)
Escherichia coli	CFT073	Urinary tract isolate, genome sequenced	TSB/TSA	37/S	(271)
	JM109	*endA1·recA1·gyrA96·hsdR17*($r_k^-m_k^-$)· *supE44· recA1* Δ(*lac-proAB*); F'(*traD36·proAB*$^+$·*lacI*^{q}·*lacZ·M15*)	LB(A), MSVG	35/R	(282)
	TG1	*supE·thi·hsd5·*Δ(*lac-proAB*); F'(*traD36·proAB*$^+$·*lacI*^{q}·*lacZ·M15*)	LB(A), MSD	35/R	(83)
	DSS640	TG1 derivative; Δ*tatABC*; Kn^r	LB(A), MSD	35/R	(211)
Pseudomonas aeruginosa	ATCC 15442	Standard reference strain for biocide susceptibility testing	LB(A)	35/S	ATCC
	ATCC 27853	Standard reference strain for antibiotic susceptibility testing	LB(A), MSVP	35/R	ATCC
	PA14	Clinical isolate, genome sequenced	TSB/TSA	35/S	(201)
Pseudomonas chlororaphis	PcO6	Environmental isolate	KB/KA	20/S	(200)
Pseudomonas fluorescens	ATCC 13525	Environmental isolate	LB(A)	27/S	ATCC
Staphylococcus aureus	ATCC 29213	Standard reference strain for antibiotic susceptibility testing	LB(A)	35/R	ATCC

[1]Abbreviations for growth media: KB = King's broth; KA = King's agar; LB = Luria-Bertani broth; LBA = Luria-Bertani agar; MSD = minimal salts dextrose; MSD-YC = minimal salts dextrose enriched with yeast extract and casamino acids; MSVP = minimal salts vitamins pyruvate; RQMB = RPMI supplemented with glutamine and buffered with MOPS and sodium bicarbonate; TSA = tryptic soy agar; TSB = tryptic soy broth

[2]Denotes the incubation temperature and CBD assay format used: R = rocking table for trough format; S = gyrorotary shaker for microtiter plate format

2.2.2 Biofilm cultivation using the Calgary Biofilm Device (CBD)

Bacterial biofilms were grown in the CBD as previously described by Ceri *et al*. (39, 40); this method is summarized here and this device and the initial workflow are illustrated in Figure 2.1. The lid of the CBD has 96 polystyrene pegs that point downwards, and each peg bears an overall neutral electrostatic charge and has a surface area of approximately 109 mm^2. In this work, there were two formats of the CBD that were routinely used to cultivate biofilms: the first method involved the use of a corrugated trough (the MBEC™-High Throughput assay) (40), the second utilized a microtiter plate (the MBEC™-Physiology and Genetics assay) (60). To begin, the desired bacterial or fungal strain was streaked out twice on agar, and colonies were suspended into fresh broth to match the optical density of a 1.0 McFarland standard[18]. For the bacterial strains, this corresponded to approximately 3.0×10^8 cfu mL^{-1}; for *Candida tropicalis* this was approximately 3.0×10^6 cfu mL^{-1} (as verified by viable cell counts, see below). The cultures matching the optical standard were then diluted 30-fold in the appropriate broth medium, which subsequently served as the inoculum for the CBDs.

For the first format of this assay, 22 mL of the inoculum was transferred into the trough and the peg lid was then fitted inside of this. The assembled CBD was then placed on a rocking table (Bellco Biotechnology, Vineland, NJ, USA) at ~3.5 rocks per minute in a humidified incubator. For the second method of biofilm cultivation, 150 µL of the inoculum was added to each well of a 96-well microtiter plate. The peg lid was then fitted inside of this and the assembled device was placed on a gyrorotary shaker at 75 to 150 revolutions per minute (rpm) in a humidified incubator. The cultivation method used

---

[18] The McFarland standard is used by the CLSI as a reference to adjust the turbidity of microbial suspensions so that the number of microbes will be within a given range. This can be done by mixing solutions of $BaCl_2$ and H_2SO_4 together – at specific ratios – to generate $BaSO_4$ precipitates in ddH_2O (for a McFarland 1.0, it is 0.1 ml of 1.0% $BaCl_2$ and 9.9 ml of H_2SO_4). Alternatively, commercially prepared suspensions, which contain latex particles, can be purchased from most suppliers. The McFarland standard is compared visually to a suspension of microbes in saline. If the suspension is too turbid, it can be diluted with more saline; conversely, if the suspension is not turbid enough, more bacteria can be added.

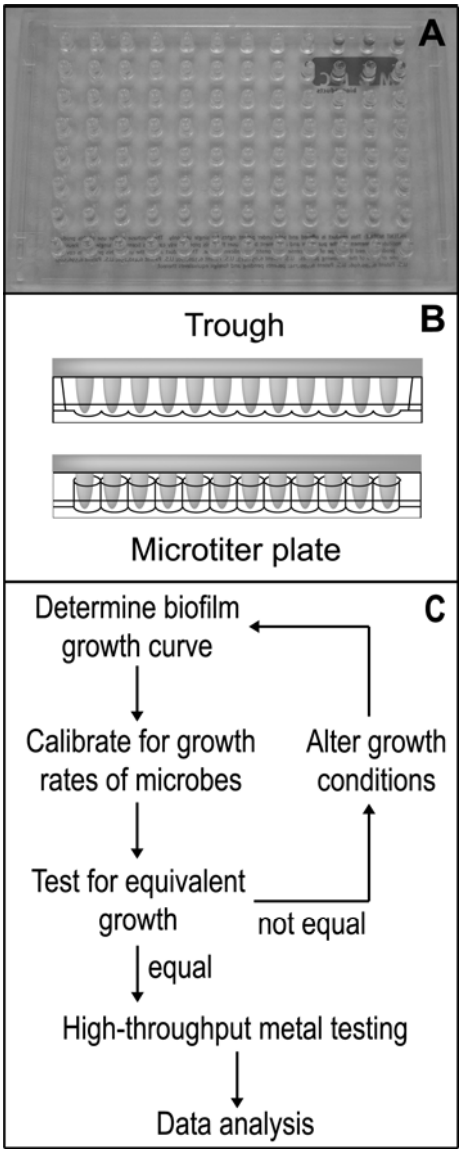

Figure 2.1. An example workflow for cultivating biofilms in the Calgary Biofilm Device (CBD). (A) A photograph of the CBD lid showing the 96 plastic pegs that (B) fit into a corrugated trough or into a 96-well microtiter plate. (C) A typical workflow for optimizing biofilm growth in the CBD might include calibrating the growth times of the organisms so to produce biofilms of similar cell density (if desired). In all cases, the biofilms are tested for equivalent cell densities, using one-way analysis of variance, with data categorically arranged by the row of pegs in the device (see section 2.3.5). If this test is passed, then it is possible to proceed with high-throughput testing, otherwise the growth conditions are modified and this optimization process is repeated.

for each bacterial or fungal strain is indicated in Table 2.1, and the method used was chosen based on which approach gave the greatest biofilm cell density, with the stipulation that the growth was statistically equivalent between the different rows of pegs (see Section 2.3.5). Following the desired period of incubation, the biofilms were rinsed by inserting the peg lids into microtiter plates with 200 μL of either 0.9% saline or PBS in each well for ~1 min.

The rounded "tip" of each CBD peg extends approximately 6 mm into the growth medium. Corresponding to this, the "air-liquid-surface interface" occurs approximately 7 mm above the tip after the inoculated device is agitated on a rocking table or gyrorotatry shaker. Typically, the greatest biofilm growth occurs at the air-liquid-surface interface of each peg, which also corresponds to the region of greatest shear force (R. J. Martinuzzi, personal communication).

2.2.3 Surface modification of the CBD

To facilitate the growth of *C. tropicalis* 99916 on the surface of the CBD, the pegs were coated with L-lysine to introduce an overall positive charge to the surface. This was accomplished by immersing the pegs into a solution of 1.0% L-lysine for 1 h, then by drying the peg lids upside down in a laminar flow hood for 30 min prior to use (103). In the case of *C. albicans*, the CBD pegs were coated with a solution of 100% w/v trichloroacetic acid (TCA), dried upside down in a laminar flow hood, and then treated with ethylene oxide gas (Anprolene®, Anderson Products Inc, Oyster Bay, NY, USA). In principle, this latter treatment may introduce an overall negative charge to the surface.

2.2.4 Viable cell counting

Viable cell counts were determined after biofilms had been rinsed (as described above). Sample pegs were broken from the lid of the CBD using a pair of flamed pliers, then inserted into 200 μL of 0.9% saline in the wells of microtiter plate (Figure 2.2 E). Biofilms were disrupted from the peg surface using an Aquasonic 250HT ultrasonic

cleaner (VWR International, Mississauga, ON, Canada) set at 60 Hz for 5 min[19]. The disrupted biofilm cells were serially diluted in either 0.9% saline or PBS, and then plated onto the appropriate agar medium. Agar plates were incubated for up to 48 h at the temperatures summarized in Table 2.1 and then enumerated. Viable cell counts for planktonic cultures (for example, the starting inoculum) were similarly determined by serial dilution in 0.9% saline or PBS, and then by plating onto agar as described for biofilm cells.

2.2.5 Tests for equivalent biofilm growth

An important control for using the CBD as a research and development tool was to test microorganisms grown in this assay system for equivalent biofilm formation across the different rows of pegs on the lid of the device. This was accomplished by growing a biofilm in the CBD as described in section 2.2.2 above. The biofilms were rinsed and then disrupted by sonciation into neutralization medium (or a physiological saline solution) and then plated for viable cell counting as described in section 2.2.4. A viable cell count was obtained for 48 of the pegs in the device; typically, this included rows A to H and columns 1 to 6. The biofilm cell density on each peg was determined by enumerating spot plates after a suitable period of incubation. These values were $\log_{10}$-transformed and arranged into columns in a spreadsheet corresponding to rows in the CBD assay. The viable cell counts were then analyzed using one-way analysis of variance (ANOVA). Highly reproducible results from this assay were attained when growth conditions were optimized to produce statistically equivalent biofilms (i.e. a *p*-value ≥ 0.05 rejects the alternative hypothesis that the mean viable cell counts for each row of pegs are non-equivalent).

---

[19] It is important to acknowledge the limitations of using sonication to recover biofilm cells for viable counting. Sonication likely recovers cohesive clumps of cells as well as single cells from surfaces. Since clumps and single cells would in principle each give 1 colony forming units (CFU), 1 CFU is directly proportional, but not equal, to the number of viable cells. Nonetheless, the CFU will be the standard measure of bacterial viability used throughout this Thesis.

2.2.6 High-throughput susceptibility testing using the CBD

2.2.6.1 Stock solutions of metal compounds

Preparations of the metal compounds used throughout this thesis research are summarized here. Sodium hydrogen arsenate (Na_2HAsO_4), silver nitrate ($AgNO_3$), aluminum sulfate ($Al_2(SO_4)_3 \bullet 18H_2O$), zinc sulfate ($ZnSO_4 \bullet 7H_2O$), stannous chloride ($SnCl_2 \bullet 2H_2O$) and copper sulfate ($CuSO_4 \bullet 5H_2O$) were obtained from Fisher Scientific Company of Fairlawn, NJ, USA. Potassium dichromate ($K_2Cr_2O_7$) was obtained from J.T. Baker Chemical of Phillipsburg, NJ, USA. Sodium arsenite ($NaAsO_2$), nickel sulfate ($NiSO_4 \bullet 6H_2O$), lead nitrate ($Pb(NO_3)_2$), mercuric chloride ($HgCl_2$), sodium selenite (Na_2SeO_3), potassium tellurite (K_2TeO_3) and sodium tungstate (10 % w/v aqueous solution Na_2WO_4) were obtained from Sigma Chemical Company of St. Louis, MO, USA. Cadmium chloride ($CdCl_2 \bullet 5/2H_2O$) was obtained from Terochem Laboratories of Edmonton, AB, Canada, selenous acid (H_2SeO_3) from The British Drug Houses Limited of Poole, England, manganous sulfate ($MnSO_4 \bullet H_2O$) from BDH Inc. of Toronto, ON, Canada, potassium tellurate (K_2TeO_4) from Johnson Mathey Electronics of Ward Hill, MA, USA and sodium molybdate (Na_2MO_4) from Matheson Coleman and Bell of Norwood, CA, USA. Reagent grade metal and metalloid salts were purchased for the purposes of these studies to minimize the potential influence of contaminating, residual metals.

All stock metal solutions, with the exception of Sn^{2+}, were made up in double-distilled water at 5 times the highest concentration desired in the challenge plates. These stock solutions were passed through a 0.22 μm syringe filter into sterile glass vials and stored at room temperature. As the exception, Sn^{2+} was disolved in 50% ethanol and stored in a sterile polypropylene tube and 10% ethanol was added to the growth controls for Sn^{2+} assays. Stock solutions of Sn^{2+}, TeO_3^{2-}, and TeO_4^{2-} were heated to 60°C to aid with dissolution of these stock metal compounds.

2.2.6.2 Biofilm metal susceptibility determinations

Susceptibility testing and exposure of biofilms to toxic metal ions is illustrated in Figure 2.2. Unless otherwise noted in this research, serial 2-fold dilutions of metal ions were prepared in flat bottom 96-well microtiter plates (NuncBrand® cell culture treated polystyrene plates, Nalge Nunc International, Rochester, NY, USA) with a final volume of 200 µL (termed the 'challenge plate'), allowing the first and last wells of each row to serve as a sterility and growth control, respectively. Unless otherwise noted, the challenge plates were incubated for the desired exposure time at the temperatures indicated in Table 2.1 and at 95% relative humidity. After exposure, the peg lid was removed and rinsed twice with 0.9% NaCl (or PBS) and the biofilm disrupted by sonciation into the appropriate recovery medium (termed the 'recovery plate', see section2.2.6.4). After removal of the peg lid, the challenge plate was covered with a new, sterile lid to protect the planktonic cultures in the challenge plate wells (see Section 2.2.6.3 for details of planktonic cell susceptibility testing).

Twenty µL aliquots of the neutralized cultures containing the recovered biofilm cells were spot plated onto the appropriate agar medium and incubated for up to 48 h to allow for maximum recovery of surviving microbes. In this high-throughput approach, MBC_b values were determined by qualitatively scoring the spot plates for bacterial growth. When possible, MBC_b values were redundantly determined by reading the OD_{650} of the recovery plates after 48 h incubation at 35 °C using a Thermomax® microtiter plate reader with Softmax Pro® data analysis software (Molecular Devices, Sunnyvale, CA, USA).

2.2.6.3 Planktonic cell susceptibility determinations

In the CBD assay system, planktonic cells shed from the surface of the biofilms serve as the inoculum for a simultaneous determination of MIC and MBC_p values. In this regard, the CBD might represent the natural duality of the bacterial ecological cycle, and as a model, this may reflect environmental conditions where the biofilm forms a recalcitrant nidus of cells that may repopulate the surroundings after an exposure to a toxic compound.

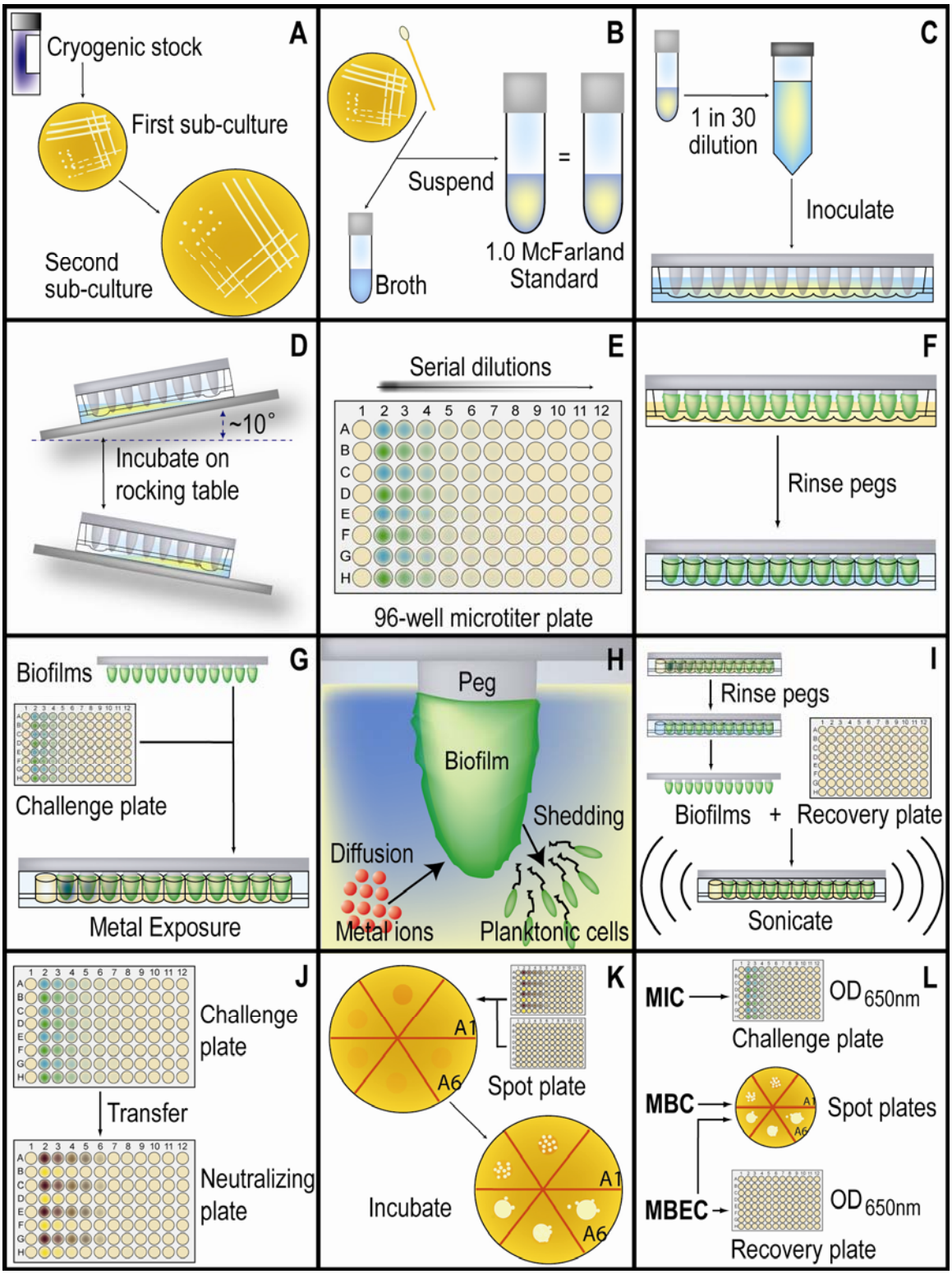
A
Cryogenic stock
First sub-culture
Second sub-culture
B
Suspend
=
Broth
1.0 McFarland Standard
C
1 in 30 dilution
Inoculate
D
~10°
Incubate on rocking table
E
Serial dilutions
1 2 3 4 5 6 7 8 9 10 11 12
A
B
C
D
E
F
G
H
96-well microtiter plate
F
Rinse pegs
G
Biofilms
Challenge plate
Metal Exposure
H
Peg
Biofilm
Shedding
Diffusion
Metal ions
Planktonic cells
I
Rinse pegs
Biofilms + Recovery plate
Sonicate
J
Challenge plate
Transfer
Neutralizing plate
K
A1
A6
Spot plate
Incubate
A1
A6
L
MIC
OD 650nm
Challenge plate
MBC
Spot plates
MBEC
OD 650nm
Recovery plate

Figure 2.2. An overview of the standard method for high-throughput metal susceptibility testing of microbial biofilms using the CBD. (A) Frozen stocks of bacteria were streaked out on the appropriate agar medium to obtain a first- and a subsequent second-subculture. (B) Colonies were collected from second-subcultures and suspended in broth medium to match a 1.0 McFarland Standard. (C) This suspension was diluted 30-fold in broth, and the 1 in 30 dilution was used to inoculate the CBD. (D) The inoculated device was placed on a rocking table in an incubator. As an alternative approach, the 1 in 30 dilution of the 1.0 McFarland Standard was used to inoculate a microtiter plate, which served as the bottom half of the CBD. This format of the device was placed on a gyrorotary shaker (see section 2.2.2 for details). (E) Serial dilutions of metal cations or oxyanions were set up along length of a microtiter plate (the challenge plate). (F) The biofilms were rinsed to remove loosely adherent planktonic bacteria. (G) The first peg from each row was removed. These pegs were used to verify growth of the biofilms on the pegs. The peg lid was then inserted into the challenge plate. (H) During exposure, metals diffused into the biofilm while planktonic cells were shed from the surface of the biofilm. Sloughed cells serve as the inoculum for MIC and MBCp determinations. (I) The exposed biofilms were rinsed twice and the peg lid was inserted into fresh recovery medium containing the appropriate neutralizing agent (the recovery plate). The biofilms were disrupted into the recovery medium by sonciation on a water table sonicator. (J) Aliquots of planktonic cultures were transferred from the challenge plate to a microtiter plate containing the appropriate neutralizing agents (the neutralizing plate). (K) An aliquot from the recovery and neutralizing plates were spotted onto rich agar media. (L) MIC values were determined by reading the optical density at 650 nm (OD650) of the challenge plate after the desired period of incubation using a microtiter plate reader. Spot plates were qualitatively scored for growth to obtain MBCp (denoted as MBC) and MBCb values (which in some instances are also denoted as MBEC values in the literature). MBCb values were redundantly determined by determining the OD650 of the recovery plates after incubation. (This figure has been reproduced from Harrison et al. (2005) BMC Microbiology 5:53).

Here, planktonic cultures from challenge plates were also treated with the appropriate neutralizing agent (see section 2.2.6.4) and 25 μL aliquots of the neutralized planktonic cultures were spot plated onto agar in a fashion similar to that described for biofilms. MBC_p values were determined by qualitatively scoring the spot plates for bacterial growth. After a suitable period of incubation, planktonic MIC values were determined by reading the optical density of the challenge plate at 650 nm (OD_{650}) using a microtiter plate reader as described in section 2.2.6.2.

2.2.6.4 Neutralizing agents and recovery medium

To differentiate between the static and cidal actions of the tested metal ions, a two-step neutralizing protocol was designed to reduce the residual toxicity of tested compounds. First, the metal ion exposed cultures were treated with a chemical known to chelate or to react with the tested compound. Second, neutralized cultures were plated onto a rich agar medium. Ideally, this latter step might facilitate additional complexation of metals with components of the medium (such as phosphates, sulfates, and amines) and might also allow diffusion of the residual metal ions into the agar. Thus, the recovered microbes were left on top of the agar medium to grow where there is a reduced concentration of biologically available toxic metal species. There are several ways to accomplish neutralization and the approach used by our research group has changed as our use of this technique has improved. A list of agents used for the purpose of neutralizing toxic metal ions appears in Table 2.2 and the rationale for using these particular agents is summarized here.

The metal oxyanions were reacted with 5 mM reduced glutathione (GSH, Sigma Chemical). GSH is used by the bacterial cell as a redox buffer to reductively eliminate a diverse array of inorganic oxidants (9, 65), including SeO_3^{2-} and TeO_3^{2-} (257, 258), and this is the basis for its use as a neutralizing agent here. Similarily, GSH was used to counter the effects of Zn^{2+}, Co^{2+}, Pb^{2+}, Hg^{2+}, and Cd^{2+} toxicity. Many metals are postulated to exert toxicity through oxidative stress on the thiol (-SH) groups of proteins and thus addition of GSH or L-cysteine may partially counteract this mechanism (100, 241). Sodium diethyldithiocarbamate (Na_2DDTC) was used to chelate Ni^{2+} and Cu^{2+},

which rapidly formed metal precipitates with this organic compound (87). Citrate was used to coordinate Ag^{+} (98) and Sn^{2+} was complexed using the amino acid glycine (66). It has been previously reported that 5-sulfosalicylic acid may be used as a chelator of Al^{3+} and Mn^{2+} (88, 98, 163); however, as an improvement to this technique, we suggest that crushed Asprin® might be used as an alternative. Salicylate derivatives can be toxic to bacteria and the less soluble acetylated form may be employed with a wider range of bacterial strains (J.J. Harrison, H. Ceri, and R.J. Turner, unpublished data).

Stock solutions of citrate (0.5 M), Na_2DDTC (0.25 M), GSH (0.25 M), acetylsalicylic acid (ASA, ~0.01 M), glycine (0.25 M), and L-cysteine (0.25 M) were prepared in ddH_2O and sterile filtered. With the exception of ASA, which was stored at room temperature, all of these stocks were stored at –20 °C until use. Neutralizing agents for biofilm cultures were added directly to the broth used in the recovery plates. Neutralizing agents for the planktonic cultures were prepared at 5 times the desired neutralizing concentration in 0.9% saline. Aliquots (10 µl) of the diluted stock solutions were then added to the wells of a sterile 96-well plate (the neutralizing plate) to which 40 µl from each well of the challenge plate were added. The final concentration of neutralizing agent used to treat the planktonic cultures was thus equal to that used to treat the recovered biofilm cells.

In later studies, the individual neutralizing agents in the recovery medium were replaced by a universal neutralizer (growth medium supplemented with 1% Tween-20, 2.0 g L^{-1} reduced glutathione, 1.0 g L^{-1} L-histidine, and 1.0 g L^{-1} L-cysteine). This latter formulation is similar to that suggested for biocide susceptibility testing by the Association of Official Analytical Chemists (AOAC) and its use is required by several American regulatory agencies to demonstrate product label claims for novel hard-surface disinfectants (Merle E. Olson, personal communication).

Table 2.2. Potential neutralizing agents for the microbiological application of inactivating toxic metal ions*

Metal species	Neutralizing agent	Recommended concentration[1]	Reference(s)
All ions	Universal neutralizer	See section 2.2.6.4	AOAC
All oxyanions	Glutathione	10 mM	(257, 258)
Al^{3+}, Mn^{2+}	Crushed acetylsalicylic acid	~ 1-2 mM[2]	(88, 163)
Hg^{2+}, Cd^{2+}	Glutathione	10 mM	(98, 209)
	L-cysteine	10 mM	(209)
Cu^{2+}, Ni^{2+}	Diethyldithiocarbamic acid[3]	~2 mM (*E. coli*) up to 5 mM (*P. aeruginosa*)	(87)
Sn^{2+}	Glycine	10 mM	(66)
Ag^{+}	Sodium citrate	10 mM	(98)
Zn^{2+}, Co^{2+}, Pb^{2+}	Glutathione	10 mM	(105)

* This is the first part of a two-part strategy to reduce the *in vitro* toxicity of metals
[1] Unless otherwise noted, this is the maximum concentration tested and employed in the high-throughput metal susceptibility testing method presented in this thesis.
[2] Application is limited by the low solubility of salicylic acid and its acetylated derivatives in water.
[3] The concentration listed is inhibitory to bacterial growth in broth culture. Recovery broth media must be spot plated onto agar to allow bacterial growth and determination of accurate MBC and MBEC values.

2.2.6.5 Stock antibiotic solutions

All antibiotics were purchased from Sigma-Aldrich unless otherwise indicated. Amikacin (ICN Biomedicals), ampicillin, cefazolin, ceftrioxone, ciprofloxacin (Bayer), gentamicin, piperacillin, and tobramycin were prepared as stock solutions in ddH_2O at 5120 μg mL^{-1}, split into 1.1 mL aliquots in Eppendorf® tubes, and stored at -70°C until used. Chloramphenicol was prepared in 50% ethanol and treated identically to the other

antibiotics. Ten percent ethanol was added to the growth controls for chloramphenicol assays.

2.2.6.6 Antibiotic and biocide susceptibility testing

Biofilm susceptibility to antibiotics and biocides was determined in a fashion identical to that described above for metal susceptibility testing with the following exceptions. Biofilms formed on the lid of the CBD were transferred to standard 96-well plates in which serial 2-fold dilutions of the antibiotics were prepared in cation-adjusted Mueller-Hinton broth (CA-MHB). Universal neutralizer was added to the recovery medium for biofilms exposed to these agents.

2.2.6.7 Quantitative determination of cell survival

For viable cell counts of biofilms or planktonic cultures after antimicrobial treatment, 50 μL of the recovery medium (containing the recovered cells) was transferred from the recovery or neutralizing plate to row A of a microtiter plate. These recovered cells were then diluted 10-fold in 0.9% NaCl (or PBS) and were plated, in 20 μL aliquots, on to appropriately labelled agar plates. These plates were incubated for a minimum of 48 hours to ensure maximum recovery of the surviving microorganisms.

To rigorously evaluate bacterial growth and survival, a series of calculations were routinely carried out. First, the sample viable cell count (VCC), mean sample viable cell count (MVCC) and sample standard deviation (SD) were determined for the dilution factor (DF) corrected, $\log_{10}$-transformed plate counts for every strain and/or antimicrobial concentration tested. These familiar statistical calculations, which are used to represent the number of cells in populations following antibiotic exposure, may be expressed by the following equations:

$$\text{VCC} = \log_{10}(\text{plate count} \times \text{DF}) \qquad (1)$$

$$\text{MVCC} = \frac{\Sigma \text{VCC}}{n} = \frac{\Sigma[\log_{10}(\text{plate count} \times \text{DF})]}{n} \qquad (2)$$

$$SD = \sqrt{\frac{\Sigma(VCC - MVCC)^2}{n}} \qquad (3)$$

where n is the number of measurements. Note that as a matter of convention, a plate count of zero will result in a value of 1, as $\log_{10}(0) = 1$. This approach has been adopted since it is not mathematically possible to plot a zero value on a logarithmic scale.

Next, the sample log-kill (LK) and mean sample log-kill (MLK) for microbial populations may be calculated from this data. This was done by subtracting each of the post-exposure VCC values from the pooled, initial mean viable cell counts ($MVCC_i$) for each strain. $MVCC_i$ calculations were based on plate counts for growth controls that were determined before exposure of populations to antimicrobials, and this calculation was carried out using equation *(2)*. This approach was used to normalize cell death calculations to the starting number of cells as well as to average out sampling error. These calculations may be represented by the general equations:

$$LK = MVCC_i - VCC \qquad (4)$$

$$MLK = \frac{\Sigma LK}{n} = \frac{\Sigma(MVCC_i - VCC)}{n} \qquad (5)$$

Note that if these calculations have been performed correctly, SD will be equal in both the cases of MVCC and MLK calculations (proof not shown). This allows for the propagation of error during subsequent calculations. Moreover, the survival dynamics reflected in MLK calculations allow the dose-dependent action of the antimicrobial to be categorized in the following ways: if during an antibiotic exposure the $MLK < 0$, then the population was resistant and the antimicrobial agent was ineffective; if $MLK \approx 0$, then the population size did not change and therefore the antimicrobial concentration was inhibitory; if $MLK > 0$, then cell death has occurred and the antimicrobial concentration was bactericidal.

I will also introduce the concept of relative log-kill (RLK). Here, calculations for the wild-type and mutant strains will be denoted by the subscripts $_{wt}$ and $_{\Delta}$, respectively (for example, SD_{wt} and SD_{Δ}). The mean relative log-kill (MRLK) calculation was used to mathematically compare survival in mutant populations relative to the average killing of wild-type populations by a single antimicrobial agent (this concept is first applied in Chapter 7 for examining a bank of *E. coli* thiol-redox mutants). This may be expressed as:

$$RLK = MLK_{wt} - LK_{\Delta} \qquad (6)$$

$$MRLK = \frac{\Sigma RLK}{n} = \frac{\Sigma(MLK_{wt} - LK_{\Delta})}{n} \qquad (7)$$

Measurements with viable cell counting inherently have high variance; moreover, susceptibility testing with the CBD generally has greater variance than broth microdilution methods used for testing planktonic cells (107). Although this will not be discussed in detail here, I have previously used an experimental approach to define thresholds for significance for to compare wild type *E. coli* K12 BW25113 (which is Δ*lacZ*) to its isogenic mutants. Here, a strain of *E. coli* K12 BW25113 – which had a deletion mutation in *lacA* – was tested side-by-side with its parental strain and exposed to cefazolin, rifampicin, deoxycycline and tobramycin (J. J. Harrison, C. Vacchi-Suzzi and H. Ceri, unpublished data). Since *E. coli* K12 BW25113 is Δ*lacZ*, it was reasonable to expect that the Δ*lacA* strain should have the same susceptibility as its isogenic parent. The cut-offs, which are defined below, were thus set so that the mathematical criteria used for analyzing the data identified no differences between the *ΔlacA* and parental Δ*lacZ* strains (data not shown).

In order for the survival in mutant populations to be considered significantly different from the wild type population, both of the following conditions must have been met: 1) there must have been at least a 50-fold difference in MRLK values for the mutant versus the wild-type populations at 1 or more tested concentration(s) of an antimicrobial

(note that $\log_{10}(50) = 1.7$) , and 2) the MLK_{wt}, plus or minus one standard deviation (SD_{wt}), must have been mutually exclusive of MLK_{Δ}, plus or minus one standard deviation (SD_{Δ}). In other words, there must have been no overlap between the SDs of the compared means. The interval (I) between the SDs may be calculated using one of the following equations; if MRLK $\leq$ -1.7, then:

$$I = (MLK_{\Delta} - SD_{\Delta}) - (MLK_{wt} + SD_{wt}) \qquad (8)$$

and, if $I \geq 0$, the inactivating mutation was deleterious to population survival under the tested exposure conditions. In contrast, if MRLK $\geq$ 1.7, then:

$$I = (MLK_{wt} - SD_{wt}) - (MLK_{\Delta} + SD_{\Delta}) \qquad (9)$$

and, if $I \geq 0$, the inactivating mutation was advantageous to population survival under the tested exposure conditions.

Several additional calculations were carried out as required during this Thesis research. To calculate percent kill, the following formula was used:

$$\%\ \text{kill} = \left(1 - \frac{(\text{plate count} \times DF)}{10^{MVCCi}}\right) \times 100 \qquad (10)$$

To calculate percent survival, the following formula was used:

$$\%\ \text{survival} = \left(\frac{(\text{plate count} \times DF)}{10^{MVCCi}}\right) \times 100 \qquad (11)$$

To calculate log percent survival, the following formula was used:

$$\log\ \%\ \text{survival} = \log_{10}(\%\ \text{survival}) \qquad (12)$$

I will also define the ratio of MBC_b:MBC_p as the 'fold tolerance' of the biofilm relative to the derived planktonic cell population. Note that when calculating this value, it is important to consider logic boundaries set by maximum (>) and minimum ranges (<) in susceptibility assays; nonetheless, in the simplest form:

$$\text{fold tolerance} = \frac{MBC_b}{MBC_p} \qquad (13)$$

The data produced from the CBD is high-throughput and there is a requirement to exclude single measurements and as well as entire assay plates that may be in error when data is analysed *en masse*. By contrast, it is also important to ensure that data within the normal range of biological variation are included. I have adhered to the following list of objective criteria when analyzing biofilm cell survival and I will suggest that these conditions must always be met when performing an analysis with CBD data:

- The microbial strain examined must have formed statistically equivalent biofilms, as averaged out by row of the CBD and tested by one-way ANOVA (at the 95% level of significance), as described in section 2.2.5.
- The initial mean viable cell count per biofilm peg, as determined from the pegs removed from the CBD before susceptibility testing, must be within 1 $\log_{10}$ CFU/peg of the pooled mean for all growth controls (for that strain) determined in this manner.
- In general, post-exposure growth controls from a single CBD must have a mean negative log-kill when the exposure times are 24 h or greater. Note that it is normal for cells to be lost from the biofilm during the process of exposure; however, these biofilm cells must recommence growth during an appropriate incubation time (the time required this varies by species and by strain).
- Single measurements where dilution or experimental errors are suspected should be excluded from the analysis; however, the remaining data from the CBD assay may be included if the other criteria are met.

- If there is interfering contamination in test spots used for verifying the microbial inoculum or any of the growth controls, the data obtained from that CBD should be discarded and the assay should be repeated.
- In the standard protocol, dilutions and spot plating are carried out on a row-by-row basis. Data from single rows of the device should be excluded when there is contamination in the sterility control (the first well) of that row.
- Since the variation in biofilm mean viable cell counts may be in excess of 1 $\log_{10}$ CFU/peg (particularly if the population is killed by an antimicrobial and low cell counts are obtained), a test for outlying measurements is not appropriate. Rather, the approach taken here has been to perform a large number of replicates so that the influence of an outlier on the mean biofilm cell count is averaged out.

An example of viable cell count and log-kill curves is illustrated in Figure 2.3.

2.2.7 Scanning electron microscopy (SEM)

Pegs were broken from the lid of the CBD using pliers and then rinsed once with 0.9% saline to disrupt loosely adherent planktonic cells. Typically, one of two approaches were used for fixing the biofilms, and these different protocols are illustrated in Figure 2.3. In the first approach, biofilms were fixed with 2.5% glutaraldehyde in 0.1 M cacodylate buffer (pH 7.2) at 4 °C for 20 hours. Following this, pegs were washed with 0.1 M cacodylate buffer and then rinsed with ddH_2O (for 10 min at each step). Subsequently, the pegs were dehydrated with 70% ethanol and then air dried for 72 h before mounting. An alternate approach was used to examine ECM production. In this case, the rinsed biofilms were fixed with 0.1 M cacodylate buffer (pH 7.2) at room temperature for 2 h, then air dried for 120 h before mounting. SEM was performed using a Hitachi model 450 scanning electron microscope as previously described (166). SEM images were contrast and brightness enhanced using Adobe® Photoshop® CS3 (Adobe Systems Inc., San Jose, CA, USA).

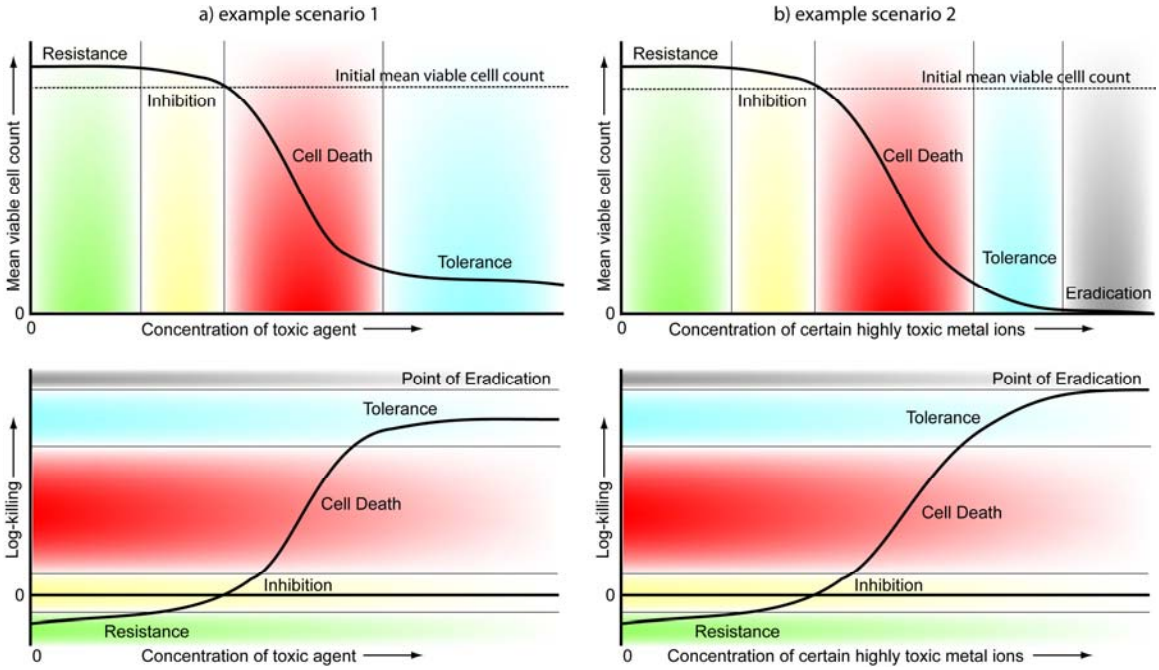

Figure 2.3. A simple guide to interpreting graphs of mean viable cell counts and log-killing of microbial populations exposed to antimicrobial agents. This figure illustrates two scenarios frequently observed in this thesis research, a) the incomplete killing of microbial populations by an antimicrobial, and b), the chemical sterilization of a microbial culture. Here, the action of antimicrobial agents – and by extension the response of microbial populations exposed to them – can be categorized in five ways (colour coded on the figure panels above). First, agents that are ineffective or that are present at non-toxic concentrations have no effect on population growth, and therefore the microbes are resistant (green). Secondly, antimicrobials present at concentrations that reduce or arrest the population growth rate are inhibitory. Thirdly, bactericidal concentrations of antimicrobial agents trigger cell death (red). Fourthly, a plateau or reduction in antimicrobial efficacy that occurs even when agent concentrations are further increased indicates that the microorganisms might be tolerant (blue). Lastly, highly toxic agents, such as certain metal ions, may act as chemical sterilizers, which eradicate the microbial population (grey). (J. J. Harrison, unpublished).

2.2.8 Confocal Laser Scanning Microscopy (CLSM)

Pegs were broken from the lid of the CBD using pliers and then rinsed once with 0.9% saline to disrupt planktonic bacteria. Prior to examination by CLSM, biofilms were fluorescently stained with one of the five following treatments (Table 2.3): 1) acridine orange (AO), 2) Syto-9 and propidium iodide (PI), 3) AO and tetramethylrhodamine isothiocyanate conjugated concanavalin A (TRITC-ConA), 4) Syto-9 and tetramethylrhodamine isothiocyanate conjugated peanut agglutinin (TRITC-PNA), or 5) Syto-9 and TRITC-ConA. The mechanism and procedure for cell staining are described here for each of these fluorescent compounds, and the general process for staining biofilms on pegs is illustrated in Figure 2.4 (I to K).

AO is a membrane permeant nucleic acid stain that intercalates dsDNA and binds to ssDNA as well as to ssRNA through dye-base stacking to give broad spectrum fluorescence when excited at 476 nm (21). This compound stains all cells in a biofilm, live or dead, and may also bind to nucleic acids that are present in the extracellular matrix. To stain biofilms, pegs were immersed in 0.1% w/v acridine orange (Sigma Chemical Co., St. Louis, MO, USA) in PBS for 5 min at room temperature.

Syto-9 and PI are packaged together as part of the Live/Dead® BacLight™ Kit for bacterial cell viability staining (Molecular Probes, Burlington, ON, Canada). Syto-9 (488 nm excitation, green emission) is a freely diffusible, nucleic acid intercalator that labels all cells in the microbial population regardless of viability. The counterstain, PI (543 nm excitation, red emission), is a membrane impermeant DNA intercalator that only stains cells with compromised membrane integrity. In principle, live cells stain green and dead cells stain orange-red. This has been shown to correlate well with viable cell counts for calibrated suspensions of many bacteria as well as for *C. albicans* (126). Here, cell viability staining of bacteria and fungi was carried out by incubating biofilms concomitantly with Syto-9 (6.7 μM) and PI (40 μM) at 30°C for 30 min as previously described by Jin *et al.* (126).

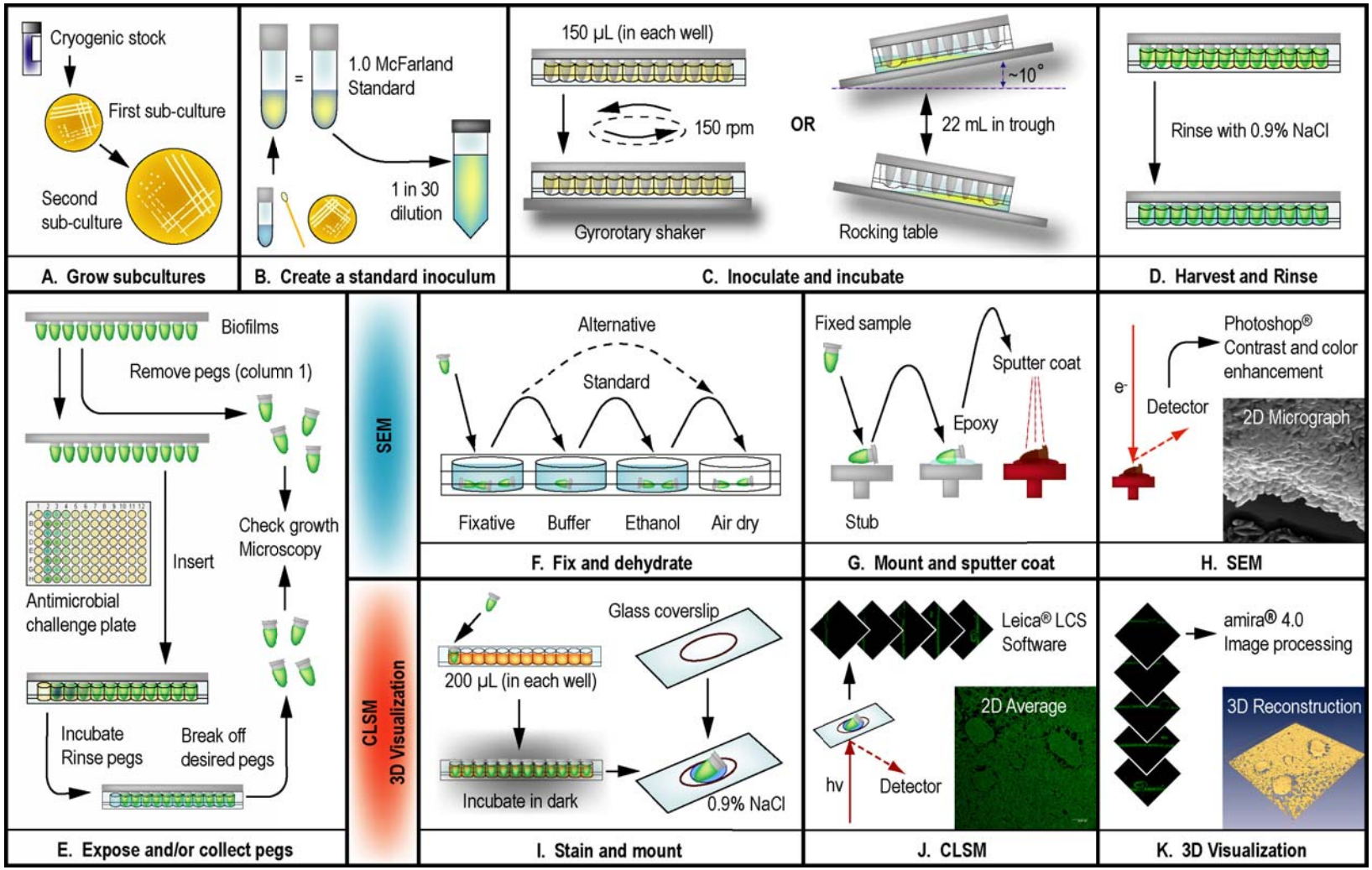
Cryogenic stock
First sub-culture
Second sub-culture
A. Grow subcultures
1.0 McFarland Standard
1 in 30 dilution
B. Create a standard inoculum
150 µL (in each well)
150 rpm
Gyrorotary shaker
OR
~10°
22 mL in trough
Rocking table
C. Inoculate and incubate
Rinse with 0.9% NaCl
D. Harvest and Rinse
Biofilms
Remove pegs (column 1)
Insert
Check growth Microscopy
Antimicrobial challenge plate
Incubate Rinse pegs
Break off desired pegs
E. Expose and/or collect pegs
SEM
Alternative
Standard
Fixative
Buffer
Ethanol
Air dry
F. Fix and dehydrate
Fixed sample
Sputter coat
Epoxy
Stub
G. Mount and sputter coat
Photoshop® Contrast and color enhancement
e-
Detector
2D Micrograph
H. SEM
CLSM 3D Visualization
Glass coverslip
200 µL (in each well)
Incubate in dark
0.9% NaCl
I. Stain and mount
Leica® LCS Software
hv
Detector
2D Average
J. CLSM
amira® 4.0 Image processing
3D Reconstruction
K. 3D Visualization

Figure 2.4. An overview for using the CBD for the purpose of microscopy and 3D visualization of microbial biofilms. (A) To begin, fresh subcultures of the microbial strain were grown on the appropriate agar medium. (B) Using a cotton swab, colonies from a fresh second subculture were suspended in broth medium to match a 1.0 McFarland standard. This was diluted 30-fold in broth to create the inoculum for the CBD. (C) The peg lid of the CBD was either inserted into a microtiter plate (containing 150 μL of inoculum in each well) or a corrugated trough (with 22 mL of inoculum inside). The inoculated devices were placed in a humidified incubator on a gyrorotary shaker or platform rocker, respectively. (D) After cultivation, biofilms were rinsed with saline to remove loosely adherent cells. (E) Pegs were removed from the CBD using pliers and the biofilms then were enumerated by viable cell counting. A second set of pegs was removed for examination by microscopy. There is an option to expose biofilms to an array of antimicrobial agents or other test conditions and then to remove a second set of pegs for microscopy. (F) For scanning electron microscopy (SEM), pegs were first fixed and then dehydrated, which was carried out using 1 of 2 protocols. (G) The fixed samples were mounted on stubs using epoxy resin, dried, and then sputter coated with gold-palladium. (H) The biofilms were then examined by SEM, and the resulting images were contrast enhanced. (I) For CLSM, pegs were immersed in the appropriate stain and then placed in 2 drops of 0.9% saline on a glass coverslip. (J) Images of the biofilms were captured using CLSM, and the instrument software was used to generate 2D averages of image z-stacks. (K) The z-stacks were imported into amira™ for advanced image processing and 3D visualization. (This figure has been reproduced from Harrison et al. (2006) Biological Procedures Online 8:194-215).

To stain the extracellular polysaccharides in the matrix of *P. aeruginosa* and *C. tropicalis* biofilms, pegs were immersed in 200 µg ml-1 TRITC-ConA (Molecular Probes) and incubated at 30°C for 90 min. ConA is a lectin with high specificity for mannose sugars present in the cell walls and biofilm matrix of *Candida* spp. (126) as well as *P. aeruginosa* (278). These pegs were subsequently treated with AO as described above. By contrast, the extracellular polysaccharide component of *B. cenocepacia* biofilms was labeled by immersing pegs in 50 µg mL^{-1} TRITC-PNA and incubating at 30 °C for 60 min. Peanut lectin specifically binds to D-galactose, which occurs three times in the heptasaccharide repeating unit that makes up the exopolysaccharide cepacian (which is specific to *Burkholderia cepacia* complex bacteria) (57). To preserve structure and extracellular biomass in the case of *B. cenocepacia*, biofilms were fixed with 5% glutaraldehyde for 1 h at room temperature prior to staining. These fixed biofilms were rinsed 5 times with 0.9% saline before mounting for microscopy.

Syto-9 was also used in some of this thesis research to stain cells in conjunction with TRITC-ConA. This may be a superior choice, as Syto-9 does not have the broad range fluorescence emission that is characteristic of AO. Syto-24 was also used as an alternative to AO or Syto-9, as this fluorophore preferentially binds to DNA over other nucleic acids, and thus, Syto-24 may be used to stain microbial chromosomes.

In all cases, fluorescently labelled biofilms were placed in two drops of 0.9% saline on the surface of a glass coverslip. These pegs were examined using a Leica DM IRE2 spectral confocal and multiphoton microscope with a Leica TCS SP2 acoustic optical beam splitter (AOBS) (Leica Microsystems, Richmond Hill, ON, Canada). To minimize or eliminate artefacts associated with single and/or simultaneous dual wavelength excitation, all dual labelled samples were sequentially scanned, frame-by-frame, first at 488 nm and then at 543 nm. Fluorescence emission was then sequentially collected in the green and red regions of the spectrum, respectively. Line averaging (×2) was used to capture images with reduced noise. A 63 × water immersion objective was used in all imaging experiments. Image capture, two-dimensional (2D) projections of z-stacks and 3D reconstructions were performed using Leica Confocal Software (LCS, Leica Microsystems).

Table 2.3. Fluorescent stains for CLSM of microbial biofilms cultivated in the CBD (as used throughout this thesis).

Stain 1[1]	Stain 2[1]	Excitiation (nm)		Collected emission (nm)		Incubation time (min)	
		λ_1	λ_2	λ_1	λ_2	Stain 1	Stain 2
AO (0.1% in PBS)	na	476	na	505 – 535	na	5	na
TRITC-ConA (200 μg ml^{-1})	AO (0.1% in PBS)	543	476	555 – 615	505 – 535	90	5
TRITC-ConA (200 μg ml^{-1})	Syto-9[b] (10.1 μM)	543	488	555 – 615	510 – 540	90	5
TRITC-ConA (200 μg ml^{-1})	Syto-24[b] (10.1 μM)	543	488	555 – 615	510 – 540	90	10
Syto-9[1] (10.1 μM)	PI[1] (60 μM)	488	543	510 – 540	610 – 670	30 (concomitant)	
TRITC-PNA (50 μg ml^{-1})	Syto-9[b] (10.1 μM)	543	488	555 – 615	510 – 540	60	5

[1]Abbreviations for fluorescent stains: AO = acridine orange; PI = propidium iodide; TRTIC-ConA = tetramethylrhodamine isothiocyanate conjugated concanavalin A; TRITC-PNA = tetramethylrhodamine isothiocyanate conjugated peanut agglutinin.
[2]Syto-9 and PI were diluted 333-fold from the stock solutions provided by the manufacturer (Molecular Probes).
na denotes an item that is not applicable.

2.2.9 Three-dimensional (3D) visualization

Three-dimensional (3D) visualization of CLSM data was created using amira™ 4.0 (Mercury Computer Systems Inc., Chelmsford, MS, USA). The principle and application of using this software to the analysis of biofilm structure are briefly summarized here. CLSM data consists of a set of two-dimensional (2D), cross-sectional images in the x-y plane that is captured along a z-axis. Collectively, a set of x-y images through the z-axis is termed a z-stack. Here, each individual x-y image was a 1024 × 1024 pixel tagged image file format (TIFF) file that corresponded to a cross-section through the biofilm. Points in 2D and 3D data sets are termed pixels and voxels, respectively. For instance, the x-y images in the z-stack are composed of pixels, whereas the same point in the 3D

volume data set is a voxel. There were two different methods used to visualize the microbial biofilms.

First, the method of surface rendering was used to create biofilm 3D visualizations; in this approach 3D surfaces were created to encase the biomass by interconnecting its boundary voxels. Therefore, biofilm visualizations created in this manner were a geometric representation of a surface (termed an isosurface) from a 3D volume data set. CLSM z-stacks were processed by re-sampling and segmenting the images according to a threshold that was selected according to a fluorescence intensity histogram of the TIFF files. In this manner, segmentation partitioned the images into background and biomass voxels and this was further user verified by manually comparing segmented biomass to its 2D original.

An alternative method was to use volume rendering, whereby biomass was a 3D visualization of the 3D volume data set, without the use of thresholding segmentation. Briefly, this method, termed ray tracing or ray casting, was based on the amount of light (in terms of colour and opacity values) that every pixel in an image was emitting and absorbing. For every pixel in the image a ray was shot into the data volume, and at a predetermined number of locations along the ray path, the colour and opacity values were obtained by interpolation, subject to a predetermined range of light intensity. In other words, every pixel displayed in the image had a colour and opacity as displayed relative to the viewing plane of the user. In comparison to surface rendering, volume rendering was computationally intense as it required more processor time and special hardware.

In both cases, 3D visualization using amira™ allowed for dynamic display of the biofilm, such that the visualization of biomass could be examined from any viewpoint. This allowed for the detection of 3D features in these biological systems that were not perceptible from static 2D CLSM image stacks or from wireframe isosurface rendering carried out using LCS. Animations produced using amira™ were edited for screen resolution using Quicktime 7.1 Pro (Apple Computers Inc., Cupertino, CA, USA).

2.2.10 Statistical tests and data analysis

Statistical tests described in this thesis, such as the Mann-Whitney U-test and one-way ANOVA of viable cell counts, were performed using MINITAB® Release 14 (Minitab Inc., State College, PA, USA) to analyze $\log_{10}$-transformed raw data. Alternate hypotheses were tested at the 95% level of confidence. All other calculations were performed using Microsoft® Excel 2003 (Microsoft Corporation, Redmond, WA, USA). Data were plotted as required using either SigmaPlot® 10.0 (SyStat Software Inc., Chicago, IL, USA) or Prism® 4.0 (GraphPad Software Inc., San Diego, CA, USA).

2.3 Proof-of-principle experiments and discussion

2.3.1 Mean biofilm cell densities in the CBD

Throughout this thesis research and as a standard practice within our research group, every time an assay has been performed using the CBD, 3 or 4 pegs have been removed from the lid and the number of cells growing on the surface has been determined by viable cell counting. I have pooled the cumulative data from all of the studies previously undertaken by myself and the rest of our research team that have specifically examined the microbial strains summarized in Table 2.1. The mean viable cell counts and standard deviations (in units of $\log_{10}$ CFU peg^{-1}) for these bacterial and fungal strains (under all of the test conditions examined in this chapter) are summarized in Table 2.4. The studies used to compile these data are indicated (where applicable), and this meta-analysis allowed the number of viable cells growing in CBD biofilms to be quantified based on 3 to 202 replicates for each strain. The rationale for this approach is that analyzing the results from a group of studies will allow for an accurate representation of the average biofilm growth and variation that can be expected in future studies.

Another routine matter in studies involving the CBD is to test that the selected assay format and growth conditions have resulted in statistically equivalent biofilm formation throughout the device. Although it is not possible to show these data for all of the strains examined here, an example of this is shown for *E. coli* TG1 and *P. aeruginosa* ATCC 27853 (Figure 2.5). To do this, the cell counts for each row were pooled and

compared using one-way ANOVA, which suggested that the cell density of biofilms grown on the different rows of pegs in the CBD assay were statistically equivalent (p = 0.274 and p = 0.842, for *E. coli* TG1 and *P. aeruginosa* ATCC 27853, respectively).

Here, it was also possible to calibrate growth times so as to generate biofilms of similar cell density, which is an important consideration for comparing the relative susceptibilities of different microbial species or different isogenic mutants of the same species. In this case, *E. coli* TG1 and *P. aeruginosa* ATCC 27853 were grown in LB broth at 35 °C for 24 and 9.5 h, respectively (Table 2.4). Under these conditions, the biofilm cell counts for these two species were statistically equivalent (as judged by a Mann-Whitney U-test, p = 0.209). This microbial growth calibration was essential for the susceptibility comparison described in section 2.3.2.

E. coli TG1 and *P. aeruginosa* ATCC 27853 biofilms were also examined *in situ* using SEM (Figure 2.5). SEM pictures showed the growth of surface-adherent bacteria in thin layers and mounds distributed heterogeneously across the surfaces of the CBD pegs. These layers were estimated to be up to 10 μm in height in some areas, although admittedly, these structures were dehydrated. A more detailed discussion of comparative SEM using the CBD is provided in section 2.3.4.

Table 2.4. Meta-analysis of mean viable cell counts for microbial biofilms grown in the CBD.

Genus and species	Strain	Growth medium[1]	Time (h)	Viable cell count (log_{10} CFU peg^{-1})	n	Reference(s)
B. cenocepacia	K56-2	MSD-YC	72	6.6 ± 0.4	4	this work
C. albicans	3153A	RPMI	48	2.9 ± 0.5	4	(106)
C. tropicalis	99916	TSB	48	4.3 ± 0.4	202	(101, 103)
			72	4.3 ± 0.3	3	this work
		RPMI	48	4.4 ± 0.3	4	(106)
E. coli	CFT073	TSB	24	5.9 ± 0.3	71	unpublished data
	JM109	LB	24	6.2 ± 0.5	119	(97, 98, 104)
		MSVG	24	5.0 ± 0.5	36	(104)
	TG1	LB	24	7.0 ± 0.3*	84	(96, 104)
		MSD	24	6.1 ± 0.6**	40	(96)
	DSS640	LB	24	6.8 ± 0.5*	80	(96)
		MSD	24	4.9 ± 0.7**	40	(96)
P. aeruginosa	ATCC 15442	TSB	24	6.8 ± 0.5	181	unpublished data
	ATCC 27853	LB	9.5	6.9 ± 0.8	55	(98, 105)
		MSVP	22	6.1 ± 0.4	133	(105), this work
	PA14	TSB	24	6.3 ± 0.2	12	(60), this work
P. chlororaphis	PcO6	KB	24	7.3 ± 0.2	4	this work
P. fluorescens	ATCC 13525	LB	24	6.0 ± 0.8	99	(277)
S. aureus	ATCC 29213	LB	24	6.2 ± 0.9	76	(98, 99)

[1] Abbreviations for growth media are the same as those listed in Table 1.
* These values are significantly different by means of a Mann-Whitney U-test ($p < 0.01$)
** These values are significantly different by means of a Mann-Whitney U-test ($p < 0.01$)

2.3.2 Comparative susceptibility of E. coli *and* P. aeruginosa *to Te oxyanions*

Since the bulk of the data presented in this thesis comes from high-throughput metal susceptibility testing, I have only included a single example in this chapter of how the CBD may be used to compare the metal susceptibility of biofilms and planktonic cells of two different microbial strains. Here, *E. coli* TG1 and *P. aeruginosa* ATCC 27853 were exposed to TeO_3^{2-} for 4 hours (a highly toxic metalloid oxyanion that is a favourite of my PhD co-supervisor, Dr. Raymond J. Turner). The means and standard deviations for TeO_3^{2-} MIC, MBC_p and MBC_b values (based on 4 to 8 independent replicates each) are listed in Table 2.5. Using this approach, it was possible to show that biofilms of *E. coli* and *P. aeruginosa* were up to 266- and 4.8-times more tolerant to TeO_3^{2-} than the corresponding planktonic cultures, respectively. Furthermore, based on planktonic MIC values, *P. aeruginosa* ATCC 27853 was 80 times more resistant to TeO_3^{2-} than *E. coli* TG1. This simple example illustrates two simple but important concepts – first, that biofilms are generally highly tolerant to toxic metal species, and second, that the innate susceptibility to metal toxicity varies greatly between microbial species.

Table 2.5. The susceptibility of biofilm and planktonic *Escherichia coli* and *Pseudomonas aeruginosa* to tellurite.

Bacterial strain	MIC (mM)	MBC_p (mM)[1]	MBC_b (mM)[1]	Fold tolerance[1]
E. coli TG1	0.02 ± 0.01	0.03 ± 0.02	> 2.0	≥133
P. aeruginosa ATCC 27853	1.6 ± 0.8	6.6 ± 3.0	> 16	≥4.8

[1] The MBC values were qualitatively determined here as the lowest concentration where there were fewer than 20 colonies per test spot on the recovery plates.

2.3.3 Comparative SEM analysis of biofilm structure

Over the years, SEM examination of biofilms cultivated in the CBD has revealed that different bacterial strains may adopt various structural conformations that are distinct from the "stalk" and "mushroom cap" biofilms formed in flow cells by *P. aeruginosa*. For instance, *P. chlororaphis* PcO6 formed thick cell layers with high cell density (Figure

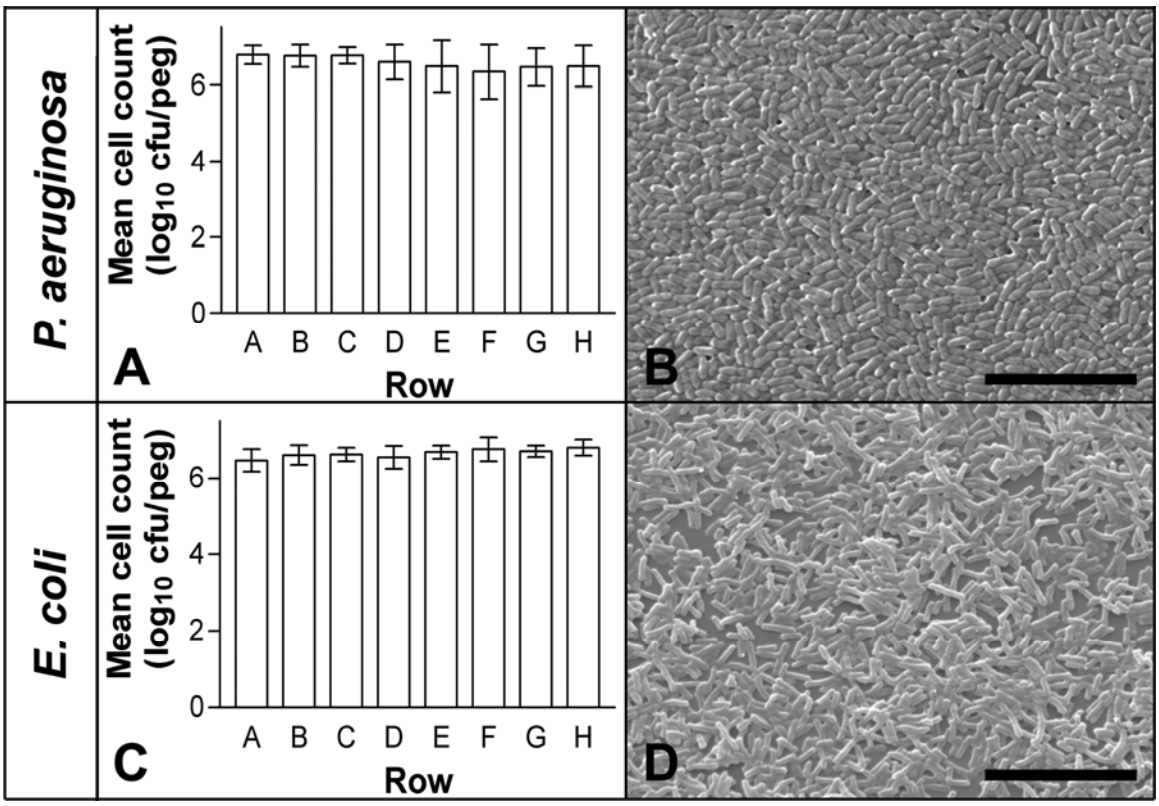

Figure 2.5. Biofilms may be grown to statistically equivalent cell densities in the CBD. (A) Mean cell densities of *Pseudomonas aeruginosa* ATCC 27853 biofilms on the pegs in different rows of the CBD. Each value is expressed as the mean and standard deviation of 4 to 6 trials. There is no significant difference between cell density of biofilms in the different rows (p = 0.842 using one-way ANOVA). (B) SEM photomicrograph of a *P. aeruginosa* biofilm on the peg surface. (C) Mean cell densities of *Escherichia coli* TG1 on the pegs in different rows of the CBD. Each value is expressed as the mean and standard deviation of 4 to 6 trials. There is no significant difference between cell density of biofilms in the different rows (p = 0.274 using one-way ANOVA). There is also no significant difference between the mean biofilm cell densities of *P. aeruginosa* and *E. coli* (as compared by a Mann-Whitney U-test, p = 0.209). (D) SEM photomicrograph of an *E. coli* biofilm on the peg surface. The bars represent 5 μm. (This figure has been reproduced from Harrison *et al*. (2005) BMC Microbiology 5:53).

2.5 A) whereas *S. aureus* ATCC 29213 adhered to the pegs in clumps of approximately 2 to 20 cells (Figure 2.6 B). In another example, *E. coli* JM109 formed uneven layers of single and multiseptate cells that were clustered into mounds (Figure 2.6 C). The formation of multiseptate cells, which were chains of cells that did not separate from one another as is normal during planktonic cell replication and division, is commonly observed for many biofilm bacteria (J. J. Harrison and H. Ceri, unpublished observations).

As researchers have begun to dissect the molecular mechanisms of biofilm formation, the concepts of "good," "poor," and "hyper-" biofilm forming bacterial strains have emerged. This is particularly relevant with regards to transposon mutants identified from strain libraries in experiments designed to identify genes important for biofilm growth. For example, wild type *P. aeruginosa* is considered a good biofilm former under many growth conditions (Table 2.4, Figure 2.6 D and G). As discussed later in this thesis, strains of this microorganism bearing inactivating mutations in the two-component regulatory system GacA/GacS have been labeled poor biofilm formers (60, 183), whereas small colony variant (SCV) strains of this microorganism have been labeled hyper-biofilm formers (134). In another example examined in this thesis work, an *E. coli* mutant lacking the twin-arginine translocase (*tat*) may be considered a poor biofilm former when compared to its wild type parental strain using comparative SEM analysis. However, this type of comparison must be carried out with care, and I will touch on this briefly here.

When grown in rich medium and examined using a standard fixing protocol, biofilms of *E. coli* TG1 (wild type) and DSS640 (*tatABC*$^-$) similarly produced surface-adherent layers of cells that had small amounts of extracellular polymers, and similarly, were thickest near the air-liquid-surface interface (Figure 2.6 E and F). The mean number of viable cells in *E. coli* DSS640 biofilms was significantly less than that of the isogenic wild type strain TG1 (Table 2.4, by means of a two-population Mann-Whitney U-test, $p < 0.001$) (96). It is important to note that this difference was not perceptible from examination by SEM (Figure 2.6). Therefore, a first caveat to comparative studies

using the techniques described in this thesis is that viable cell counts (with statistical analysis) are required to give meaning to microscopy (Table 2.4).

Another variable influencing biofilm formation in the CBD was the choice of growth medium. For instance, biofilms of *E. coli* TG1 and DSS640 had a cell density that was 8 and 79 times greater in LB than it was in MSD, respectively. To provide another cross comparison, biofilms of *E. coli* TG1 grown in MSD had a mean viable cell count that was 16 times greater than biofilms of *E. coli* DSS640 grown in MSD. This was a statistically significant difference (Table 2.5, by means of a Mann-Whitney U-test, $p < 0.001$) that was readily observable by SEM (Figure 2.6 H and I). Therefore, under conditions of nutrient restriction, *E. coli* DSS640 may be considered a poor biofilm former relative to the isogenic wild type strain. It is interesting to contrast these results to those for biofilms of *E. coli* TG1 and DSS640 grown in rich medium, which, when compared by SEM without the additional context of viable cell counts, appeared to be good biofilm formers. Nonetheless, a caveat that emerges from this data set is that growth conditions are an important consideration when evaluating biofilm formation, as a good biofilm former in a one medium may be a poor biofilm former in another.

A final feature of SEM that warrants attention is that samples must be fixed and dehydrated, which may introduce experimental artifacts that affect the interpretation of biofilm structure. This was examined here by using two different protocols for fixing biofilms of *E. coli* TG1 and DSS640 to the CBD pegs. The first (standard) protocol employed two rinse steps after incubation of biofilm pegs in a glutaraldehyde fixative, followed by ethanol dehydration (Figure 2.6 E and F). The alternative protocol required extended air drying after the incubation of pegs in a glutaraldehyde fixative, but did not utilize rinse or ethanol dehydration steps (Figure 2.6 J to L). The alternative protocol preserved biofilm extracellular polymers and revealed a tight organization of biofilm cells *in situ*. Using this latter protocol, biofilms of *E. coli* TG1 and DSS640 biofilms appeared similar to those we have previously reported for hyper-biofilm forming SCV strains of *P. aeruginosa* PA14 that had been fixed with the standard protocol (60). By comparison, the standard protocol removed much of the adherent biomass and exposed a portion of the underlying cells. In other words, the method of fixing biofilm cells to pegs

may introduce artifacts that affect the judgment concerning the capacity of a particular microbe to form biofilms. Together, these data emphasize the importance of a consistent experimental approach to create valid comparisons in SEM analysis. In this case, *E. coli* DSS640 may be considered a poor biofilm former in minimal media, a good biofilm former in rich media, or mistaken for a hyper-biofilm former when treated with an alternative fixing protocol.

2.3.4 Acridine orange staining of microbial biofilms

Although SEM has been a staple technique in biofilm research for many decades, fluorescent microscopy, particularly CLSM, is quickly replacing SEM as the technique of choice. Two principle advantages to this approach are that it is aqueous, and so samples are not dehydrated, and that images may be collected and quantified in the z-dimension. For example, in conjunction with CLSM, AO may be used as a fluorescent biofilm biomass indicator as it stains cells as well as the nucleic acids that are a normal component of the biofilm ECM (34). Here, this technique was used to illustrate the variety of structural formations that may be adopted by biofilm bacteria grown in the CBD. In the following examples, CLSM z-stacks were processed using Leica Confocal Software (LCS), which was used to generate 2D average projections as well as 3D visualizations of biofilms using an isosurface rendering algorithm. Each experiment was performed in triplicate and a representative example of each is shown here.

The first bacterium examined was *E. coli* CFT073 (a urinary tract isolate), which formed thin layers of cells across the surfaces of the CBD pegs that were 5 to 10 μm thick (Figure 2.7 A and D). Under similar growth conditions in the CBD (Table 2.1), *P. aeruginosa* PA14 formed biofilms with microcolonies that were up to 25 μm thick, particularly in the region of the air-liquid-surface interface (Figure 2.7 B and E). These microcolonies were shaped into high-cell density ridges that were interspersed by regions that contained few adherent cells. In contrast, *P. chlororaphis* PcO6 formed a flat, heterogeneous layer of cells that was 10 to 15 μm thick at the air-liquid-surface interface (Figure 2.7 C and F). It is interesting to note that biofilms of all three of these

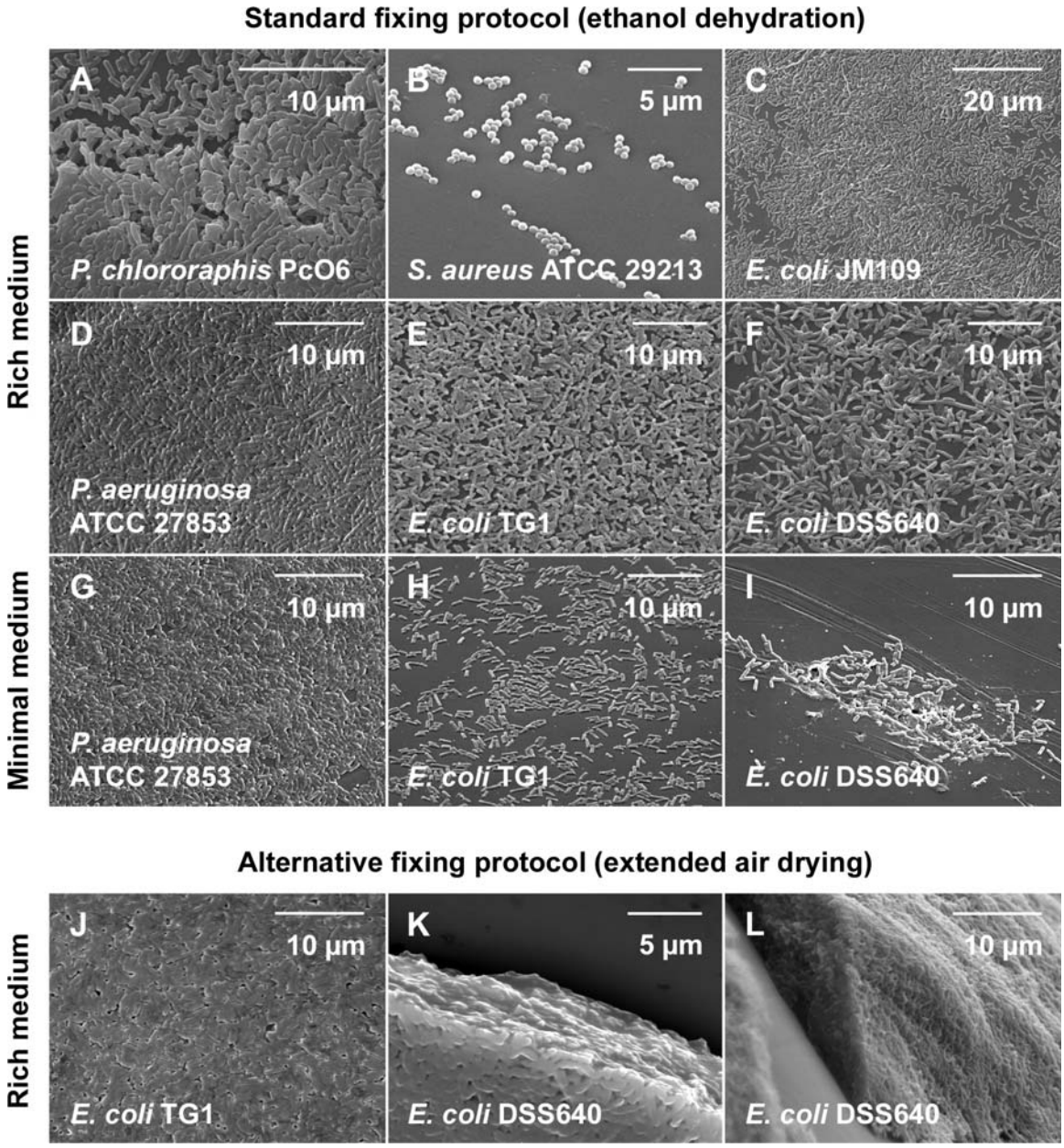

Figure 2.6. SEM of bacterial biofilms grown in the CBD. For a comparison, biofilms were grown in rich or minimal medium (as summarized in Table 2.1) and then fixed using different protocols. These micrographs illustrate that medium composition has an impact on bacterial biofilm formation, which also varies between genus, species and strains. Moreover, the choice of fixing protocols influences how well microstructures may be preserved, which impacts on interpretation of SEM data. (This figure has been reproduced from Harrison *et al*. (2006) Biological Procedures Online 8:194-215).

microorganisms were formed by growing bacteria in rich medium using the microtiter plate format of the CBD. In conjunction with the data from Figure 2.6, these AO stained biofilms illustrate an important fact – that different organisms may form different biofilm structures, even when cultivated in a similar fashion.

2.3.5 Viability staining of microbial biofilms

An important issue to address in biofilm microbiology is the contribution of dead biomass to community structure. In terms of the emergent properties of adherent populations, dead cells represent both a nutrient reservoir as well as chemically reactive biomass that together may enhance population survival during periods of starvation or antimicrobial exposure, respectively. Dead cells cannot be discerned from live cells using SEM, but may be assessed by using a variety of fluorescent stains in conjunction with CLSM. One example of this is the use of Syto-9 and PI, the components of the Live/Dead® cell viability kit, which cause live and dead cells to fluoresce green and red, respectively. Here, I have used this technique to assess the number of dead cells present in microbial biofilm populations that were cultivated in the CBD. Each experiment was performed in triplicate and a representative example of each is shown here.

Dead cells were a component of every biofilm sample examined in this research. In the cases of *E. coli* CFT073 and *C. tropicalis* 99916 grown for 24 and 48 h, respectively (Figure 2.8 A and B), the fields of view examined generally contained fewer than 20 dead cells (representing less than 1% of the population). For *P. aeruginosa* ATCC 15442, *P. fluorescens* ATCC 13525 and *P. aeruginosa* ATCC 27853 (Figure 2.8 C and D, and 2.9 C, respectively), the number of dead cells in the population was highly variable. In some instances, the number of dead cells in a field of view was less than 20; in other samples the dead cells represented an estimated 30 to 50% of the biofilm population. Similarly, dead cells represented a significant proportion of *C. tropicalis* 99916 biofilm populations incubated for extended periods of time on the gyrorotary shaker, even with medium changes (Figure 2.11, discussed below). Syto-9 and PI also stained extracellular nucleic acids and this was observed as a yellow-orange hue surrounding the microbial cells, in particular for *P. aeruginosa* biofilms (Figure 2.8 C and 2.8 A).

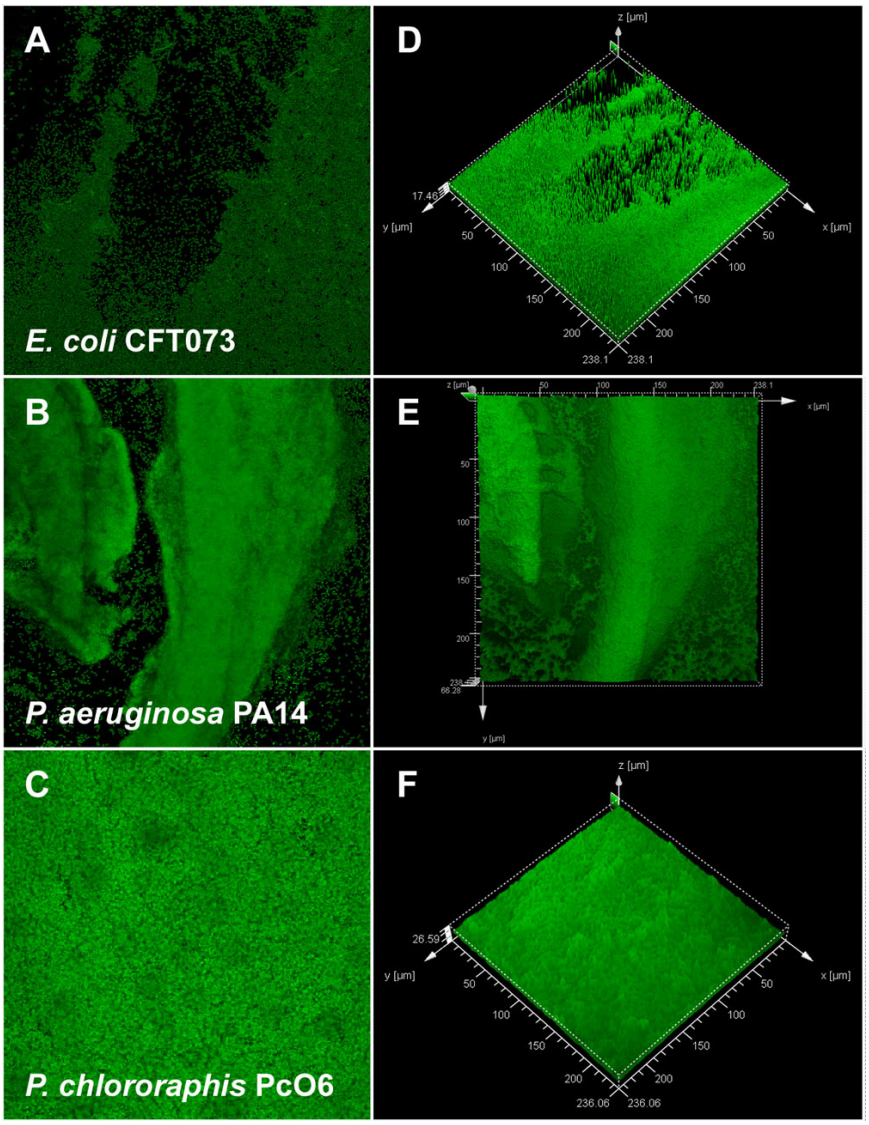

Figure 2.7. CLSM of acridine orange stained bacterial biofilms grown in the CBD. The images on the left are 2D averages of image z-stacks, whereas the images on the right are isosurface rendered 3D visualizations of the same data set (prepared using Leica® Confocal Software). These data sets illustrate that mature biofilms of different organisms that are grown under similar conditions can adopt a number of structures that are distinct from the archetypal "stalk and mushroom" microcolony structures that are well characterized for *P. aeruginosa*. Each panel represents a square surface area of approximately 238 × 238 μm. (This figure has been reproduced from Harrison *et al.* (2006) Biological Procedures Online 8:194-215).

There are many limitations to the interpretations that may be drawn from viability staining of biofilms using Syto-9 and PI; however, here I will address the limitation of sampling. A single field of view in a microscope does not represent a random sample from the entire biofilm population on the peg. Systematic collection of fields of view is a possible (but impractical) solution to quantify population survival in the CBD, which is more simply done through viable cell counting. Therefore, Live/Dead staining of CBD biofilms (as described here) is qualitative, and the discussion of semi-quantitative image analysis using this method is beyond the scope of this thesis.

Despite pragmatic limitations on sampling, this type of assay is very useful for spatial localization of dead cells in CBD biofilms following many different antimicrobial treatments (103, 126, 250). To illustrate this, biofilms of *P. aeruginosa* ATCC 27853 were grown in the CBD and then exposed to tobramycin for 24 h. From here, it was possible to quantitatively determine the concentration-dependent killing of the population by this aminoglycoside as well as to stain representative biofilms with Syto-9 and PI (Figure 2.9). Correlative to previous reports described in the literature (128), bactericidal concentrations of this drug killed biofilm cells in outer regions of the surface-adherent population while cells in the interior regions survived (Figure 2.9 D and E). This pattern of killing is consistent with the hypothesis that restricted penetration of the drug into the biofilm might contribute to aminoglycoside tolerance. However, it is equally as interesting to note that there are some surviving cells sticking to the peg surface on the exterior of these microcolonies.

Here, I must acknowledge that dead cells are also a normal component of late logarithmic and stationary phase planktonic cell suspensions cultured in the CBD (J. J. Harrison, H. Ceri and R. J. Turner, unpublished data), and thus part of this dead biomass may be incorporated into the biofilm during growth. Nonetheless, this reinforces the notion that control groups are of pivotal importance when using Syto-9 and PI to evaluate the efficacy of anti-biofilm treatments, as every growing biofilm population normally contains a portion of dead biomass.

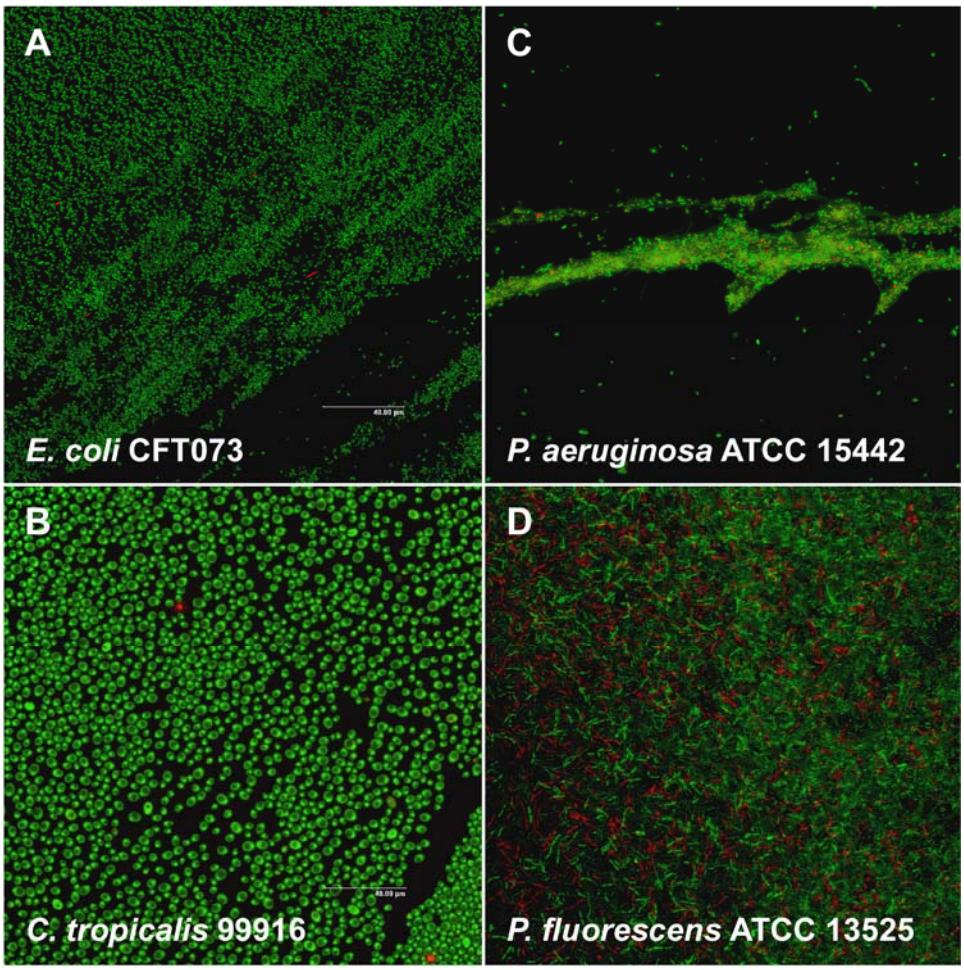

Figure 2.8. CLSM of Live/Dead® stained biofilms grown in the CBD. (A to D) Cell death is a normal part of biofilm development (the extent of which may vary) and therefore dead biomass constitutes a portion of every microbial biofilm. Each panel represents a square surface area of approximately 238 × 238 μm. These biofilms were grown for 24 h, except for *C. tropicalis* which was grown for 48 h, using the standard conditions described in Table 2.1 (This figure has been reproduced from Harrison *et al*. (2006) Biological Procedures Online 8:194-215).

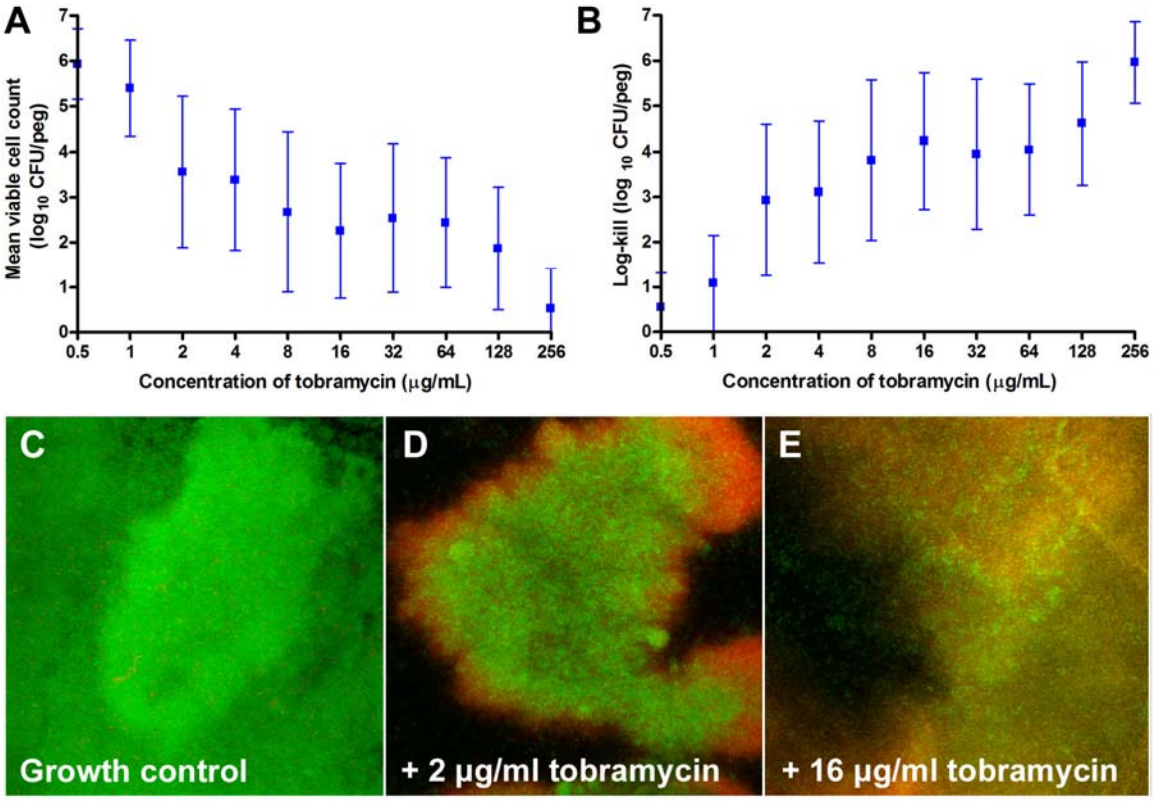

Figure 2.9. Quantitative killing and Live/Dead® staining of *P. aeruginosa* ATCC 27853 biofilms exposed to tobramycin. The Live/Dead® kit is a qualitative assay that is very useful for identifying spatial patterns in biofilm cell killing. Moreover, these killing patterns may be correlated to quantitative viable cell counts determined at the same time from these devices. (A) Killing of biofilm cells by tobramycin is concentration-dependent. (B) In general, bactericidal concentrations of this aminoglycoside kill the majority of biofilm cells at a relatively low concentration (MBC_b is 2 μg mL^{-1}); however there are a few cells (<0.1% of the starting population) that can be recovered at concentrations in excess of 256 μg mL^{-1}. The means and standard deviations here are based on 19 independent replicates each. (C to E) In this example, the positively charged aminoglycoside antibiotic tobramycin may kill cells in the outer regions of biofilm microcolonies first, while those in the interior regions are spared. Nonetheless, it is interesting to note that there are some surviving, single cells adhering to the surface on the exterior of these microcolonies. Each panel represents a square surface area of approximately 238 × 238 μm. (J. J. Harrison and H. Ceri, unpublished data).

2.3.6 Staining of biofilm extracellular polysaccharides using fluorescent lectins

A distinguishing feature of biofilms is an extracellular matrix that is composed of short and long chain oligonucleotides (274), species specific proteins (33) and polysaccharides (34), as well as the biochemical derivatives and monomeric units of these compounds (246, 278). A strategy that has been employed to visualize extracellular polymers relies upon fluorophore-conjugated lectins. Here, I used TRITC-ConA and TRITC-PNA in conjunction with AO and Syto-9, respectively, to stain the biofilm ECM and surface-attached cells of *C. tropicalis* 99916 (Figure 2.10 A to C) and *B. cenocepacia* K56-2 (Figure 2.10 D to F). Each experiment was performed in triplicate and a representative example of each is shown here.

Correlative to previous reports, ConA highlighted *C. tropicalis* 99916 cell walls and stained extracellular polysaccharides to a lesser extent (44, 103). An overlay of AO and TRITC-ConA 2D average images revealed that yeast cells were in physical contact with their neighbours, joined either by their cell walls or a thin layer of extracellular polysaccharides (Figure 2.10 A). The distribution of the extracellular biomass was also uneven, a feature that was shared in common with *P. aeruginosa* PA14 biofilms stained in a similar fashion (Figure 2.10, discussed below with regards to 3D visualization). An overlay of Syto-9 and TRITC-PNA 2D average images additionally showed that *B. cenocepacia* K56-2 biofilms were encased in a heterogeneously distributed layer of extracellular polysaccharides (Figure 2.10 D). I have also included additional examples of lectin staining in conjunction with various fluorescent nucleic acid indicators for *C. tropicalis* 99916 and *C. albicans* 3153A (Figure 2.10 G to I). Collectively, these data suggest that the production of extracellular polymers occurs non-uniformly throughout microbial biofilms.

In the case of *B. cenocepacia* K56-2, biofilms were fixed using glutaraldehyde and rinsed several times following staining with TRITC-PNA. As discussed for SEM, any method used to preserve the biofilm may affect community structure and in particular, remove components of the ECM. Based on the data presented in Figure 2.6, it is likely that ethanol dehydration of samples for SEM is for the most part responsible for the removal of the ECM. The advantage of CLSM is that the samples remain in an aqueous

environment and as such it is reasonable to expect that a larger portion of ECM is retained using this technique than with SEM.

2.3.7 3D visualization of CLSM data

Image processing and analysis methods are widely used in microbiological research to qualitatively and/or semi-quantitatively characterize microorganisms growing in biofilms. There are three open-source software packages that have been applied to the examination of multiple channel CLSM data sets from biofilms: *daime* (58), PHLIP (169), and COMSTAT (113). Here I describe the use of amira™, a professional software package for 3D visualization of volume data sets that utilizes hardware accelerated OpenGL 3D graphics with texture mapping. This software package was used to examine two additional CLSM data sets that were part of the proof-in-principle experiments described in this chapter. First, *P. aeruginosa* PA14 biofilms were examined by staining samples with AO and TRITC-ConA (Figure 2.11 A to G). This was carried out with the specific aim of visualizing the heterogeneous distribution of extracellular polymers throughout the surface-attached community. Second, *C. tropicalis* 99916 biofilms (grown for 72 h on a gyrorotary shaker) were stained with Syto-9 and PI (Figure 2.11 H to N). This visualization was performed to illustrate that dead cells were a prevalent component of these biofilm communities. With regards to biofilm cultivation in the CBD and fluorescent staining, each of these experiments was performed in triplicate and a representative example of each was visualized using computer graphics (CG), as shown in the data presented here. Furthermore, two computational methods were used to examine these biofilm CLSM data sets.

The first visualization method used was isosurface rendering, whereby biofilm biomass was illustrated as a hollow shell that corresponded to the interconnected boundary voxels of the fluorescent, 3D volume data set. This method required that CLSM z-stacks were segmented, a user refined step carried out to separate background noise from biomass voxels. The advantage of this method was fast computer time and real-time user manipulability of the models without the requirement of specialized hardware (ex. expanded computer memory and specialized graphics cards). Isosurface

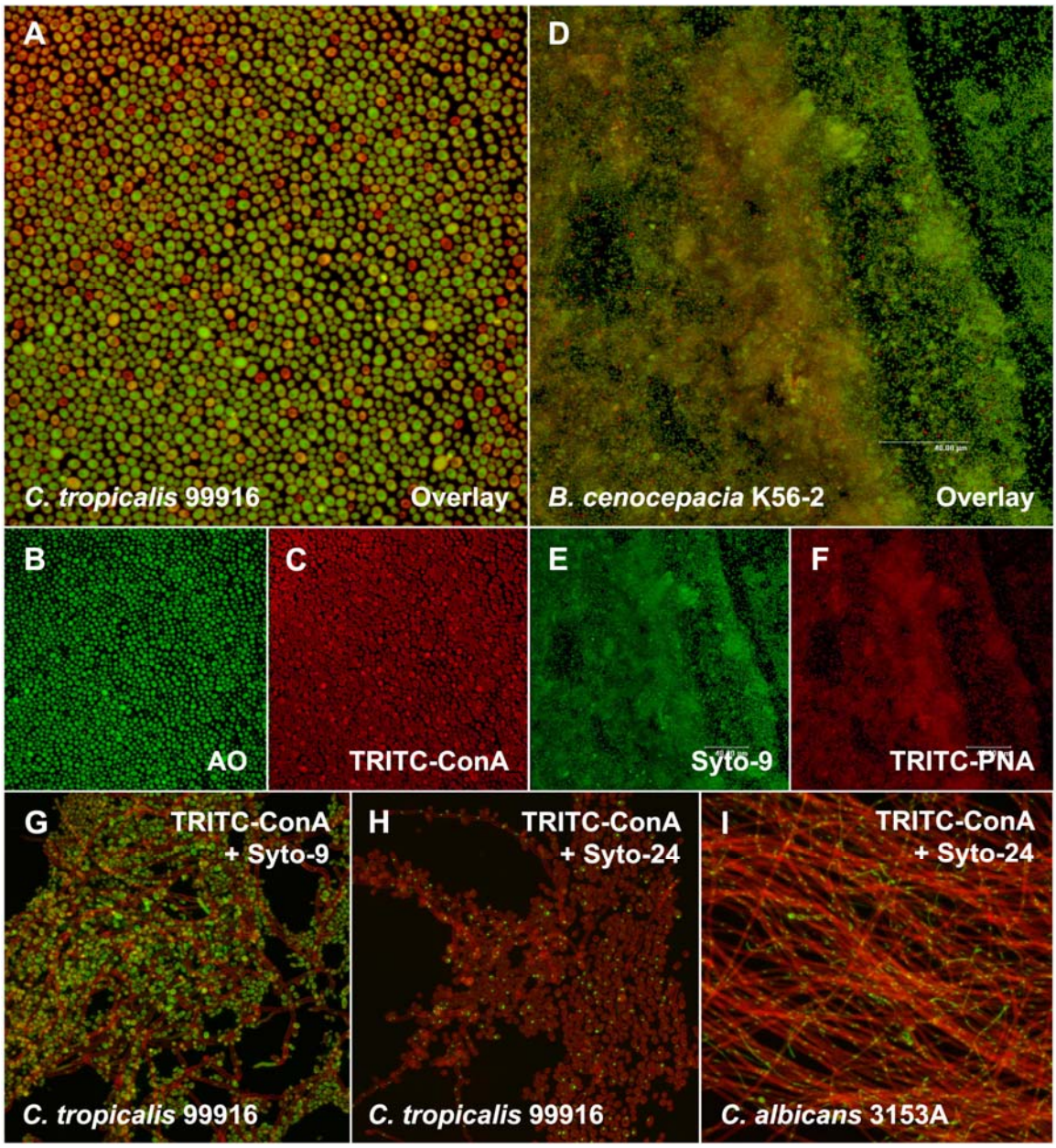

Figure 2.9 TRITC-conjugated lectin staining of biofilms grown in the CBD. (A) An overlay image of a *C. tropicalis* biofilm that was stained with (B) AO (green emission) and (C) TRITC-ConA (red emission). (D) An overlay image of a *B. cenocepacia* biofilm that was stained with (E) Syto-9 and (F) TRITC-PNA. (G to I) Biofilms of *Candida* spp. grown in RQMB and stained with TRITC-ConA and Syto-9 or Syto-24. Each panel represents a square surface area of approximately 238 × 238 μm. (This figure has been adapted from Harrison *et al*. (2006) Biological Procedures Online 8:194-215).

rendering of CLSM data for *P. aeruginosa* PA14 and *C. tropicalis* 99916 is illustrated in Figure 2.11 (panels B to D and O for *P. aeruginosa*; panels I to K and Q for *C. tropicalis*).

The second method used to visualize biofilms was volume rendering, whereby 3D visualizations were a direct representation of the 3D volume data set. This method did not require the use of image segmentation to separate noise from the emitted fluorescence signals, thereby reducing user manipulation of the CLSM data sets. This method required greater processor time as well as hardware acceleration. Volume rendering of CLSM data for *P. aeruginosa* PA14 and *C. tropicalis* 99916 is illustrated in Figure 2.11 (panels E to G and P for *P. aerugionsa*; panels L to N and R for *C. tropicalis*).

In summary, 3D visualization was used to dynamically illustrate 3D volume data sets from CLSM of biofilms cultivated in the CBD. With regards to the underlying biology of microbial biofilms, these data illustrated two important points that were the focus of the proof-in-principle experiments carried out here. First, biofilms cultivated in the CBD displayed heterogeneity in the production of extracellular polysaccharides. Second, CBD biofilms contained a significant proportion of dead cells amongst the population. In this example, *C. tropicalis* 99916 biofilms grown for 72 h had a number of viable cells equivalent to those cultivated for 48 h (Table 2.4). However, the aged biofilms were thicker, contained multiple cell morphotypes, had a much greater proportion of dead cells in the population.

2.4 Summary

In this chapter I have described the Calgary Biofilm Device (CBD) and how it may be applied to the cultivation, high-throughput susceptibility testing and microscopy of microbial biofilms. My work with this assay has allowed for the combinatorial experiments of growth media, metal ions, antibiotics, exposure times, microbial species and isogenic strains that have helped to elucidate many components of the multifactorial model of multimetal resistance and tolerance summarized in the final chapter of this thesis. The salient features and considerations for using this device as a research tool are briefly summarized here.

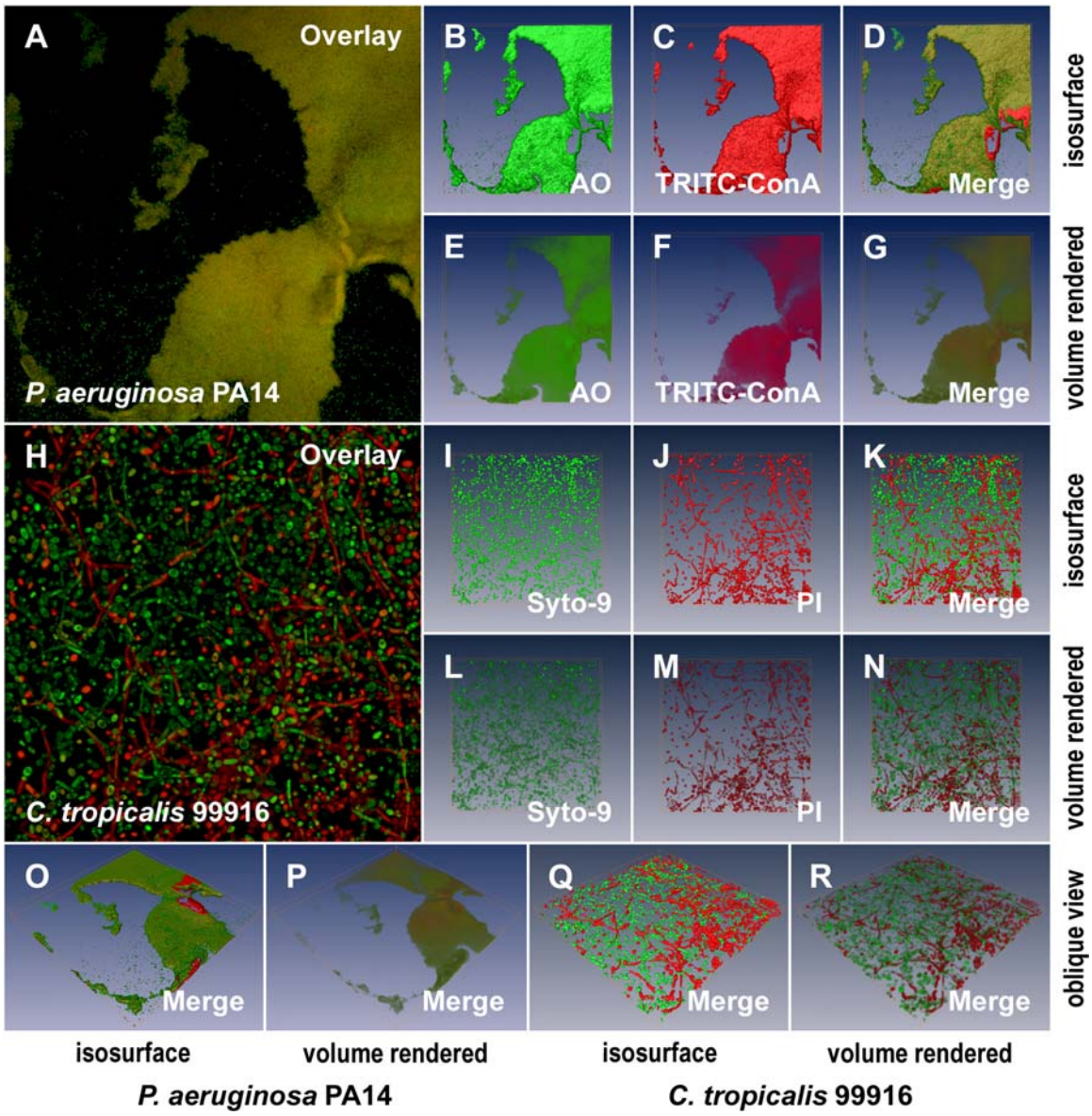

Figure 2.11. 3D visualization of microbial biofilms using amira®. A. A 2D average of an image z-stack for a *P. aeruginosa* PA14 biofilm stained with AO and TRITC-ConA. B and C. Isosurface rendering of the 3D volume data sets for AO and TRITC-ConA, respectively, extrapolated from the image z-stacks used to create the image in panel A. D. The merged, isosurface rendered 3D volume data set for AO and TRITC-ConA. E to G. Volume rendering corresponding to the data sets presented in panels B to D. H. A 2D average of an image z-stack for a *C. tropicalis* 99916 biofilm stained with the Live/Dead® cell viability kit. I and J. Isosurface rendering of the 3D volume data

sets for Syto-9 and PI respectively, extrapolated from the image z-stacks used to create the image in panel H. K. The merged, isosurface rendered 3D volume data set for Syto-9 and PI. L to M. Volume rendering corresponding to the data sets presented in panels I to K. O and P. The oblique view of the *P. aeruginosa* PA14 biofilm pictured in panel A visualized using isosurface and volume rendering, respectively. Q and R. The oblique view of the *C. tropicalis* 99916 biofilm pictured in panel H visualized using isosurface and volume rendering, respectively. Each 2D image panel or 3D model represents a square surface area of approximately 238 × 238 μm. (This figure has been reproduced from Harrison *et al*. (2006) Biological Procedures Online 8:194-215).

1. Successful cultivation of biofilms of different fungal and bacterial microorganisms in the CBD may require an iterative process of optimization that involves testing growth media formulations or polystyrene surface modifications.
2. Biofilm growth must be tested for equivalence in the device and differences between the mean biofilm cell densities in each row of the CBD must be non-significant.
3. High-throughput biofilm susceptibility data may be qualitatively or quantitatively determined depending on the application.
4. An objective set of criteria must be universally applied to analyze the high-throughput susceptibility data, which includes a clear definition of end-points (discussed later in this thesis).
5. The CBD is amenable to several different microscopy techniques and is not limited to those described in this chapter.
6. When performing comparative microscopy it is important to correlate pictures to quantitative growth data. It is also important to consider that biofilm structure is dependent on nutrient status and that biomass is distributed heterogeneously on the peg surfaces. Therefore, microscopy must be performed in a systematic and consistent way.
7. CLSM image stacks of biofilms may be further analyzed using specialized computer algorithms in a way that may reveal features that are otherwise not possible to see using the software included with the microscope.
8. It is possible to correlate killing patterns in microbial biofilm populations to quantitative survival data.

2.5 Contributions

2.5.1 Author's contributions to this work and personal acknowledgements

I helped to design and troubleshoot the protocols described in this chapter, and in the process, performed the vast majority (>85%) of the bench work described here. Expert technical assistance and invaluable input were provided by Carol A. Stremick, a senior laboratory technician in Dr. Howard Ceri's lab. Electron microscopy was performed by Liz Middlemiss, a technician employed by Innovotech Inc. The protocol

for three-dimensional (3D) visualization of biofilm confocal microscopy image stacks was developed in collaboration with Jerome Yerly, Dr. Yaoping Hu, and Dr. Robert J. Martinuzzi from the Schulich School of Engineering, University of Calgary.

2.5.2 Relevant publications

I wrote the protocols described in this chapter for Innovotech Inc., the company that manufactures and distributes the CBD, as part of my obligations for sponsorship of a NSERC Industrial Postgraduate Scholarship (2004-2006). I also wrote the instruction booklets that are shipped with every CBD sold by the company, and these are available on the Innovotech Inc. website (http://www.innovotech.ca/products_instructions.php). These protocols were originally published in Harrison *et al*. (2004) Environmental Microbiology 6:1220-1227, Harrison *et al*. (2005) BMC Microbiology 5:53, and Harrison *et al*. (2006) Biological Procedures Online 8:194-215.

Chapter Three: Persister cells, biosorption and the killing of *Pseudomonas aeruginosa* biofilm populations by toxic metal ions

3.1 Introduction

Bacteria have developed a diverse array of strategies – which are enabled by both chromosomal and mobile genetic determinants – to counter the deleterious effects of toxic metal species. These strategies may include, reduction or modification of the metal ion to a less toxic form, sequestration or chelation of the metal ion, efflux or reduced uptake, and increased expression of cellular repair machinery (178, 225, 256). In addition to these mechanisms of metal resistance, it has been identified that biofilms may be intrinsically less susceptible to metal toxicity than planktonic cells (250).

As summarized in Chapter One, it has been well documented that biofilm bacteria are 10- to 1000-fold less susceptible to killing by antibiotics relative to planktonic cells of the same organism (80, 92, 151, 152, 236). Similarly, Teitzel and Parsek (250) reported that with short (5 h) exposure times, biofilms of the soil bacterium and opportunistic pathogen *Pseudomonas aeruginosa* are 2- to 600-fold less susceptible to killing by cationic metal species of Cu, Zn, and Pb. In contrast to these results, I have previously found that with longer (24 h) exposure times, biofilm and planktonic cells of *Escherichia coli* and *Staphylococcus aureus* may be equally susceptible to eradication by these toxic metal species as well as by other cations and oxyanions (98). Why might this be?

Although my earlier results were apparently contradictory to the established model of biofilm susceptibility to antimicrobials, it may be possible to reconcile these different outcomes if biofilm multimetal tolerance (MMT) were correlated to the existence of persister cells in bacterial populations. Persister cells are metabolically quiescent cells that, with respect to time and antibiotic concentration, characteristically give rise to biphasic cell survival following exposure of bacterial populations to microbicidal drugs (see Chapter One for a review of this subject). Therefore, the aim of the research in this Chapter was to establish time- and concentration-dependent killing kinetics for biofilm and planktonic *P. aeruginosa* by different toxic metal species, with a particular focus on environmentally relevant toxic metal cations.

To begin, 17 metal cations and oxyanions, chosen to represent groups VIB to VIA of the periodic table, were each tested on biofilms and planktonic cultures *P. aeruginosa* ATCC 27853. Similar to *E. coli* and *S. aureus*, biofilms of *P. aeruginosa* had a level of metal tolerance that was comparable to that of planktonic populations when the MIC, MBC_p and MBC_b values were qualitatively measured at 24 h of exposure. From this, the time- and concentration-dependent killing of biofilms by a subset of six metals – Co, Ni, Cu, Zn, Al, and Pb – were characterized in further detail. These six representative metals are commonly released into the environment in industrial emissions and each of these metals has been surveyed as part of environmental impact reports (62, 112). As example levels of pollutants, Zn and Cu have been reported at concentrations of 3.4 mM and 1.7 mM in the Tinto River, Spain, originating from acid mine drainage run-off (159). Al has been measured at 94 μmol per gram of soil in the industrially impacted spruce zones of the Ukranian Carpathian forests (219). In these polluted areas, metal cations may be at concentrations comparable to the bactericidal concentrations at the lower end of the concentration gradients examined *in vitro* during this work.

Here, each of these six metals was tested at 2, 4, 6, 8, 10, 24 and/or 27 h exposure times in either rich or minimal media. With exposure times of less than 4 h, biofilms were observed to be 2- to >16-times more tolerant to toxic metal cations than the corresponding planktonic cell cultures. However, with exposure times of around 1 day, biofilm and planktonic bacteria were eradicated at approximately the same concentration in many instances. Viable cell counts revealed that at higher concentrations, many of the metal cations had killed greater than 99.9% of biofilm and planktonic cell populations. The survival of less than 0.1% of the bacterial population corresponds well with the hypothesis that a small population of persister cells may be partly responsible for the observed tolerance of both planktonic cells and biofilms to high concentrations of metals.

In addition to this cellular mechanism of tolerance, I show that metal cations may be adsorbed by biofilm biomass. Here, it was possible to use a chelator to cause visible precipitates to form in biofilms exposed to Cu^{2+} and Ni^{2+}. This process of biosorption may also contribute to biofilm multimetal tolerance. However, it is important to note that the proportion of bacterial cells killed by toxic metal cations reached a plateau at any

given exposure time and further increases in metal ion concentrations did not eliminate this phenomenon. Collectively, this suggests that both persister cells and the restricted diffusion of metal cations into the surface-adherent population may be components of biofilm multimetal tolerance.

3.2 Materials and methods

3.2.1 Standard Protocols

P. aeruginosa ATCC 27853 was stored, handled and cultured as described in Chapter Two. Biofilms were cultivated by growing this microorganism at 35 °C in the trough format of the Calgary Biofilm Device (CBD) for either 9.5 or 22 h in LB or MSVP medium, respectively. In addition to this method of biofilm cultivation, antibiotic and metal susceptibility testing as well as scanning electron microscopy (SEM) were carried out according to the standard protocols described in Chapter Two.

3.2.2 Precipitation of adsorbed Cu and Ni with sodium diethyldithiocarbamate

Sodium diethyldithiocarbamate (Na_2DDTC) has historically been used as an analytical reagent for determining the concentration of transition metals, As and Te in aqueous solutions and in biological fluids (48, 260). *P. aeruginosa* biofilms formed on pegs of the CBD device in MSVP media were exposed to Cu^{2+} or Ni^{2+} for 24 h. The exposed biofilms were then rinsed twice for 5 min in 0.9% NaCl. The rinsed peg lids were inserted into 96-well microtiter plates containing 200 μL of 5 mM Na_2DDTC in each well. Biofilms were treated with Na_2DDTC for ~1 min then photographed using a Sony 4.0 megapixel Cyber-shot digital camera.

3.2.3 Calculations and definitions of measurements

Calculations of mean viable cell counts, mean log-kill measurements and fold-tolerance were performed according to the guidelines set in Chapter Two. Here, it is important to explicitly define the endpoints used to measure antimicrobial susceptibility in this Chapter. The minimum inhibitory concentration (MIC) was defined as the lowest

dilution of an antimicrobial required to slow the growth of the microorganism such that there was no visible change in turbidity of the growth medium after 24 h ($MIC_{24\ h}$) or after 72 h incubation ($MIC_{72\ h}$). The guidelines of the American Clinical Laboratory Standards Institute (CLSI, formerly the National Committee for Clinical Laboratory Standards) define the minimum bactericidal concentration (MBC) as the minimum concentration of an antimicrobial agent that is required to kill 99.9% (or 3 $\log_{10}$) cells of a bacterial population. Here, this will be denoted as the $MBC_{p\text{-}99.9}$ and $MBC_{b\text{-}99.9}$ for planktonic and biofilm bacterial populations, respectively. However, this definition is inadequate for examining the survival of less than 0.1% of the bacterial population. In this research, I will define the $MBC_{p\text{-}100}$ and $MBC_{b\text{-}100}$ as the concentrations of antibiotics or toxic metal ions required to kill 100% of the planktonic and biofilm bacterial populations, respectively. As such, $MBC_{99.9}$ and MBC_{100} measurements are based on quantitative survival data obtained through viable cell counting. In addition to this, qualitative determinations of MBC endpoints, based on the high-throughput method of biofilm testing illustrated in Figure 2.2, will be denoted as $MBC_{p\text{-}q}$ and $MBC_{b\text{-}q}$ for planktonic and biofilm populations, respectively. In this case, $MBC_{p\text{-}q}$ and $MBC_{b\text{-}q}$ endpoints will be defined as the lowest concentration of an antimicrobial that resulted in ≤20 colonies per 20 μL test spot on an agar plate. I will use the term 'killing' to denote the death of any portion of the bacterial population of less than 100% and the term 'eradication' will be used to denote sterilization (i.e. 100% destruction of the bacterial population and thus no recoverable viable cells from a susceptibility assay).

3.3 Results

3.3.1 Biofilm formation by P. aeruginosa ATCC 27853 in the CBD

As indicated in Table 2.1, *P. aeruginosa* ATCC 27853 formed biofilms with a mean cell density of 6.9 ± 0.8 and 6.4 ± 0.4 $\log_{10}$ CFU peg^{-1} when grown for 9.5 and 22 h in LB and MSVP, respectively. These biofilms were statistically equivalent across the different rows of pegs in the CBD (Figure 2.5 as well as data not shown). SEM revealed that biofilms grown in LB formed a bacterial layer several cell widths in thickness on the surface of the pegs (Figure 3.1 A and B). By contrast, biofilms grown in MSVP covered

the surface of the peg in heterogeneously distributed lumps and mounds (Figure 3.1 C and D). This microscopy indicates that *P. aeruginosa* forms viable biofilms on the surfaces of the CBD pegs and that the biomass is not simply adherent single-celled organisms.

3.3.2 Susceptibility of P. aeruginosa to antibiotics

As a quality control for this experimental system, I examined the susceptibility of *P. aeruginosa* ATCC 27853 biofilms and planktonic populations to the antibiotics gentamicin (an aminoglycoside) and ciprofloxacin (a fluoroquinolone) in LB medium. Ciprofloxacin is known to rapidly penetrate through *P. aeruginosa* biofilms (5, 223). On the other hand, gentamicin is an antibiotic that does not readily diffuse across the biofilm extracellular matrix (ECM) (223). The median values and ranges of $MIC_{24\ h}$, $MBC_{p\text{-}100}$ and $MBC_{b\text{-}100}$ measurements for *P. aeruginosa* ATCC 27853 to these antibiotics at 2 and 20 h of exposure in LB medium are reported in Table 3.1 (3 or 4 replicates each). While ciprofloxacin efficaciously eradicated planktonic cells by 2 h of exposure, 20 h of exposure to gentamicin was required to eradicate planktonic cultures. By contrast, neither gentamicin nor ciprofloxacin eradicated biofilms of *P. aeruginosa* at the highest concentrations of antibiotics assayed (regardless of exposure time). It is also interesting that the fold tolerance of biofilms exposed to ciprofloxacin increased marginally with time. For example, given the time-dependent killing of planktonic cells, the observed fold tolerance of $\geq$16 at 2 h of exposure to ciprofloxacin was slightly lower than the fold tolerance of $\geq$32 at 20 h. A similar trend was observed for gentamicin and these observations correlated well to previous reports of biofilm antibiotic susceptibility (35, 40, 180, 230). A logical next step towards validating this system was to evaluate the number of surviving cells in the biofilm and planktonic bacterial populations.

3.3.3 Cell survival in planktonic and biofilm populations exposed to antibiotics

Viable cell counts were determined for a range of antibiotic concentrations following either 2 or 20 h of exposure in LB. Figure 3.2 summarizes the mean viable cell counts and log-killing data of biofilm and planktonic cells with respect to concentration

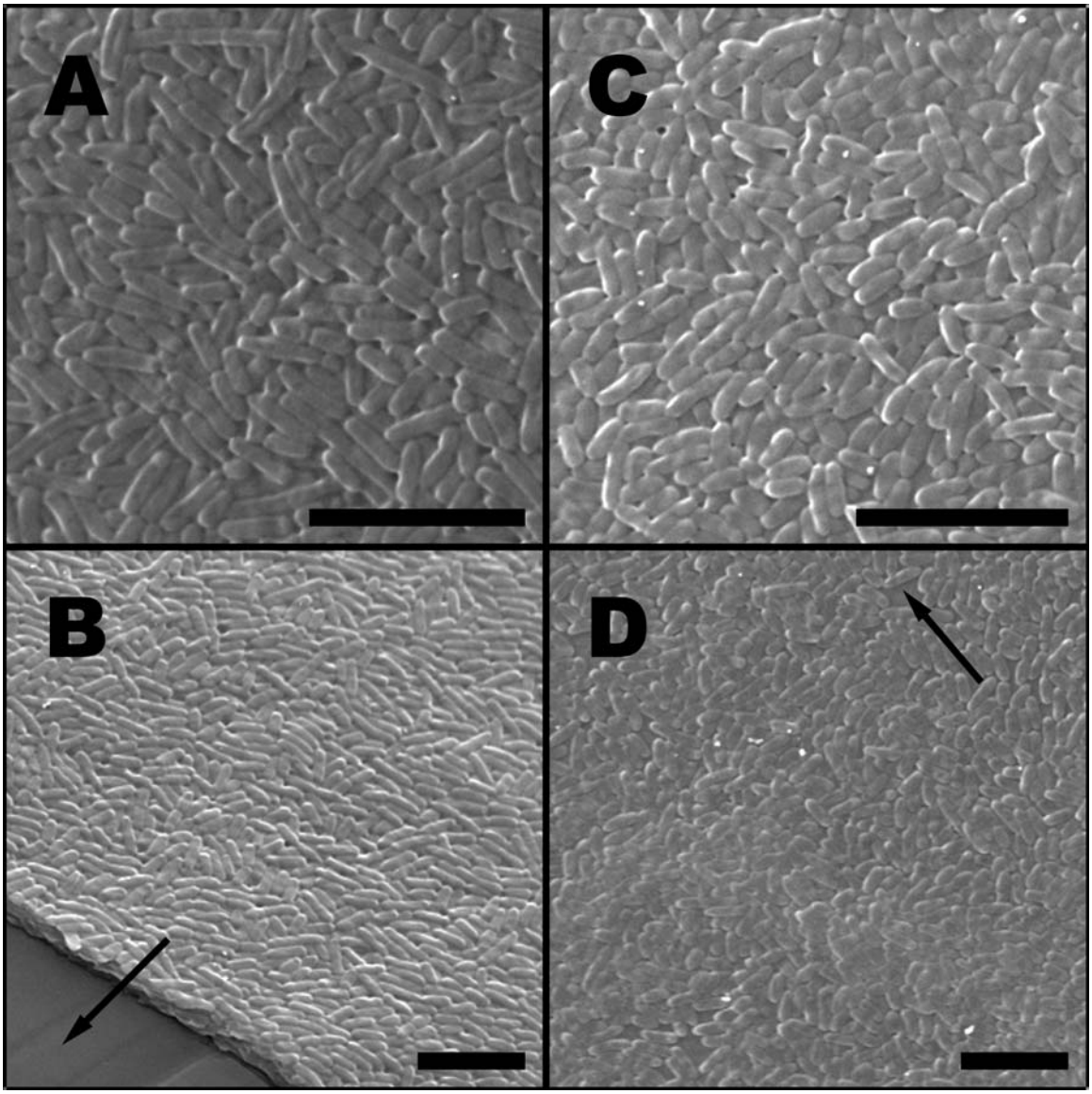

Figure 3.1. SEM of *Pseudomonas aeruginosa* ATCC 27853 biofilms grown in the CBD using rich or minimal media. (A) Biofilms grown in rich media (LB) formed a bacterial layer that covered the entire surface of the plastic peg. (B) A breakaway cross-section shows that these biofilms were several cell widths in thickness. (C and D) Biofilms grown in minimal media (MSVP) were unevenly distributed across the peg surface, forming lumps and mounds. The arrows indicate the exposed surface of the peg and the bars represent 5 μm. (This figure has been reproduced by permission from Harrison *et al*. (2005) Environmental Microbiology 7:981-994).

of ciprofloxacin (3.2 A and B) and gentamicin (3.2 C and D). Ciprofloxacin killed the vast majority of planktonic and biofilm populations at concentrations of less than 8 μg mL^{-1}. However, a very small portion of the planktonic population survived up to 64 μg mL^{-1}. For the corresponding biofilms, 10^{-3} to 10^{-5} cells tolerated ciprofloxacin up to 256μg mL^{-1}, which was the highest concentration used in this study. This subpopulation remained recalcitrant to killing by this antibiotic even after 20 h of exposure. By contrast to this, by 20 h exposure, gentamicin had eradicated planktonic cells in the range of 128-512 μg mL^{-1}. A small portion of the corresponding biofilm cultures exposed to gentamicin remained viable even at 512 μg mL^{-1}. This data corresponds well with Spoering and Lewis's (230) previous description of biofilm tolerance to antibiotics and supports the idea that antibiotic penetration into biofilms, in some cases, may be independent of antibacterial activity. The data in Figure 3.2 support a time-dependent relationship for the killing of planktonic cells by antibiotics; however, it is important to note that in these assays only gentamicin killed biofilm cells in a time-dependent fashion following 2 h exposure.

Table 3.1. Susceptibility of *Pseudomonas aeruginosa* ATCC 27853 to antibiotics with 2 or 20 h of exposure in rich (LB) medium.

Antibiotic	Exposure time (h)	$MIC_{24\ h}$ (μg/ml)	$MBC_{p\text{-}100}$ (μg/ml)	$MBC_{b\text{-}100}$ (μg/ml)	Fold tolerance
Ciprofloxacin	2	1 (1 to 2)	32 (16 to 32)	>256	≥16
	20		16 (16 to 64)	>256	≥32
Gentamicin	2	8 (8 to 16)	>512	>512	na
	20		256 (128 to 512)	>512	≥4

na indicates a measurement that is not applicable

3.3.4 Susceptibility of P. aeruginosa to toxic metal cations and oxyanions

To begin, metal susceptibility testing for 17 different toxic metal species was performed under similar conditions to antibiotic assays, as these conditions were also similar to the 24 h assays I had previously performed to examine the metal susceptibility

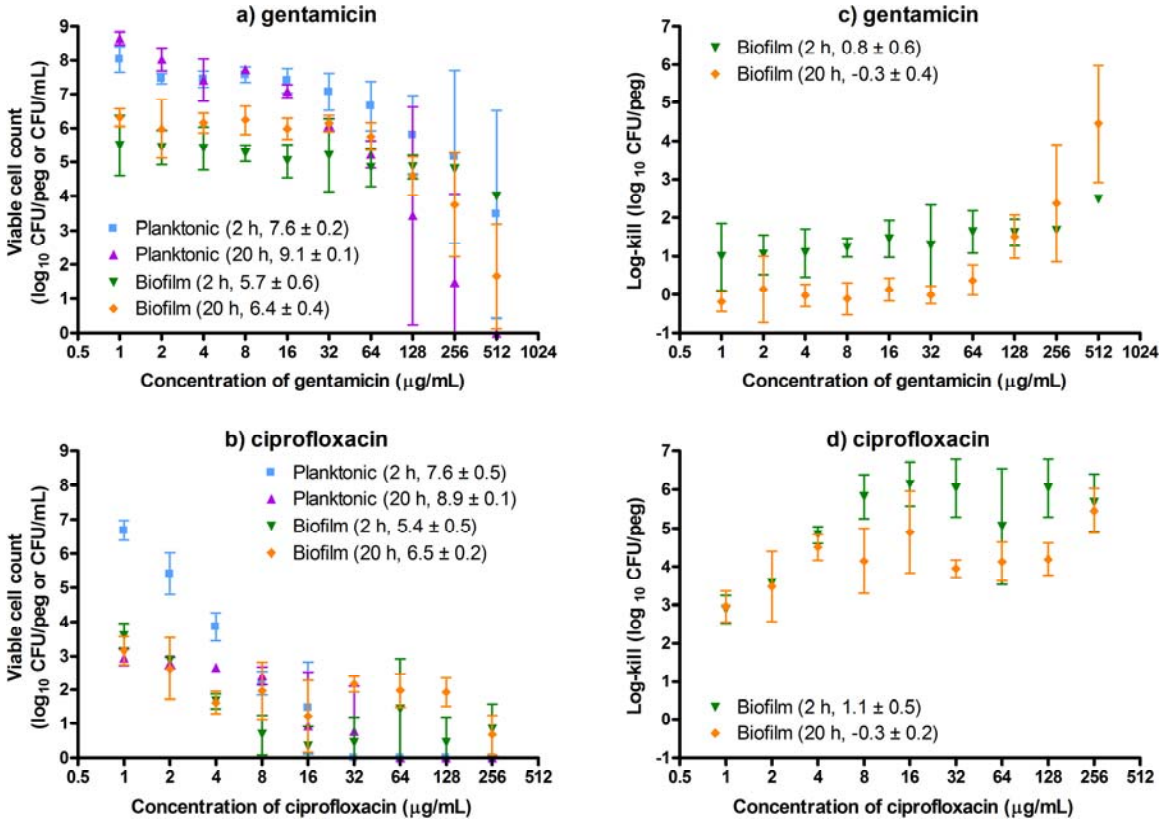

Figure 3.2. Time-dependent killing of *Pseudomonas aeruginosa* ATCC 27853 planktonic and biofilm populations by gentamicin and ciprofloxacin. The mean viable cell counts for (A) gentamicin and (B) ciprofloxacin indicate that bactericidal drugs kill bacterial populations in a time-dependent fashion. Log-killing calculations for (C) gentamicin and (D) ciprofloxacin indicate that it is only a small sub-population of cells in biofilms that survive this antibiotic exposure. Each data point in these graphs is the mean and standard deviation of 3 independent replicates. Similar calculations were also performed for the post-exposure growth controls (i.e. identical exposure conditions without the addition drug) and these values are indicated in parentheses for the specified population at the indicated exposure time. (This figure has been adapted from data originally published in Harrison *et al*. (2005) Environmental Microbiology 7:981-994).

of *E. coli* and *S. aureus* biofilms (98). Here, the susceptibility of *P. aeruginosa* biofilms to this diverse range of toxic metal species is reported in Table 3.2 (medians and ranges of $MIC_{72\ h}$, $MBC_{p\text{-}q}$ and $MBC_{b\text{-}q}$ values were based on 3 to 7 replicates each). Generally, there was less than 1 $\log_2$ deviation between the values obtained in independent replicates for the same metal ion (i.e. one well on the serial two-fold dilution challenge plate), and frequently the same value was obtained in every replicate for the same compound. In all cases, the median $MBC_{p\text{-}q}$ and $MBC_{b\text{-}q}$ measurements were similar, if not equal.

To extend these observations, and to look for time-dependent relationships in these data, the CBD assay was additionally used to screen biofilm susceptibility to Co^{2+}, Ni^{2+}, Cu^{2+}, Zn^{2+}, Al^{3+}, and Pb^{2+} in LB medium at 2 and 27 h of exposure (Co and Pb were not examined in the original panels of antimicrobial agents). The median values and ranges for these $MIC_{72\ h}$, $MBC_{p\text{-}q}$ and $MBC_{b\text{-}q}$ determinations are reported in Table 3.3 (4 replicates each). It was observed that with 2 h of exposure, biofilms were at least 2- to 4-times more tolerant to metal toxicity than the corresponding planktonic cultures. In those cases where the toxic metal ion had eradicated the populations, by 27 h, biofilms were as susceptible to metal toxicity as planktonic cells. These data indicate that, in contrast to antibiotics, toxic metal cations may eradicate biofilms in a time-dependent fashion (Figure 3.3). Here, it is important to note that endpoints could not be measured in many instances because these assays were performed using rich medium and at high concentrations the metal may precipitate out, thereby reducing its biological availability.

3.3.5 Time-dependent eradication of P. aeruginosa biofilms by toxic metal cations

To eliminate the possibility that the observed time-dependent tolerance was an artefact of the growth conditions, these assays were repeated using minimal (MSVP) medium at multiple time intervals. The median values and ranges of all $MIC_{72\ h}$, $MBC_{p\text{-}100}$ and $MBC_{b\text{-}100}$ measurements under these conditions are reported for Co^{2+}, Ni^{2+}, Cu^{2+}, Zn^{2+}, Al^{3+}, and Pb^{2+} in Table 3.4. The $MIC_{72\ h}$ values determined using the CBD assay did not change with exposure time (data not shown) and the values reported in Table 3.4 were derived from a total of 28 replicates. By contrast, $MBC_{p\text{-}100}$ and $MBC_{b\text{-}100}$ determinations were repeated 4 to 7 times each. Reproducibility of $MIC_{72\ h}$

Table 3.2. Relative levels of resistance of *Pseudomonas aeruginosa* ATCC 27853 planktonic and biofilm bacteria to metal toxicity (in LB with 24 h exposure)

Metal ion	Periodic Group	n	$MIC_{72\ h}$ (mM)	$MBC_{p\text{-}q}$ (mM)	$MBC_{b\text{-}q}$ (mM)
CrO_4^{2-}	VI B	4	4.7 (2.4 to 4.7)	3.6 (2.4 to 4.7)	3.6 (2.4 to 4.7)
MoO_4^{2-}		5	>103	>103	>103
WO_4^{2-}		6	>66	>66	>66
Mn^{2+}	VII B	4	>149	>149	>149
Ni^{2+}	VIII B	4	18	>140	>140
Cu^{2+}	I B	4	16 (8.1 to 16)	16 (8.1 to 16)	16 (8.1 to 16)
Ag^{+}		**5**	**0.30**	**0.30**	**0.30 (0.30 to 0.60)**
Zn^{2+}	II B	4	63 (63 to 125)	>125	>125
Cd^{2+}		5	4.6	36	36
Hg^{2+}		**6**	**0.38 (0.38 to 1.5)**	**0.38 (0.38 to 0.76)**	**0.38 (0.38 to 0.76)**
Al^{3+}	III A	3	9.5	19 (9.5 to 38)	19 (19 to 38)
Sn^{2+}	IV A	5	17	17 (17 to 34)	17 (17 to 34)
AsO_2^{-}	V A	4	>77	>77	>77
AsO_4^{2-}		4	>59	>59	>59
SeO_3^{2-}	VI A	4	32 (16 to 32)	32 (16 to 32)	32 (16 to 32)
TeO_3^{2-}		**5**	**0.73**	**5.8 (2.9 to 5.8)**	**4.4 (2.9 to 5.8)**
TeO_4^{2-}		5	>1.3	>1.3	>1.3

bold denotes the three most toxic metal compounds to *Pseudomonas aeruginosa* ATCC 27853
n denotes the principal quantum number

determinations served as an internal control to eliminate dilution error of the metal compounds in the challenge plates. In principle, the use of MSVP medium may also minimize metal precipitation and metal coordination with medium components, and it is likely because of this that the $MIC_{24\ h}$, $MBC_{p\text{-}100}$ and $MBC_{b\text{-}100}$ values were to some extent greater in LB than in MSVP.

3.3.6 Cell survival in planktonic and biofilm populations exposed to toxic metal ions

To quantify the survival of planktonic and biofilm bacterial populations following exposure to metal cations, viable cell counts were determined for a range of

concentrations following either 2 or 27 h of exposure in MSVP. Mean viable cell counts and log-killing of biofilm cultures for Co^{2+}, Ni^{2+}, and Cu^{2+} (Groups 8B and 1B) are reported in Figure 3.3, and for Zn^{2+}, Al^{3+}, and Pb^{2+} (Groups 2B to 4A) are reported in Figure 3.4. In all of these assays, high concentrations of metals were observed to kill 90% to 99.9% (or an even greater portion) of both planktonic and biofilm bacterial populations with 27 h exposure. This was also the case with Cu^{2+}, Al^{3+}, and Pb^{2+} by 2 h of exposure. In contrast, Co^{2+}, Ni^{2+} and Zn^{2+} killed 50 to 90% of the bacterial population with 2 hours of exposure. Unlike planktonic cultures, which were quickly eradicated by metal cations, in no instance were biofilms eradicated within 2 h of exposure. In contrast, with 27 h of exposure to Co^{2+}, Cu^{2+} Al^{3+} and Pb^{2+}, biofilm bacteria in the CBD were eradicated at concentrations similar to those required to eradicate planktonic cell populations.

The survival of less than 0.1% of the bacterial population was particularly relevant in the cases of Ni^{2+} (Figure 3.3 B and E) and Zn^{2+} (Figure 3.4 A and D). *P.*

Table 3.3. Susceptibility of *Pseudomonas aeruginosa* ATCC 27853 to toxic metal cations with 2 or 27 h of exposure in rich (LB) medium.

Metal ion	Periodic Group	Time (h)	$MIC_{72\ h}$ (mM)	$MBC_{p\text{-}q}$ (mM)	$MBC_{b\text{-}q}$ (mM)	Fold tolerance
Co^{2+}	VIII B	2	4.3 (4.3 to 8.7)	105 (70 to 140)	>140	≥2.7
		27		>140	>140	na
Ni^{2+}	VIII B	2 or 27	17	>140	>140	na
Cu^{2+}	I B	2	16 (8.1 to 16)	16	64 (32 to 64)	4
		27		16 (8.1 to 32)	16 (8.1 to 64)	**1.0**
Zn^{2+}	II B	2	62 (62 to 125)	>125	>125	na
Al^{3+}	III A	2	81 (9.5 to 152)	152 (152 to 303)	>303	≥2.0
		27		19	19 (9.5 to 76)	**1.0**
Pb^{2+}	IV A	2	9.9 (9.9 to 20)	>40	>40	na
		27		>40	>40 (40 to >40)*	na

na indicates a measurement that is not applicable
bold indicates the fold tolerance at 27 h of exposure
*indicates that the bacterial culture was eradicated at the threshold of the maximum concentration of metal ion used in this study

Table 3.4. Susceptibility of *Pseudomonas aeruginosa* ATCC 27853 to toxic metal cations with 2 or 27 h of exposure in minimal (MSVP) medium.

Metal ion	Group	Time (h)	$MIC_{72\ h}$ (mM)	$MBC_{p\text{-}q}$ (mM)	$MBC_{b\text{-}q}$ (mM)	Fold tolerance
Co^{2+}	VIII B	2 to 6	2.2 (1.1 to 4.4)	139 (139 to >139)	>139	≥2.0
		8		105 (70 to >139)	139	1.3
		10		139 (139 to >139)	>139	≥2.0
		27		139 (35 to 139)	139 (70 to 139)	**1.0**
Ni^{2+}	VIII B	2 to 27	0.54 (0.27 to 1.1)	>140	>140	na
Cu^{2+}	I B	2	4.0 (1.0 to 8.1)	16 (16 to 32)	>129	≥16
		4		32 (16 to 32)	48 (32 to 129)	1.5
		6		16 (4 to 32)	32 (32 to 64)	2.0
		8 to 10		16	32	2.0
		27		12 (8.1 to 16)	16	**1.3**
Zn^{2+}	II B	2 to 8	7.8 (7.8 to 16)	>125	>125	na
		10		125 (63 to >125)	>125	≥2.0
		27		125 (32 to 125)	125 (32 to 125)	**1.0**
Al^{3+}	III A	2 to 4	9.5 (4.8 to 9.5)	19 (19 to 38)	>303	≥16
		6		19	152 (38 to 152)	8.0
		8		19	2.4 (2.4 to 9.5)	0.13
		10		19	9.5	0.5
		27		38 (19 to 38)	19 (19 to 38)	**0.5**
Pb^{2+}	IV A	2 to 6	1.2	20	>40 (40 to >40)	≥2.0
		8		9.9 (9.9 to 20)	>40 (40 to >40)	≥4.0
		10		20	>40 (40 to >40)	≥2.0
		27		20 (4.9 to 20)	30 (9.9 to 40)	**1.5**

na indicates a measurement that is not applicable
bold indicates the fold tolerance at 27 h of exposure
*indicates that the bacterial culture was eradicated at the threshold of the maximum concentration of metal ion used in this study

aeruginosa did not grow at low concentrations of these divalent heavy metal cations (MIC = 0.60 and 9.5 mM, respectively). However, the surviving population was observed to tolerate Ni^{2+} and Zn^{2+} at concentrations in excess of 140 mM and 125 mM, respectively. This phenomenon coincided with less than 0.1% survival of the biofilm and

planktonic cell populations. Panels D, E and F (Figures 3 and 4) indicate the proportion of the biofilm killed (i.e. log-kill) at 2 and 27 h of exposure. In every instance, the higher exposure time corresponded with an increase in the log-kill of the biofilm. As a control, biofilms not exposed to metals were enumerated after an equal exposure time and were shown to be similar to and, in most instances, greater than the initial biofilm counts before exposure (these values are indicated in parentheses in the figure panels for viable cell counts and log-killing). These controls rule out the possibility that the observed increase in log-kill was simply due to the dispersion of the biofilm due to the technique itself. Collectively, these data indicate that a small portion of the biofilm population mediates the time-dependent tolerance of *P. aeruginosa* biofilms to toxic ions of Co, Ni, Cu, Zn, Al and Pb. However, these cell death kinetics immediately raise an important question: are these survivors mutants or adapted bacteria that may grow at elevated levels of toxic metals in subsequent challenges? Or are these bacteria phenotypic variants that may revert to the starting cell type when propagated and tested for a second time, thereby giving rise to similar population killing kinetics similar to those determined for the parent population?

3.3.7 Propagation of biofilm persister cells

To investigate the possibility that the surviving cells of metal exposure were a genetically distinct or adapted sub-population as opposed to phenotypic variants, I propagated survivor cells by inoculating a CBD with cells isolated from recovery plates from biofilms previously exposed to Cu^{2+} for a period of 24 h. The re-cultured survivors gave rise to planktonic and biofilm populations with normal susceptibility to Cu^{2+} (Figure 3.5). The MIC for planktonic bacteria derived from re-cultured survivor populations was the same as the MIC for the parental culture from which the survivors were recovered.

In summary, these data indicate that 0.1% or less of the bacterial population is responsible for the observed tolerance of both planktonic and biofilm *P. aeruginosa* to high concentrations of toxic metal cations. Furthermore, a comparable portion of the biofilm population (less than 0.1%) survived for a longer period of time than it did for

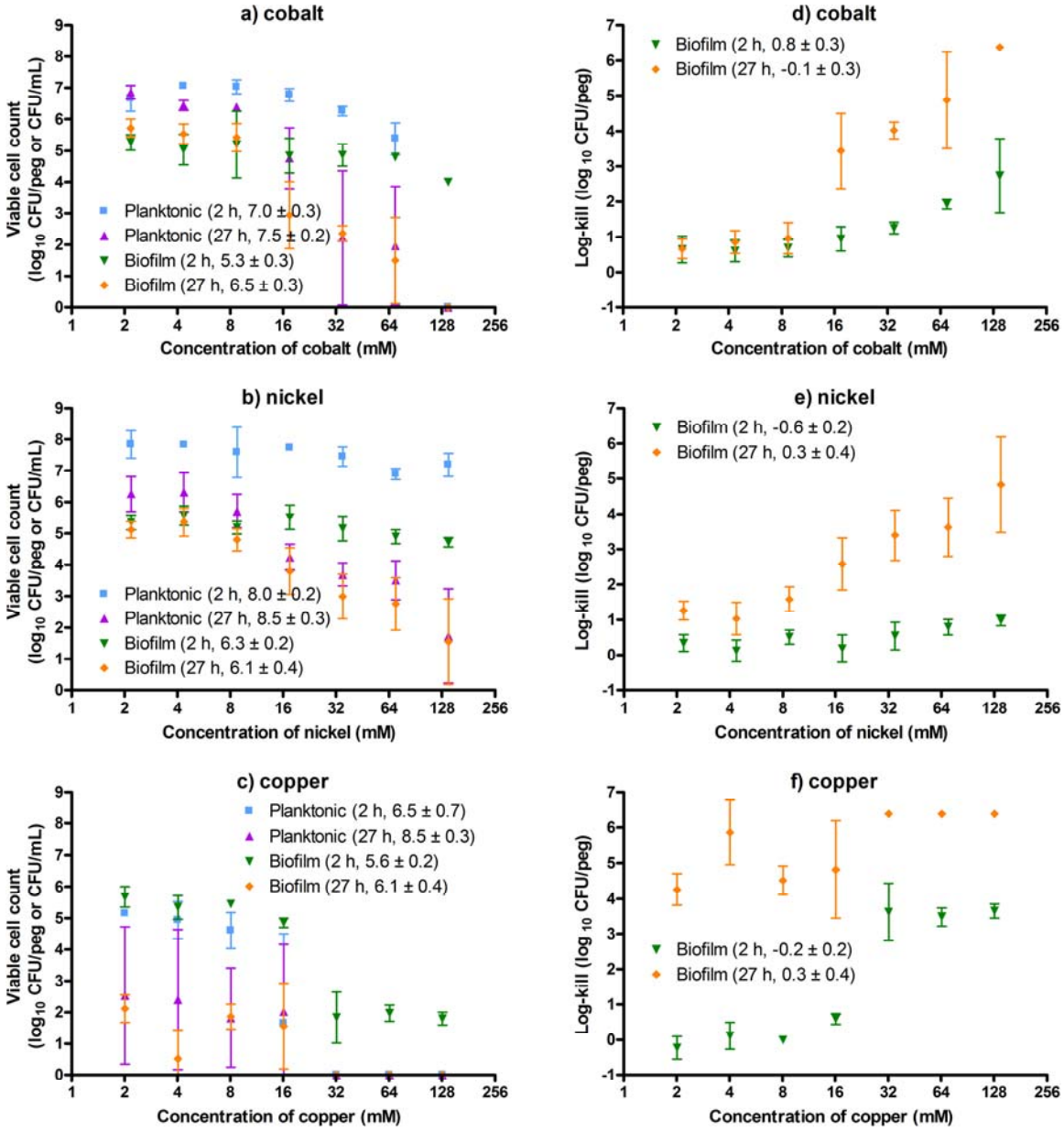

Figure 3.3. Time-dependent killing of *Pseudomonas aeruginosa* ATCC 27853 planktonic and biofilm populations by representative metals from groups 8B and 1B of the periodic table. Biofilm and planktonic cells (which were shed from the surface of biofilms) were exposed to (A) Co^{2+}, (B) Ni^{2+} or (C) Cu^{2+} for 2 or 27 hours in minimal (MSVP) medium and then plated for viable cell counts. Log-killing of biofilm cultures for (D) Co^{2+}, (E) Ni^{2+} or (F) Cu^{2+} indicate that 0.1% to 10% of the bacterial population was able to survive exposure to high concentrations of these heavy metals for prolonged periods of time. In the cases of Co and Cu, 27 h of exposure to toxic metal species

eradicated the biofilm population. Each data point in these graphs is the mean and standard deviation of 3 or 4 independent replicates. Similar calculations were also performed for the post-exposure growth controls (i.e. identical exposure conditions without the addition metal) and these values are indicated in parentheses for the specified population at the indicated exposure time. (This figure has been adapted from data originally published in Harrison *et al*. (2005) Environmental Microbiology 7:981-994).

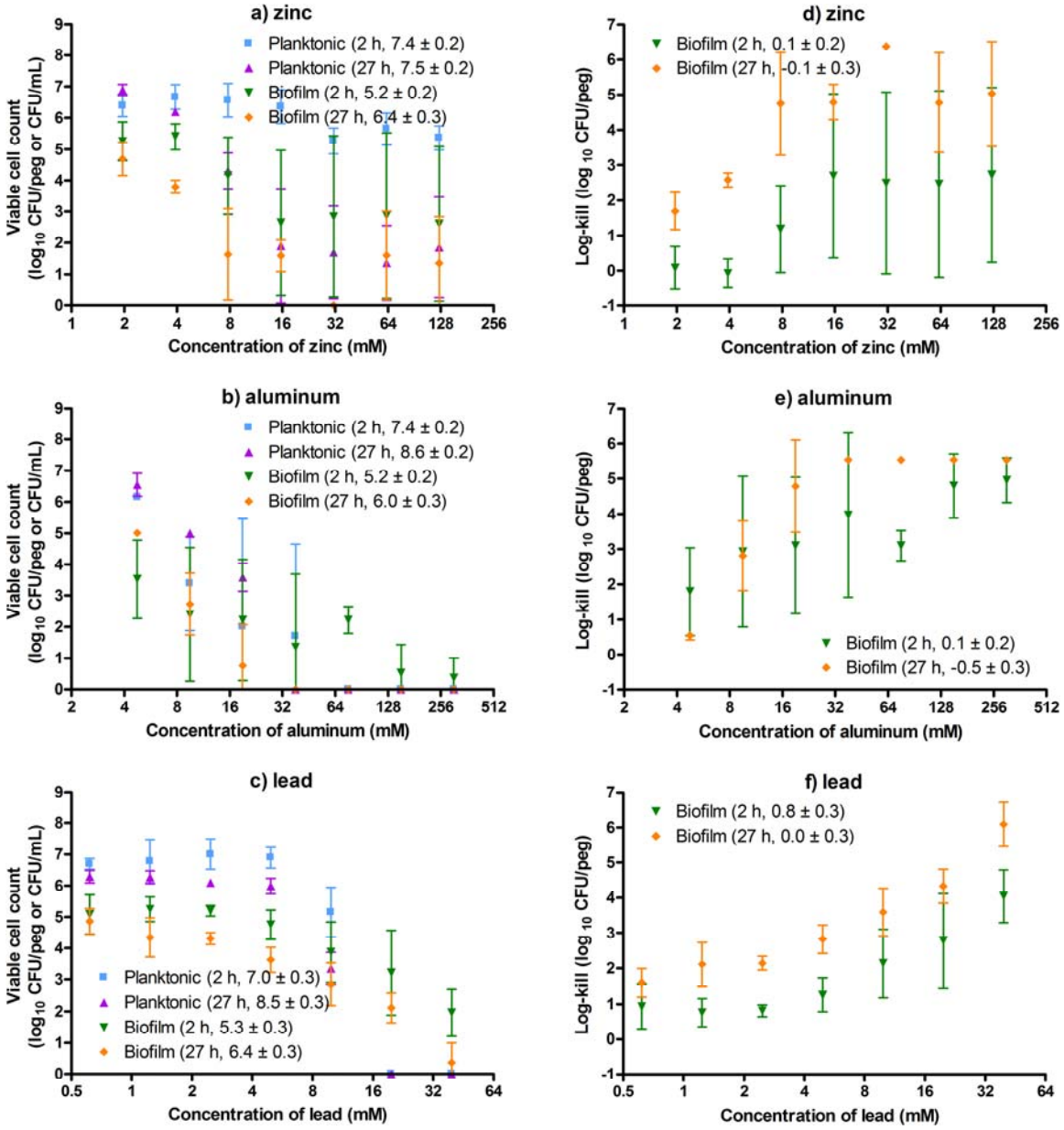

Figure 3.4. Time-dependent killing of *Pseudomonas aeruginosa* ATCC 27853 planktonic and biofilm populations by representative metals from groups 2B to 4A of the periodic table. Biofilm and planktonic cells (which were shed from the surface of biofilms) were exposed to (A) Zn^{2+}, (B) Al^{3+} or (C) Pb^{2+} for 2 or 27 hours in minimal (MSVP) medium and then plated for viable cell counts. Log-killing of biofilm cultures for (D) Zn^{2+}, (E) Al^{3+} or (F) Pb^{2+} indicate that less than 0.1% of the bacterial population survived 27 h exposure to high concentrations of these heavy metals. In all cases, biofilm and planktonic populations were killed time-dependently by metal cations and in the

cases of Al and Zn, there were instances in which 27 h exposure to the toxic metal species eradicated these populations. Each data point in these graphs is the mean and standard deviation of 3 or 4 independent replicates. Similar calculations were also performed for the post-exposure growth controls (i.e. identical exposure conditions without the addition metal) and these values are indicated in parentheses for the specified population at the indicated exposure time. (This figure has been adapted from data originally published in Harrison *et al*. (2005) Environmental Microbiology 7:981-994).

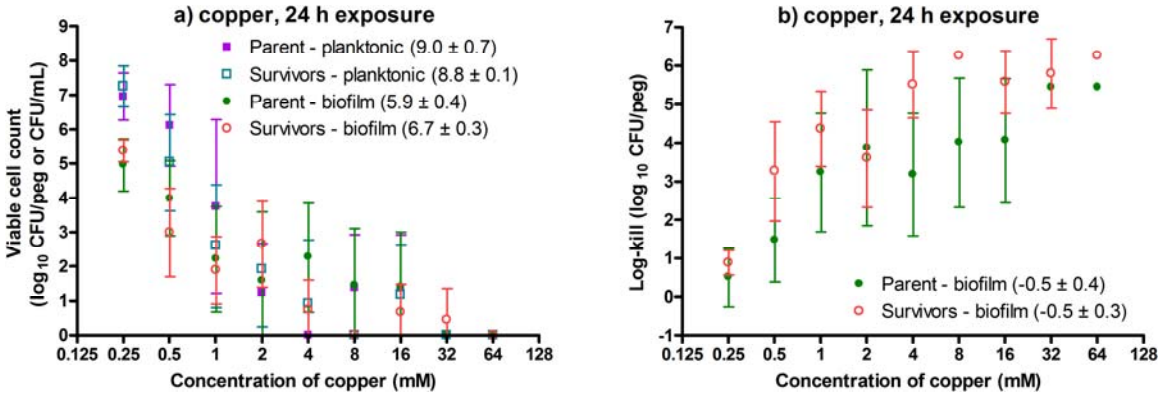

Figure 3.5. Propagation of *Pseudomonas aeruginosa* persister cells surviving exposure to copper gives rise to biofilm and planktonic populations with normal susceptibility to copper. Biofilm and planktonic cultures of *Pseudomonas aeruginosa* ATCC 27853 were exposed to Cu^{2+} for 24 hours and then plated for viable cell counting. Persister cells were isolated from agar recovery plates, grown in the CBD device, exposed to Cu^{2+} for 24 h again and then plated for viable cell counting. The re-cultivated persister cells produced persisters at similar levels to parental cultures (given the high error associated with viable cell counting) and were eradicated at similar concentrations of metals. Note that the mean and standard deviation intervals of viable cell counts for the persister populations from the different generations overlap. (A) Mean viable cell counts for parental and persister cell seeded cultures exposed to Cu^{2+}. (B) Log-killing for biofilms of parental and persister cell seeded cultures exposed to Cu^{2+}. Each data point in these graphs is the mean and standard deviation of 4 independent replicates. Similar calculations were also performed for the post-exposure growth controls (i.e. identical exposure conditions without the addition copper) and these values are indicated in parentheses for the specified population. (This figure has been adapted from data originally published in Harrison *et al*. (2005) Environmental Microbiology 7:981-994).

planktonic cultures. However, the metals Co^{2+}, Cu^{2+}, Al^{3+}, and Pb^{2+} all allowed for complete eradication of the biofilm cultures with extended exposure times (27 hours).

3.3.8 Adsorption of heavy metals to biofilm biomass

Conspicuously, the MIC values for metal cations reported in Tables 3.3 and 3.4 were generally greater than the concentrations required to kill 50 to 90% of the corresponding biofilm cultures enumerated in Figures 3.3 and 3.4. A potential explanation for this phenomenon was that the biofilm may have adsorbed metal ions. Removal of biofilm pegs from the challenge media would then effectively reduce the concentration of metals in the wells of the 96-well microtiter plates. Consequently, bacteria shed from the surface of the biofilm which had seeded the planktonic culture would then begin to grow in a milieu with lower concentrations of toxic, biologically available metals. To investigate this hypothesis, I developed a simple, qualitative assay for retention of metals in biofilms exposed to Cu^{2+} or Ni^{2+} (see section 3.2.2 for a discussion of the rationale). Essentially, biofilms exposed to Cu^{2+} and Ni^{2+} for 24 h were rinsed and then treated with the chelator sodium diethlydithiocarbamate (Na_2DDTC).

Cu^{2+} and Ni^{2+} rapidly formed brown and pale yellow metal complexes with Na_2DDTC, respectively. Pictures of Cu^{2+} exposed biofilm and planktonic cultures treated with Na_2DDTC appear in Figure 3.6 (the data for Ni^{2+} is not shown). Green discoloration of growth controls occurred because of pigmented siderophore production by *P. aeruginosa* ATCC 27853 as it reached late logarithmic-phase. The brown precipitate in biofilms was qualitatively indicative that copper cations were coordinated (or trapped) within the biofilm during metal exposure.

3.4 Discussion

In this Chapter, I have used the CBD to examine *P. aeruginosa* biofilm susceptibility to metal toxicity. The principle strength of this high-throughput approach lies in the potential to conduct combinatorial susceptibility assays with different media, metal ions and exposure times. This research study was designed to address the apparent incongruity existing between three sets of observations: 1) my observations that biofilms

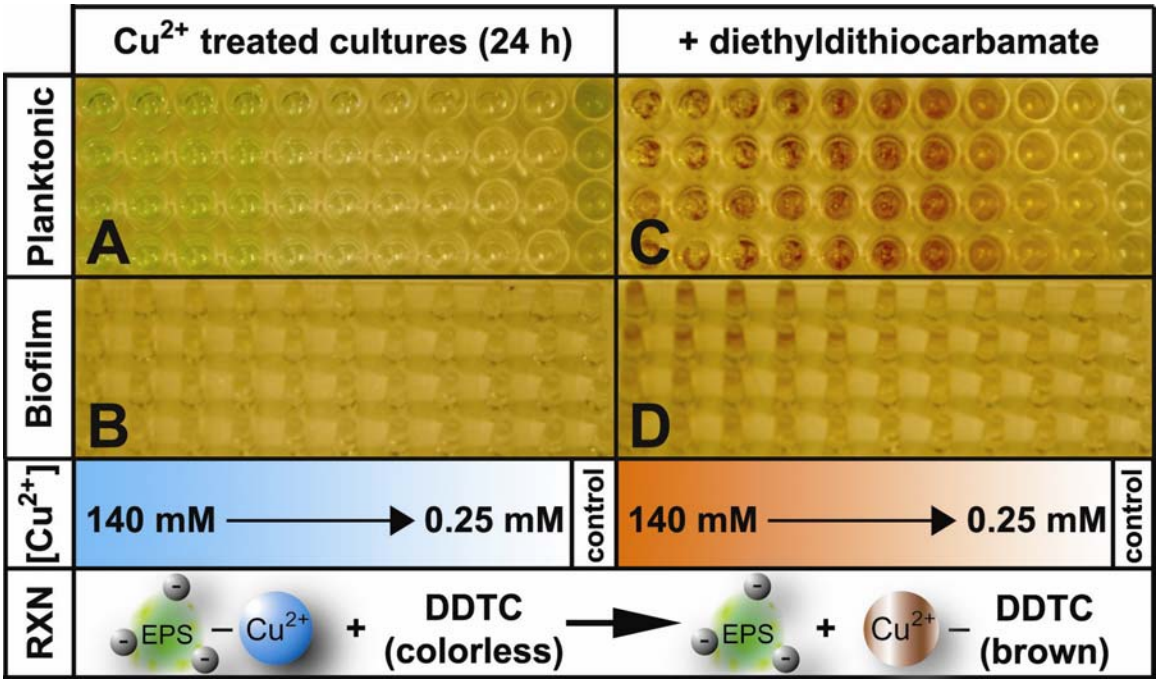

Figure 3.6. Copper cations were adsorbed by the biomass of *Pseudomonas aeruginosa* ATCC 27853 biofilms. The concentration gradient of Cu^{2+} present in the challenge media and the coordination reaction that produces the colour change are depicted below the photographs. In each panel, the far right hand well or peg is a growth control not exposed to copper. The photographs of biofilm pegs are mirror images digitally processed to align pegs with the corresponding planktonic wells. (A) Planktonic cultures and (B) biofilms after 24 h of exposure to Cu^{2+} are green-blue and colorless, respectively. The biofilms pictured here were rinsed twice with 0.9% NaCl. (C) Planktonic cultures and (D) biofilms after treatment with 5 mM sodium diethyldithiocarbamate causes brown precipitates to form. In the case of biofilms, precipitates on the peg are qualitatively indicative of copper deposition (or retention) within the biofilm. (This figure has been reproduced by permission from Harrison *et al*. (2005) Environmental Microbiology 7:981-994).

and planktonic cells of *P. aeruginosa* are equally susceptible to killing by metal cations with 24 h exposure (in rich media); 2) the report by Teitzel and Parsek (250) that biofilms of *P. aeruginosa* are 2- to 600- times less susceptible to divalent heavy metal cations than planktonic bacteria with 5 h exposure (in minimal media or MOPS buffered saline and carried out using the CDC biofilm reactor); and 3) the evidence that persister cells may mediate, in part, the observed tolerance of biofilms and planktonic cells to microbicidal agents (12, 35, 130, 168, 230, 235). The data in this Chapter suggest that all of these observations may be in agreement.

In either rich or minimal media, the concentration of toxic metal cations required to eradicate a biofilm decreased with exposure time (a phenomenon that was very different from control antibiotic assays). With long enough exposures, biofilms were eradicated at approximately the same concentration required to eradicate logarithmic-growing planktonic bacteria. In general, at high concentrations of metal cations, 90 to 99.9% (and sometimes a greater proportion) of both planktonic and biofilm bacterial populations were killed. Remarkably, the short term tolerance of biofilms to concentrations of toxic metal cations greater than the $MBC_{p\text{-}100}$ was mediated by the survival of a small fraction ($\leq$0.1%) of cells from the bacterial population. Furthermore, the proportion of bacterial cells killed by toxic metal cations reached a plateau at any given exposure time and further increases in metal ion concentrations did not eliminate this phenomenon. This suggests that biosorption cannot solely account for this phenomenon. I would propose two potential explanations for these observations, both of which may be at work here: 1) that persister cells in a biofilm are killed at a reduced rate by metal cations relative to the planktonic persister population, or 2) that there is a greater population of persisters in a biofilm that are killed at the same rate as planktonic persister cells.

One of the features of the CBD is that the wells of the microtiter plates containing serial dilutions of metals are inoculated with bacteria shed from the surface of the peg lid. Consequently, precise initial numbers of planktonic bacteria are unknown and log-killing of planktonic bacteria cannot be calculated using this method. However, this situation *in vitro* may reflect naturally existing environmental systems (or infections) where a biofilm

forms a recalcitrant nidus that sheds planktonic cells into its surroundings. A detailed comparison of the CBD method for planktonic cell susceptibility testing and a modified CLSI protocol for planktonic cell susceptibility testing is presented in Chapter Four.

Notable challenges to studying the 'persistent' phenotype are the natural low frequency of persister cells and our limited knowledge about the functional significance of these cell types. Within the limits of our current understanding, persisters may only be defined as the small, slow-growing and thus physiologically distinct subpopulation of bacterial cells capable of withstanding environmental duress (12).

A model based on the available data suggests that bacterial growth in a biofilm provides bacteria with time-dependent tolerance to high concentrations of toxic metal cations. In this model, persister cells may represent a protected, quiescent subpopulation that mediates, at least in part, the short term tolerance of the biofilm to toxic metal species. This model does not refute that the reduced susceptibility of biofilms to metal cations may occur at multiple levels. Although there were declines in biofilm mean viable cell counts at the lowest concentrations of metal cations assayed in this study, this neither confirms nor dismisses the possibility that biofilms may continue to grow in the presence of toxic metal cations under different cultivation or test conditions.

In this model system, the dissemination of planktonic cells is linked to the survival of the biofilms from which they are derived. Based on the data presented in this Chapter, a mature biofilm may function to protect the planktonic cells released from it because the biofilm may adsorb and sequester certain toxic metal species from the surrounding aqueous milieu. This was observed as recovery of planktonic cultures in wells of the challenge plate after the exposed biofilms were removed. In the context of this assay, the associated $MIC_{72\ h}$ values (expressed in mM of metal added to the challenge plate) were in some instances greater than concentrations of metals required to kill a portion of the biofilm. In an ecological context, biofilm formation may hypothetically function as a strategy for resistance of bacteria shed from it. Sequestration of toxic metal cations within the biofilm matrix would allow shed cells an opportunity to migrate away from the local site of metal contamination.

In conjunction with the qualitative observation that Cu^{2+} and Ni^{2+} were retained by the biofilm matrix, the time-dependent killing kinetics of biofilms by metal ions are consistent with the restricted-penetration hypothesis (153) and may putatively represent a reaction-diffusion phenomenon (234). Biochemically, the extracellular polymeric matrix of *P. aeruginosa* is an ionic mixture of amino acids (246), nucleotides (274), and derivatized sugars (278). Simple diffusion of a non-reactive ion across a biofilm matrix is slow. Using chloride (Cl^-) as an example, diffusion across a 1000 μm thick biofilm requires more than 16 minutes (238). Diffusion of chloride ions may be restricted through ionic interactions with positively charged chemical groups in the biofilm. By contrast, metal cations may interact with negatively charged ionic groups resulting in the slower diffusion of the metal species into the biofilm. It is also important to note that metal cations may also covalently react with various microbial metabolites and this may effectively sequester the compounds in the biofilm ECM (100). This sequestration would keep toxic metals away from cells and would provide protection until the ECM saturates, and in principle, this may result in local metal concentrations greater than the bulk media. The kinetics of the reaction equilibriums likely influence both biological availability and diffusion dynamics of the toxic metal species.

Based on evidence in the literature as well as data presented in this Chapter, it is not yet possible to label biofilms as multimetal resistant since they do not seem to grow in concentrations of toxic metal species in excess of the planktonic MIC. Rather, biofilms may be considered multimetal tolerant as they do not die as fast as planktonic cells exposed to toxic metal ions. Although persister cells are known to survive high levels of antibiotics for prolonged exposure times, as it pertains to our model system and *P. aeruginosa* ATCC 27853, the data here suggest that the same statement is not true for toxic metal cations. In this study, I observed that ~0.1% or less of the biofilm population survived for short periods of time at concentrations of metal cations in excess of the concentration required to eradicate planktonic bacteria ($MBC_{p\text{-}100}$). Persister cells may mediate a high level of tolerance to metal toxicity in both biofilm and planktonic cultures; however, in biofilms, persisters only appear to survive concentrations of metal cations in excess of the $MBC_{p\text{-}100}$ for a finite period of time. I thus propose that bacterial growth in

a biofilm may be a time-dependent mechanism of tolerance to high concentrations of metal cations, and that this might be linked to persister cells as well as to the adsorption of metals to biofilm biomass.

3.5 Contributions

3.5.1 Author's contributions to this work and personal acknowledgements

I performed all of the experimental work described in this Chapter. I would like to extend my thanks to Carol A. Stremick for insightful discussions about this work. Electron microscopy was performed by Liz Middlemiss, a technician employed by Innovotech Inc.

3.5.2 Relevant publications

These data sets were originally published in Harrison *et al*. (2004) Environmental Microbiology 6:1220-1227 and in Harrison *et al*. (2005) Environmental Microbiology 7:981-994.

Chapter Four: Toxin-antitoxin genes and persister cell mediated tolerance to metal oxyanions in planktonic and biofilm *Escherichia coli*

4.1 Introduction

Bacterial cultures produce subpopulations of persister cells that mediate tolerance to high concentrations of antibiotics. With respect to exposure time and concentration of the drug, these cells characteristically give rise to a biphasic pattern of cell survival in bacterial populations (Figure 3.2). In the previous chapter, it was established that *Pseudomonas aeruginosa* biofilm populations were also killed in a time- and concentration-dependent fashion by toxic metal cations. Mechanistically, this is a difficult problem to experimentally dissect, as the killing kinetics of biofilms by metal ions might be linked to both restricted diffusion as well as to multimetal tolerant persister cells. The reduced susceptibility of biofilms to metal ions is important, as toxic metal species are constant pressures in the environment that are spread by human pollution, volcanic activity, physical and chemical weathering of minerals as well as by biogeochemical cycling (36). The research in this chapter was undertaken to expand these observations of multimetal tolerance to another Gram-negative bacterial species, *Escherichia coli*, and to examine a different type of toxic metals – metal oxyanions. These compounds have a significant environmental impact, as oxyanions of chromium, arsenic, selenium and tellurium are prevalent industrial pollutants with high biological toxicity (for reviews, see 41, 47, 170, 181).

Although the precise molecular mechanism of bacterial persistence remains a mystery, the frequency at which persister cells occur in populations of *E. coli* is known to be genetically regulated (139, 167, 168) and has been linked to chromosomal toxin-antitoxin (TA) genes (see Chapter One for a review). The best studied example is the TA pair *hipBA*, and a mutant allele of *hipA*, *hipA7*, is known to increase the proportion of multidrug tolerant persister cells in stationary phase populations approximately 10- to 1000-fold (139, 140). Korch and Hill (140) have shown that ectopic overexpression of wild-type HipA at levels in excess of HipB inhibits protein, RNA and DNA synthesis *in vivo*, and that this triggers a reversible, dormant state in a sizable fraction of cells;

however, it is not clear whether HipA7 functions through this mechanism. Nonetheless, the HipA7 mutant may be useful in this research for ascertaining whether persister cells mediate bacterial tolerance to metal oxyanions. If persister cells mediate multimetal tolerance, the proportion of cells in the *hipA7* mutant population that survive exposure to toxic metal oxyanions should be increased relative to a population of wild type cells.

In this Chapter, I investigated whether bacterial persistence may play a role in the tolerance of *E. coli* to the toxicity of metal oxyanions. Here, six water soluble metal oxyanions were examined: chromate (CrO_4^{2-}), arsenate (AsO_4^{3-}), arsenite (AsO_2^{-}), selenite (SeO_3^{2-}), tellurate (TeO_4^{2-}), and tellurite (TeO_3^{2-}). Similar to the time-dependent tolerance of *P. aeruginosa* biofilms to metal cations, *E. coli* biofilms were up to 250-times more tolerant to metal oxyanions than corresponding planktonic cultures (after 2 h exposure). However, with 24 h of exposure, metal oxyanions eradicated biofilm and planktonic cultures at approximately the same concentration in every instance. Viable cell counts indicated that all of the metal oxyanions had killed greater than 99% of biofilm and planktonic cell populations at concentrations slightly in excess of the planktonic minimum inhibitory concentration (MIC). Notably, there was no precipitation and/or colorimetric coordination of oxyanions in exposed biofilms treated with the organic chelator sodium diethyldithiocarbamate (Na_2DDTC). This observation would suggest that metal oxyanions may have low affinity for the *E. coli* biofilm matrix, and consequently, that metal sequestration in the extracellular matrix (ECM) may not be a large contributor to the tolerance of *E. coli* biofilms to metal oxyanions. Finally, I tested *E. coli* HM22, a strain bearing the *hipA7* gain-of-function allele that increases the proportion of persisters in stationary phase populations. Here I show that this multidrug tolerant HipA7 mutant also has a multimetal tolerant phenotype. I concluded that the survival of less than 1% of the bacterial population fits well with the hypothesis that a small population of persister cells may be responsible for the *in vitro* tolerance of both logarithmic-growing planktonic and biofilm cultures to high concentrations of metal oxyanions. Furthermore, the production of multimetal tolerant persister cells in *E. coli* populations may be linked to the chromosomal TA module *hipBA*.

4.2 Materials and methods

4.2.1 Standard Protocols

E. coli JM109, HM21 and HM22 were stored, handled and cultured as described in Chapter Two. Biofilms were cultivated by growing this microorganism at 35 °C in the trough format of the Calgary Biofilm Device (CBD) for 24 h in LB medium. In addition to this method of biofilm cultivation, antibiotic and metal susceptibility testing as well as scanning electron microscopy (SEM) using the CBD were carried out according to the standard protocols described in Chapter Two. All growth media used for *E. coli* strains HM21 (AT984 *dapA zde-264::Tn10*) and HM22 (AT984 *dapA zde-264::Tn10 hipA7*) were supplemented with 75 μg mL^{-1} diaminopimelic acid (DAPA) as previously described (130).

4.2.2 Additional susceptibility testing of logarithmic-growing planktonic cells

To validate the CBD assay system, which has been used throughout the rest of this thesis, susceptibility determinations with logarithmic growing *E. coli* JM109 cells were repeated using a protocol designed to reflect the Clinical Laboratory Standards Institute (CLSI) method for antibiotic susceptibility testing. The inoculum for these tests was prepared by direct colony suspension from streak plates to match a 1.0 McFarland Standard as described in Chapter Two for creating a standard biofilm inoculum. This standard was diluted 30-fold in LB medium and 5 μL aliquots of this 1 in 30 dilution were added to each well of the challenge plates. This corresponded to an initial cell load of approximately 5.0 to 6.0 $\log_{10}$ CFU mL^{-1}. Challenge and recovery media, neutralizing agents, serial dilution and incubation times were identical to those used for CBD susceptibility testing.

4.2.3 Susceptibility testing of stationary phase planktonic cells

To directly test whether known high persistence (*hip*) mutants may have a multimetal tolerant phenotype, I examined *E. coli* HM21 (wild type) and HM22 (*hipA7*). These strains were grown in batch cultures by inoculating 24 mL of LB + DAPA with 1

mL of a 1.0 McFarland Standard. These cultures were grown in sterile 50 mL polypropylene tubes for 16 h at 35 °C on a gyrorotary shaker set to 125 rpm. Stationary phase planktonic cells were harvested by centrifugation (3000 × g for 10 min) then suspended in fresh medium containing the appropriate concentration of metal oxyanions. There was no significant loss of cell viability during centrifugation of either strain (data not shown). 20 µL aliquots were removed from the tubes after 6 h of exposure, neutralized, serially diluted and plated for viable cell counting as described for biofilm susceptibility testing in Chapter Two. HipA7 has a temperature sensitive mutation (131) and during exposure to metals *E. coli* HM21 and HM22 cultures were incubated at 30 °C.

4.2.4 Precipitation of adsorbed Cu, Te and Cr with sodium diethyldithiocarbamate

As described in Chapter Three, the chelator Na_2DDTC may be used as an analytical reagent for determining the concentration of transition metals, As and Te in aqueous solutions and in biological fluids (48, 260). As it pertains to this study, Na_2DDTC forms dark brown, green and yellow colored complexes with Cu^{2+}, CrO_4^{2-} and TeO_3^{2-}, respectively. A visible color change (mediated by Na_2DDTC) on the biofilm pegs in the CBD following metal exposure would indicate that these metal cations and oxyanions had been adsorbed and/or retained by the biofilm (105). Here, biofilms were formed on pegs of the CBD and then exposed to Cu^{2+}, CrO_4^{2-} or TeO_3^{2-} for 24 h. Biofilms exposed to these metal ions were rinsed twice for 5 min in sterile 0.9% NaCl. Subsequently, the peg lid was inserted into a 96-well microtiter plate which contained 200 µL of 37.5 mM Na_2DDTC in each well. Biofilms were treated with Na_2DDTC for ~2 min then photographed using a Sony 4.0 megapixel Cyber-shot digital camera.

4.2.5 Calculations and definitions of measurements

Calculations of mean viable cell counts, mean log-kill measurements and fold-tolerance were performed according to the guidelines set in Chapter Two. The calculation of fold tolerance was based on data obtained from the CBD, but not from measurements obtained from the CLSI protocol typically used for antibiotic susceptibility assays. The definitions of endpoints used to measure bacterial susceptibility (MIC,

$MIC_{24\ h}$, $MBC_{p\text{-}99.9}$, $MBC_{b\text{-}99.9}$, $MBC_{p\text{-}100}$ and $MBC_{b\text{-}100}$, $MBC_{p\text{-}q}$ and $MBC_{b\text{-}q}$) are the same as those used in Chapter Three.

4.3 Results

4.3.1 Biofilm formation by E. coli JM109 in the CBD

Biofilms were grown on the peg lid of the CBD to a point that corresponded to stationary phase for the associated planktonic cells in the trough of the device. Data from 54 control assays were pooled to calculate the population mean and standard deviation of biofilm growth on the pegs. At 24 h, biofilms had a mean cell density of 6.4 ± 0.4 $\log_{10}$ CFU per peg in the CBD. SEM was used to examine biofilm formation *in situ*. SEM images of *E. coli* JM109 biofilms are presented in Figure 4.1 and these pictures show the growth of mature biofilms on the peg surfaces.

4.3.2 Susceptibility of E. coli to antibiotics

As a standard of comparison to metal oxyanions and as a quality control for the CBD as an experimental system, I examined the growth inhibition and eradication of *E. coli* JM109 by three different antibiotics: amikacin, ceftrioxone and tobramycin. The median values and ranges for observed $MIC_{24\ h}$, $MBC_{p\text{-}100}$ and $MBC_{b\text{-}100}$ values are summarized in Table 4.1. Each reported value is based on 4 to 8 independent replicates. In no instance did antibiotics eradicate biofilms of *E. coli* with 2 h of exposure. By 24 h, planktonic cultures were eradicated at relatively low concentrations of amikacin (16 μg mL^{-1}), ceftrioxone (96 μg mL^{-1}) and tobramycin (32 μg mL^{-1}). Regardless of exposure time, biofilms were not eradicated at the highest concentrations of amikacin or ceftrioxone examined (512 μg mL^{-1}). Tobramycin eradicated biofilms time-dependently at very high concentrations (256 to 512 μg mL^{-1}). However, these assays show that *E. coli* biofilms remained at least 11 to 64 times more tolerant to antibiotics than planktonic cells (even with prolonged exposure time). This observation is consistent with previously reported results (40, 98, 270).

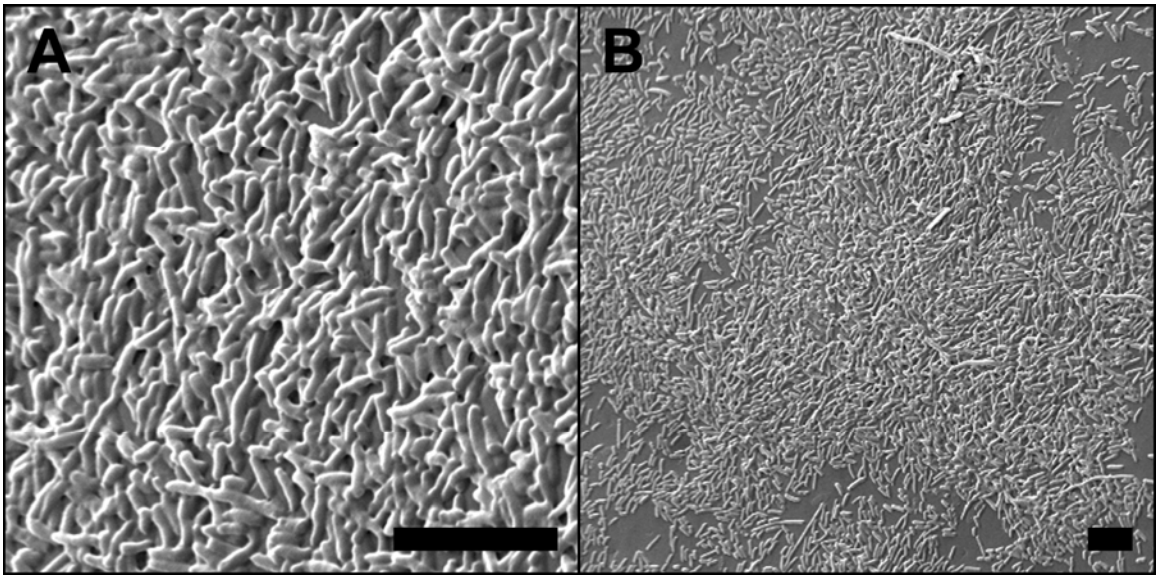

Figure 4.1. SEM of *Escherichia coli* JM109 biofilms grown in the CBD using rich medium. The bacteria formed (A) slimy mounds and layers that (B) covered the peg surfaces with a heterogeneous distribution. In both panels, the bar represents 5 μm. (This figure has been reproduced by permission from Harrison *et al*. (2005) Microbiology 151:3181-3195).

Table 4.1. Susceptibility of planktonic and biofilm *Escherichia coli* JM109 to antibiotics with 2 or 24 h of exposure in rich (LB) medium.

Antibiotic	Exposure time (h)	$MIC_{24\ h}$ (μg/mL)	$MBC_{p\text{-}100}$ (μg/mL)	$MBC_{b\text{-}100}$ (μg/mL)[1]	Fold tolerance
Amikacin	2	2 (2 to 4)	>512 (512 to >512)	>512	na
	24	6 (4 to 16)	16 (16 to 32)	>512	≥64
Ceftrioxone	2	6 (4 to 8)	>512	>512	na
	24	24 (8 to 64)	96 (32 to 128)	>512	≥11
Tobramycin	2	12 (4 to 32)	32 (16 to 64)	>512	≥32
	24	24 (16 to 32)	32 (16 to 64)	384 (128 to 512)	12

na indicates a measurement that is not applicable
[1]These values also include determinations of endpoints made using OD_{650} measurements of recovery plates.

4.3.3 Cell survival in planktonic and biofilm populations exposed to antibiotics

The bactericidal action of amikacin, ceftrioxone and tobramycin with respect to antibiotic concentration was evaluated by determining the viable cell counts for planktonic and biofilm *E. coli* JM109 after 2 or 24 h exposure in the CBD. Mean viable cell counts and log-killing for biofilms are illustrated in Figure 4.2. Each value is reported as the mean and standard deviation of 4 independent replicates. The majority of biofilm and planktonic populations were eradicated at very low concentrations of amikacin (approximately 20 μg mL^{-1}). However, 1% or less of the population tolerated this antibiotic up to 512 μg mL^{-1}, which was the highest concentration used in this assay. A similar trend was observed for ceftrioxone. In the case of planktonic cultures, the surviving cells were killed time-dependently (Figure 4.2 A), a trait that has been attributed to persister cells (12). When the bacteria were grown in a biofilm, a small fraction of cells were also recalcitrant to killing by ceftrioxone even with 24 h exposure (Figure 4.2 B and E). Tobramycin showed time-dependent killing kinetics of *E. coli* biofilms (Figure 4.2 C and F). At 24 h of exposure, tobramycin was the only antibiotic to reproducibly eradicate biofilms and this occurred at the threshold of the highest concentrations examined (128 to 512 μg mL^{-1}). These results are consistent with previous reports in the literature that have examined antibiotic susceptibility of *P. aeruginosa* biofilms (230). In general, these data show that, although biofilms may be

killed time-dependently by antibiotics, biofilms are many times more resilient to these drugs than planktonic cells (even with long exposures).

4.3.4 Susceptibility of E. coli to toxic metal oxyanions

E. coli JM109 $MIC_{24\ h}$, $MBC_{p\text{-}100}$ and $MBC_{b\text{-}100}$ values for CrO_4^{2-}, AsO_4^{3-}, AsO_2^{-}, SeO_3^{2-}, TeO_4^{2-}, and TeO_3^{2-} at 2 and 24 h exposure are presented in Table 4.2. Each value is reported as the mean and standard deviation of 3 to 7 independent replicates. With short exposures (i.e. 2 h), *E. coli* biofilms and planktonic cells were, in general, relatively tolerant to very high concentrations of metal oxyanions. In the case of TeO_3^{2-}, biofilms presented with a transient 250-fold increased tolerance relative to the corresponding planktonic cultures. The bacterial survivors of TeO_3^{2-} exposure represented a small enough portion of the population that they were only reliably detected using the (qualitative) OD_{650} measurements of the 96-well microtiter recovery plate. This may imply the number of surviving cells in the biofilm was approximately equal to or less than the threshold of detection using viable cell counts (approximately 10 CFU peg^{-1}). A similar phenomenon was observed for CrO_4^{2-}. In all instances, the highly tolerant survivors were eradicated by metal oxyanions by 24 h of exposure. As a comparison to literature values, the $MIC_{24\ h}$ values obtained using the CBD method for SeO_3^{2-} and TeO_3^{2-} are approximately equal to the MIC values obtained using alternate microbiological techniques (256, 258).

As a quality control for the CBD experimental system, planktonic cell susceptibility testing was repeated with logarithmic growing planktonic cells prepared similar to a CLSI protocol used for antibiotic susceptibility testing. In these assays, the mean initial cell load was similar to the biofilm cell density per peg of the CBD (see section 4.3.6). $MIC_{24\ h}$, $MBC_{p\text{-}100}$ and $MBC_{b\text{-}100}$ values obtained using this method are also presented in Table 4.2. These values were in most cases similar and consistent with those obtained using the CBD assay. Each value represents the median and range of 4 independent replicates.

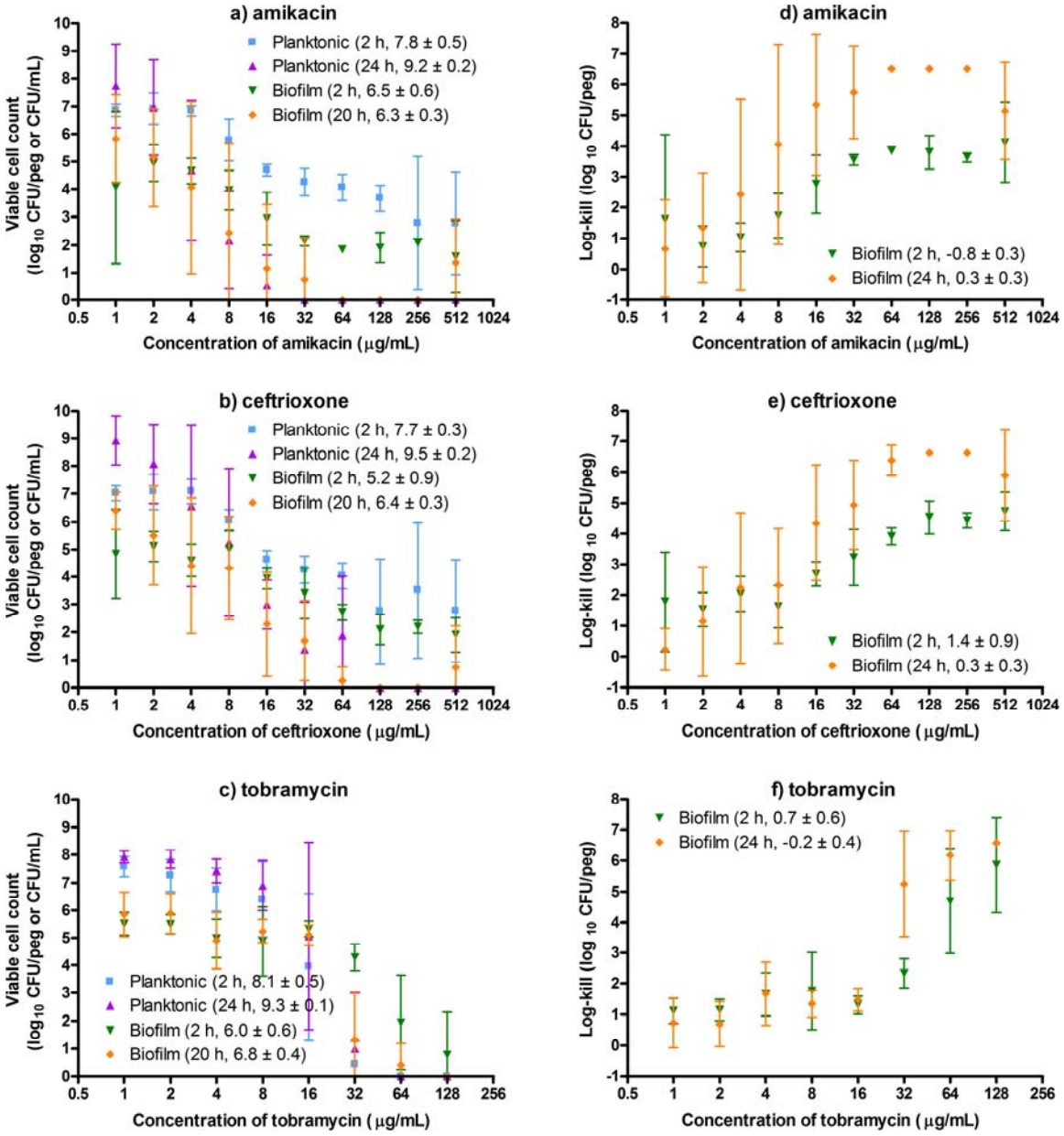

Figure 4.2. Killing of *Escherichia coli* JM109 biofilms and planktonic cells by antibiotics. Biofilms were grown for 24 h on the peg lid of the CBD, then exposed for 2 or 24 h to amikacin, ceftrioxone, or tobramycin in rich (LB) medium. Biofilm and planktonic cultures were recovered in fresh LB media, serially diluted ten-fold, then plated onto agar for viable cell counts. Each data point is the mean of 3 or 4 independent replicates, and error bars denote standard deviation. The mean viable cell counts are reported with respect to concentration of (A) amikacin, (B) ceftrioxone and (C)

tobramycin. The log-killing of biofilm populations is also reported with respect to concentration of (D) amikacin, (E) ceftrioxone and (F) tobramycin. Values in parentheses indicate the means and standard deviations for the viable cell counts or the log-kill calculations for the identically treated growth controls with no added antibiotics. Low concentrations of antibiotics rapidly destroyed the majority of planktonic and biofilm populations. A very small fraction of the population (10^{-3} to 10^{-6}) survived exposure to the highest concentrations of amikacin and ceftrioxone tested (512 μg mL^{-1}). In the case of planktonic cultures, these cells were eradicated by 24 h of exposure. Only tobramycin could effectively eradicate biofilms with 24 h of exposure – in this case at the threshold of the highest concentration assayed (128 μg mL^{-1}). (This figure has been adapted from Harrison *et al*. (2005) Microbiology 151:3181-3195).

Table 4.2. Susceptibility of planktonic and biofilm *Escherichia coli* JM109 to toxic metal oxyanions with 2 or 24 h exposure in rich (LB) medium.

Metal ion	Periodic Group	Time (h)	CLSI method		CBD method			Fold tolerance
			$MIC_{72\ h}$ (mM)	$MBC_{p\text{-}100}$ (mM)	$MIC_{72\ h}$ (mM)	$MBC_{p\text{-}100}$ (mM)	$MBC_{b\text{-}100}$ (mM)[1]	
CrO_4^{2-}	VI B	2	0.54	2.2 (1.1 to 2.2)	1.1 (0.27 to 1.1)	8.8 (8.8 to 18)	18 (8.8 to 32)	2.0
		24		0.54 (0.27 to 0.54)		0.54	0.54	1.0
AsO_4^{3-}	V A	2	nd	>60	29 (7.4 to 60)	>60	>60	na
		24		>60		>60	>60	na
AsO_2^-	V A	2	9.4	>77	4.8 (2.4 to 4.8)	>77	>77	na
		24		75		77	77	1.0
SeO_3^{2-}	VI A	2	8.1	64	8.1 (8.1 to 16)	32	32 (32 to 64)	1.0
		24		16 (8.1 to 16)		8.1	8.1 (8.1 to 16)	1.0
TeO_4^{2-}	VI A	2	nd	1.3	6.7×10^{-2} (4.2 to $8.4\ 10^{-2}$)	>1.1 (1.1 to >1.1)	>1.1 (1.1 to >1.1)	na
		24		1.3 (0.65 to 1.3)		0.33 (0.33 to 0.67)	0.67 (0.33 to 0.67)	2.0
TeO_3^2	VI A	2	1.4×10^{-3} (1.4 to 2.8×10^{-3})	2.2×10^{-2} (2.2 to 4.5×10^{-2})	1.1×10^{-2} (0.55 to 1.1×10^{-2})	3.4×10^{-2} (3.4 to 6.7×10^{-2})	8.7 (9.1×10^{-2} to 8.7)	2.5×10^2
		24		1.1×10^{-2} (0.55 to 1.1×10^{-2})		3.4×10^{-2} (1.7 to 3.4×10^{-2})	3.4×10^{-2} (1.7 to 3.4×10^{-2})	1.0

na indicates a calculation that is not applicable
nd indicates an MIC that was not determined
[1]These values also include determinations of endpoints made using OD_{650} measurements of recovery plates.

4.3.5 Cell survival in planktonic and biofilm **E .coli** *exposed to toxic metal oxyanions*

To examine the survival of planktonic and biofilm bacterial populations following exposure to metal oxyanions, viable cell counts were determined for a range of concentrations following either 2 or 24 h of exposure. Mean viable cell counts and log-killing of biofilm cultures with respect to concentration of CrO_4^{2-}, AsO_4^{3-}, and AsO_2^{-} are presented in Figure 4.3. The data for SeO_3^{2-}, TeO_4^{2-}, and TeO_3^{2-} are presented in Figure 4.4. Every metal oxyanion examined in this study killed a large portion (1 $\log_{10}$ cells or greater) of the biofilm at relatively low concentrations. To continue with the example of TeO_3^{2-}, the majority of both planktonic and biofilm populations were killed at 7 μM TeO_3^{2-} (approximately 1-2 μg mL^{-1}). However, a small fraction of biofilm cells (10^{-5} to 10^{-3}) survived for at least 2 hours at concentrations well in excess of 0.1 mM (16-32 μg mL^{-1}). Together with the data from Table 4.2, a very small number of survivors (below the threshold of detection by viable cell counts) tolerated TeO_3^{2-} at concentrations up to 12 mM (approximately 2048 μg ml^{-1}). This surviving fraction was eradicated by 24 h exposure. Only AsO_4^{3-} did not eradicate biofilm or planktonic cultures with 24 h exposure, and it was only ~1000 CFU per biofilm peg that survived this toxic exposure. High concentrations of CrO_4^{2-}, AsO_2^{-}, SeO_3^{2-}, TeO_4^{2-}, and TeO_3^{2-} completely eradicated biofilms and planktonic cultures with extended exposure times.

There are two features of the CBD that must be addressed here. First, the wells of the microtiter plates containing serial dilutions of metals are inoculated with bacteria shed from the surface of the peg lid. As a consequence, precise initial numbers of planktonic bacteria are unknown and log-killing of planktonic cells cannot be calculated using this method. Here, I address this shortcoming by repeating the susceptibility assays using a defined inoculum (section 4.3.6). However, the former situation *in vitro* may be reflective of naturally existing environmental systems (or as a model of infection) where a biofilm forms a recalcitrant nidus that sheds planktonic cells into its surroundings.

Second (and critical to the seeding of planktonic wells), transfer of the peg lid from the CBD into challenge media disperses a portion of the *E. coli* JM109 biofilm. I have previously noted that for *P. aeruginosa* ATCC 27853 biofilms, this dispersion event is not statistically significant (J.J. Harrison, R.J. Turner and H. Ceri, unpublished

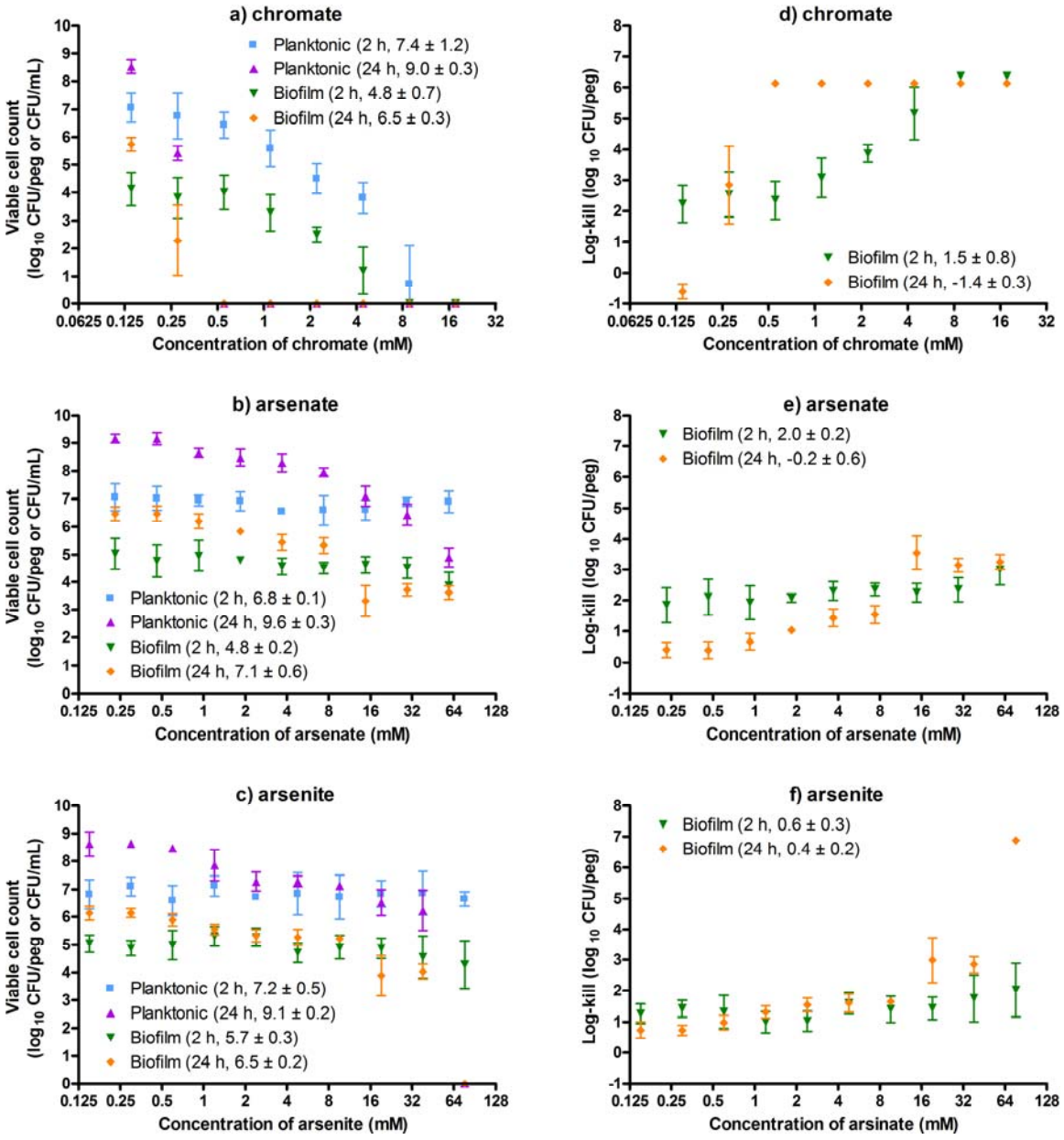

Figure 4.3. Killing of *Escherichia coli* JM109 biofilms and planktonic cells by chromium and arsenic oxyanions. Biofilms were grown for 24 h on the peg lid of the CBD, then exposed for 2 or 24 h to CrO_4^{2-}, AsO_4^{3-}, or AsO_2^{-} in rich (LB) medium. Biofilm and planktonic cultures were recovered in fresh LB media containing a neutralizing agent, serially diluted ten-fold, then plated onto agar for viable cell counts. Each data point is the mean of 3 or 4 independent replicates, and error bars denote standard deviation. The mean viable cell counts are reported with respect to

concentration of (A) CrO_4^{2-}, (B) AsO_4^{3-} and (C) AsO_2^-. The log-killing of biofilm populations is also reported with respect to concentration of (D) CrO_4^{2-}, (E) AsO_4^{3-} and (F) AsO_2^-. Values in parentheses indicate the means and standard deviations for the viable cell counts or the log-kill calculations for the identically treated growth controls with no added metals. In the case of As oxyanions, concentrations in excess of ~5 mM resulted in the death of 99% (or greater a portion) of the biofilm population. The surviving 1% of the population tolerated these highly toxic, heavy metalloids in excess of 50 mM. AsO_4^{3-} did not eradicate these surviving population even at the highest concentration examined (60 mM). Cr oxyanions began to kill bacteria at concentrations as low as 400 μM, however ≤1% of the bacterial population survived for at least 2 h at concentrations of up to 8.8 mM. Notably, CrO_4^{2-} and AsO_2^- eradicated biofilm cultures time-dependently. (This figure has been adapted from Harrison *et al*. (2005) Microbiology 151:3181-3195).

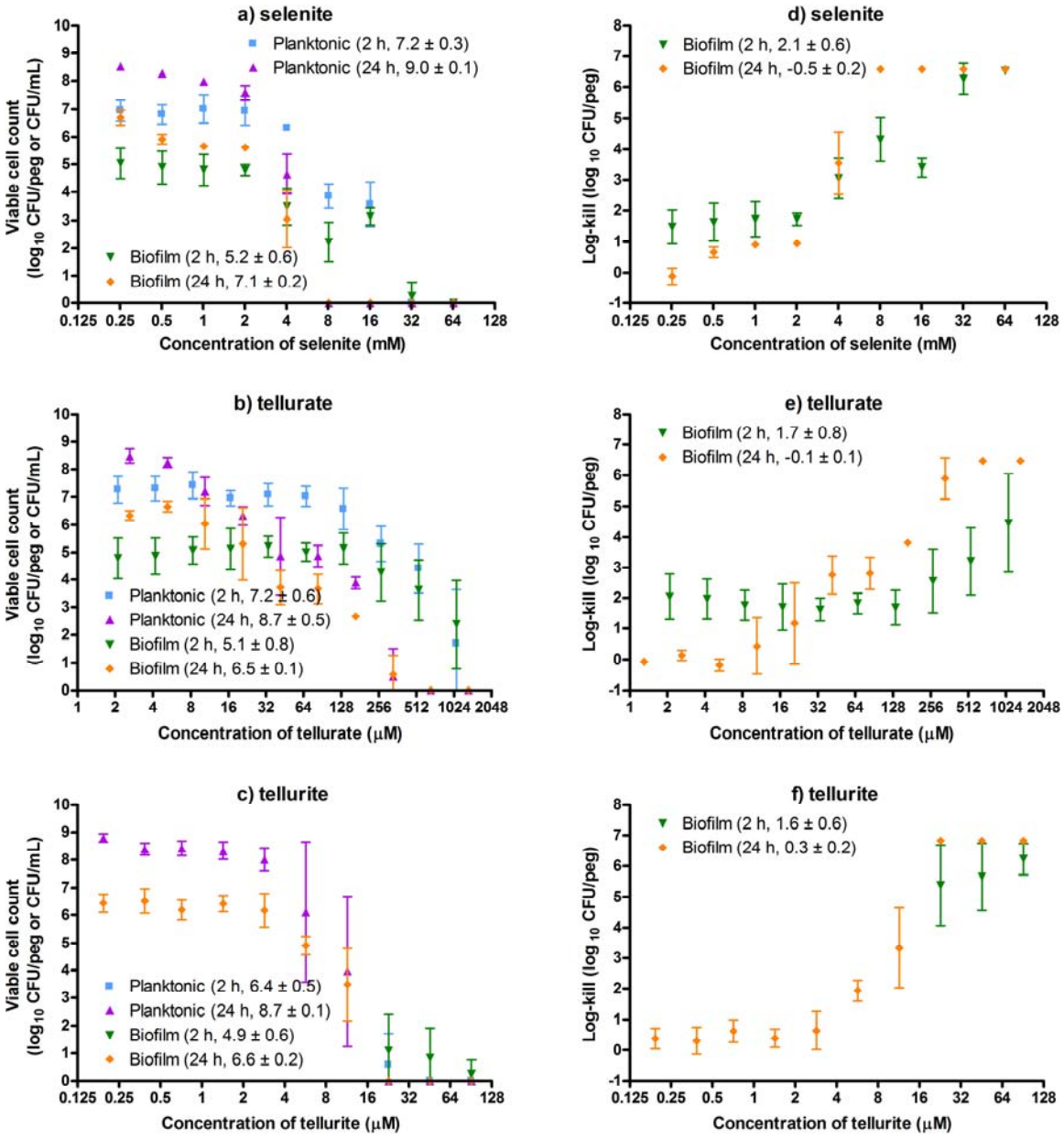

Figure 4.4. Killing of *Escherichia coli* JM109 biofilms and planktonic cells by selenium and tellurium oxyanions. Experimental conditions and data analysis were identical to the conditions described in the legend of Figure 4.3. Mean viable cell counts are reported for 2 and 24 h exposures to (A) SeO_3^{2-}, (B) TeO_4^{2-} and (C) TeO_3^{2-}. The log-killing of biofilm populations is also reported with respect to concentration of (D) SeO_3^{2-}, (E) TeO_4^{2-} and (F) TeO_3^{2-}. Values in parentheses indicate the means and standard deviations for the viable cell counts or the log-kill calculations for the identically treated

growth controls with no added metals. Consistently, only a small percentage of the bacterial population (approximately ≤1%) was observed to survive to high concentrations of these highly toxic metalloid oxyanions. Although the number of survivors in the case of biofilms was somewhat larger, this subpopulation was eradicated time-dependently. In other words, biofilm and planktonic cultures were equally susceptible to these toxic metal species with extended exposure times. (This figure has been adapted from Harrison *et al*. (2005) Microbiology 151:3181-3195).

data). However, the portion of the *E. coli* JM109 biofilm disrupted is larger. In the absence of shear and given sufficient exposure time, the disrupted biofilms resume growth. Here, this may work as an advantage. Mean viable cell counts reported in Figures 4.2 to 4.4 were based on the number bacteria recovered from pegs (including growth controls) after transfer and exposure. However, log-killing was calculated relative to the initial number of bacteria formed in the biofilm before transfer to the challenge media (i.e. log-killing was based on the growth controls used to calculate the mean biofilm cell density of 6.4 ± 0.4 $\log_{10}$ CFU peg^{-1} as described above). From this, it is possible to discern that growth of biofilms occurred during exposure to low concentrations of metal oxyanions. When comparing where the transition between growth and cell death occurs on the log-killing curves in Fig. 4.3 (B, D and F) and Figure 4.4 (B, D and F), biofilms were not observed to grow at concentrations of metal oxyanions greater than the planktonic MIC values reported in Tables 4.2 and 4.3. As noted above, the MIC values in these tables are consistent with literature MIC values and those obtained using a modified CLSI protocol (Table 4.3). This results in the interesting concept that biofilms and planktonic cells may be similarly resistant to growth inhibition by metal oxyanions.

4.3.6 Susceptibility testing of planktonic cells using alternative methods

When comparing the resistance and/or tolerance of planktonic cells and biofilms to metals, there is a possibility that differences in susceptibility may arise due to disparity in starting cell numbers used for MIC, MBC_p and MBC_b determinations. To check for this possibility, a representative oxyanion for each metal was chosen and cell viability testing was repeated using a protocol similar to CLSI guidelines for antibiotic susceptibility assays. Here, the mean and standard deviation of viable cell counts were determined for CrO_4^{2-}, AsO_2^-, SeO_3^{2-} and TeO_3^{2-} and these values are reported in Figures 4.5 and 4.6. The initial cell load using this complimentary method was 6.0 ± 0.5 $\log_{10}$ CFU mL^{-1} and log-killing of planktonic cultures was calculated based on this number. This starting cell number was similar to the starting cell densities of the biofilms tested in the preceding sections ($\sim 10^6$ cells). $MBC_{p\text{-}100}$ values obtained using this alternate method

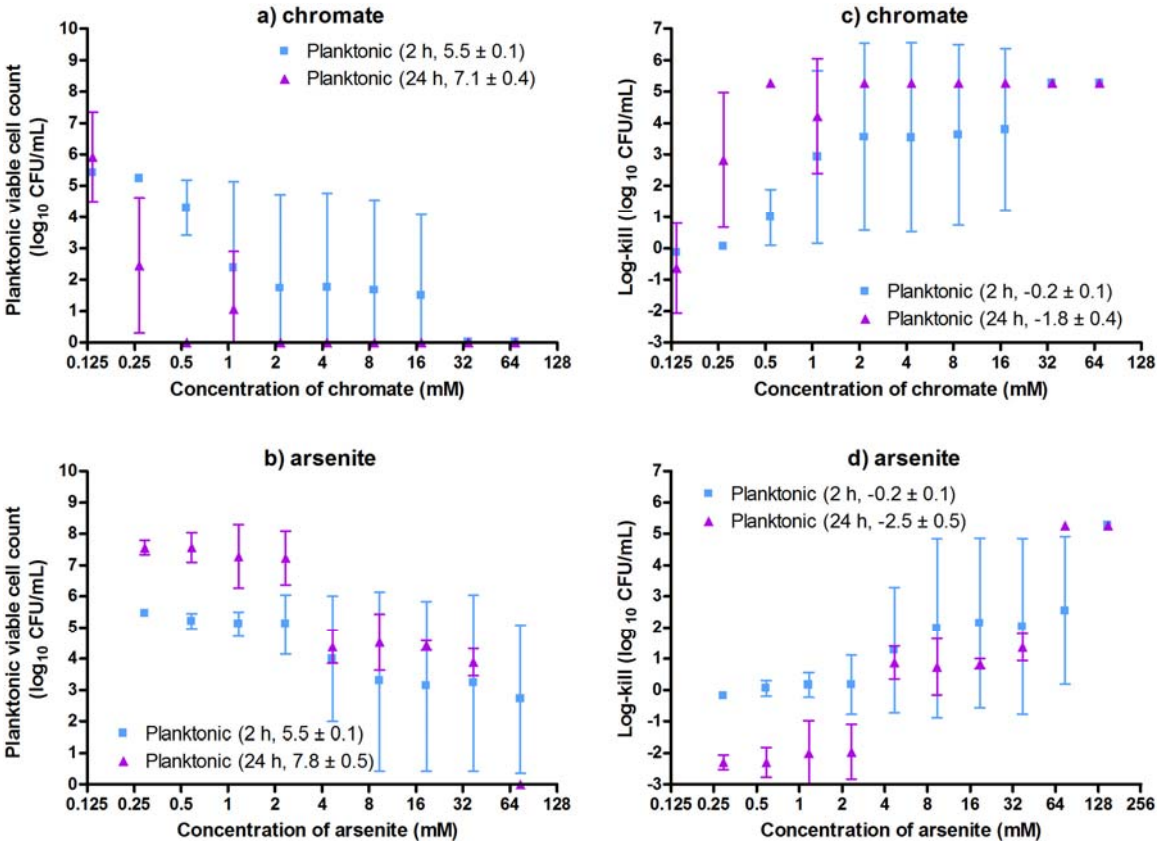

Figure 4.5. Killing of *Escherichia coli* JM109 logarithmic planktonic cells by chromate (CrO_4^{2-}) and arsenite (AsO_2^-). These assays were performed using a protocol designed to reflect a CLSI assay for antibiotic susceptibility testing; however, cell recovery, serial dilution and data analysis were identical to the conditions described in the legend of Figure 4.3 for CBD assays. The log-killing of planktonic cells by metal oxyanions may be calculated using this method since the starting cell number is known. Here, mean viable cell counts are reported for 2 and 24 h exposures to (A) CrO_4^{2-} and (B) AsO_2^-. Log-killing of planktonic cultures is also reported with respect to concentration of (C) CrO_4^{2-} and (D) AsO_2^-. Values in parentheses indicate the means and standard deviations for the viable cell counts or the log-kill calculations for the identically treated growth controls with no added metals. Approximately 0.01 to 1% of planktonic cell populations survived exposure to bactericidal concentrations of these metal oxyanions and this was smaller than the fraction of survivors recovered from biofilms. These kill

kinetics were similar to those obtained using the CBD assay. (This figure has been adapted from Harrison *et al*. (2005) Microbiology 151:3181-3195).

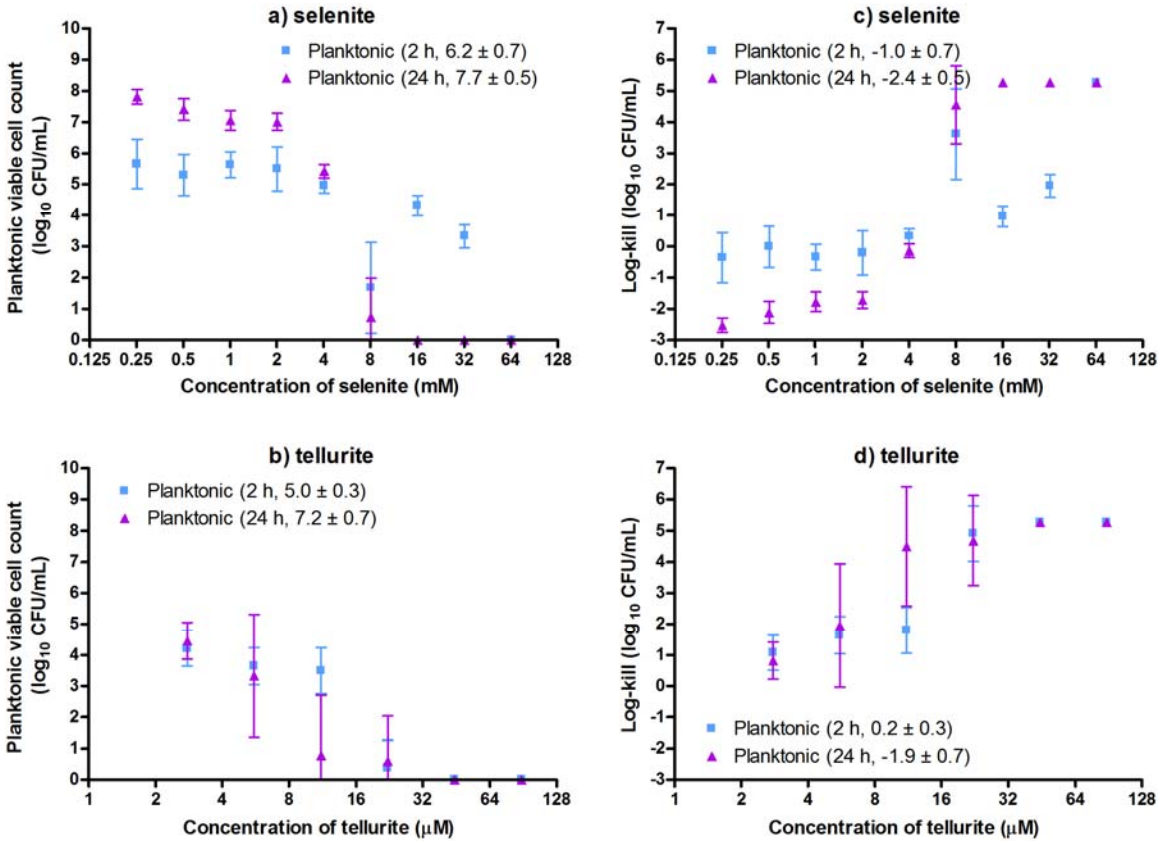

Figure. 4.6. Killing of *Escherichia coli* JM109 logarithmic planktonic cells by selenite (SeO_3^{2-}) and tellurite (TeO_3^{2-}). These assays were performed using a protocol designed to reflect a CLSI assay for antibiotic susceptibility testing; however, cell recovery, serial dilution and data analysis were identical to the conditions described in the legend of Figure 4.3 for CBD assays. The log-killing of planktonic cells by metal oxyanions may be calculated using this method since the starting cell number is known. Here, mean viable cell counts are reported for 2 and 24 h exposures to (A) SeO_3^{2-} and (B) TeO_3^{2-}. Log-killing of planktonic cultures is also reported with respect to concentration of (C) SeO_3^{2-} and (D) TeO_3^{2-}. Values in parentheses indicate the means and standard deviations for the viable cell counts or the log-kill calculations for the identically treated growth controls with no added metals. Less than 1% of planktonic cell populations survived exposure to highly toxic metal oxyanions. These kill kinetics were similar to those obtained using the CBD assay. (This figure has been adapted from Harrison *et al*. (2005) Microbiology 151:3181-3195).

were generally within $\log_2$ of the values obtained using the CBD method. Notably, the proportion of surviving cells was smaller than the fraction of survivors recovered from biofilms. This supplementary work serves as an important quality control to for making comparisons between the susceptibility of planktonic cells and biofilms to metals using the CBD.

4.3.7 Adsorption and reduction of metal oxyanions by E. coli biofilms

As described in Chapter Three, biofilms of *P. aeruginosa* ATCC 27853 adsorb copper cations (105). Here, I addressed the question whether the observed time-dependent killing of *E. coli* JM109 may be partly due to oxyanion adsorption to the biofilm matrix. As a control, I exposed biofilms of *E. coli* JM109 to Cu^{2+} for 24 h, rinsed the biofilms with 0.9% NaCl, then treated the exposed biofilms with Na_2DDTC. Correlative to my previous observations, Na_2DDTC caused the formation of dark brown metal-chelates in the biofilm (Figure 4.6 A, D and G). However, Na_2DDTC did not cause the characteristic colorimetric coordination of oxyanions in biofilms exposed to either CrO_4^{2-} (Figure 4.7 B, E and H) or TeO_3^{2-} (Figure 4.7 C, F and I). Surprisingly, this would suggest that adsorption of oxyanions by biofilm biomass may not be the primary mechanism of the observed time-dependent tolerance of biofilms to either CrO_4^{2-} or TeO_3^{2-}.

Of note, the reduction of periodic group 6A oxyanions, SeO_3^{2-} (data not shown) and TeO_3^{2-} (Figure 4.7 C and I) to orange and gray-black end products, respectively, was mediated by both planktonic and biofilm cultures of *E. coli* JM109. For planktonic cultures exposed to TeO_3^{2-}, this was observed as gray discoloration in the challenge media after 24 h exposure (Figure 4.7 C). In biofilms, gray-black bands could be observed at the biofilm air-liquid-surface interface (Figure 4.7 I).

4.3.8 Survival of the E. coli hipA7 mutant after exposure to toxic metal oxyanions

To directly test if persister cells might be responsible for bacterial tolerance to metal oxyanions, a *hipA7* strain of *E. coli* was examined. *hipA7* is a gain-of-function allele of *hipA* that increases the proportion of persisters in biofilms and stationary phase

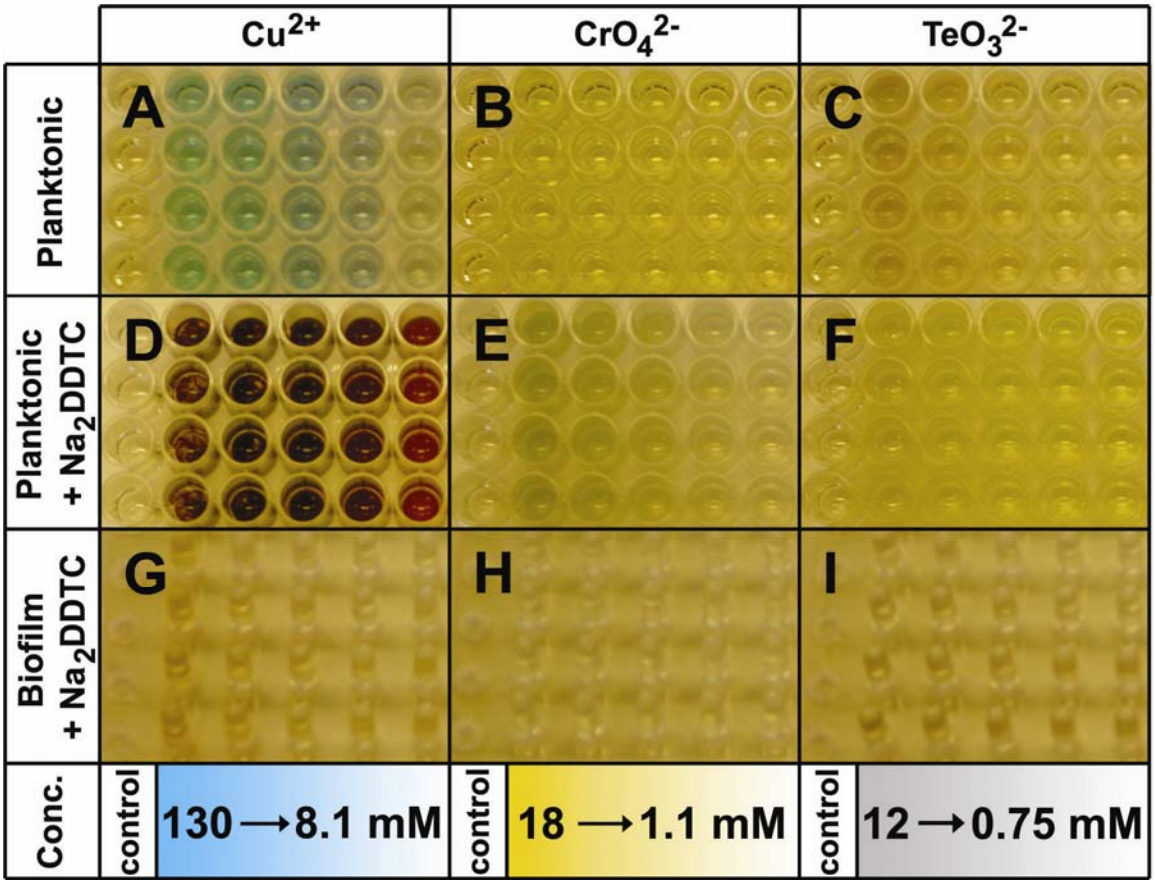

Figure 4.7. Metal oxyanions were not trapped in biofilms of *Escherichia coli* JM109. Planktonic cultures of *E. coli* JM109 were exposed to (A) Cu^{2+}, (B) CrO_4^{2-} or (C) TeO_3^{2-} for 24 h, then reacted with 37.5 mM sodium diethyldithiocarbamate (Na_2DDTC). Complexation of Cu^{2+}, CrO_4^{2-}, and TeO_3^{2-} with Na_2DDTC resulted in an instantaneous color change of planktonic cultures to (D) dark brown, (E) green and (F) bright yellow, respectively. Biofilms exposed to (G) Cu^{2+} also underwent a color change, indicating that this metal may be retained within *E. coli* biofilms. By contrast, (H) CrO_4^{2-} and (I) TeO_3^{2-} exposed biofilms did not change to a color characteristic of the metal-chelator complex. However, with 24 h exposure to TeO_3^{2-}, biofilms and planktonic cultures turned grey-black, a hallmark of intracellular Te reduction. These observations suggest that negatively charged metal ions may have low affinity for biofilm biomass. The left hand well of every panel is a sterility control. Growth controls not exposed to metals (not shown) did not change color in any assay. (This figure has been reproduced by permission from Harrison *et al*. (2005) Microbiology 151:3181-3195).

planktonic cultures (131). Stationary phase *E. coli* HM21 (wild type) and HM22 (*hipA7*) were exposed to AsO_4^{3-}, AsO_2^{-}, SeO_3^{2-}, TeO_3^{2-}, TeO_4^{2-}, and CrO_4^{2-} for 6 h then enumerated. Relative to the wild type strain, *E. coli* HM22 (*hipA7*) had an 82-, 76- and 5-fold increased proportion of survivors after exposure to TeO_3^{2-}, TeO_4^{2-}, and CrO_4^{2-}, respectively (Figure 4.8). At the highest concentrations of AsO_4^{3-}, AsO_2^{-} and SeO_3^{2-} tested against *E. coli* JM109, there was insufficient killing of *E. coli* HM21 and HM22 stationary phase cultures at 6 h exposure to observe a hypertolerant phenotype for the *hipA7* mutant (Figure 4.8). The starting number of cells for *E. coli* HM21 and HM22 were 8.7 ± 0.6 and 8.1 ± 0.6 $\log_{10}$ CFU mL^{-1}, respectively. It is interesting to note that *E. coli* HM22 seemed to enter stationary phase at lower cell densities than *E. coli* HM21, although this difference was not statistically significant (data not shown).

4.4 Discussion

In this Chapter, high-throughput susceptibility testing, using the CBD and CLSI broth microdilution techniques, was used to screen the time- and concentration-dependent killing of biofilm and planktonic cells of *E. coli* JM109 by metal oxyanions. *E. coli* JM109 is a laboratory strain with a long history of use in studies of metal resistance. Here, the CBD provided three internally consistent measurements from a single experiment: the $MIC_{24\ h}$, the $MBC_{p\text{-}100}$ the $MBEC_{b\text{-}100}$. In this assay system, planktonic cells used in susceptibility testing were shed from the surfaces of the biofilms, reproducing *in vitro* the characteristic duality of the natural bacterial ecological cycle. This feature is unique to the method used here. As a control for this experimental system, $MIC_{24\ h}$ and $MBC_{p\text{-}100}$ values attained using this technique were compared to those discerned using a modified CLSI protocol. Initial cell numbers used in these additional assays were similar to biofilm cell densities in the CBD. The $MIC_{24\ h}$ and $MBC_{p\text{-}100}$ values obtained from both methods were similar (serving as an important quality control for this experimental system). Subsequently, combinations of exposure times and metal concentrations were rapidly examined using the CBD, which would not have been pragmatic using alternate approaches. To validate this model, I have reexamined the biofilm persister cell hypothesis proposed by Spoering & Lewis (2001). Consistent with

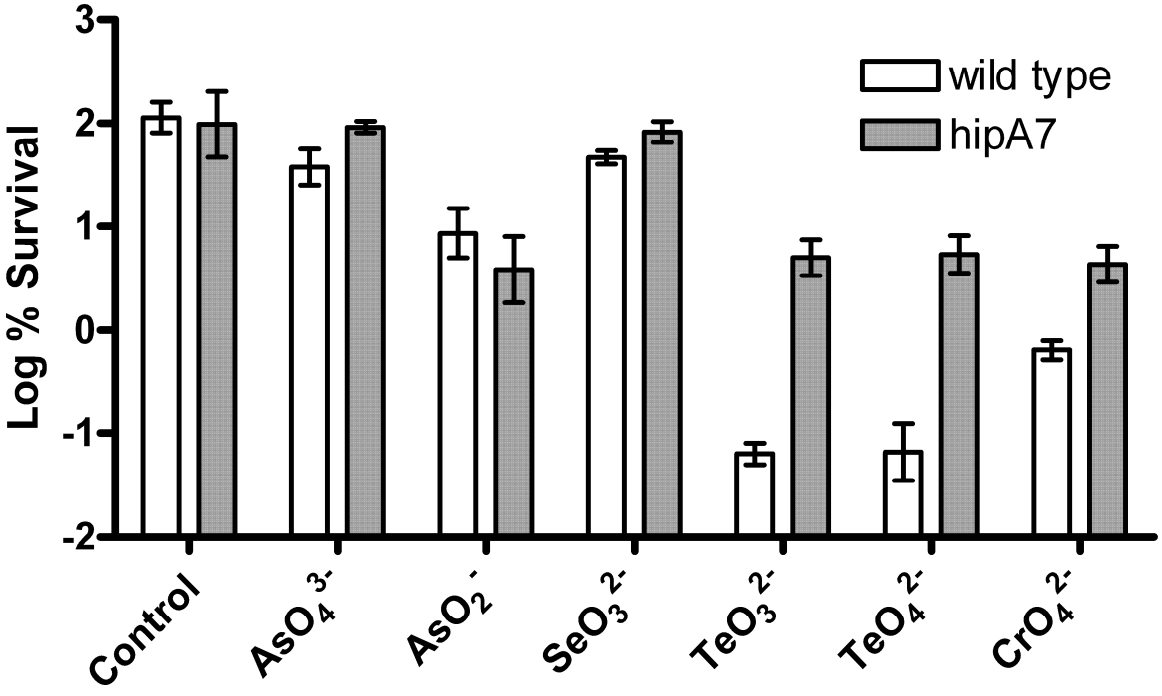

Figure 4.8. The *hipA7* allele increases the survival of stationary-phase planktonic cells of *Escherichia coli* JM109 exposure to toxic metal oxyanions. There was approximately a 5- to 82-fold increase in the fraction of *E. coli* HM22 (*hipA7*) cells that survived 6 h exposure to tellurium and chromium oxyanions relative to *E. coli* (HM21) (wild type). At the concentrations used in this assay, which were greater than or equal to the highest concentrations used in biofilm susceptibility assays, the arsenic and selenium oxyanions did not significantly decrease the number of viable stationary-phase planktonic cells. Each bar represents the mean and standard deviation of 3 replicates. The concentrations of metals used for this assay were: 308 mM AsO_4^{3-}, 152 mM AsO_2^{-}, 64 mM SeO_3^{2-}, 91 μM TeO_3^{2-}, 1.3 mM TeO_4^{2-}, and 2.2 mM CrO_4^{2-}.

previously reported results, here it was observed that biofilms of *E. coli* remained highly tolerant to antibiotics for long exposure times (98, 270). Further, this tolerance was mediated by a very small portion of the adherent bacterial population (230).

E. coli HM22 (*hipA7*) – well known for its ability to produce a large subpopulation of persister cells recalcitrant to killing by bactericidal antibiotics – also produced a subpopulation of multimetal tolerant cells that was larger than the isogenic, wild type strain. Biofilms of *E. coli* JM109 presented with a transient, time-dependent tolerance to metal oxyanions that was up to two orders of magnitude greater than planktonic cells. Long exposures to these highly toxic substances resulted in destruction of planktonic cells and biofilms at similar concentrations of metal oxyanions. Consistent with the persister cell hypothesis, this short term tolerance was mediated by a small fraction of the biofilm population (10^{-3} or less). It was also observed that the short term tolerance of planktonic cells was mediated by an even smaller subpopulation of cells. As noted in Chapter Three, two potential explanations for this phenomenon are: 1) that persister cells in a biofilm are killed at a reduced rate by metal oxyanions relative to the planktonic persister population, or 2) that there is a greater population of persisters in a biofilm that are killed at the same rate as planktonic persister cells. In the first case, it is interesting to speculate that there may be a faster persister cell to vegetative cell transition rate in planktonic as opposed to biofilm populations. Nonetheless, metal ion killing is different from antibiotic killing of biofilms, where in the case of the latter cell death typically reached a plateau characterized by a lack of further antibiotic efficacy (even with prolonged exposure or increased antibiotic concentrations). In the case of tobramycin, which eradicated biofilms by 24 h exposure, biofilms remained 12-times more tolerant to killing than the corresponding planktonic cells. Thus, these data would suggest that metal oxyanions possess a bactericidal action capable of destroying biofilm persister cells. To reaffirm this notion, we have observed in a subsequent study that stationary phase *E. coli* HM22 (*hipA7*) may be sterilized by AsO_4^{3-} with 24 h exposure (J.J. Harrison, R.J. Turner and H. Ceri, unpublished data).

The role of *E. coli* biofilm biomass in adsorption of metal cations and oxyanions had previously been unexamined. Here, metal oxyanions may have equilibrated across

the biofilm matrix at a slowed rate due to steric and/or ionic hindrance (234). Intuitively, we can be confident that complete penetration of the biofilm eventually occurred if the biofilms were eradicated. The observation that the chelator Na_2DDTC does not result in precipitation or coordination of metal oxyanions in exposed biofilms supports the idea that the *E. coli* JM109 ECM may have low affinity for adsorbing and/or binding metal oxyanions. This was not the case for the divalent heavy metal cation Cu^{2+}, which was retained and formed metal precipitates in similarly treated biofilm cultures. These observations are consistent with reports that the *E. coli* ECM is polyanionic (for a review, see 245). Colanic acid, which is known to be important in *E. coli* biofilm formation (195), is the major extracellular polysaccharide of most *E. coli* strains (86, 276). Further evidence for the low affinity of the matrix for metal oxyanions was the observed reduction of TeO_3^{2-} by biofilms.

The reduction of TeO_3^{2-} by *E. coli* is well documented (284). Reduction of TeO_3^{2-} to gray-black colored, colloidal Te^0 is an intracellular reaction potentially mediated by through several biochemical routes (284). Insoluble Te^0 closely associates with cell membranes (156), giving bacterial cultures a characteristic gray-black color. The observation that *E. coli* biofilms turn gray-black after exposure to TeO_3^{2-} is evidence of intracellular Te accumulation and entrapment. This is evidence that the biofilm matrix may not sequester metal oxyanions in the extracellular milieu. A similar case can be made for SeO_3^{2-} reduction, another group 6A chalcogen with similar chemistry to TeO_3^{2-} (258, 284). In the present study, *E. coli* biofilms also reduced SeO_3^{2-} to Se^0, which resulted in the accumulation of orange-red end products on the pegs (data not shown).

A characteristic attributed to persister cells is the ability to give rise to a new population with normal antimicrobial susceptibility (25, 130, 168, 230). I have thus addressed this question for *E. coli* JM109, but have not shown the data here. Survivor cells cultivated after exposure to mercury (Hg^{2+}), then to copper (Cu^{2+}), and finally to Cu^{2+} again, yielded a similar proportion of metal survivors in the newly generated populations, and produced cultures with normal susceptibility to metals (J.J. Harrison, H. Ceri, and R.J. Turner, unpublished data). A similar phenomenon occurred for *P. aeruginosa* ATCC 27853, which was described in Chapter Three. Collectively, this

would indicate that the survivors are not mutants within the bacterial culture, but rather specialized phenotypes produced by a genetically homogeneous population. By definition, persister cells are not mutants, and so it is possible that the survivors of metal exposures may also be persisters.

In *E. coli*, the proportion of persisters in the bacterial population is in part controlled by the high persistence (*hip*) operon (131, 139, 168). The *hipA7* mutant produces 10- to 1000-times more persister cells than wild type *E. coli* as it approaches stationary phase (131, 139). Since the *hipA7* mediated high persistence phenotype was abolished in a *relA*$^-$ *spoT*$^-$ background, Korch and colleagues (2003) postulated that (p)ppGpp synthesis may govern the 'persistent' physiological state. More than 80 homologues of the *hipA* gene have been identified in Gram-negative and Gram-positive bacteria (139). It is unknown what role the stringent response (which is also governed by (p)ppGpp synthesis) plays in the production of persister cells. However, it is known that stringent response regulated genes play an important role in both *E. coli* biofilm formation (13), entry into stationary phase, bacterial adaptation to nutrient limitation and oxidative stress (45). The 'persistent' response of *hip* mutants not only reduces cell death due to antibiotic exposure, but also reduces the lethality of heat shock (216) and metabolic block (i.e. starvation for diaminopimelic acid) (168). I acknowledge that some of these mechanisms may share overlapping features with each other and the effects of metal toxicity.

Metal oxyanions are considered to exert toxicity through oxidative stress (241, 258, 259). Additionally, AsO_4^{3-} is toxic by virtue of substitution for inorganic phosphate in glycolytic intermediates, abrogating ATP producing enzymatic steps through spontaneous hydrolysis of arsenophosphates in water (for a review, see 165). Although the precise mechanism is unknown, TeO_3^{2-} ultimately functions to uncouple the *E. coli* transmembrane ΔpH gradient (157). In both cases, ATP levels would be lowered in sensitive cells, mimicking the effects of starvation. Thus the data in this study and in the literature suggest that persistence may be part of an underlying, highly conserved and generalized mechanism for bacteria to tolerate environmental duress.

Biofilms are infamous for their ability to withstand antimicrobials. Here, biofilms did not grow at concentrations of metal oxyanions in excess of the planktonic minimum inhibitory concentration (MIC). Based on these data, biofilms may not be labeled resistant. However, biofilms did withstand concentrations of metal oxyanions far in excess of the planktonic minimum bactericidal concentration ($MBC_{p\text{-}100}$). Therefore, biofilms may be considered highly 'tolerant' to metal oxyanions.

Persisters are known to survive high levels of antibiotics for prolonged exposure times. As it pertains to our model system and *Escherichia coli* JM109, this is not true for metal oxyanions. In fact, given long exposures, metal oxyanions destroyed biofilms at concentrations similar to planktonic bacteria. In this study, I observed that 1% or less of the biofilm population survived for short periods of time at concentrations of metal oxyanions in excess of the concentration required to eradicate planktonic bacteria ($MBC_{p\text{-}100}$). Lastly, the proportion of surviving cells in stationary phase cultures of an *E. coli hipA7* mutant was greater than that for wild-type bacterial cultures. It is an unfortunate experimental limitation that the *E. coli* strains bearing *hipA7* did not form robust biofilms in the CBD. At the time of writing this thesis, I am testing a series of in-frame, markerless deletion mutants bearing singly inactivated toxin or antitoxin genes to link TA modules to the sizes of survivor populations in drug and metal exposed biofilms. Nonetheless, based on the collective data in this Chapter it is reasonable to hypothesize that persister cells might mediate the time-dependent tolerance of *E. coli* biofilms to metal oxyanions, that the production of these cells is linked to chromosomal TA modules, and that certain metal oxyanions may be lethal to the slow-growth phenotype possessed by these cells.

4.5 Contributions

4.5.1 Author's contributions to this work and personal acknowledgements

I performed about 50% of the experimental work described in this Chapter. In the process of doing this work, I trained 3 undergraduate students (Erin A. Badry, Kimberley M. Sproule and Nicole J. Roper) to assist with the remainder of the bench work. Electron

microscopy was performed by Liz Middlemiss, a technician employed by Innovotech Inc. Additonal thanks to Dr. Kim Lewis for kindly providing *E. coli* strains HM21 and HM22.

4.5.2 Relevant publications

These data sets were originally published in Harrison *et al*. (2005) Microbiology 151:3181-3195.

Chapter Five: Multimetal resistance and tolerance are linked to phenotypic variation controlled by the GacS sensor kinase in *Pseudomonas aeruginosa* PA14

5.1 Introduction

In the previous two Chapters, I have provided evidence that biofilms have increased tolerance to toxic metal species relative to planktonic cell populations. So far, the data in this thesis suggest that biofilm multimetal tolerance might be mediated by subpopulations of persister cells in bacterial cultures as well as by metal ion sequestration via reversible adsorption to biomass. However, the existence of persister cells and the restricted diffusion of ions cannot explain the resistance properties of biofilms that, at least anecdotally, are well known in many industrial and clinical settings. The research in this Chapter was undertaken to assess whether other phenotypic variants, which are known to arise at high frequency in biofilms, might contribute to biofilm multimetal resistance and tolerance. Here, I chose to investigate this problem by examining *Pseudomonas aeruginosa* and a serendipitously discovered link between colony morphology variation and the GacS/GacA signal transduction system.

P. aeruginosa is successful at adapting to a wide variety of environmental niches such as soil, water, plants and animals. GacS/GacA (global activator of antibiotic and cyanide synthesis) is one of 66 two-component regulatory systems that *P. aeruginosa* uses to alter its physiology to suit these diverse environmental conditions. The GacS/GacA system regulates the expression of virulence factors, stress tolerance genes, enzymes for secondary metabolism, as well as periplasmic proteins important for motility (84, 267). The response regulator GacA is vitally important for biofilm formation and maturation in multihost virulent *P. aeruginosa* PA14 (183). This two-component system is highly conserved among a wide range of *Pseudomonas* species (61) and has been well characterized in rhizosphere strains of *P. syringae* and *P. chlororaphis* (229).

In later stages of development, biofilm growth and behaviour may be coordinated by quorum sensing (QS), a process that relies on intercellular signalling by N-acyl-homoserine lactones (AHSLs) (127, 227). In *P. aeruginosa*, GacA is a positive transcriptional regulator of the *lasRI* and *rhlRI* operons, which are responsible for the

enzymes that synthesize N-3-oxo-dodecanoyl-homoserine lactone (3-oxo-C12-HSL) and N-butanoyl-homoserine lactone (C4-HSL), respectively. Loss-of-function mutations in *gacS* and/or *gacA* in *Pseudomonas* species reduce production of these autoinducers (49, 183). *In vitro*, these QS-systems are pivotal for *P. aeruginosa* biofilm tolerance to hydrogen peroxide, aminoglycoside antibiotics, and polymorphonuclear leukocytes (26). It is a paradox that, despite roles in stress tolerance and survival, spontaneous mutations in *gacS* and/or *gacA* have been observed in many pseudomonads under laboratory conditions as well as in the plant rhizosphere (38, 70, 213, 263).

As it turns out, mutation of *gacS* is not associated with a loss-of-fitness of pseudomonads in the environment (193, 217). Using *P. chlororaphis* as an example, studies have suggested that mixtures of *gacS*$^-$ mutants with the wild-type population may enhance the survival of this bacterium in soil (43). Preliminary evidence suggests that this may be linked to phenotypic variation (213). Our research group has recently discovered that inactivation of *gacS* in *P. chlororaphis* and in *P. fluorescens* gives rise to highly adherent colony morphotype variants from aged biofilms exposed to certain metal ions (M.L. Workentine, J.J. Harrison, L.L.R. Marques, H. Ceri, R. J. Turner, A.J. Anderson, Y.C. Kim and M.E. Olson, unpublished data). In general, these isolates are less motile and are superior at forming biofilms, which might be part of an important process for root colonization (108). Interestingly, this process has not been examined in the soil bacterium and opportunistic human pathogen *P. aeruginosa*, and here it was specifically hypothesized that GacS may be similarly involved in phenotypic variation. This may be important because GacS/GacA signalling in this microorganism has been implicated in attenuating virulence and establishing chronic infections in the cystic fibrosis (CF) lung (84, 266). Furthermore, the isolation of antimicrobial resistant colony morphology variants with an increased ability for forming biofilms has been described for many laboratory and clinical strains of *P. aeruginosa* (30, 69, 110, 111, 134).

In this Chapter, a *gacS*$^-$ strain of *P. aeruginosa* PA14, which had been previously constructed by another graduate student in the Biofilm Research Group (James A. Davies), was examined in order to assess the physiological role of this sensor histidine kinase. This loss-of-function mutation was associated with hypermotility, reduced

production of AHSLs, impaired biofilm maturation, and decreased antimicrobial resistance. Relative to controls, biofilms of the *gacS*⁻ mutant gave rise to phenotypically stable small colony variants (SCVs) with increasing frequency when exposed to some clinically used antibiotics (tobramycin, amikacin, azetronam, ceftrioxone, oxacilin, piperacillin or rifampicin), hydrogen peroxide (H_2O_2) and silver cations ($AgNO_3$). When cultured, the SCVs produced thicker biofilms with greater cell density and greater antimicrobial resistance and/or tolerance than did the wild-type or parental *gacS*⁻ strains. Similar to other colony morphology variants described in the literature, this SCV was less motile than the wild-type strain and autoaggregated in broth culture. Complementation with *gacS in trans* restored the ability of the SCV to revert to a normal colony morphotype. These findings indicate that mutation of *gacS* is associated with the occurrence of stress resistant SCV cells in *P. aeruginosa* biofilms and suggests that in some instances GacS may be necessary for reversion of these variants to a wild-type state.

5.2 Materials and methods

5.2.1 Standard protocols

The bacterial strains used in this study are summarized in Table 5.1 and these strains were stored, handled and cultured as described in Chapter Two. Biofilms were cultivated by growing *P. aeruginosa* at 35 °C in the trough format of the Calgary Biofilm Device (CBD) for the desired incubation time using TSB medium. Unless otherwise indicated, *E. coli* was grown in LB at 35°C, and alternatively, nutrient agar or LB agar was used to culture these bacteria. Biofilm antibiotic and metal susceptibility testing as well as confocal laser scanning microscopy (CLSM) were performed using the CBD and were carried out according to the standard protocols described in Chapter Two. Note that phosphate buffered saline (PBS, pH 7.2) containing the anionic surfactant Tween-20 (1% v/v) was used to assist in bacterial recovery from the peg surfaces, and here, biofilms were sonicated for 30 min instead of the standard 5 min described in Chapter Two. This

extended sonication time was required to maximally recover biofilm cells of the highly adherent SCV strain (data not shown).

5.2.2 Swim and swarm assays

Swim assays were carried out on a semisolid medium composed of LB broth ammended with 0.3% w/v agar. Swarm assays were carried out on a modified M9 medium which contained 3.0 g KH_2PO_4, 6.0 g Na_2HPO_4, 0.5 g NaCl, 0.5 g L-glutamate, 2.0 g dextrose, and 5.0 g agar per liter of double distilled water (ddH_2O). This medium was autoclaved and enriched with 1 mL of 1 M $MgSO_4$ and 1 mL of 0.01 M $CaCl_2$. One microliter aliquots of overnight bacterial cultures were spotted into the middle of the swim or swarm plates, which were incubated for 72 h at room temperature and 35 °C, respectively. Swim diameter was measured and plates were photographed using a Kodak EasyShare C340 digital camera.

Table 5.1. Strains and plasmids used in Chapter Five.

Strain or plasmid	Genotype or description	Source
Escherichia coli		
MG4	reporter strain	(186)
Pseudomonas aeruginosa		
PAO-JP2	Δ*rhlI::Tn501* derivative of wild type PAO1, Δ*lasI*, Hg^R Tc^R	(187)
UCB-PP PA14	clinical isolate	(201)
PA14 *gacA*$^-$	PA14 Δ*gacA*::gm^r	(201)
PA14 *gacS*$^-$	PA14 Δ*gacS*::gm^r	(59)
PA14 SCV	PA14 Δ*gacS*::gm^r small colony variant	(59)
Plasmids		
pUCP18mpgacS	pUCP18 containing a 3.4 kb fragment amplified from *P. aeruginosa* PA14 containing the entire *gacS* gene and flanking sequences	(59)
pECP61.5	*rhlA::lacZ* reporter construct	(187)
pKDT17	*lasB::lacZ* reporter construct	(186)

5.2.3 N-Acyl-homoserine lactone determinations

For quantification of 3-oxo-C12-HSL and C4-HSL, the AHSL biosensors *Escherichia coli* MG4 (pKDT17) (186) and *P. aeruginosa* PAO-JP2 (pECP61.5) (187) were used. These systems quantify 3-oxo-AHSL and C4-AHSL production based on the measurement of β-galactosidase activity from *lasB::lacZ* and *rhlA::lacZ* reporter constructs, respectively. The method has been previously described by Pearson *et al.* (186, 187).

5.2.4 Calculations and definitions of measurements

Calculations of mean viable cell counts, mean log-kill measurements and tests for equivalent growth using one-away ANOVA were performed according to the guidelines set in Chapter Two. The definitions of endpoints used to measure biofilm susceptibility ($MIC_{72\ h}$, $MBC_{b\text{-}q}$ and $MBC_{b\text{-}99.9}$) are the same as those used in Chapter Three.

5.3 Results

5.3.1 Creation of a gacS⁻ cell line from P. aeruginosa PA14

The *gacS* gene was inactivated by allelic exchange for a gentamicin resistance marker from a donor plasmid containing *sacB*. PA14 cells that were sucrose resistant (which selected for loss of the donor plasmid) and gentamicin resistant were assessed for interruption of *gacS* by determining the size and sequence of the PCR product based on primers corresponding to the *gacS* gene. The resulting cell line was thus verified by the production of appropriately sized PCR products and this engineered strain was denoted *P. aeruginosa* PA14 *gacS*⁻ (data not shown, note that this work was done by J. A. Davies).

5.3.2 Origin of the small colony variant

When disrupted and plated onto agar, solid surface attached biofilms of *P. aeruginosa* PA14 *gacS*⁻ that were older than 24 h produced two distinct colony morphologies. After overnight incubation at 35 °C, the majority of these colonies were shiny, smooth, light yellow or pale green, and 3-5 mm in diameter. These colonies were

similar to those produced by the wild type organism, with the exception of the slightly greater colony diameter produced by the mutant. A minority of colonies exhibited abrupt edges and were much smaller than colonies produced by either wild type or *gacS*$^-$ strains of *P. aeruginosa* PA14. It was hypothesized that these colonies represented a small colony variant (SCV) of the original *gacS*$^-$ strain.

These SCV isolates were evaluated for growth on *Pseudomonas* isolation agar and for gentamicin resistance (the marker for the *gacS*$^-$ mutation), as well as by PCR analysis and Gram-staining. These tests were consistent with the premise that the variants were derived from the parental *gacS*$^-$ strain (data not shown). The SCVs were stable and no reversion to normal colony morphology was observed, even after three days incubation in broth medium or 45 days serial culture on nutrient agar at room temperature. Phenotypically stable small colony variants were not observed originating from cultures of wild type *P. aeruginosa* PA14 or the isogenic PA14 *gacA*$^-$ mutant. Rather, these strains produced colony variants that reverted to the normal colony morphotype after subculture on LB agar (this was replicated 5 to 20 times for each strain). When PA14 SCV was transformed with the plasmid pUCP18mpgacS (bearing the wild type *gacS* gene and flanking DNA sequences), the SCV reverted to the wild type colony morphology with a frequency of approximately 10^{-1}.

5.3.3 Strain characterization and biofilm growth

Since inactivation of the response regulator GacA is known to affect the ability *P. aeruginosa* PA14 to form biofilms (183), a first logical step was to evaluate biofilm development by *P. aeruginosa* PA14 wild type (PA14 wt), the *gacS*$^-$ sensor kinase mutant (PA14 *gacS*$^-$) and the isolated small colony variant (PA14 SCV). Relative to either PA14 wt or PA14 *gacS*$^-$, PA14 SCV produced biofilms of greater cell density between 4 and 10 h of growth in Luria-Bertani (LB) medium (Figure 5.1 A). By 24 h, these three strains produced biofilms with an equivalent mean viable cell count. However, the biomass produced by these three strains was not equal. For instance, the extracellular polymeric substance produced by the SCV strain was visible to the naked eye (data not shown). There were no strain differences in the rates of planktonic cell

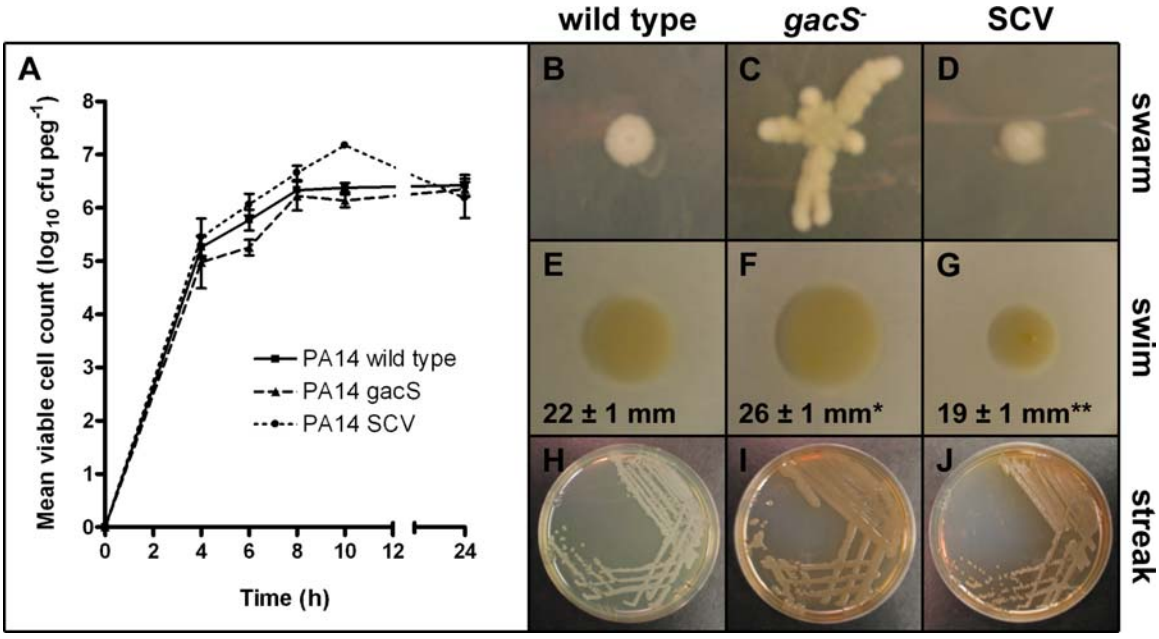

Figure 5.1. Phenotype characteristics of *Pseudomonas aeruginosa* PA14 wild type, *gacS*⁻ and small colony variant (SCV) strains. (A) Growth curves of biofilms on polystyrene pegs in the CBD. (B to D) Swarming motility of the PA14 *gacS*⁻ strain was much greater than that of the other isogenic strains. (E to G) Similarly, the *gacS*⁻ strain was significantly more motile than the wild type strain on swim agar (* $p < 0.01$ by a two sample T-test, 4 replicates each). Conversely, PA14 SCV was significantly less motile than the wild type strain (** $p < 0.02$ by a two sample T-test, 4 replicates each). (H to J) Streak plates on LB agar. (This figure has been reproduced by permission from Davies *et al*. (2007) FEMS Microbiology Ecology 59:32-46).

growth (data not shown). In broth culture, PA14 SCV had a qualitatively greater tendency to form aggregates as well as a surface pellicle (data not shown).

Each strain of *P. aeruginosa* was tested for a potential to swarm (Figure 5.1 B to D) or swim (Figure 5.1 E to G). PA14 *gacS*⁻ was highly motile relative to the other two strains, and showed an increased ability to swarm. This strain also had significantly greater motility on semisolid swim agar than either PA14 wt or SCV strains ($p < 0.01$, by a two-sample T-test, based on four replicates each). Conversely, PA14 SCV showed significantly decreased swim motility relative to the wild type strain ($p < 0.02$, by a two-sample T-test, based on four replicates each). In summary, these results show that PA14 *gacS*⁻ is hypermotile and a poor biofilm former, whereas the isogenic SCV strain is less motile but an excellent biofilm former. Streak plates of the PA14 wt, *gacS*⁻ and SCV strains are also pictured in Figure 5.1 H, I and J, respectively.

5.3.4 P. aeruginosa biofilm structure

Biofilms were examined *in situ* on pegs from the CBD using CLSM. All bacteria were stained with acridine orange (AO), a membrane permeant nucleic acid intercalator that has broad spectrum fluorescence (21). This compound stains all cells in a biofilm, live or dead, and may also bind to nucleic acids that are present in the extracellular matrix (ECM). Thus, AO functions as a general indicator of biomass present on the CBD pegs. Here, surface-adherent growths from *P. aeruginosa* PA14 wt, *gacS*⁻ and SCV strains were evaluated after 10, 24 and 48 h (Figure 5.2). Every image presented here is a representative of at least three independent replicates.

By 10 h, wild type *P. aeruginosa* PA14 formed thin layers of bacteria that were 5 to 7 μm in height at the air-liquid-surface interface of the polystyrene peg. In contrast, the *gacS*⁻ strain adhered to the surface as scattered cells or small cellular aggregates. Under the same conditions, the PA14 SCV strain formed biofilms with greater surface coverage than the wild type strain and developed into flat layers of densely packed cells that were also 5 to 7 μm in height.

After 24 h of growth, the wild type strain had formed layers up to 15 μm in height with the greatest amount of biomass present at the air-liquid-surface interface. *P.*

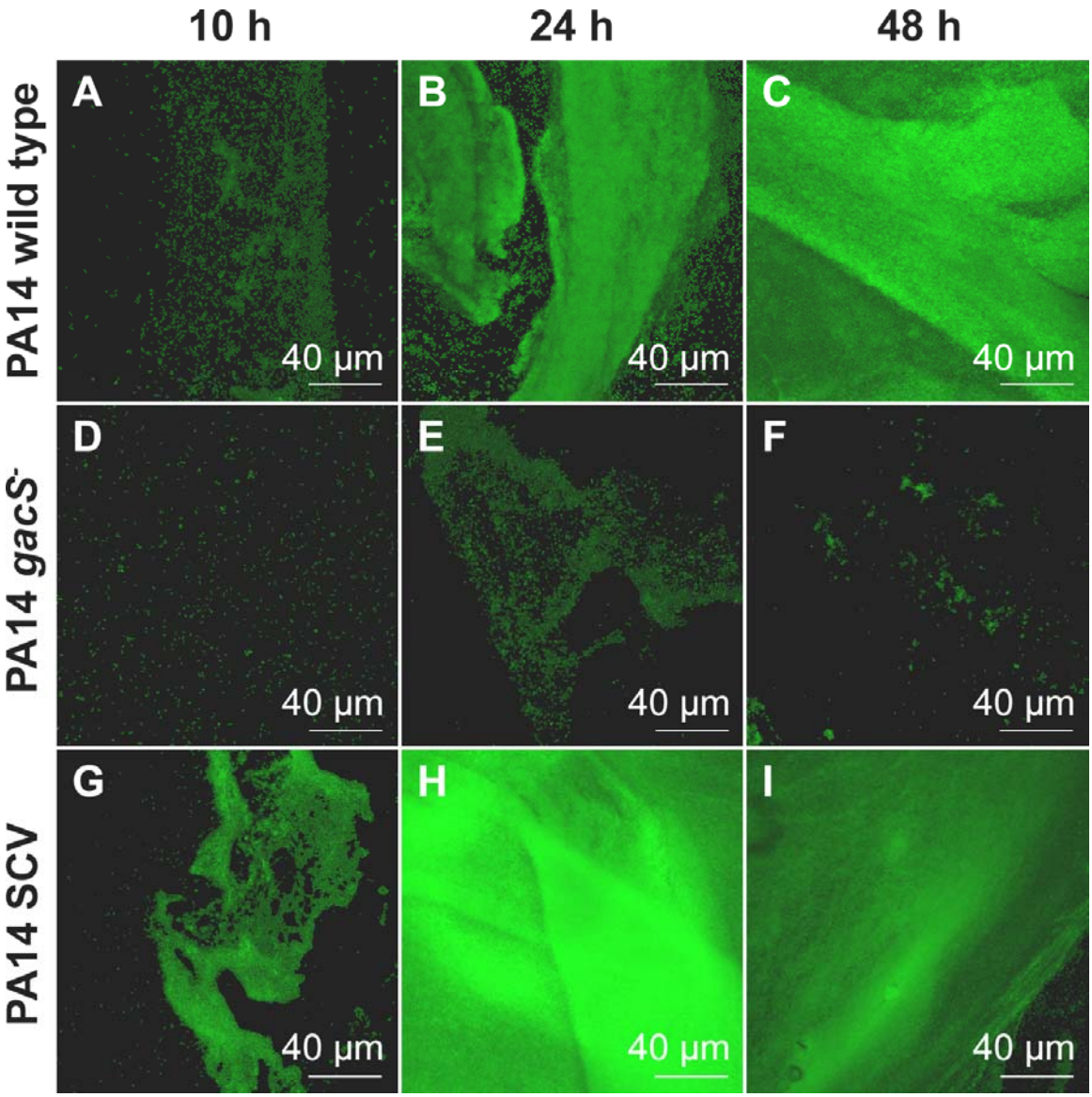

Figure 5.2. Biofilm formation by *Pseudomonas aeruginosa* PA14 wild type, *gacS*⁻ and small colony variant (SCV) strains at 10, 24 and 48 h in the CBD. Biofilms were grown in LB broth (at 35 °C and 150 rpm) in the CBD, stained with acridine orange, then imaged using CLSM. Every image presented in this figure is a two-dimensional average projection of the images captured along the z-axis. Each panel represents a square area of 238 × 238 µm. (This figure has been adapted from Davies *et al*. (2007) FEMS Microbiology Ecology 59:32-46).

aeruginosa PA14 *gacS*$^-$ formed little more than flat microcolonies and clumps that were heterogeneously distributed across the entire surface. However, the SCV strain had formed undulating layers of cells that were 20 to 25 μm thick that again gave greater surface coverage of the polystyrene pegs than wild type PA14. Biofilms examined at 48 h were similar to those examined at 24 h (Figure 5.2).

The structure of biofilms was also examined using scanning electron microscopy (SEM) at 27 h growth (J. A. Davies, data not shown). These results correlated well with CLSM data at 24 h. In particular, PA14 SCV formed very thick biofilms that lifted away from the surface of the peg when fixed and dehydrated. At lower magnifications this strain was again observed to produce undulating surface growth due to uneven thickness of the biofilm. As a control, the revertant strain PA14 SCV pUCP18mpgacS was similarly imaged using SEM. Biofilms of this revertant covered less surface area and had lost the undulating surface characteristic of the PA14 SCV biofilm (J. A. Davies, data not shown). Collectively, CLSM and SEM data suggest that the SCV has an exceptional capacity for forming surface-adherent biofilms.

5.3.5 N-acyl-homoserine lactone (AHSL) production

To determine whether there was a correlation between *gacS* inactivation and AHSL levels, the production of these metabolites by wild type PA14, *gacS*$^-$ and SCV strains was compared. *P. aeruginosa* PA14 *gacA*$^-$ was also assayed as it has been previously reported that this strain produces lower levels of 3-oxo-C12-AHSL relative to the wild type PA14 strain (183). *Escherichia coli* MG4 and *P. aeruginosa* PAO-JP2, bearing plasmids with the *lasB::lacZ* (pKDT17) or *rhlA::lacZ* (pECP61.5) reporter construct, respectively (186, 187), were used to quantify 3-oxo-C12-AHSL and C4-AHSL levels relative to β-galactosidase activity. These data are summarized in Table 5.2, and each value presented is the mean and standard deviation of three trials. C4-AHSL production was similar between *P. aeruginosa* PA14 wt and its isogenic *gacA*$^-$, *gacS*$^-$ and SCV strains. However, there were noticeable strain differences in 3-oxo-C12-AHSL production. Induction of *lasB::lacZ* expression by PA14 wt was approximately 2-fold greater than that of PA14 SCV or PA14 *gacA*$^-$, and at least 8 times greater than that of

PA14 *gacS*$^-$. In other words, inactivation of *gacA* produced a different phenotype than inactivation of *gacS*. Further, as part of the SCV phenotype, 3-oxo-C12-AHSL production was partially restored (Table 5.2). These results were corroborated by thin layer chromatography (data not shown).

Table 5.2. β-galactosidase reporter activity mediated by AHSLs from overnight cultures of *P. aeruginosa* PA14 wild type, *gacS*$^-$ mutant and SCV strains.

AHSL	Reporter	*P. aeruginosa* PA14 (all values are in Miller units)			
		wild type	*gacS*$^-$	*gacA*$^-$	*SCV*
3-oxo-C12-HSL	*lasB-lacZ*	590 ± 17	74 ± 14	322 ± 30	300 ± 50
C4-HSL	*rhlA-lacZ*	297 ± 3	250 ± 9	245 ± 5	313 ± 20

5.3.6 Antimicrobial susceptibility

Mutations in *gacA* have been shown to reduce the resistance and/or tolerance of *P. aeruginosa* PA14 biofilms to some antibiotics (183). Therefore, I determined whether the biofilms of PA14 *gacS*$^-$ or PA14 SCV strains had altered resistance to antibacterials relative to the wild type strain. Here, the inhibitory and bactericidal actions of metal cations (Cu^{2+} and Ag^{+}), hydrogen peroxide (H_2O_2) and ciprofloxacin were evaluated. Cu^{2+} and Ag^{+} are industrial pollutants that are also used as disinfectants, H_2O_2 is produced by plant and animal hosts, and ciprofloxacin is an antibiotic clinically used to treat *P. aeruginosa* infections.

Since the different strains formed biofilms at different rates, growth curve data were used to calibrate incubation times to produce biofilms of similar cell density for susceptibility testing. For these assays, PA14 wt, *gacS*$^-$ and SCV were incubated at 35 °C for 6.0, 7.0, and 5.5 h, respectively, to produce biofilms with cell densities of 5.0 ± 0.7, 5.3 ± 0.5, and 5.5 ± 0.4 $\log_{10}$ CFU per peg (based on the mean and standard deviation of 50 to 55 pooled replicates each). Biofilms formed by individual strains in the CBD were

statistically equivalent between the different rows of pegs ($0.09 < p < 0.91$ by one-way ANOVA, data not shown). $MIC_{72\ h}$, $MBC_{b\text{-}q}$ and $MBC_{b\text{-}99.9}$ values are summarized in Table 5.3 and are reported as the medians and ranges of 4 replicates. There were no significant differences in planktonic cell susceptibility to either Cu^{2+}, Ag^{+} or ciprofloxacin between the different strains (i.e. there was a $\log_2$ difference or less between these values). However, planktonic PA14 *gacS*$^{-}$ was hypersensitive to H_2O_2, whereas (by comparison) PA14 SCV was highly resistant.

The anti-biofilm activities of Cu^{2+}, Ag^{+}, H_2O_2 and ciprofloxacin were evaluated by determining mean viable cell counts and log-killing of biofilm populations of *P. aeruginosa* PA14 wt, *gacS*$^{-}$ and SCV strains (Figures 5.3 and 5.4). In these figures, each point represents the mean and standard deviation of 4 independent replicates. Although the $MBC_{b\text{-}99.9}$ values for H_2O_2 were similar for PA14 wt and SCV strains (Table 5.3), the biofilms of PA14 SCV showed increased survival at sub-$MBC_{b\text{-}99.9}$ concentrations relative to the wild type strain (see below). For ciprofloxacin, Cu^{2+} and Ag^{+}, biofilms of the SCV strain were approximately 4, 8 and 60 times more tolerant to these toxic factors than the wild type strain.

I noted that in some instances $MIC_{72\ h}$ values obtained using this method were greater than $MBC_{b\text{-}99.9}$ values. This represents an expected normality, not peculiarity, to the CBD method. For example, over the course of incubation, H_2O_2 would be gradually degraded in the challenge plates, especially by biofilms during exposure. After removing the biofilms from the challenge media, bacteria were allowed to recover for 72 h prior to MIC determination. In contrast, biofilm cell density was enumerated immediately after exposure to the peroxide (when its *in vitro* concentration would have been highest). Since there was no corresponding period of recovery for biofilms, this would result in the comparatively lower $MBC_{b\text{-}99.9}$ value.

When looking at the mean viable cell counts and log-killing data for Cu^{2+} and Ag^{+} (Figure 5.4) and for H_2O_2 and ciprofloxacin (Figure 5.5), it was possible to see the general trend that *P. aeruginosa* PA14 *gacS*$^{-}$ was much more sensitive to antimicrobials than the wild type strain. Even more interesting than this was the trend that the PA14

Table 5.3. Antimicrobial susceptibility of *Pseudomonas aeruginosa* PA14 wild type, *gacS*⁻ and small colony variant (SCV) strains.

Antibacterial	wild type		*gacS*⁻		SCV	
Growth inhibition	$MIC_{72\ h}$		$MIC_{72\ h}$		$MIC_{72\ h}$	
Cu^{2+} (mM)	8.0		8.0		4.0	
Ag^{+} (mM)	0.04 (0.04 to 0.08)		0.04 (0.02 to 0.08)		0.04	
H_2O_2 (ppm)	938		45 (30 to 60)		1875 (938 to 1875)	
ciprofloxacin (μg ml^{-1})	0.32 (0.32 to 0.64)		0.82 (0.32 to 1)		0.64 (0.32 to 1.28)	
Bactericidal activity	$MBC_{b\text{-}99.9}$	$MBC_{b\text{-}q}$	$MBC_{b\text{-}99.9}$	$MBC_{b\text{-}q}$	$MBC_{b\text{-}99.9}$	$MBC_{b\text{-}q}$
Cu^{2+} (mM)	8	48 (16 to >128)	8 (4 to 8)	8 (4 to 32)	64	>128
Ag^{+} (mM)	0.08 (0.04 to 0.15)	>9.5	0.08 (0.01 to 0.08)	2.5 (0.63 to >2.5)	4.8	>9.5 (4.8 to >9.5)
H_2O_2 (ppm)	352 (234 to 469)	1407 (938 to 3750)	29 (1.8 to 29)	968 (60 to 3750)	293 (118 to 469)	1875 (938 to 1875)
ciprofloxacin (μg ml^{-1})	0.16	5.1 (0.32 to >512)	0.12 (0.08 to 0.16)	0.32 (0.32 to >5.1)	0.48 (0.32 to 1.3)	5.1 (1 to 128)

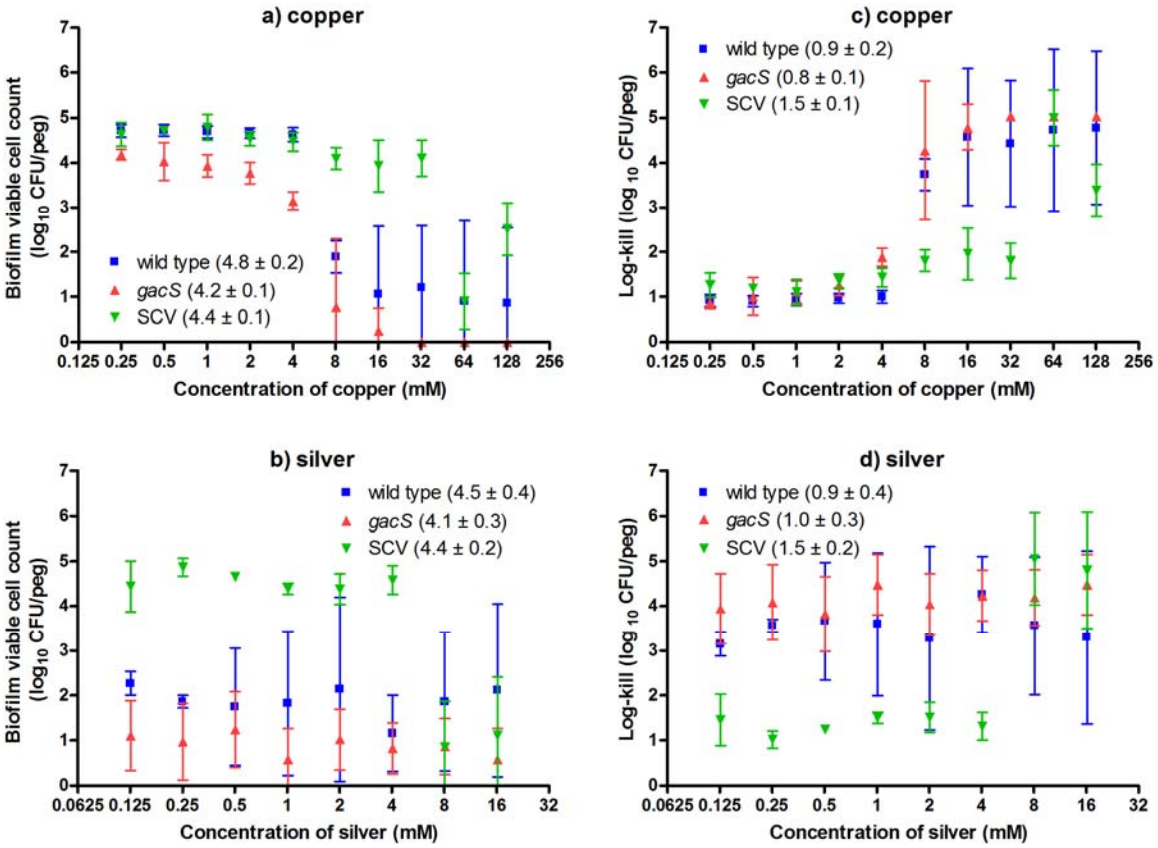

Figure 5.3. Killing of *Pseudomonas aeruginosa* PA14 wild type, *gacS*$^{-}$ and small colony variant (SCV) biofilms by Cu^{2+} and Ag^{+}. Biofilms were exposed to metal ions for 2 h, rinsed, and then disrupted into fresh medium containing neutralizing agents. Mean viable cell counts are reported here for biofilms exposed to (A) Cu^{2+} and (B) Ag^{2+}. Log-killing of biofilm populations was also calculated for (C) Cu^{2+} and (D) Ag^{2+}. Each measurement is reported as the mean and standard deviation of 3 or 4 replicates. Values in parentheses indicate the means and standard deviations for the viable cell counts or the log-kill calculations for the identically treated growth controls with no added antimicrobials. The SCV produced biofilms that were much more tolerant to metal toxicity than either of the other (presumably) isogenic strains. (This figure has been adapted from Davies *et al*. (2007) FEMS Microbiology Ecology 59:32-46).

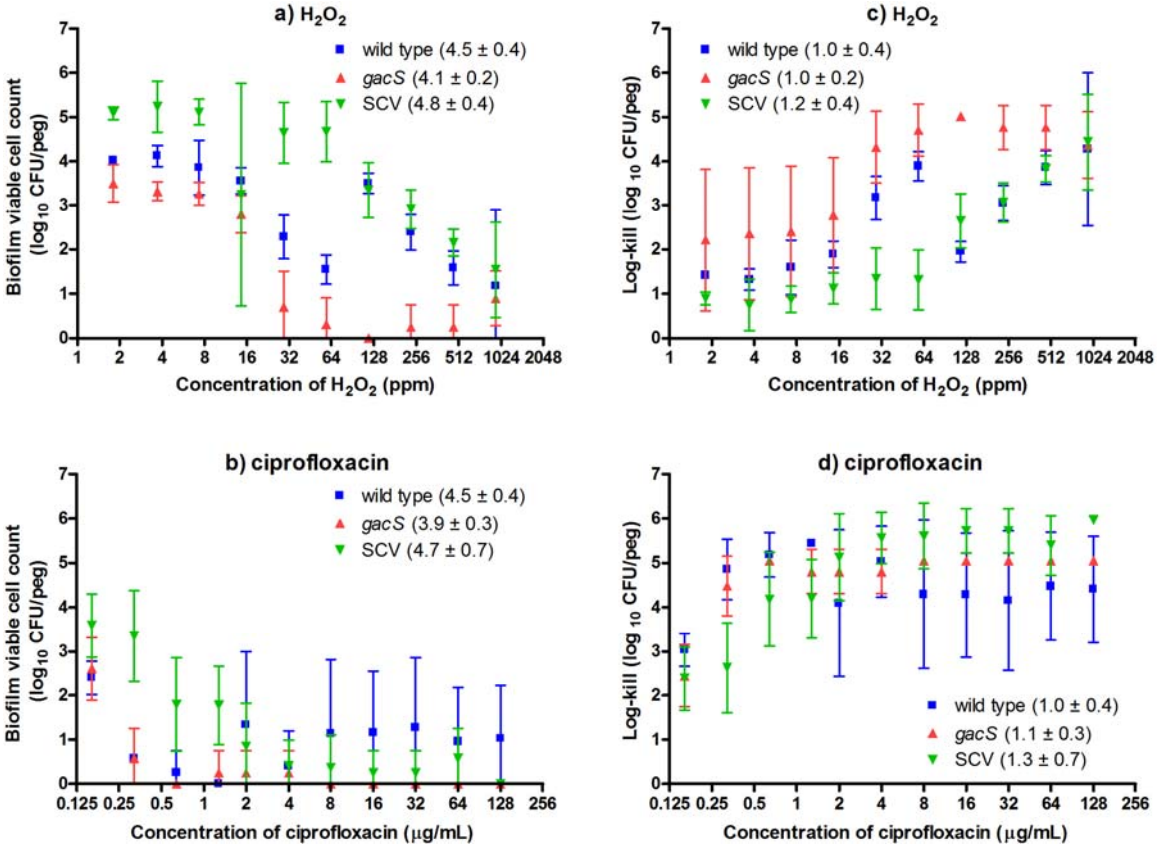

Figure 5.4. Killing of *Pseudomonas aeruginosa* PA14 wild type, *gacS*⁻ and small colony variant (SCV) biofilms by H_2O_2 and ciprofloxacin. Test conditions were similar to those described in the legend of Figure 5.3. Mean viable cell counts are reported here for biofilms exposed to (A) H_2O_2 and (B) ciprofloxacin. Log-killing of biofilm populations was also calculated for (C) H_2O_2 and (D) ciprofloxacin. Each measurement is reported as the mean and standard deviation of 3 or 4 replicates. Values in parentheses indicate the means and standard deviations for the viable cell counts or the log-kill calculations for the identically treated growth controls with no added antimicrobials. The SCV produced biofilms that were much more recalcitrant to killing by H_2O_2 or the DNA gyrase inhibitor, ciprofloxacin relative to the other (presumably) isogenic strains. (This figure has been adapted from Davies *et al*. (2007) FEMS Microbiology Ecology 59:32-46).

SCV strain produced biofilms that were more tolerant to antimicrobial exposure than the wild type strain. For example, biofilms of the small colony variant were tolerant of 2.4 mM Ag^+, whereas the vast majority of cell viability was lost from PA14 wt and *gacS*$^-$ biofilms at 0.04 mM Ag^+. Collectively, these data indicate that deletion of *gacS* reduces antimicrobial tolerance of *P. aeruginosa* PA14; however, phenotypic variation in biofilm populations may restore or even enhance antimicrobial tolerance to levels that exceed either the wild type or parental *gacS*$^-$ strains. It is also important to note that SCVs were highly resistant to H_2O_2 relative to the *gacS*$^-$ strain. This latter observation hints that this process of phenotypic variation may be linked to changes in resistance as well.

5.3.7 Frequency of phenotypic variation

During the course of susceptibility assays, I noted that the proportion of SCV cells recovered from biofilms after exposure to Ag^+ or H_2O_2 was increased relative to the corresponding growth controls. Therefore, I queried whether this may be true for other antimicrobial agents or growth conditions. An array of clinically used antibiotics, saline, goat and human sera were examined for an ability to select for these SCVs from 24 h biofilms of *P. aeruginosa* PA14 *gacS*$^-$. Biofilms were exposed to these agents for 18 h and each assay was performed in triplicate. Viable cell counts were determined for each exposure condition, and log-survival was determined. The proportion of SCV cells in bacterial populations recovered from these exposure conditions was calculated as the mean of the proportions from each individual trial. The data from these assays are summarized in Table 5.4.

Rifampicin, an RNA polymerase inhibitor, was a strong selective agent for SCVs from *P. aeruginosa* PA14 *gacS*$^-$ biofilms. At a concentration of 5 μg mL^{-1}, this drug killed 0.7 $\log_{10}$ cells from the biofilm population. On average, approximately 3 of 5 surviving cells from biofilms exposed to this concentration of rifampicin were colony morphology variants. Similarly, the β-lactams piperacillin, oxacillin and ceftrioxone selected for SCVs at a frequency of approximately 1 in 3. This occurred regardless of cell growth (ceftrioxone) or cell death (oxacillin or piperacillin). The aminoglycosides tobramycin and amikacin, both of which are used clinically to treat *P. aeruginosa*

infections, selected for SCVs at a frequency of approximately 1 in 5. This *in vitro* selection was compound specific, as in no instances were saline, erythromycin, imipenem, or ciprofloxacin observed to increase frequency of SCV cells from PA14 *gacS*⁻ biofilms. Human serum, but not goat, also gave rise to phenotypic variants at elevated frequencies compared to growth controls. These assays indicate that environmental conditions, such as antibacterial exposure or host factors, may select for SCVs from biofilms of *P. aeruginosa* PA14.

5.4 Discussion

In this work I examined an engineered strain of *P. aeruginosa* PA14 bearing an inactivating mutation in the sensor kinase *gacS*. This mutant was hypermotile and a poor biofilm former relative to the wild type strain. While characterizing this strain, it was noted that phenotypically stable SCVs could be recovered from biofilms at a proportion that was increased by three factors: 1) age of the biofilm, 2) by *in vitro* culture in human serum, or 3) exposure of biofilms to certain antibacterial agents. The SCV strain had a hyper-biofilm-forming phenotype, and was less motile and more tolerant to bactericidal agents than the parental *gacS*⁻ and wild type strains. With the exception of phenotypic stability, all of these traits have been described for *P. aeruginosa* colony morphology variants in the literature (63, 69, 111, 134). Although there may be multiple mechanisms that give rise to SCVs in *P. aeruginosa*, it is fair to conclude that GacS regulates reversion of variants to normal colony morphotypes for at least one of these pathways. This premise was supported by complementation analysis, in which SCVs reverted to normal colony phenotypes when transformed with a plasmid bearing wild type *gacS*. Thus, the inactivation of *gacS*, which frequently occurs in laboratory and rhizosphere populations of pseudomonads (213, 263), may also lead to the accumulation of stress resistant SCV cells in *P. aeruginosa* biofilms.

Genes of the GacS regulon strongly influence the later stages of biofilm formation in *P. aeruginosa* PA14. Biofilms formed by the PA14 *gacS*⁻ mutant did not proceed far beyond the irreversible attachment and proliferation stages of development (67).

Table 5.4. Cell survival rates and frequency of SCVs arising from *P. aeruginosa* PA14 *gacS*$^-$ biofilms exposed to various antibacterials and culture conditions.

Test medium	Antibiotic	Concentration (μg ml^{-1})	Survivors (log_{10} cfu peg^{-1})	Log-survival (log_{10} cfu peg^{-1})	SCV frequency (%)
Culture conditions (overnight)					
0.9% NaCl	none	na	3.8 ± 0.3	- 2.5 ± 0.3	0
goat serum	none	na	5.4 ± 0.2	- 1.0 ± 0.2	4
LB broth	none	na	6.7 ± 0.2	+ 0.3 ± 0.2	4
human serum	none	na	5.1 ± 0.2	- 1.3 ± 0.2	19
Antibiotic exposure (overnight)					
LB broth	erythromicin	5	6.4 ± 0.3	- 0.1 ± 0.3	0
	imipenem	1.25	2.7 ± 1.0	- 3.8 ± 1.0	0
	tobramicin	1.25	5.4 ± 0.5	- 1.0 ± 0.5	14
	amikacin	5	3.6 ± 0.6	- 2.8 ± 0.6	23
	azetronam	1.25	4.5 ± 0.5	- 2.6 ± 0.5	24
	ceftrioxone	1.25	6.8 ± 0.5	+ 0.4 ± 0.5	29
	oxacilin	1.25	5.6 ± 0.6	- 0.9 ± 0.6	32
	piperacillin + tazobactam	5	2.7 ± 1.7	- 3.8 ± 1.8	33
	rifampicin	5	5.7 ± 0.3	- 0.7 ± 0.3	58
Antibacterial exposure (2 h exposure, representative example from susceptibility assays)					
LB broth	none	na	4.2 ± 0.3	- 0.9 ± 0.3	0
	ciprofloxacin	0.16	2.4 ± 0.8	- 2.6 ± 0.8	0
	Cu^{2+}	16	4.2 ± 0.1	- 0.9 ± 0.1	0
	Ag^+	4	2.4 ± 0.1	- 2.6 ± 0.1	7
	H_2O_2	30	1.2 ± 1.1	- 3.8 ± 1.1	8

na denotes a variable that is not applicable

Biofilms of this mutant remained flat and lacked the characteristic layered structures of the mature biofilms formed by the parental strain. The biofilm growth process observed here for *P. aeruginosa* PA14 *gacS*$^-$ also differed from that previously reported by our research group for PA14 *gacA*$^-$, which failed to form surface-adherent aggregates under similar laboratory conditions (183).

GacS represents another piece of the cell specialization puzzle that exists in the literature for *P. aeruginosa* biofilms. GacS shares a high degree of identity with an open reading frame (ORF3) downstream and adjacent to *pvrR* (phenotype variant regulator), a hypothetical response regulator for a two-component system (PubMed accession number AF482691; http://www.ncbi.nih.gov/). Together, ORF3 and *pvrR* form a hybrid, putative sensor kinase and response regulator. Overexpression of PvrR from a plasmid reduces the frequency of phenotypic variation in *P. aeruginosa* biofilms (69). GacS/GacA are also upstream regulators of the *pel* (pellicle) operon (84). This cluster of seven adjacent genes is postulated to encode polysaccharide biosynthetic enzymes important for matrix formation in *P. aeruginosa* PA14 (79). These genes are implicated in surface adherence, and in general the *pel* locus shows increased expression in SCVs derived from biofilms of *P. aeruginosa* PAO1 (134). The data from this study suggest that a functional *gacS* limited the generation of SCVs in biofilms (although the exact mechanism remains elusive), and that this phenomenon was specific to the *gacS*$^-$ mutant as phenotypically stable small colony variants were not produced from an isogenic *gacA*$^-$ strain of *P. aeruginosa* PA14. Further indicative of the low fidelity relationship between GacA and GacS are decreases in AHSL levels of *gacS*$^-$ relative to the *gacA*$^-$ strain and the differences in biofilm structure (183). Note that two other sensor kinases, RetS and LadS, are known to modify intracellular signaling through GacA (84, 266). It is interesting to note that deletion of *retS* is similarly associated with the occurrence of hyper-biofilm forming colony morphology variants in *P. aeruginosa* (288).

QS-systems may be involved in the process of phenotypic variation and consequently may be indirectly and partly responsible for alterations in antimicrobial susceptibility. Among many other genes, these autoinducers control the expression of superoxide dismutase and catalase (109), which may account for the hypersensitivity of

PA14 *gacS*⁻ to H_2O_2. Compared to the *gacS*⁻ strain, we noted that AHSL levels were partially restored in the SCV strain, which coincided with increased resistance and tolerance to H_2O_2. The increased production of extracellular polymers associated with the SCV strain may further enhance the protective activity of these enzymes. This may contribute to resistance through a reaction-diffusion phenomenon where the substrate (H_2O_2) is degraded by catalase in the ECM before penetrating into the depths of the biofilm (234).

The extra biomass in SCV biofilms may also play a role in Cu^{2+} and Ag^{+} adsorption. Sequestration of copper cations in *P. aeruginosa* biofilms was evaluated in Chapter Three using the organic chelator sodium diethyldithiocarbamate to cause colored preciptiation of the metal (105). Using this approach, I have observed that biofilms of the PA14 SCV strain qualitatively adsorb greater Cu^{2+} than either PA14 wt or *gacS*⁻ strains (J. J. Harrison, G. R. Foglia and H. Ceri, unpublished data). This implies that the production of hyper-biofilm-forming SCVs from a genotypically diverse *Pseudomonas* population represents a strategy that may give rise to elevated heavy metal resistance and/or tolerance at the population level. A similar statement may be made for H_2O_2 and ciprofloxacin, although in the case of the latter, more precise mechanistic detail is not known, as this antibiotic rapidly equilibrates across the *P. aeruginosa* biofilm matrix (153).

Since the biofilm mode of growth is thought to be responsible for persistent infections, these *P. aeruginosa* SCVs may play an important role in pathogenesis, in particular the destructive infections of the CF lung (69, 110, 111). *P. aeruginosa* is also known for causing infections associated with burn wounds and the use of catheters (179). Here it was identified that low concentrations of clinically used antibiotics may select for hyper-biofilm-forming SCVs from biofilms of the *gacS*⁻ strain of this nosocomial pathogen. A similar trend has been previously shown for CF isolates of *P. aeruginosa* (69). The present study indicates that silver ions may be added to this list of triggers and/or selective agents. This is important as silver compounds are finding renewed use in medicine as antimicrobial surface coatings for bandages and catheters (182). Thus, an emerging and provocative theme is that antimicrobial chemotherapy may be triggering or

selecting for the phenotypic variation in *P. aeruginosa* biofilms that contributes to drug resistance and to damaging the chronically infected tissue (115, 179). This type of response would also be advantageous in soil environments, where *P. aeruginosa*, similar to other pseudomonads, would encounter other antibiotic producing microorganisms, toxic metals, or H_2O_2 produced by plants.

The stability of many types of biological systems is increased by diversity. Boles *et al.* (30) have recently identified that *P. aeruginosa* biofilm communities self-generate genetic diversity through a *recA* dependent mechanism. Analogously, Martinez-Granero *et al.* (162) (162) have identified that spontaneous mutations in *gacS* of *P. fluorescens* may be introduced by the site specific recombinases Sss and XerD, resulting in increased phenotypic variation. This variation increases the competitiveness of *P. fluorescens* in the plant rhizosphere, and similar mechanism might be at work for *P. aeruginosa*. Nonetheless, the present work suggests that *P. aeruginosa* biofilm formation and antibacterial resistance are intertwined with phenotypic variation, which itself may be linked to the underlying genetic diversity of these bacterial populations.

5.5 Contributions

5.5.1 Author's contributions to this work and personal acknowledgements

I performed about 60% of the experimental work described in this Chapter. In the process of doing this work, I trained 1 graduate student (Ginevra R. Foglia) to assist with the some of the bench work. Determinations of AHSLs were made by Jamie MacDonald, a technician for Dr. Douglas G. Storey. A portion of the CLSM work was performed by Carol A. Stremick, a technician for Dr. Howard Ceri. My many personal thanks go to James A. Davies for creating the *gacS*⁻ mutant used in this Chapter and for his discerning observations that this mutant produces stable colony morphology variants.

5.5.2 Relevant publications

These data sets were originally published in Davies *et al*. (2007) FEMS Microbiology Ecology 59:32-46, a manuscript on which I am denoted an equal first author.

Chapter Six: Metal ions may suppress or enhance cellular differentiation in multimetal resistant and tolerant biofilms of *Candida* species

6.1 Introduction

Biofilm formation is part of the ecological cycle for many yeasts including those from the genus *Candida* (92, 203). To date, more than 200 species of *Candida* have been identified, many of which are prevalent in rich soil and aquatic habitats that have been polluted with heavy metals (91, 158, 244). *Candida albicans* and *Candida tropicalis* are human opportunistic pathogens that are frequently isolated from these contaminated milieus. In fact, these two *Candida* species are known for high levels of resistance to many water soluble metal ions, such as Hg^{2+}, Pb^{2+}, Cd^{2+}, AsO_4^{3-} and SeO_3^{2-} (20, 103, 190). Yeasts may become the predominant microbial species in aqueous locales contaminated by toxic metals (91), and many of these organisms, including *Candida* species, also have the capacity to adsorb or accumulate these substances from their surroundings (190, 287). Although the research in this thesis has been primarily focused on bacterial biofilms, there are no studies in the literature that have specifically examined the susceptibility of fungal biofilms to metal toxicity. The primary aim of the research described in this Chapter was to compare the susceptibility of planktonic and biofilm *C. tropicalis* to toxic metal ions.

Similar to a few prokaryotes, polymorphic fungi such as *C. albicans* and *C. tropicalis* frequently undergo cell morphotype switching during growth in biofilms, and therefore, yeast to hyphal cell type transitioning may be an important matter to investigate. *C. albicans* forms biofilms in a step-wise process that results in a polymer entrenched arrangement of multiple cell types, typically with budding yeast attached to the surface and tentacle like chains of elongated hyphae, termed mycelia, on top (44, 102, 143). During my investigations of metal susceptibility, it was observed that metal exposure often affected the normal process of cellular differentiation that occurs during *Candida* biofilm development. Cellular polymorphism in *Candida* populations may be significant as matured biofilms are more resistant to antifungal agents than those at an earlier stage of development (44). Furthermore, the polymorphic character of *Candida*

spp. may play a role in pathogenic biofilm formation in some plants and animals, as hyphae may assist in the invasive penetration of physical barriers (203). There are a variety of environmental parameters that affect cellular differentiation in *Candida* species; these include: temperature, nutrient status, CO_2 levels, pH, as well as population density (174). A second specific aim of this research was to examine how metal ions may affect cellular differentiation in *C. albicans* and *C. tropicalis* biofilms.

By using a modification of the CBD technique described in Chapter Two, fifteen water soluble metal ions, chosen to represent groups 6A to 6B of the periodic table, were tested against *C. tropicalis*. With *in vitro* exposures as long as 1 day, biofilms were up to 65 times more resistant and/or tolerant to toxic metal ions than corresponding planktonic cultures. By using the sodium diethyldithiocarbamate (Na_2DDTC) assay described in Chapter Three, metal-chelator precipitates were formed in *C. tropicalis* biofilms following exposure to Cu^{2+} and Ni^{2+}. This suggests that *Candida* biofilms may also adsorb and trap metal cations from their surroundings. Lastly, by using both light microscopy and confocal laser scanning microscopy (CLSM) in conjunction with three-dimensional (3D) visualization, I examined the multicellular architecture of *C. albicans* and *C. tropicalis* biofilms before and after exposure to metal ions. This last approach identified that many of the tested metal compounds functioned as environmental cues with the potential to block or to trigger a switch from yeast to hyphal cell morphotypes. At the level of the microbial community, metal exposure thus resulted in specific biofilm structure types. In other words, *C. albicans* and *C. tropicalis* coordinately differentiated in response to metal ions to form biofilms with distinct spatial arrangements of cells.

6.2 Materials and methods

6.2.1 Standard protocols

C. albicans 3153A (147) and *C. tropicalis* 99916 (an isolate from the Foothills Hospital in Calgary, Alberta, Canada) were stored, handled and cultured as described in Chapter Two. For biofilm cultivation, these yeasts were grown either in trypticase soy broth (TSB) or in RPMI 1640 medium that was supplemented with 5 mM L-glutamine, 0.165 M 3-*N*-morpholino-propanesulfonic acid and 2.0 g L^{-1} sodium bicarbonate

(RQMB). *C. tropicalis* biofilms were grown in CBD devices that had been coated with L-lysine (also as described in Chapter Two). The CBD, when used as supplied by the manufacturer or when modified with L-lysine, did not support the growth of *C. albicans* (data not shown). Here, I will note that the CBD is made of raw polystyrene and this hydrophobic substratum might interfere with *C. albicans* surface adhesion (142). Other than surface modification, the procedures for CBD susceptibility testing, CLSM and 3D visualization were also the same as those described in Chapter Two.

In an additional set of experiments, CBD biofilms of *C. tropicalis* 99916 were grown for the initial 48 h period and then placed into microtiter plates with fresh medium containing one of the following: TSB, TSB + 2.0 mM SeO_3^{2-} or TSB + 0.25 mM CrO_4^{2-}. In other words, SeO_3^{2-} and CrO_4^{2-} were added at sub-inhibitory concentrations that were otherwise sufficient to shift the predominant cell morphotype in *C. tropicalis* biofilms (see section 6.3). The biofilms were then returned to the gyrorotary shaker (at 100 rpm) and incubated for an additional 24 h at 35°C and 95% relative humidity. Viable cell counts for these 72 h biofilms were then determined as outlined in Chapter Two.

6.2.2 Planktonic cell susceptibility testing

Planktonic yeast susceptibility testing was carried out using procedures modified from those suggested by Fothergill and McGough (76). Here, challenge plates of metals were prepared as described in Chapter Two for biofilms. A 1.0 McFarland standard was prepared in a manner identical to that used for biofilm cultivation, and from this, a two-fold dilution was made in TSB of which 5 μL was added to each well of the challenge plates. After the desired exposure time, 40 μL aliquots of the planktonic cultures were transferred into 96-well microtiter plates (which additionally contained 10 μL of the appropriate 5 × concentrated neutralizing agent in each well). From this, 25 μL aliquots of the neutralized planktonic cultures were plated onto TSA. Spot plates were incubated for 48 h and scored for growth to obtain minimum lethal concentrations for planktonic cells (MLC_P see section 6.2.6 for definitions). Alternatively, log-killing was evaluated by serial dilution of neutralized cultures and by plating onto TSA. Minimum inhibitory concentration (MIC) values were obtained after 48 h incubation at 35 °C by reading the

optical density at 650 nm (OD_{650}) of the challenge plates using a THERMOmax microplate reader with SOFTmax Pro data analysis software.

6.2.3 Biofilm cultivation in microtiter plates.

The method of Ramage and Lopez-Ribot (202) was used to cultivate biofilms of *C. albicans* 3153A and *C. tropicalis* 99916 in flat bottom, 96-well Nunc™ microtiter plates (VWR International Ltd., Mississauga, ON, Canada). Nunc™ cell culture plates are made from polystyrene that is chemically modified to introduce charged functional groups to the polymer. This plastic is a suitable substratum for both *C. albicans* and *C. tropicalis* biofilm growth. In this approach, serial two-fold dilutions of metal cations and oxyanions were made along the rows of wells in microtiter plates using RQMB medium. For each metal ion, ten concentrations were examined in quadruplicate, leaving the first and last well of each row to serve as sterility and growth controls, respectively. In this regard, biofilms were grown in challenge plates prepared in a similar fashion to those used for antifungal susceptibility testing (76).

To inoculate these microtiter plates, *C. albicans* and *C. tropicalis* were streaked out twice on TSA and an inoculum was prepared by suspending colonies from the second agar subculture into 0.9% saline to match a 1.0 McFarland Standard. Five µL of the inoculating suspension was added to each well of the microtiter plates and this resulted in a starting cell number of approximately 1×10^5 cfu mL^{-1}. The inoculated plates were then placed on a gyrorotary shaker at 100 rpm, 35 °C and 95% relative humidity for 48h. Again, $MIC_{48\ h}$ values were determined to assess the growth inhibition of *C. albicans* and *C. tropicalis* by metal ions by using a method adapted from Fothergill and McGough (76). Here, this was accomplished by reading the OD_{650} of these growth plates using a microtiter plate reader as described above.

6.2.4 Tetrazolium reduction assays

Metal or antifungal exposed CBD biofilms were rinsed twice with 0.9% saline and then inserted into microtiter plates that contained the following in each well: 150 µL of phosphate buffered saline (PBS, pH 7.2), 25 µL of TSB and 25 µL of CellTiter 96®

AQ_{ueous} One Solution (Promega Corporation, Madison, WI, U.S.A.). AQ_{ueous} One Solution contains the tetrazolium salt 3-(4,5-dimethylthiazol-2-yl)-5-(3-carboxymethoxyphenyl)-2-(4-sulfophenyl)-2H-tetrazolium (MTS), which is presumably reduced to a colored formazan product by NADH and NADPH from metabolically active cells (22). These plates were wrapped in tin foil and incubated at 35 °C for 120 min. Biofilm metabolic activity was assessed by reading the OD_{490} of these plates on a microtiter plate reader as described above.

6.2.5 Light microscopy

C. albicans and *C. tropicalis* biofilms cultivated in the bottoms of microtiter plate wells were examined using an inverted light microscope (Wild of Canada Limited, Ottawa, ON, Canada). Alternatively, an upright light microscope was used to examine pellicle formation (Wild of Canada Limited). Pictures were captured using a DCM130 1.3 megapixel digital video eyepiece camera with ScopePhoto 2.0 image software (TrueVision Microscopes Incorporated, St. Louis, MO, USA). Images were contrast and brightness enhanced using Adobe® Photoshop® 7.0 (Adobe Systems Inc., San Jose, CA, USA).

6.2.6 Calculations and definitions of measurements

Calculations of mean viable cell counts and mean log-kill measurements as well as tests for equivalent growth using one-away ANOVA were performed according to the guidelines set in Chapter Two. The definitions of endpoints used to measure fungal susceptibility as planktonic cells and as biofilms must be defined here. The minimum inhibitory concentration (MIC) was defined as the lowest concentration of an antimicrobial required to result in no visual turbidity of a planktonic suspension following 48 h of incubation ($MIC_{48\ h}$). The minimum lethal concentration (MLC) has been defined as the concentration of an antimicrobial required to kill 99.95% of the fungal population (76). This definition will be retained for planktonic cell susceptibility assays and will be referred to here as the MLC_P. The minimum lethal concentration for biofilms (MLC_b) will be similarly defined here as the lowest concentration of an

antimicrobial that is required to kill 99.95% of the fungal biofilm population. In terms of our assays, this implies that any plate with 1 or no colonies (from a single test spot) was scored negative for growth. Similar to the definition provided for bacteria in Chapter Two, I will define the fold tolerance as the ratio of MLC_B:MLC_P.

6.3 Results

6.3.1 Evaluation of the model systems used for studying Candida biofilm formation

Although biofilm formation by *C. albicans* is well characterized, little is known about biofilm formation by *C. tropicalis*. In this Chapter, I used two complementary approaches to address this problem. First, biofilm formation by *C. albicans* 3153A was examined side-by-side with *C. tropicalis* 99916 using the microtiter plate growth method of Ramage and Lopez-Ribot (202). This method allowed for the direct examination of *Candida* biofilms by light microscopy. Biofilm formation by *C. albicans* 3153A and *C. tropicalis* 99916 in microtiter plates was similar in many regards to the step-wise developmental process described for *C. albicans* biofilm formation in the literature (44). However, mature *C. tropicalis* biofilms had fewer hyphae than similarly aged *C. albicans* biofilms. This will be evident in the data presented in the sections to come.

The curved polystyrene pegs in the CBD are detachable; therefore, the peg surfaces were modified to facilitate yeast surface adhesion and most importantly, were removed as required to facilitate CLSM. Note that the CBD, either used as supplied by the manufacturer or modified in a way that supported biofilm growth for *C. tropicalis*, could not be used to cultivate *C. albicans* biofilms (see section 6.2.1). However, biofilm formation by *C. tropicalis* in the CBD followed a similar stepwise progression to that observed in microtiter plates. An advantage of the CBD is the easy transfer of biofilms to subsequent microtiter plates and therefore this system was additionally used for high-throughput biofilm susceptibility testing of *C. tropicalis*.

C. tropicalis grew to a mean cell density (with standard deviation) of 4.3 ± 0.4 $\log_{10}$ CFU per peg (based on 202 pooled measurements). To ensure that biofilm growth was even across the rows of pegs in the CBD, all of the biofilms from a single peg lid were plated for viable cell counting. Growth of *C. tropicalis* biofilms was statistically

equivalent between the different rows of pegs by means of one-way ANOVA ($p = 0.402$). For planktonic susceptibility assays, each well of a separate set of challenge plates was inoculated with 4.5 ± 0.1 $\log_{10}$ cfu of planktonic *C. tropicalis* (a starting number derived from 6 viable cell counting assays of the inoculum). This starting cell number was calibrated to approximately match the initial biofilm cell density.

6.3.2 Susceptibility of planktonic and biofilm C. tropicalis to metals

Medians and ranges for metal cation and oxyanion $MIC_{48\ h}$, MLC_p and MLC_b values determined for *C. tropicalis* planktonic cells and biofilms are summarized in Table 6.1. The values reported represent 4 to 8 independent replicates each. From these qualitative endpoints, it was possible to determine that planktonic *C. tropicalis* could withstand exposure to the highest concentrations of three of the metals tested: Ni^{2+}, Zn^{2+} and Al^{3+} (corresponding to maximum concentrations of 279, 501 and 592 mM, respectively). However, planktonic yeast cells were killed in a time-dependent fashion by other metals. In the cases of CrO_4^{2-}, Mn^{2+}, Co^{2+}, Cd^{2+}, AsO_4^{3-} and AsO_2^{-}, there was a minimum fold decrease in the MLC_P of 8.3, 4.0, 33, 7.7, 4.1, and 2.6, respectively, between 5 and 24 h exposure. These data indicate that planktonic *C. tropicalis* exhibits time-dependent tolerance to high concentrations of these metals. Hg^{2+} was the most toxic heavy metal tested, inhibiting yeast growth and killing both planktonic cells and biofilms over a narrow concentration range of 0.5 to 2.0 mM. As the sole exception, biofilms were no more tolerant to Hg^{2+} than planktonic cells.

In contrast to planktonic cells, *C. tropicalis* biofilms were, in general, highly tolerant to metal toxicity and survived added concentrations of more than 120, 140 and 500 mM of the metals AsO_4^{3-}, Co^{2+} and SeO_3^{2-}, respectively. Ag^{+} was highly toxic to planktonic cells, inhibiting growth and killing this form of *Candida* at concentrations of approximately 1.2 mM and 19 mM, respectively. In contrast, biofilms were highly tolerant to Ag^{+} and were not killed at the highest concentration added *in vitro* (152 mM). Given the sensitivity of this assay on a $\log_2$ scale, this implied that *C. tropicalis* biofilms were minimally 16-times more tolerant to Ag^{+} than corresponding planktonic cells. By comparison to MLC_p measurements, MLC_b values did not decrease with increasing

exposure time to metals. Since there was no time-dependent eradication of these surface-adherent microbes, it is possible that biofilms may have been resistant and/or tolerant to metal toxicity. Here, it may be feasible to distinguish between these two possibilities by using viable cell counting.

6.3.3 Candida tropicalis biofilms are multimetal resistant and tolerant

To discriminate between metal resistance and metal tolerance in these fungal biofilms, the lethality of one metal cation and one metalloid oxyanion was evaluated using viable cell counting and Live/Dead® staining in conjunction with CLSM. Co^{2+} was selected as a representative heavy metal cation since *Candida* biofilms had the greatest fold tolerance (≥ 65) to this compound. SeO_3^{2-} was chosen as a representative oxyanion since relative to Co^{2+} (as well as to other metals) planktonic cells were not killed in a time-dependent fashion by this compound. Biofilms were at least 21 times more tolerant to SeO_3^{2-} than planktonic cells at both 5 and 24 h exposure (Table 6.1).

Mean viable cell counts and log-killing of *C. tropicalis* biofilm and planktonic cells by Co^{2+} are presented in Figure 6.1. At concentrations above the planktonic MIC (4.3 mM), both planktonic and biofilm cells were killed by Co^{2+}. In the case of planktonic cells, every cell in the population had died by 24 h exposure to 8.6 mM of this heavy metal. In contrast, although a portion of the biofilm population died on exposure to high concentrations (35 or 140 mM) of Co^{2+}, there were many survivors even after an *in vitro* exposure of 1 day (Figure 6.1 D to H). The size of Co^{2+} exposed yeast cells was larger than that in growth controls (compare Figure 6.1 C or F to H). Biofilms thus contained fewer but bigger cells after exposure to high concentrations of this heavy metal, which is reflected in a marked decrease in mean viable cell counts. These data indicate that *C. tropicalis* biofilms were highly tolerant to Co^{2+}.

A different scenario existed for SeO_3^{2-}. Mean viable cell counts and log-killing of *C. tropicalis* biofilm and planktonic cells by this oxyanion are presented in Figure 6.2. At concentrations above the MIC (56 mM), planktonic *C. tropicalis* was rapidly killed (which correlated closely to the data in Table 6.1). Strikingly, at an *in vitro* concentration of 125 mM SeO_3^{2-}, mean viable cell counts for biofilms increased during the first 5 h of

Table 6.1. Susceptbility of planktonic and biofilm *C. tropicalis* to toxic metal ions.

Metal ion	Group	n	Time (h)	Broth microdilution assay		CBD	Fold tolerance
				MIC (mM)	MLC_P (mM)	MLC_B (mM)	
CrO_4^{2-}	6B	4	5	4.4	35 (35 to 70)	70 (70 to >70)	2.0
			24		5.5 (1.1 to 8.8)	>70	≥26
Mn^{2+}	7B	4	5	nd	>596	>596	na
			24		298	>596	≥4.0
Ni^{2+}	8B	4	5	70	>279	>279	na
			24		>279	>279	na
Co^{2+}		4	5	4.3	>139	>139	na
			24		4.3	>139	≥65
Cu^{2+}	1B	4	5	64	64	64	1.0
			24		64	>129	≥4.0
Ag^{+}		5	5	1.2	19 (19 to 38)	>152	≥16
			24		19	>152	≥16
Zn^{2+}	2B	4	5	31 (31 to 62)	>501	>501	na
			24		>501	>501	na
Cd^{2+}		5	5	2.3 (2.3 to 4.5)	73 (37 to 73)	>146	≥4.0
			24		6.8 (1.1 to 18)	>146	≥43
Hg^{2+}		6	5	1.3	1.3	1.2 (1.2 to 2.5)	0.9
			24		1.3	1.9 (1.3 to 2.6)	1.5
Al^{3+}	3A	3	5	607	>592	>592	na
			24		>592	>592	na
Pb^{2+}	4A	6	5	39	79	>77	≥2.0
			24		>79 (79 to >79)	>77	na
AsO_4^{3-}	5A	4	5	59	>122	>122	na
			24		22 (15 to 61)	>122	≥11
AsO_2^{-}		4	5	19	>306	>306	na
			24		306 (19 to 306)	>306	≥2.0
SeO_3^{2-}	6A	4	5	56	48 (32 to 64)	>516	≥21
			24		48 (32 to 64)	>516	≥21
TeO_3^{2-}		5	5	> 11	>11	>11	na
			24		>11	>11	na

n denotes the principal quantum number
na indicates a calculation that is not applicable
nd indicates an MIC that could not be determined due to precipitate formation in test wells

exposure. CLSM of Live/Dead stained biofilms exposed to SeO_3^{2-} (Figure 6.2 D) showed a corresponding increase in the number of live cells in the biofilms, which generally gave greater surface coverage of the peg. By 24 h exposure to 125 mM SeO_3^{2-} (Figure 6.2 G), mean viable cell counts of biofilms were similar to the starting number of cells in biofilms. In contrast, 500 mM SeO_3^{2-} resulted in rapid yeast cell death in biofilms (Figure 6.2 E and H). By 24 h many of the dead cells had been lost from the peg and the biofilm covered less surface area than it did before exposure. These data indicate that under certain conditions, biofilm *C. tropicalis* was more resistant to SeO_3^{2-} than planktonic cells.

Although the majority of the fungal biomass in these assays was composed of yeast cells, some sparsely distributed pseudohyphae and hyphal cell types could be observed near the air-liquid-surface interface of the pegs. For example, formation of hyphae was evident after 24 h in growth controls for metal exposure; however, there was little if no differentiation in biofilms exposed to metals. A logical course of action was to investigate whether metal ions might be affecting cellular differentiation in biofilms.

6.3.4 Metal ions alter development and 3D organization of C. tropicalis biofilms

The development, structure and survival of metal exposed *C. tropicalis* biofilms (cultivated in the CBD) were further investigated by CLSM, by 3D visualization and by viable cell counting. CLSM imaging was performed in triplicate for at least one sub-inhibitory and at least one fungicidal concentration for several representative metal ions, of which a representative example is illustrated in Figures 6.3 and 6.4. The reported mean viable cell counts and standard deviations were based on 3 to 8 independent replicates each.

After 48 h of incubation in the CBD (the start point for these experiments), *C. tropicalis* formed a surface adherent layer of yeast cells that was up to 20 μm thick. Growth was greatest near the air-liquid-surface interface at the top of the peg and in some regions, yeast cells were organized into circular formations (Figure 6.3 A). After the initial 48 h incubation period, the growth medium was changed and the biofilms were returned to the incubator for an additional 24 h (with or without shaking to generate shear

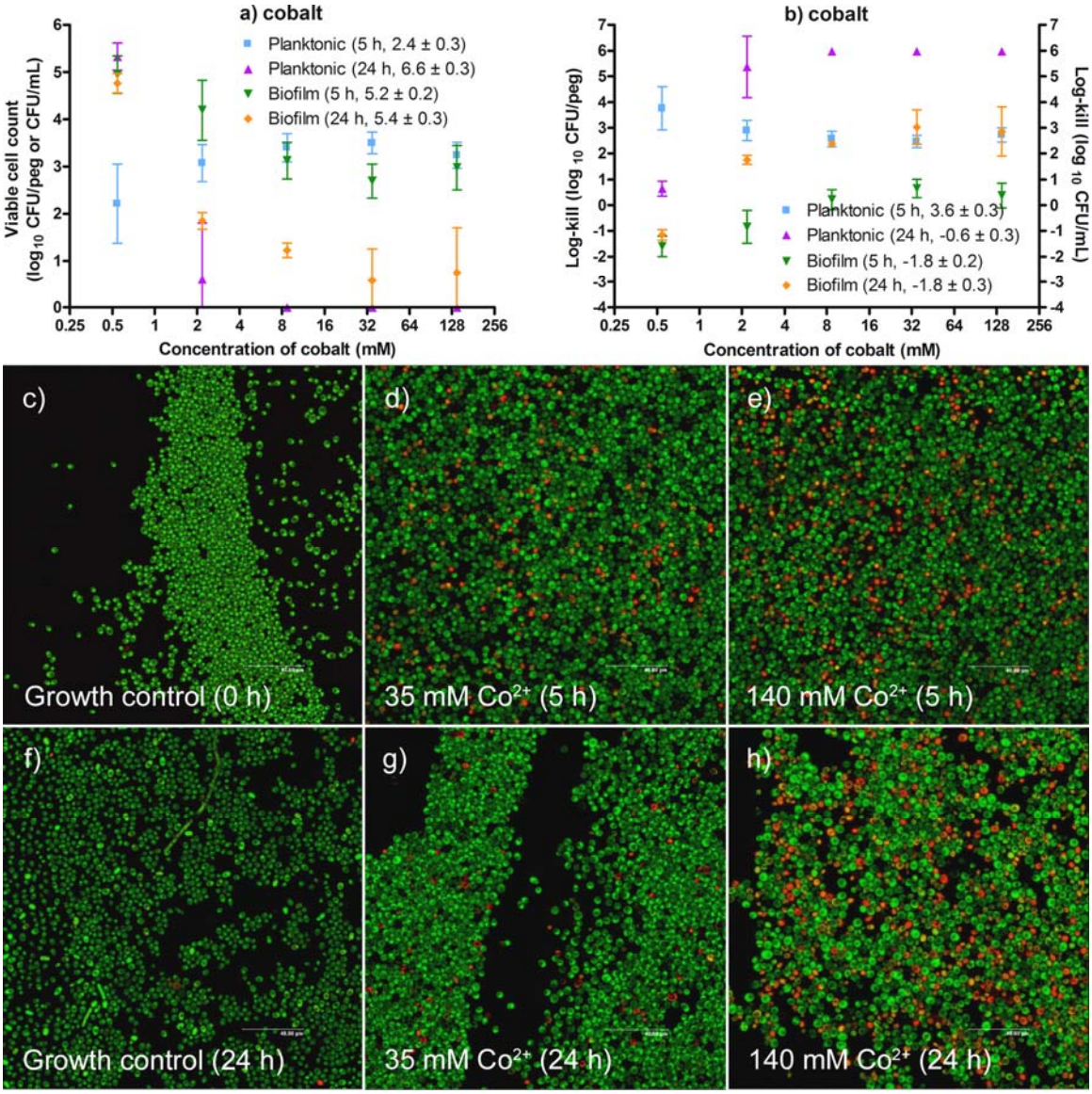

Figure 6.1. *Candida tropicalis* 99916 biofilms are highly tolerant to the heavy metal Co^{2+}. Biofilms were grown for 48 h on the peg lid of the CBD then exposed to Co^{2+} for 5 or 24 h. Here, this was compared to survival of an equivalent number of planktonic cells that had been added to identically prepared challenge plates. Biofilm and planktonic cells were recovered in 0.9% NaCl, serially diluted ten-fold then plated onto agar for viable cell counts. Here, each data point is reported as the mean and standard deviation of 3 or 4 independent replicates. CLSM and Live/Dead® staining were also used to evaluate fungal survival in cobalt exposed biofilms grown in the CBD. (A) Mean viable cell counts and (B) log-killing of biofilm and planktonic cells of *C. tropicalis* with

respect concentration of Co^{2+}. Planktonic cell populations were killed (completely) in a time-dependent fashion by Co^{2+}, and although many biofilm cells were killed by prolonged exposure to cobalt, some cells in the biofilm population survived exposure to this highly toxic metal even with 1 day of exposure *in vitro*. (C) Before exposure to Co^{2+}, the vast majority of biofilm biomass was yeast cells and the vast majority of cells were alive. (D and E) With 5 h exposure, Live/Dead® staining corroborated that the number of dead cells in biofilms increased with concentration of the cobalt added to the growth medium. (F) With an additional 24 h growth, there was some differentiation of yeast cells into pseudohyphae and hyphae within CBD biofilm populations. Biofilms after 24 h exposure to (G) 35 mM and (H) 140 mM Co^{2+}, respectively, had fewer cells and covered less area on the CBD pegs. Yeast cells were notably larger at 24 h exposure to Co^{2+} than at 5 h. Each CLSM panel is a 2D average of a 3D z-stack of images representing an area of 238 × 238 μm. (This figure has been adapted from Harrison *et al.* (2006) FEMS Microbiology Ecology 55:479-491).

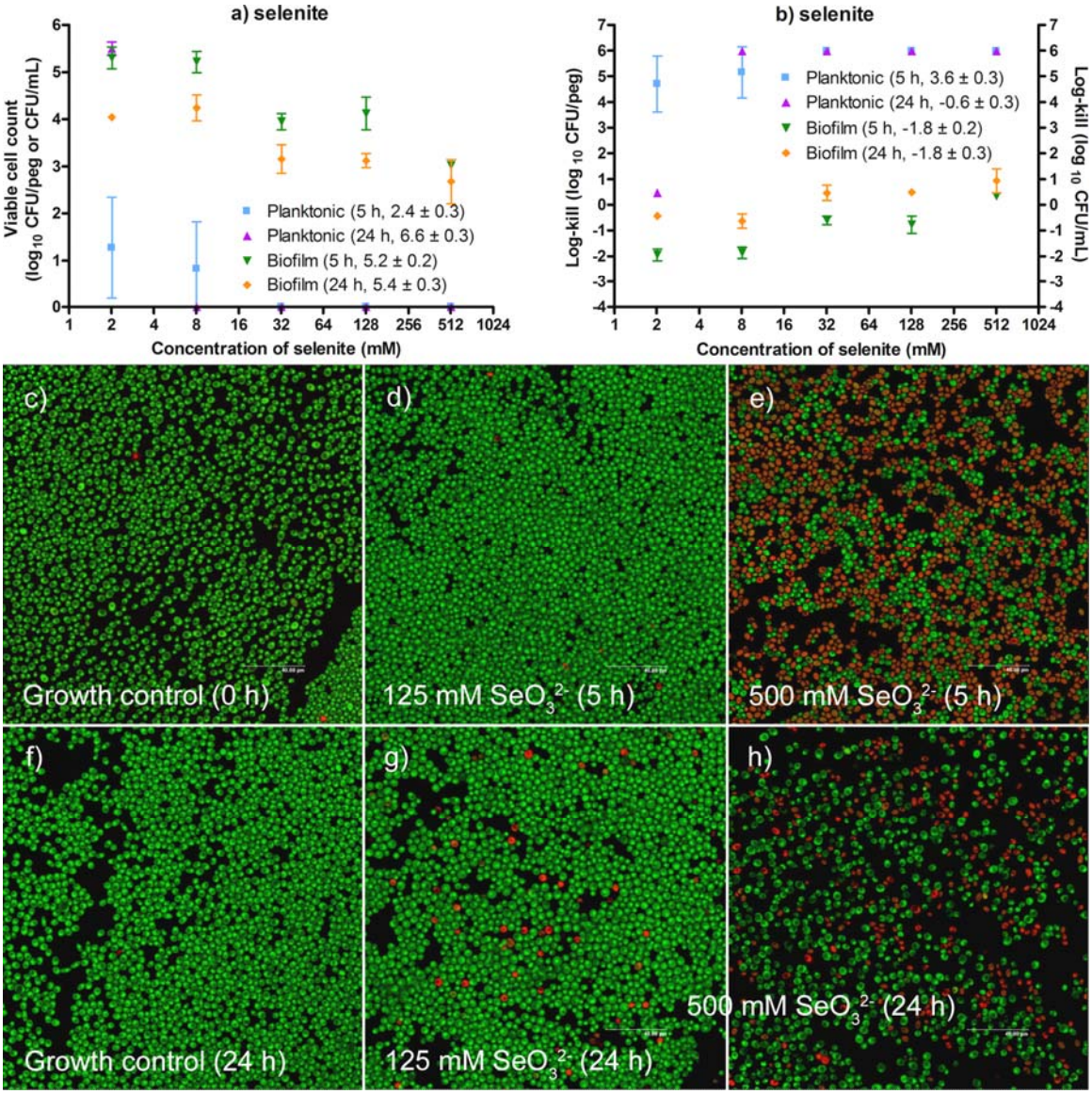

Figure 6.2. ***Candida tropicalis*** **99916 biofilms are highly resistant to the metalloid oxyanion SeO_3^{2-}.** Experimental conditions were similar to those described in the legend of Figure 6.1. (A) Mean viable cell counts and (B) log-killing of biofilm and planktonic cells of *C. tropicalis* with respect concentration of SeO_3^{2-}. (C) Live/Dead® staining of biofilms before exposure to SeO_3^{2-} and after 5 h exposure to (D) 125 mM and (E) 500 mM SeO_3^{2-}, respectively. Here, I observed that *C. tropicalis* biofilms continued to grow in 125 mM SeO_3^{2-}, a concentration that was 2- to 4-fold larger than the planktonic MIC. In contrast, 500 mM SeO_3^{2-} killed a large portion of biofilm cell populations. Biofilms in (F) growth controls after an additional 24 h incubation, were chiefly viable cells.

However, 24 h exposure to (G) 125 mM and (H) 500 mM SeO_3^{2-}, killed many cells in the biofilm population. Viable cell counts as well as the number of cells in biofilms were generally lower at longer exposure times. Yeast cells were notably larger at 24 h exposure to SeO_3^{2-} than at 5 h. Each CLSM panel is a 2D average of a 3D z-stack of images representing an area of 238 × 238 μm. (This figure has been adapted from Harrison *et al.* (2006) FEMS Microbiology Ecology 55:479-491).

and flow forces). A similar process of cellular differentiation occurred in both static and dynamic shear conditions; therefore, I initially chose to focus on static exposure conditions.

In the untreated controls, *C. tropicalis* biofilms continued to grow and to differentiate; hyphae and pseudohyphae were prominent near the air-liquid-surface interface (Figure 6.3 C). Biomass was heterogeneously distributed across the peg surface and biofilms were up to 80 μm thick in some regions. Single-cell layers of yeast covered most of the remaining peg surface. Correlative to viable cell counts, Live/Dead® staining qualitatively revealed that the vast majority (>95%) of *C. tropicalis* cells were viable. In contrast to growth controls, less than 2 mM concentrations of Zn^{2+} (Figure 6.3), Co^{2+}, Cu^{2+}, Ag^{+}, Cd^{2+}, Pb^{2+}, arsenite (AsO_2^-) and selenite (SeO_3^{2-}), as well as 0.08 mM Hg^{2+}, suppressed hyphal formation (Figure 6.4). Strikingly, biofilms exposed to CrO_4^{2-} produced the opposite result, triggering the formation of mycelia (Figure 6.3 F).

Collectively, four biofilm structure types were discerned from the data presented here and an example of each was analyzed using 3D visualization; I have denoted these 1) 'domed' (Figure 6.3 B), 2) 'layer cake' (Figure 6.3 D), 3) 'flat' (Figure 6.3 F) and 4) 'mycelial' (Figure 6.3 G). To summarize, domed resulted from an extended, initial incubation of *C. tropicalis* on a shaker, where it formed mushroom-cap shaped microcolonies composed entirely of yeast cells. Layer cake describes the archetypal mature *Candida* biofilm structure that had a basal layer of yeast cells with hyphae protruding into the bulk media. This occurred after spent medium from biofilm cultures was replaced with fresh medium following the initial 48 h incubation period and biofilms were returned to the incubator. The flat structure type resulted from the addition of metal cations, AsO_2^- and SeO_3^{2-} to the growth medium. Finally, the mycelial structure type resulted from exposure of *C. tropicalis* biofilms to low levels of CrO_4^{2-}.

6.3.5 Metal ions affect differentiation in C. albicans and C. tropicalis at sub-MIC levels

To further explore the effect of metal ions on cellular differentiation, an alternate growth method was used to examine in *C. albicans* and *C. tropicalis* biofilms. Here biofilms were cultivated in individual wells of microtiter plates and these were

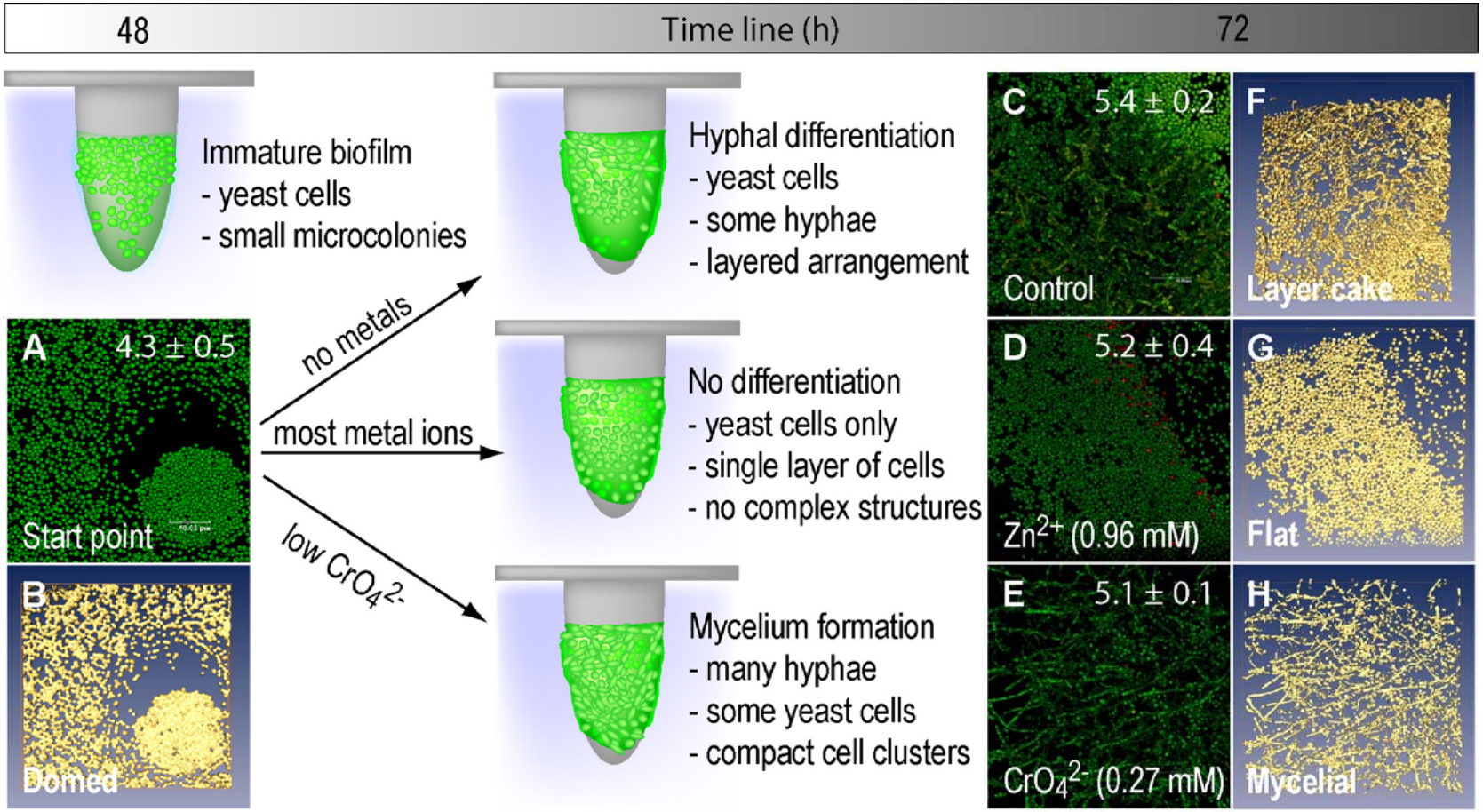
48
Time line (h)
72
Immature biofilm
- yeast cells
- small microcolonies
A 4.3 ± 0.5
Start point
B
Domed
no metals
most metal ions
low CrO_4^{2-}
Hyphal differentiation
- yeast cells
- some hyphae
- layered arrangement
No differentiation
- yeast cells only
- single layer of cells
- no complex structures
Mycelium formation
- many hyphae
- some yeast cells
- compact cell clusters
C 5.4 ± 0.2
Control
D 5.2 ± 0.4
Zn^{2+} (0.96 mM)
E 5.1 ± 0.1
CrO_4^{2-} (0.27 mM)
F
Layer cake
G
Flat
H
Mycelial

Figure 6.3. *Candida tropicalis* 99916 forms biofilm communities with characteristic 3D structure that may be influenced by metal ions. Here, the heavy metal ions Zn^{2+} and CrO_4^{2-} influenced the maturation of *C. tropicalis* communities at an intermediate stage of biofilm development. In these experiments, *C. tropicalis* was grown on pegs in the CBD and was then exposed to Zn^{2+} and CrO_4^{2-} for 24 h. The exposed biofilms were stained with the Live/Dead® BacLight™ kit, imaged by CLSM and then visualized using amira™ 3.1. The mean and standard deviation of biofilm cell densities were evaluated by viable cell counting (log_{10} CFU per peg) and this is indicated where appropriate. (A) The 2D average projection and (B) isosurface rendering of a *C. tropicalis* biofilm grown for 48 h on the CBD. This "domed" biofilm structure type was named for the formation of small microcolonies of yeast cells in surface-adherent communities. (C and F) The 2D average projection and isosurface rendering of an untreated *C. tropicalis* biofilm grown for a total of 72 h. This structure type was named "layer cake" for the biphasic arrangement of yeast and hyphal cells in the community. (D and G) The 2D average projection and isosurface rendering of a *C. tropicalis* biofilm exposed to 0.96 mM Zn^{2+} for 24 h. These "flat" biofilms had few hyphae and lacked microcolony structures. (E and H) The 2D average projection and isosurface rendering of a *C. tropicalis* biofilm exposed to 0.27 mM CrO_4^{2-} for 24 h. "Mycelial" biofilms consisted of masses of hyphal cells attached to the polystyrene surface with few yeast cells remaining in the community. Each panel represents an area of 238 × 238 μm. Green cells are alive and red cells are dead. (This figure has been reproduced by permission from Harrison *et al*. (2007) Applied and Environmental Microbiology 73:4940-4949).

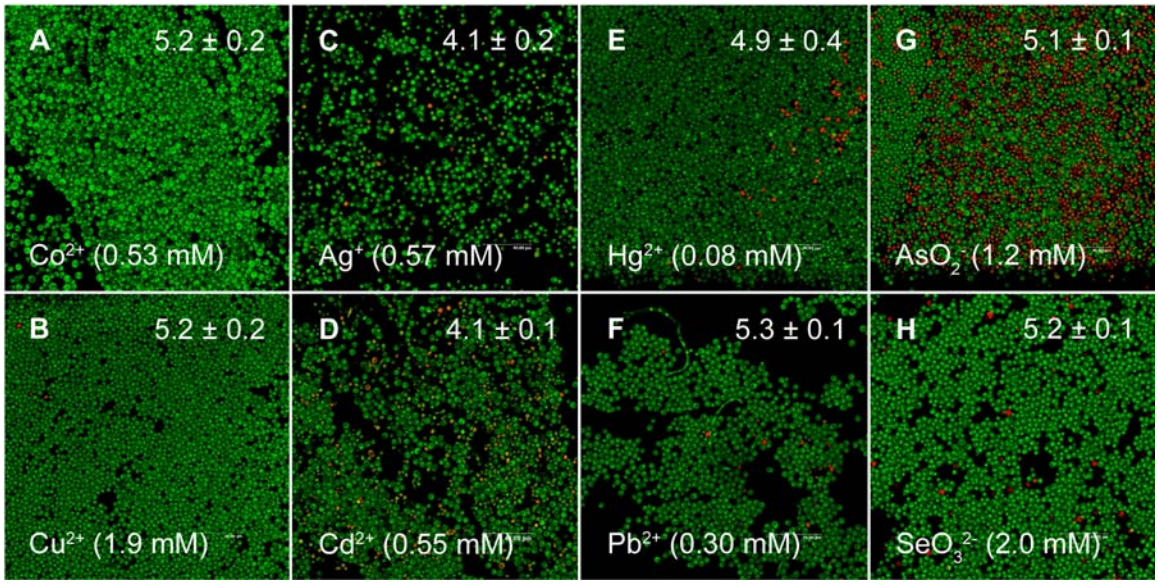

Figure 6.4. Many metal ions (Co^{2+}, Cu^{2+}, Ag^{+}, Cd^{2+}, Hg^{2+}, Pb^{2+}, AsO_2^{-}, SeO_3^{2-}) inhibited hyphal formation by *Candida tropicalis* 99916 at an intermediate stage of biofilm development. In every case, treating biofilms with these compounds resulted in the "flat" biofilm community structure type. Biofilm populations were grown, imaged and enumerated as described in the legend of Figure 6.3. Each panel represents an area of 238 × 238 μm. Green cells are alive and red cells are dead. (This figure has been reproduced by permission from Harrison *et al*. (2007) Applied and Environmental Microbiology 73:4940-4949).

systematically examined using light microscopy. Cell morphology in biofilms was qualitatively ranked on a five point scale (all ranks were relative to the growth control; 1 = a large shift towards the hyphal cell type; 2 = a small shift towards the hyphal cell type; 3 = approximately the same proportion of yeast and hyphal cells as the growth control; 4 = a small shift towards the yeast cell type; 5 = a large shift towards the yeast cell type). The minimum concentration blocking or enhancing the yeast-hyphal cell morphotype transition was defined as the lowest concentration resulting in a rank score of ≤ 2 or ≥ 4. These data are presented in Table 6.2 and each value represents the median and range of 4 to 8 independent replicates and the predominant cell type at that concentration.

Under these growth conditions, almost all of the metal ions examined blocked or triggered the transition between yeast and hyphal cell types in *Candida* biofilms. Light microscopy images of these biofilms were captured using a digital camera and representative pictures are illustrated in Figure 6.5. In most instances, metal ions (Co^{2+}, Cu^{2+}, Ag^{+}, Cd^{2+}, Hg^{2+}, Pb^{2+}, AsO_2^{-} and SeO_3^{2-}) inhibited hyphal cell type formation in biofilms of *C. albicans* and *C. tropicalis*.

It is worth noting that *C. albicans* and *C. tropicalis* did not respond the same way to all metal ions; for example, CrO_4^{2-} triggered the transition to the hyphal cell morphotype in *C. tropicalis* 99916 biofilms (Figure 6.5 L), whereas *C. albicans* 3153A biofilms exposed to this metal oxyanion were mostly yeast cells (Figure 6.5 B). A similar situation was observed for Zn^{2+} (Figure 6.5 H and R). In the cases of Co^{2+}, Ag^{+} and Hg^{2+}, concentrations in the micromolar range were sufficient to affect the yeast-hyphal cell type transition (Table 6.2). The response of *C. albicans* and *C. tropicalis* to Hg^{2+} was particularly interesting, as fungal growth was inhibited at an intermediate range of concentrations (0.16 – 0.64 mM), but resumed above a threshold concentration (1.24 mM) (Figure 6.6). Furthermore, the location of biofilm formation in the microtiter plate wells changed with Hg^{2+} concentration. At low concentrations of Hg^{2+} (≤ 0.08 mM), the majority of biofilm growth was surface adherent (Figure 6.6 B and E), whereas at higher concentrations (≥ 2.5 mM), *C. albicans* and *C. tropicalis* abandoned surface-adherent growth to form pellicles at the air-liquid interface (Figure 6.6 C and F).

Table 6.2. Minimum concentrations of metal ions that inhibit growth or that affect the cellular differentiation of *C. albicans* 3153A and *C. tropicalis* 99916 during the initial stages of biofilm development[1]

Metal ion	Minimum inhibitory concentration (mM)[2]	Minimum concentration blocking or enhancing the yeast-hyphal cell type transition (mM)[2]	Predominant cell type[3]
C. albicans 3153A			
CrO_4^{2-}	6.8 (6.8 – 14)	0.85 (0.43 – 1.7)	Yeast
Co^{2+}	0.70 (0.31 – 0.78)	0.03 (0.02 – 0.04)	Yeast
Cu^{2+}	3.1 (3.1 – 6.3)	1.6 (1.6 – 3.1)	Yeast
Ag^{+}	0.06 (0.04 – 0.08)	0.01 (0.01 – 0.02)	Yeast
Zn^{2+}	15	1.4 (0.9 – 1.9)	Hyphae
Cd^{2+}	nd	nd	Yeast
Hg^{2+}	0.16	0.04	Yeast
Pb^{2+}	> 24.1	no change	
AsO_2^{-}	55	41 (14 – 55)	Yeast
SeO_3^{2-}	58 (29 – 58)	15 (7.3 – 15)	Yeast
C. tropicalis 99916			
CrO_4^{2-}	1.7	0.21	Hyphae
Co^{2+}	0.69 (0.31 – 0.75)	0.02	Yeast
Cu^{2+}	6.3	3.1	Yeast
Ag^{+}	0.06 (0.05 – 0.08)	0.08 (0.04 – 0.08)	Yeast
Zn^{2+}	6.3 (6.3 – 13)	1.8 (0.45 – 3.1)	Hyphae
Cd^{2+}	nd	nd	Yeast
Hg^{2+}	0.15 (0.15 – 0.31)	0.04	Yeast
Pb^{2+}	> 24.1	6.0 (3.0 – 12)	Yeast
AsO_2^{-}	62	10 (6.8 – 13.6)	Yeast
SeO_3^{2-}	29	7.3 (7.3 – 14)	Yeast

[1]Biofilms were grown in the presence of metal ions in microtiter plates using RQMB medium.
[2]Values are expressed as the median of 4 to 8 replicates with the range (if applicable) indicated in parentheses.
[3]the indicated metal ion concentration (in the column to the left) caused a population shift towards this cell morphotype.
nd denotes an assay that was "not determined" due to the formation precipitates.

I performed a similar, systematic light-microscopy analysis for *C. tropicalis* 99916 biofilms cultivated in the CBD. In this model system, which was used in section 6.3.4, biofilms were grown for an initial 48 h period (corresponding to an intermediate

Table 6.3. Minimum concentrations of metal ions that inhibit growth or that affect the cellular differentiation of *C. tropicalis* 99916 at an intermediate stage of biofilm development[1]

Metal ion	Minimum inhibitory concentration (mM)[2]	Minimum concentration blocking or enhancing the yeast-hyphal cell type transition (mM)[2]	Predominant cell type[3]
CrO_4^{2-}	4.4 (4.4 – 18)	0.27 (0.27 – 2.2)	Hyphae
Co^{2+}	4.2 (2.2 – 4.3)	≤ 0.53	Yeast
Cu^{2+}	48 (31 – 64)	0.49 (≤ 0.49 – 0.49)	Yeast
Ag^{+}	0.59	≤ 0.59	Yeast
Zn^{2+}	nd	≤ 0.96	Yeast
Cd^{2+}	4.5 (1.8 – 7.2)	1.1	Yeast
Hg^{2+}	0.46 (0.31 – 0.62)	≤ 0.08	Yeast
Pb^{2+}	40	2.4	Yeast
AsO_2^{-}	29 (19 – 39)	≤ 1.2	Yeast
SeO_3^{2-}	63	≤ 2.0	Yeast

[1]Biofilms were grown for 48 h in the CBD using TSB medium and were then exposed to metal ions for an additional 24 h.
[2]Values are expressed as the median of 4 to 8 replicates with the range (if applicable) indicated in parentheses.
[3]The indicated metal ion concentration (in the column to the left) caused a population shift towards this cell morphotype.
nd denotes an assay that was "not determined" due to the formation of precipitates.

stage of biofilm development), and then were transferred into challenge plates containing metal ions. These data are summarized in Table 6.3 and each value represents the median and range of 4 to 8 independent replicates and the predominant cell type at that concentration is indicated. When comparing *C. tropicalis* biofilm formation in microtiter plates (RQMB) to the CBD (TSB), metal ions had a similar effect on cellular differentiation, with the exception of Zn^{2+}.

In every case, the shift in the predominant cell morphotype of *C. albicans* 3153A and *C. tropicalis* 99916 biofilms occurred at concentrations of metal ions that were less than the corresponding MIC values (Table 6.2 and 6.3). Therefore, these data indicate that metal cations and oxyanions may suppress or enhance the interconversion of yeast and hyphal cell morphotypes independently of growth inhibition.

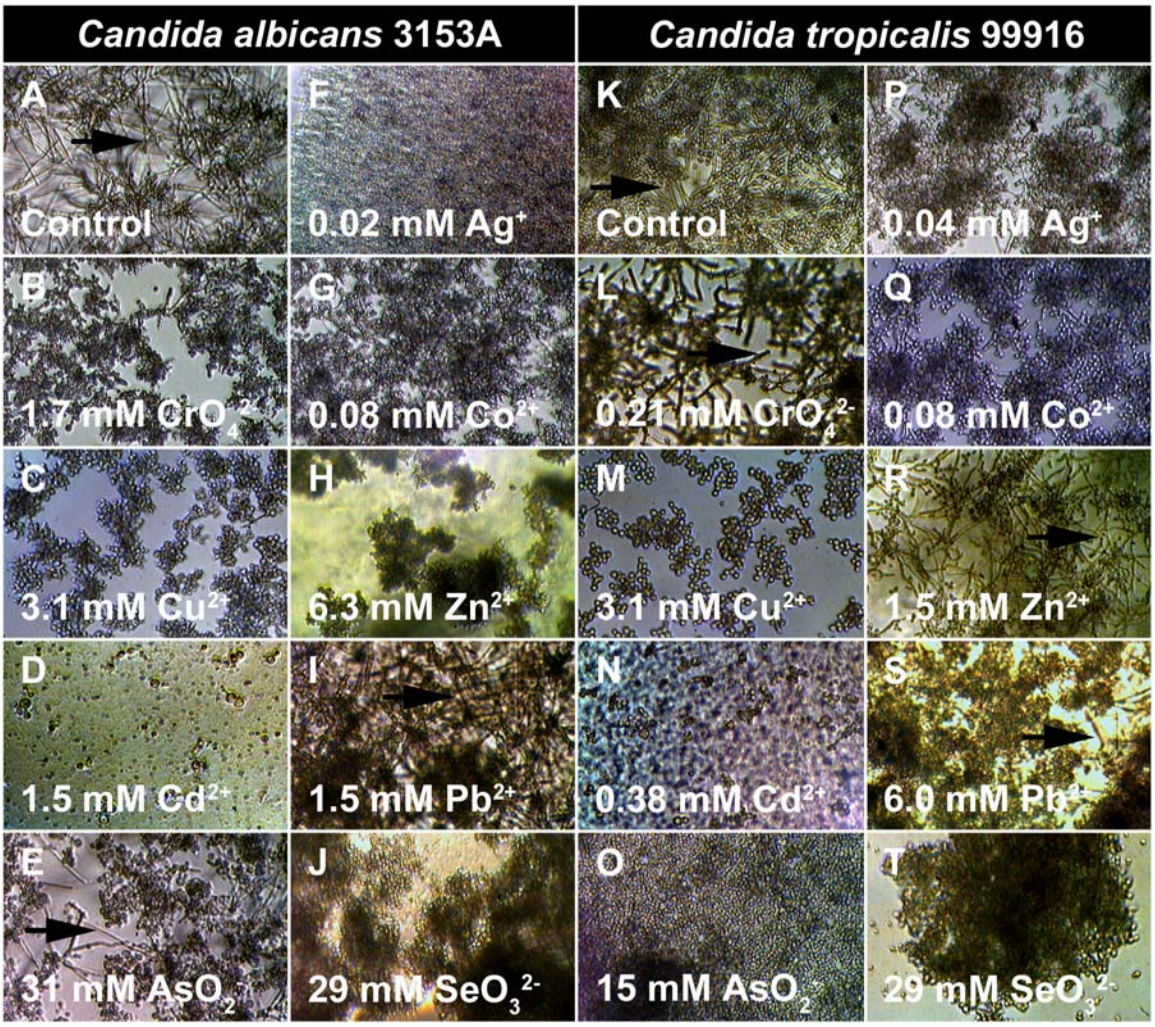

Figure 6.5. Metal ions may promote or inhibit cellular differentiation during biofilm growth of *C. albicans* 3153A and *C. tropicalis* 99916. Biofilms were grown in RQMB in microtiter plates for 48 h at 35°C on a gyrorotary shaker. (A) The untreated *C. albicans* 3153A biofilms consisted of yeast cells interspersed with many hyphae. (B to J) *C. albicans* 3153A biofilms were grown in media containing the indicated metal ion, and with the exception of Pb^{2+}, all of the metal ions inhibited hyphal formation. (K) The untreated *C. tropicalis* 99916 biofilms consisted of yeast cells intertwined with hyphae. In comparison to *C. albicans*, *C. tropicalis* produced fewer hyphae in the community. (L to T) *C. tropicalis* 99916 biofilms were grown in medium containing the indicated metal ion. For *C. tropicalis* grown in these conditions, CrO_4^{2-} and Zn^{2+} triggered the formation of hyphal cells, whereas the remaining metal ions inhibited the formation of hyphal cells.

For the sake of comparison, an inhibitory concentration of Cd^{2+} has been shown for *C. albicans* and *C. tropicalis*. These digital photos were captured at 100 × magnification and the images were contrast and brightness enhanced using Adobe® Photoshop® 7.0. Arrows indicate the hyphal cells in the biofilm populations. (This figure has been reproduced by permission from Harrison *et al*. (2007) Applied and Environmental Microbiology 73:4940-4949).

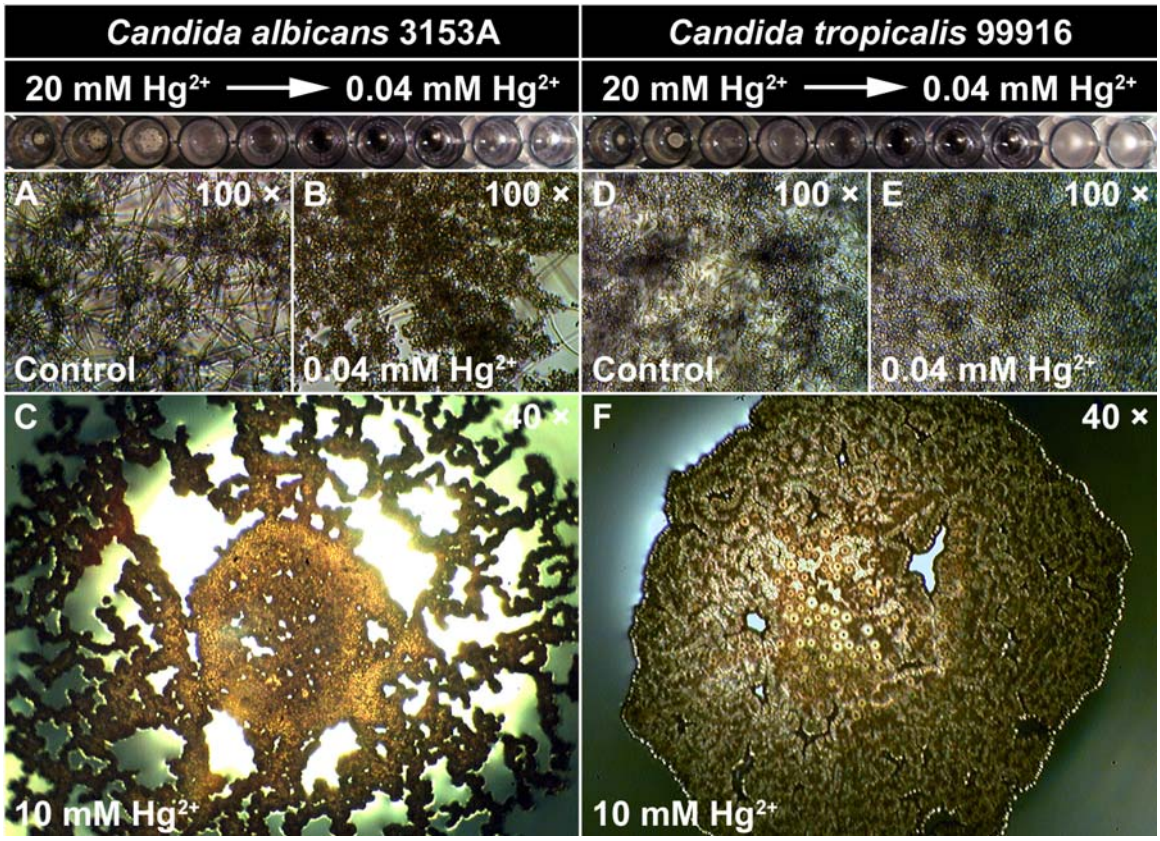

Figure 6.6. *C. albicans* 3153A and *C. tropicalis* 99916 undergo multiple shifts in growth rate and biofilm community structure when cultivated in a concentration gradient of divalent mercury cations (Hg^{2+}). Biofilms were grown in RQMB in microtiter plates for 48 h at 35°C on a gyrorotary shaker. Pictured at the top of each column are rows from a microtiter plate that contained a $\log_2$ concentration gradient of Hg^{2+} (ranging from 20 mM to 0.04 mM). (A and E) Untreated *C. albicans* 3153A and *C. tropicalis* 99916 biofilms contained yeast cells interspersed with hyphae. (B and E) *C. albicans* 3153A or *C. tropicalis* 99916 biofilms cultivated in as little as 0.04 mM Hg^{2+} consisted of yeast cells only. (C and F) As the concentration of Hg^{2+} increased, *C. albicans* 3153A and *C. tropicalis* 99916 gradually abandoned solid-surface attachment, and at $\geq$ 10 mM Hg^{2+}, these microorganisms formed a pellicle of yeast cells at the air-liquid interface. (This figure has been reproduced by permission from Harrison *et al*. (2007) Applied and Environmental Microbiology 73:4940-4949).

6.3.6 Metal ions alter the resistance of C. tropicalis biofilms to antimicrobials

Previous studies have indicated that the multidrug resistance of *C. albicans* biofilms arises during community maturation, a process that is linked to cellular differentiation (44). Since metal ions may alter the normal process of *Candida* biofilm development, I specifically hypothesized that growing biofilms in sub-inhibitory concentrations of metal ions may alter the antifungal resistance of the surface-adherent population. In this set of experiments, *C. tropicalis* 99916 biofilms were grown in the CBD for an initial 48 h and then the growth medium was replaced with one of the following: TSB, TSB + 2.0 mM SeO_3^{2-} or TSB + 0.25 mM CrO_4^{2-}. This approach was taken to produce *C. tropicalis* biofilm communities with the layer cake, flat and mycelial structure types, respectively.

To rigorously investigate the process of cellular differentiation in these biofilm communities (under dynamic, as opposed to static, shear and flow force conditions), I stained these biofilms using Syto-9 and TRITC-ConA (to label cellular biomass and extracellular polysaccharides, respectively). Each CLSM imaging experiment was performed in triplicate and a representative of each was analyzed by volume rendering. These additional data, illustrated in Figure 6.7, indicate that in all instances *C. tropicalis* biofilm cells were encapsulated in a layer of extracellular polysaccharides (or that these cells were attached to their neighbours by cell wall material) and that the process of cellular differentiation mirrored that described for static exposure conditions.

Lastly, biofilms cultured under these conditions were exposed to Cu^{2+} or amphotericin B. The metabolic capacity of the exposed biofilms, as a measure of community resistance, was evaluated by reduction of MTS, a tetrazolium salt (Figure 6.7). Although neither directly correlative nor conclusive, the loss of phenotypic variation in *C. tropicalis* 99916 biofilms induced by CrO_4^{2-} and SeO_3^{2-} was associated with a decrease in the biofilm resistance to Cu^{2+} and amphotericin B, respectively. Similar results were obtained using an Alamar Blue™ viability assay (data not shown). These data suggest that metal ion exposure may in some instances change the process of community maturation that gives rise to antifungal resistance.

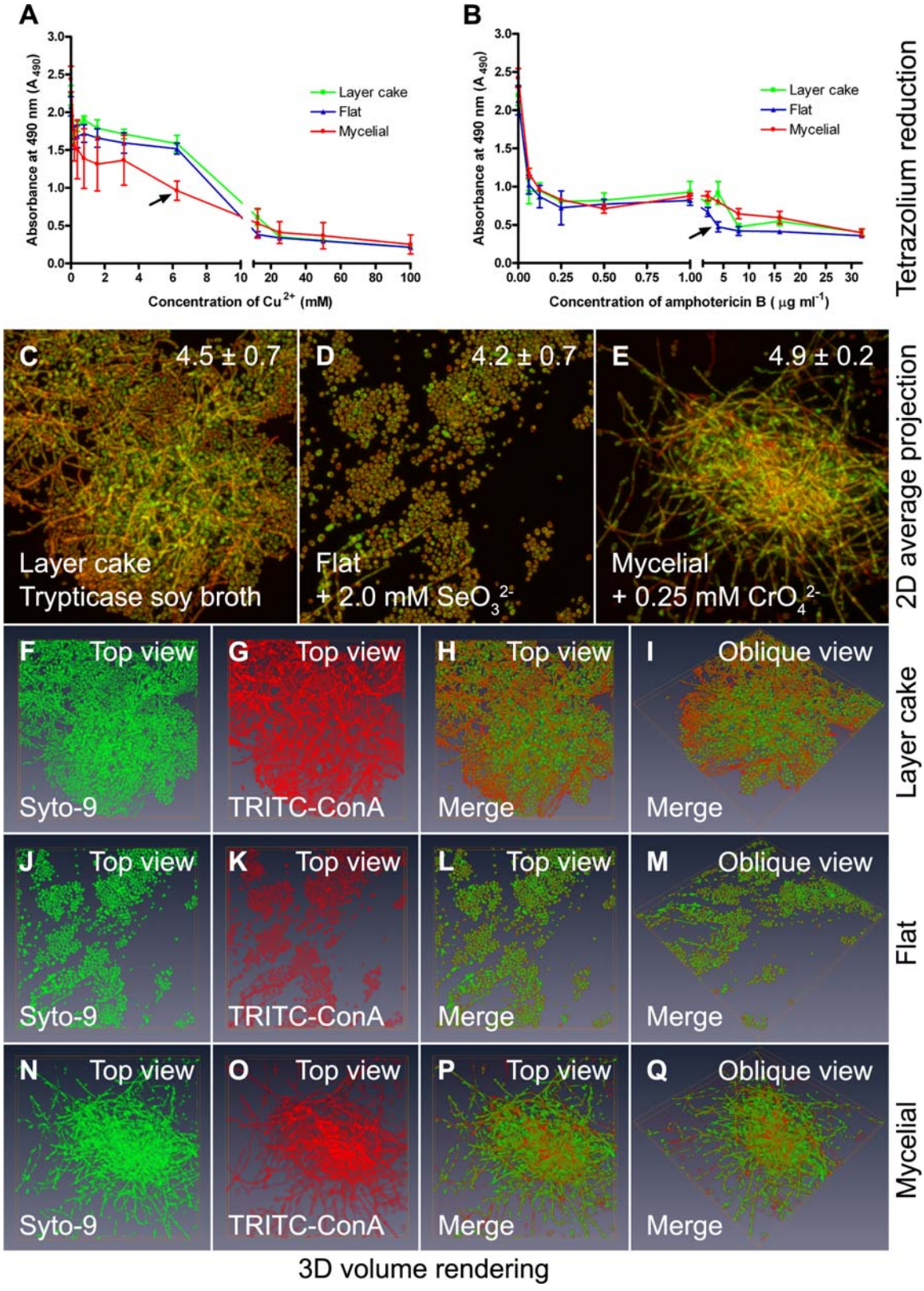
A
B
Absorbance at 490 nm (A490)
Layer cake
Flat
Mycelial
Concentration of Cu2+ (mM)
Concentration of amphotericin B (μg ml-1)
Tetrazolium reduction
C 4.5 ± 0.7
D 4.2 ± 0.7
E 4.9 ± 0.2
Layer cake
Trypticase soy broth
Flat
+ 2.0 mM SeO3 2-
Mycelial
+ 0.25 mM CrO4 2-
2D average projection
F Top view
G Top view
H Top view
I Oblique view
Syto-9
TRITC-ConA
Merge
Merge
Layer cake
J Top view
K Top view
L Top view
M Oblique view
Syto-9
TRITC-ConA
Merge
Merge
Flat
N Top view
O Top view
P Top view
Q Oblique view
Syto-9
TRITC-ConA
Merge
Merge
Mycelial
3D volume rendering

Figure 6.7. Cultivation of *Candida tropicalis* 99916 biofilms in SeO_3^{2-} and CrO_4^{2-} decreases the resistance of the biofilm population to amphotericin B and Cu^{2+}, respectively. In these experiments, *C. tropicalis* biofilms were grown on pegs in the CBD for 48 h in TSB, and then transferred into fresh media containing no additive, SeO_3^{2-} or CrO_4^{2-} for an additional 24 h. Biofilms cultivated in this manner were either exposed to antifungals (Cu^{2+} and amphotericin B), or fixed and then stained with Syto-9 and TRITC-ConA (for CLSM and 3D visualization). The mean and standard deviation of biofilm cell densities were evaluated by viable cell counting ($\log_{10}$ cfu peg^{-1}) and this is indicated in panels C, D and E. (A) Reduction of MTS, a tetrazolium salt, by *C. tropicalis* "layer cake", "flat" and "mycelial" biofilms after a 24 h exposure to Cu^{2+}. (B) Reduction of MTS by *C. tropicalis* "layer cake", "flat" and "mycelial" biofilms after a 24 h exposure to amphotericin B. (C to E) The 2D average projections of CLSM image stacks for biofilms grown on the CBD pegs. (F to Q) Volume rendering of the Syto-9 and TRITC-ConA labeled 3D volume data sets extrapolated from the image z-stacks used to create the images of the "layer cake", "flat" and "mycelial" biofilms in panels C to E. Each panel represents an area of 238 × 238 μm. Green fluorescence corresponds to cellular biomass, whereas red fluorescence corresponds to extracellular polymers. (This figure has been reproduced by permission from Harrison *et al*. (2007) Applied and Environmental Microbiology 73:4940-4949).

6.3.7 Retention of divalent heavy metal cations in yeast biofilms

The last characteristic of *Candida* biofilms examined here was their ability to trap metal cations, as this has been examined for bacterial biofilms in previous chapters. Here, I investigated if yeast biofilms may similarly sequester metal cations or oxyanions from their aqueous surroundings. Biofilms exposed to the metals Cu^{2+}, Ni^{2+} and TeO_3^{2-} were rinsed then treated with Na_2DDTC (Figure 6.8). In the cases of Cu^{2+} and Ni^{2+} exposed biofilms, Na_2DDTC caused the rapid formation of brown and yellow metal-chelates, respectively. However, biofilms exposed to the metalloid oxyanion tellurite did not change color when immersed in this chelator. This suggests that *C. tropicalis* biofilms may adsorb positively charged metal ions. Conversely, negatively charged metal ions may not be sequestered as easily by the biomass of *C. tropicalis* biofilms.

6.4 Discussion

Species of the polymorphic yeast *Candida* are prevalent in soil and aquatic environments and in these niches microorganisms frequently encounter highly toxic, water soluble metal ions. The research in this Chapter used a variety of *in vitro* techniques to examine the susceptibility of planktonic and biofilm *Candida* to metal toxicity. These experiments suggested that relative to planktonic cells, *C. tropicalis* biofilms are much more resistant and tolerant to metal toxicity. Moreover, the data presented here indicate that metal ions may suppress or enhance cellular differentiation in *C. albicans* and *C. tropicalis* biofilms, thereby giving rise to multicellular aggregates with spatially distinct distributions of cell morphotypes. This evidence implies that metal ions either may function as regulators (i.e. signals), or that sub-inhibitory concentrations of metal ions may induce stress that interferes with the transition of yeast to hyphal cell morphotypes. There is some evidence to support the direct interaction of certain metal ions with a *C. albicans* transcription factor, CaMac1 (122); however the latter explanation fits well with the observed microbicidal synergy between metal ions and antifungals (either amphotericin B or Cu^{2+}).

A contributing factor to metal resistance in *C. tropicalis* biofilms may be sequestration of cations in the ECM. A previous report has shown that the diffusion of

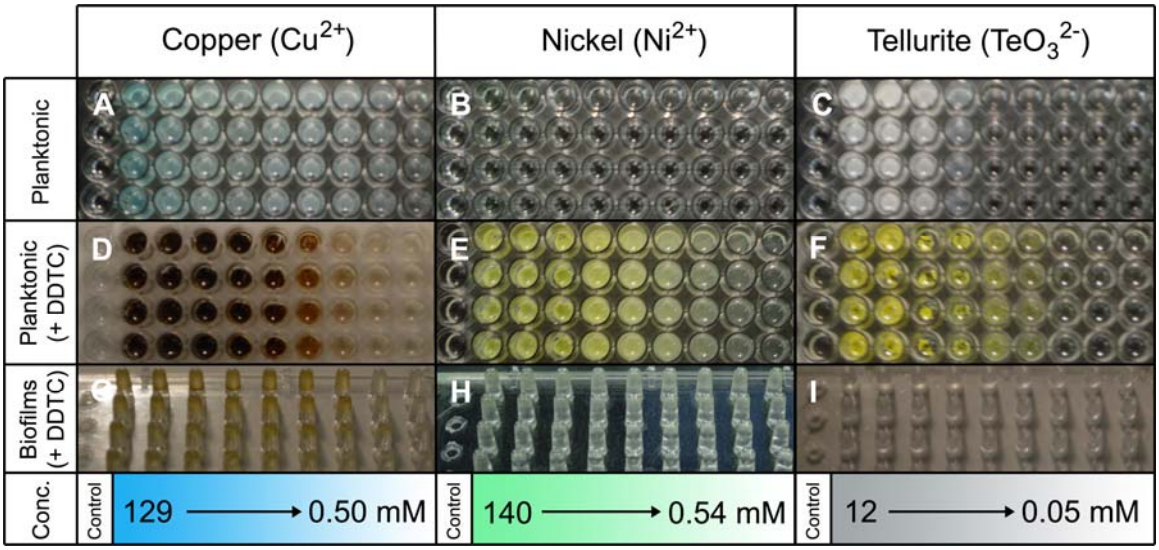

Figure 6.8. Cu^{2+} and Ni^{2+} cations were adsorped by the biomass of *Candida tropicalis* 99916 biofilms. Biofilms grown in CBD were exposed to $\log_2$ concentration gradients of the heavy metals copper (Cu^{2+}), nickel (Ni^{2+}) and tellurite (TeO_3^{2-}) for 5 hours (these gradients are illustrated in the bottom panel of each column). Planktonic cultures exposed to (A) Cu^{2+}, (B) Ni^{2+} and (C) TeO_3^{2-} are pictured above. The addition of the organic chelator Na_2DDTC to aliquots of these planktonic cultures produced (D) brown, (E) light yellow and (F) dark yellow precipitates, respectively. The biofilms from the corresponding wells illustrated in panels A, B and C were removed from the metals and rinsed twice with 0.9% NaCl. These pegs were subsequently treated with Na_2DDTC. Brown and light yellow precipitates formed in biofilms exposed to (G) Cu^{2+} and (H) Ni^{2+}. There was no color change in biofilms exposed to (I) TeO_3^{2-}. This suggests that biofilms of *C. tropicalis* have the ability to trap and sequester positively charged metal ions. Each panel shows 4 assays run in parallel in the same CBD apparatus. (This figure has been reproduced by permission from Harrison *et al.* (2006) FEMS Microbiology Ecology 55:479-491).

fluconazole and 5-fluorocytosine through *Candida* biofilms is slowed, requiring 3 to 6 h to equilibrate across these surface-adherent communities (1). However, *Candida* biofilms exposed for this period of time continued to grow in the presence of these agents, indicating that poor penetration cannot solely account for drug resistance. Similarly, the formation of visible precipitates of metal cations in biofilms suggests that sequestration and limited penetration may be a contributing factor to resistance. However, metal oxyanions could not be precipitated in a similar fashion, indicating that these negatively charged compounds may diffuse across the biofilm matrix. Furthermore, although CrO_4^{2-}, AsO_2^- and AsO_4^{3-} killed planktonic *C. tropicalis* time-dependently, biofilms survived high concentrations of these antimicrobials at the longest exposure time assayed. Together, these data suggest that restricted penetration of metals into the biofilm matrix of *C. tropicalis* is only one contributing factor for biofilm resistance and/or tolerance. Nonetheless, the experiments in this Chapter indicate that biofilm formation is an innate strategy for fungal multimetal resistance and tolerance.

Biofilm formation by yeasts is best characterized for *C. albicans*. In this microorganism, biofilm formation is a step-wise developmental process that proceeds through three stages: 1) an 'early' phase characterized by adhesion of blastospores (yeast cells) to the surface, 2) an 'intermediate' phase where yeast have proliferated to cover a large surface area and have begun to produce extracellular polymers, and 3) a 'maturation' phase. Mature *C. albicans* biofilms are matrix entrenched and arranged into layers, with yeast cells attached to the surface and hyphae on top (44, 143). The data here indicate that metal ions may act at the intermediate stage of *C. albicans* and *C. tropicalis* biofilm development to redirect the final pattern of cellular differentiation in the solid-surface attached community.

It is unlikely that the counter ions of metal salts – such as Na^+, K^+, Cl^-, NO_3^- or SO_4^{2-} – influenced the observed morphological changes in *C. albicans* and *C. tropicalis* biofilms. For example, nitrate (NO_3^-) salts of both Pb^{2+} and Ag^+ were used in this study. In the case of Ag^+, morphological changes occurred in *C. albicans* biofilms around 0.04 mM, whereas for Pb^{2+} there was no observed change in cell morphology at

concentrations of 24 mM. Further, Na^+, K^+, Cl^-, NO_3^- and SO_4^{2-} are present in the rich and minimal media formulations used to grow the biofilms in control and test groups.

The interaction of *C. albicans* and *C. tropicalis* with metal ions may represent a fundamental biotic-abiotic interaction. Since biofilm maturation involves the emergence of drug resistance in parallel with multiple cell morphotypes (44), metal ions may alter biofilm susceptibility to natural or synthetic antimicrobial agents. Furthermore, metal ions may be important regulators affecting a cell type switch that is co-regulated with a transition from commensalism to virulence, suppressing the disease process of an otherwise infectious fungal biofilm (68). At the very least, the effect of metal ions on the differentiation of highly resistant *Candida* spp. may be a preliminary biological indicator of metal pollution in the environment.

6.5 Contributions

6.5.1 Author's contributions to this work and personal acknowledgements

I performed about 70% of the experimental work described in this Chapter. In the process of doing this research, I trained 1 post-doctoral fellow (Dr. Maryam Rabiei) and 2 undergraduate students (Erin A. Badry and Kimberley M. Sproule) to assist with the remainder of the experiments. I would like to extend thanks to Jerome Yerly, Dr. Yaoping Hu and Dr. Robert Martinuzzi for expert technical assistance with 3D visualization using amira™.

6.5.2 Relevant publications

These data sets were originally published in Harrison *et al.* (2006) FEMS Microbiology Ecology 55:479-491, a manuscript on which I am denoted an equal first author with Dr. Maryam Rabiei, and in Harrison *et al*. (2007) Applied and Environmental Microbiology 73:4940-4949.

Chapter Seven: Cellular defence against oxidative stress protects *Escherichia coli* biofilms from the distinct chemical toxicities of different metal ions

7.1 Introduction

Deleterious reduction-oxidation[20] (redox) reactions have the potential to damage all biological macromolecules, and the survival of a cell therefore depends on its ability to control the levels of biochemical oxidants (191). Unwanted oxidants may be produced as by-products of normal metabolism or they may be introduced by environmental agents that induce oxidative stress[21] (191, 192). It is generally assumed, although it has not been systematically tested in prokaryotes, that the toxicity of metal ions might be derived from their ability to participate in redox reactions that both oxidize sensitive cellular thiol (-RSH) groups (100, 241, 262) and produce reactive oxygen species (ROS) – such as superoxide ($O_2^{\bullet-}$), hydroxyl radicals ($^{\bullet}OH^-$), hydrogen peroxide (H_2O_2) and singlet oxygen ($^1O_2$). Microbes possess an array of antioxidant defenses that range from small, oxidant scavenging molecules to self-regulating homeostatic gene networks (191). Here, it was hypothesized that these antioxidant defenses might be chromosomal determinants affecting the susceptibility of bacterial cells to metal toxicity. This may be significant, as the chromosomal determinants responsible for basal levels of bacterial multimetal resistance and tolerance, other than those genetic elements encoding metal efflux pumps, are for the most part unknown.

In *E. coli* cells, redox homeostasis is managed by a complex thiol-redox system which consists of the glutathione and thioredoxin pathways (251). The *oxyRS* regulon is generally considered an integrated part of this system. *E. coli* also possesses the redox-sensing *soxRS* system, which activates genes that render the cell resistant to $O_2^{\bullet-}$ and other antibacterials. It is interesting to note that *E. coli marR* – which was identified and named because of its ability to confer multiple antibiotic resistance when inactivated by

---

[20] Oxidation is the loss of electrons from an atom, ion or molecule, whereas reduction is the gain of electrons.

[21] Oxidative stress may result from excess production of various reactive species (ROS, free radicals, etc.) or from insufficient antioxidant defences in the cell.

mutation (81) – may also play a role in antioxidant defense. In fact, several isolated mutations at this locus have been associated with some of the phenotypes of *soxRS* mutants, and as a result, this same chromosomal locus was independently named *soxQ* (89). Some of the genetic parts that make up the molecular anatomy of these systems are summarized in Table 7.1 and here this has served as a preliminary list of *E. coli* genes of interest that have a known function in defense against oxidative stress.

In *E. coli*, the thiol-redox system, OxyR , MarR and SoxR regulons may work together as an integrated, homeostatic oxidative stress response system. The *E. coli* thiol-redox system senses and catalyzes thiol-disulfide exchange reactions that repair damaged cell constituents and coordinate the expression of stress response genes (251). In contrast, SoxR and OxyR are redox operated transcription factors that sense and initiate responses to superoxide and H_2O_2, respectively (192). The collective involvement of these pathways in cellular metabolism is highly complex, as many of the key transcription factors in this stress response network are parts of dense overlapping regulons (DORs) (3, 222). Here, it was specifically hypothesized that the thiol-redox system, *soxRS* and *marR*, as well as the associated enzymatic defence against oxidative stress, may contribute to basal levels of biofilm defence against metal toxicity, as several genes in these systems have a differential averaged expression profile in biofilms relative to planktonic cells (17, 18, 206).

At the time of writing this Chapter, many of the experiments described here are "work-in-progress" and it is my hope that future students or strong collaborators might help to complete this research in the months (or years) following my Thesis defence. At this point, I am in the process of using *in vitro* and *in vivo* fluorescent indicators of reactive oxygen species (ROS) (and have plans to examine thiol specific probes in the near future) to show that different toxic metal species (CrO_4^{2-}, Co^{2+}, Cu^{2+}, Ag^{+}, Zn^{2+}, AsO_2^{-}, SeO_3^{2-} and TeO_3^{2-}) participate in different and distinct oxidative reactions with bacterial cell biomass. Moreover, I have recently completed comprehensive high-throughput susceptibility testing of several *E. coli* strains with inactivating mutations in genes important for both defense against ROS and for maintaining cellular thiol-disulfide poise – this includes: the Mn- and Fe-dependent superoxide dismutases (*sodAB*),

glutathione oxidoreductase (*gorA*), thioredoxin (*trxA*), glutathione synthetase (*gshA*), glutaredoxin (*grxA*), and the repressor for the multiple antibiotic resistance and oxidative stress regulon (*marR*/*soxQ*). I am also in the process of constructing a series of promoter-*luxCDABE* reporters to look at metal ion concentration-dependent expression at several genes of interest in this stress response network. The strength of this research has been in using a combinatorial experimental design to comparatively examine different metal ions as well as logarithmic-phase, stationary-phase and biofilm cells of *E. coli*.

By compiling the data obtained from the experiments performed thus far, it is possible to show that certain genes play distinct roles in protecting bacteria from different toxic metal ions. Surprisingly, I discovered that in some cases, certain genes may increase the detrimental effects of metal toxicity, and in this regard, parts of cellular systems required for redox homeostasis may be a double edged sword. I have also functionally identified several genes that behave differently in their ability to protect planktonic cells from toxic metal ions when compared to biofilms and, in most cases, intact systems for defense against oxidative stress were essential for biofilm cell survival. Based on these data, I have concluded that enzymes for cellular defense against oxidative stress may protect biofilms from the distinct chemical toxicities of different metal ions. Moreover, these experiments have been a first step towards deducing the biochemical pathways through which metal ions exert oxidative toxicity on bacterial cells.

7.2 Materials and Methods

7.2.1 Standard Protocols

All of the *E. coli* strains used in this Chapter are summarized in Table 7.1 and all were stored, handled and cultured as described in Chapter Two. Biofilms were cultivated by growing these strains at 35 °C in the trough format of the Calgary Biofilm Device (CBD) for 24 h in LB medium. In addition to this method of biofilm cultivation, metal susceptibility testing of *E. coli* biofilms was carried out according to the standard protocols described in Chapter Two, except that 4-fold dilution gradients of toxic metal species were prepared instead of the standard 2-fold dilution gradients. Susceptibility

Table 7.1. Representative genes that function in the adaptive response of *Escherichia coli* to oxidative stress.

Gene(s)	Name	Function, relevant details or mediated enzymatic reaction	Relevant regulation	References
Thiol-redox system				
oxyR	oxidative stress response regulator	LysR family transcription factor	H_2O_2(+)	(192)
oxyS	oxidative stress response regulator	small regulatory RNA	OxyR*(+)	(192)
katE	catalase	$H_2O_2 \rightarrow H_2O + ½O_2$	RpoS(+)	(171, 191)
katG	peroxidase	bifunctional catalase-peroxidase	OxyR*(+), RpoS(+)	(191, 192)
ahpCF	alkyl hydroperoxidase	ROOR' + NADPH → ROH + R'OH + $NADP^+$ + H^+	OxyR*(+)	(129, 192)
gorA	glutathione reductase	GSSG + NADPH + H^+ → 2GSH + $NADP^+$	OxyR*(+), RpoS(+)	(129, 191)
grxA	glutaredoxin A (Grx1)	General mechanism: 2GSH + Grx(ox) → GSSG + Grx(red)	OxyR*(+)	(129, 192)
grxB	glutaredoxin B (Grx 2)		MarA(+)	(14)
grxC	glutaredoxin C (Grx 3)		unknown	(129)
gshA	γ-glutamylcysteine synthetase	L-Cys + L-Glu + ATP → L-γ-glutamylcysteine + P_i + ADP	unknown	(129)
gshB	glutathione synthase	Gly + L-γ-glutamylcysteine + ATP → GSH + P_i + ADP	unknown	(129)
trxA	thioredoxin A	Function in a wide variety of cellular processes.	unknown	(129)
trxC	thioredoxin C	Protein disulfide reductases, catalyze thiol-disulfide exchange.	OxyR*(+)	(129, 197)
trxB	thioredoxin reductase	Trx(ox) + NADPH + H^+ → Trx(red) + $NADP^+$	OxyR*(+)	(129, 197)
nrdAB	ribonucleotide reductase	Trx(red) + NDP → Trx(ox) + H_2O + 2'-dNDP (reversible)	unknown	(129)
tpx	thiol peroxidase	Trx(red) + H_2O_2 → Trx(ox) + H_2O	MarA(+)	(14)
dps	DNA-binding protein in starved cells	ferritin-like, protects DNA from electrophilic attack	OxyR*(+), RpoS(+)	(173, 191)
fur	ferric uptake regulator	Fe-binding repressor of iron transport	OxyR*(+), SoxR*(+)	(191, 192)
Superoxide regulon				
soxR	regulator of superoxide regulon	MerR family transcription factor	$O_2^{\bullet-}$(+)	(191, 192)
soxS	activator of superoxide regulon	AraC family transcription factor, activator of SoxRS regulon	SoxR*(+)	(192)
zwf	G6P dehydrogenase	G6P + $NADP^+$ + H^+ → 6-phosphoglucono-6-lactone + NADPH	SoxS(+), MarA(+)	(14, 197)
sodA	Mn-dependent superoxide dismutase	$2O_2^{\bullet-} + 2H^+ \rightarrow O_2 + H_2O_2$	SoxS(+), MarA(+), Fur(-)	(14, 176, 197)
sodB	Fe-dependent superoxide dismutase	$2O_2^{\bullet-} + 2H^+ \rightarrow O_2 + H_2O_2$	constitutive	(78)
nvd	endonuclease IV	apurinic or apyrimidinic (AP) endonuclease	SoxS(+)	(42, 192)
Multiple antibiotic resistance (Mar) regulon				
marR/soxQ	repressor of Mar regulon	MerR family transcription factor	MarR(-), MarA(+)	(14)
marA	activator of Mar regulon	AraC family transcription factor, activator of Mar regulon	MarR(-), MarA(+)	(2)

Table 7.2. *Escherichia coli* strains used in Chapter Seven.

Strain	Genotype	Relevant gene(s) inactivated	Biofilm growth (log_{10} c.f.u./peg)[1]	n[2]	Source
DH5α	*supE44 hsdR17* Δ*lacU169 recA1 endA1 gyrA96 thi1 relA1 deoR* (ϕ80 *lacZ*ΔM15)	none, cloning strain	na	na	(95)
K12 BW25113	F$^-$ *rrnB53 lacZ4787 hsdR514 araBAD567 rhaBAD568 rph-1*	none, reporter strain	na	na	(10)
JM109	F′ *traD36 proAB*$^+$ *lacIq* Δ*lacZM15* Δ*lac-proAB glnV44 e14- gyrA96 recA1 relA1 endA1 thi1 hsdR17*	none, reporter strain	na	na	(97)
GC4468	F$^-$ Δ*lacU169 rpsL* Sm^r	parental strain	5.7 ± 0.7	103	(8)
QC1725	GC4468 Δ*sodA*	Mn^{2+}-dependent superoxide dismutase	5.1 ± 0.7	16	(53)
QC1799	GC4468 Δ*sodAB*	Mn^{2+} and Fe^{2+}-dependent superoxide dismutase	5.4 ± 0.7	84	(254)
JHC1072	GC4468 *soxQ::Tn10* Km^r	Repressor for multiple antibiotic resistance and oxidative stress regulon	5.6 ± 0.6	127	(8)
JHC1096	GC4468 *marR::Tn9* Km^r	Repressor for multiple antibiotic resistance and oxidative stress regulon	5.8 ± 0.6	60	(8)
JF1070	F$^-$ *thi1 thr1 leuB6 his4 argE3 ara14 lacY1 galK2 xyl5 mtl1 rpsL31kdg K51 tsx33 supE44 proAB lacIPOZYA*	parental strain	6.0 ± 0.5	56	(261)
JF420	JF1070 Δ*gor1*	glutathione oxidoreductase	5.1 ± 0.4	56	(261)
JF2062	JF1070 *trxA::kan* Km^r	thioredoxin	5.7 ± 0.6	55	(261)
JF2200	JF1070 *gshA::kan* Km^r	glutathione synthetase	5.7 ± 0.6	104	(261)
BPR100	JF1070 *grxA::kan* Km^r	glutaredoxin	5.5 ± 0.8	103	(261)

Abbreviations: Km^r = kanamycin resistant, Sm^r = streptomycin resistant, na = not applicable
[1]Biofilm growth is reported as the mean and standard deviation of n viable cell counts
[2]n denotes the number of pooled control measurements

testing was performed in minimal salts vitamins glucose (MSVG) medium (250) for metal cations, and LB broth for metal oxyanions, and recovery medium contained "universal neutralizer," the composition of which was described in Chapter Two. Tests for equivalent biofilm growth were also carried out as described in Chapter Two.

7.2.2 Susceptibility testing of logarithmic- and stationary-phase planktonic cells

Susceptibility determinations with logarithmic growing *E. coli* cells were done using a protocol designed to reflect the Clinical Laboratory Standards Institute (CLSI) method for antibiotic susceptibility testing. The inoculum for these tests was prepared by direct colony suspension from streak plates to match a 1.0 McFarland Standard as described in Chapter Two for creating a standard biofilm inoculum. This standard was diluted 30-fold in LB medium and 5 µL aliquots of this 1 in 30 dilution were added to each well of the challenge plates.

Susceptibility determinations with stationary-phase cells were carried out in a slightly different fashion. First, 25 mL of LB was inoculated with a single colony that was picked with a sterile cotton swab from a first agar sub-culture. The *E. coli* cells in these cultures were grown to early stationary phase by incubating overnight (18 to 20 h) on a gyrorotary shaker set at 225 rpm and 37 °C. Stationary-phase cells were collected by centrifugation (5000 × g for 10 min) after which the spent medium was discarded. Cell pellets were suspended in 12.5 mL of fresh growth medium thereby concentrating cells into half of the original volume. In contrast to susceptibility determinations for biofilms and logarithmic-phase planktonic cells, challenge plates were prepared with metal ions at twice the desired concentration but in 100 µL, as opposed to 200 µL, volumes in the wells of the microtiter plates. To these challenge plates, 100 µL of the 2 × concentrated stationary-phase cells were added to each well.

In the cases of logarithmic-phase and stationary-phase planktonic cells, the challenge and recovery media, neutralizing agents, serial dilution, incubation conditions and viable cell counting protocols were identical to those used for CBD susceptibility testing. In all cases, the starting numbers of cells in these suspensions were determined by viable cell counting.

7.2.3 Molecular methods

7.2.3.1 Materials and standard molecular protocols

A complete list of plasmids used in this Chapter appears in Table 7.2. Standard molecular methods were carried out according to the protocols of Sambrook and Russell (212). *E. coli* K12 genomic DNA was purified from overnight cultures using a DNeasy Blood and Tissue kit (QIAGEN Inc., Mississagua, ON, Canada). The pCS26pac plasmid was purified from *E. coli* DH5α using a Plasmid Maxi Kit (QIAGEN) and the protocol for very low copy number plasmids. Products from PCR and restriction digestions were cleaned up using a QIAquick® PCR purification kit (QIAGEN). DNA sequencing was carried out by University Core DNA Services (University of Calgary, Calgary, AB, Canada). All enzymes were purchased from Invitrogen and all primers were purchased from Sigma.

7.2.3.2 Construction of promoter-*luxCDABE* fusions

Primers were designed to flank regions between the two adjacent open reading frames (ORFs) that border each of the promoter regions of the genes of interest. This was done in a fashion similar to that described by Zaslaver *et al*. (285). Here, my approach was to design primers to amplify the entire regions between the two ORFs with an extension of 10 to 25 bp into each flanking ORF. Each forward or reverse primer was designed with a 5' XhoI or BamH1 restriction site, respectively, and each primer was designed to have a melting temperature (T_m) of 60 to 62 °C. A complete list of primers used in this Chapter appears in Table 7.2.

Promoter regions were amplified from *E. coli* K12 genomic DNA by PCR under the following conditions: 95 °C for 10 min, followed by 24 cycles of 95 °C for 1 min, 55 °C for 1 min and 68 °C for 1 min, and a final step at 68 °C for 10 min. Product size was verified on a 1% agarose gel. PCR was optimized and repeated, as required, by varying the concentration of $MgCl_2$ in the reaction mixture from 2.0 to 4.5 mM. The PCR products were purified and then digested in a 45 µL reaction volume with XhoI for 7 h at 37 °C (in React® 2 buffer: 50 mM Tris-HCl, 10 mM $MgCl_2$, 50 mM NaCl, pH 8.0). To

conserve the PCR products, 2.5 μL of 1 M NaCl was added to this mixture (to bring the concentration to 100 mM NaCl, thereby mimicking React® 3 buffer), and then the PCR products were digested with BamH1 for 5 h at 37 °C. A similar protocol was performed to digest the pCS26pac plasmid, and all digested PCR products and plasmids were then purified using a QIAGEN PCR purification kit.

The pCS26pac vector has the reporter operon *luxCDABE* with an upstream cloning region containing 5' XhoI and 3' BamH1 restrictions sites that allowed for directional insertion of the cloned promoter fragments. The digested PCR products were ligated overnight with the digested pCS26pac vector using T4 DNA ligase under the following conditions: 4 °C for 10 h, 10 °C for 3 h and then 16 °C for 3h. The ligated promoter-*luxCDABE* fusions were then transformed into *E. coli* K12 BW25113. The digested pCS26pac vector was checked for background by self-ligation followed by transformation. Transformants were selected on LB agar with 50 μg mL^{-1} kanamycin and insertions were confirmed by colony PCR using the sequencing primers pZE.05 and pZE.06 as previously described (27). The PCR products from promoter inserts on pCS26 plasmids were additionally verified by DNA sequencing.

7.2.4 Fluorescent sensors for metal ion mediated ROS production

Three different sensors were used to evaluate the production of ROS during the reaction of *E. coli* biomass with toxic metal species. First, synthesis of the ROS sensor 4[*N*-methyl-*N*(4-hydroxyphenyl)amino]-7-nitrobenzofurazan (NBFhd) was carried out according to the method of Heyne *et al*. (114). NBFhd is composed of the fluorophore *N*-methyl-4-amino-7-nitrobenzofurazan (NBF) (excitation maximum 468 nm, emission maximum at 540 nm) that has been covalently linked to a quencher, 4-hydroxyphenol. The NBFhd sensor may react with oxygen radicals to release the strongly fluorescent NBF moiety as well as the by-product 1,4-benzoquinone (114). The second reagent used was an isomeric mixture of 5-(and 6)-carboxy-2',7'-difluorodihydrofluorescein diacetate (carboxy-H_2DFFDA, Invitrogen). Upon oxidation, this probe forms highly fluorescent

Table 7.3. Plasmids and primers used in Chapter Seven.

Name	Description or sequence	Source
Plasmids		
pCS26pac	Low copy number *luxCDABE* reporter vector	(16)
pQE30HyPer	hydrogen peroxide biosensor	Axxora Inc., (19)
pCS26pmarR	pCS26 containing 347 bp insert with *marR* promoter	this study
pCS26psodA	pCS26 containing 370 bp insert with *sodA* promoter	this study
pCS26psodB	pCS26 containing 210 bp insert with *sodB* promoter	this study
pCS26pgorA	pCS26 containing 148 bp insert with *gorA* promoter	this study
pCS26ptrxA	pCS26 containing 157 bp insert with *trxA* promoter	this study
pCS26pgshA	pCS26 containing 337 bp insert with *gshA* promoter	this study
pCS26pgrxA	pCS26 containing 215 bp insert with *grxA* promoter	this study
pCS26poxyR	pCS26 containing 144 bp insert with *oxyR* promoter	this study
pCS26psoxR	pCS26 containing 128 bp insert with *soxR* promoter	this study
pCS26psoxS	pCS26 containing 128 bp insert with *soxS* promoter	this study
pCS26pkatE	pCS26 containing 229 bp insert with *katE* promoter	this study
pCS26pfliA	pCS26 containing 365 bp insert with *fliA* promoter	this study
Primers		
marRF02	5’-ATCCGGCTCGAGCCAGCCCCAGGCCAATTG-3’	this study
marRR02	5’-ATCCGGGGATCCCAGATACTCGTTAAGCAGGC-3'	this study
sodAF02	5’-ATCCGGCTCGAGGCCGATCAAATGCCAAAATATC -3’	this study
sodAR02	5’-ATCCGGGGATCCGCATCGTAAGCATACGGCAG-3’	this study
sodBF02	5’-ATCCGGCTCGAGTGGCGCTCGTCGGGTAATG -3’	this study
sodBR02	5’-ATCCGGGGATCCGAGCATCTTTAGCATATGGTAG -3’	this study
gorF02	5’-ATCCGGCTCGAGCACCGGGCACGCCACCG-3’	this study
gorR02	5’-ATCCGGGGATCCCGCCGCCGATGGCGATG-3’	this study
trxAF02	5’-ATCCGGCTCGAGAGTCGGAAAACTTCTGTTCTG-3’	this study
trxAR02	5’-ATCCGGGGATCCGGAATAAGCCTGGCGTGTTGG -3’	this study
gshAF02	5’-ATCCGGCTCGAGGTCGGAGGTTCGAATCCTC-3’	this study
gshAR02	5’-ATCCGGGGATCCATTAAACCTGCATAACGCTCG-3’	this study
grxAF02	5’-ATCCGGCTCGAGCTTTAGGCAATTTACCGATCG-3’	this study
grxAR02	5’-ATCCGGGGATCCCCGAACGACCAAAAATAACGG-3’	this study
oxyRF02	5’-ATCCGGCTCGAGGTTAAAAGAGGTGCCGCTCC-3’	this study
oxyRR02	5’-ATCCGGGGATCCGTACTCAAGATCACGAATATT C-3’	this study
soxRF02	5’-ATCCGGCTCGAGAATTTTCTGATGGGACATAAATC-3’	this study
soxRR02	5’-ATCCGGGGATCCTAATGCGGGGTAATTTCTTTTC -3’	this study
soxSF02	5’-ATCCGGCTCGAGTAATGCGGGGTAATTTCTTTTC-3’	this study
soxSR02	5’-ATCCGGGGATCCAATTTTCTGATGGGACATAAATC-3’	this study
katEF02	5’-ATCCGGCTCGAGATTACTGGCTTCACTAAACGC-3’	this study
katER02	5’-ATCCGGGGATCCGTTCTTTTCGTTATGTTGCGAC-3’	this study
fliAF01	5’-ATCCGGCTCGAGTCTGTCTCTGCTGCAGGG -3’	this study
fliAR01	5’-ATCCGGGGATCCTCAGCGGTATAGAGTGAATTC -3’	this study
pZE.05	sequencing primer, 5’-CCAGCTGGCAATTCCGA-3’	(27)
pZE.06	sequencing primer, 5’-AATCATCACTTTCGGGAA -3’	(27)

carboxy-2',7'-difluorofluorescein (DCF, excitation maximum 485 nm, emission maximum at 530 nm), and since this molecule carries a double negative charge under physiological conditions, this dye is less likely to leak out of cells than other halogenated fluorescein analogues. Lastly, a fluorescent biosensor for intracellular H_2O_2 accumulation, pQE30HyPer (Axxora, San Diego, CA, USA), was used to detect metal ion mediated ROS production *in vivo*. This biosensor consists of circularly permuted yellow fluorescent protein (cpYFP) that has been inserted into the regulatory domain (RD) of *E. coli oxyR*. OxyR-RD contains two key cysteine residues (Cys199 and Cys208). When oxidized, a sulfenic acid is first formed at Cys199 and then a disulfide bond may be formed between Cys199 and Cys208. This conformational change prevents proper folding of the fluorescent domain in the cpYFP (19). Changes in fluorescence may be measured as the fold change in excitation ratio (500 nm/420 nm) while measuring emission at 530 nm (19).

7.2.5 Fluorimetry and luminometry

All reactions were prepared in 3 mL final volumes directly in cuvettes used for fluorescent measurements. Here, *E. coli* K12 BW25113 was streaked out and cultured twice in succession on LB agar to obtain fresh second subcultures of this organism. A 1.0 McFarland suspension of this microorganism was prepared in 0.9% NaCl as described above. In all cases, these standardized *E. coli* cell suspensions were diluted 10-fold in the reaction mixtures. Concentrated stock metal solutions were added to the cuvettes to obtain the final concentrations indicated throughout this Chapter. Where indicated, the probe NBFhd (5 mM stock in DMSO) and the antioxidant TROLOX (Sigma, 5 mM stock in DMSO) were used at final concentrations of 0.1 mM.

Fluorescent measurements were obtained using a Fluorolog-3 spectrofluorometer with DataMax for Windows^{TM} (Horiba Jobin Yvon Instruments S. A. Inc., Edison, NJ, USA). For NBF, these measurements were carried out using an excitation wavelength of 468 nm to obtain an emission spectrum from 480 to 650 nm in 1 nm increments, using a 1 s integration time and 5 nm slit widths. At the time of writing this thesis, measurements of metal-ion mediated ROS production using carboxy-H_2DFFDA and

pQE30HyPer were still in progress. Similarly, no measurements using the *luxCDABE* reporters had been made at the time of thesis submission.

7.2.6 Calculations, definitions of measurements and criteria for significant differences

Calculations of mean viable cell counts, mean log-kill measurements and one-way ANOVA to test for equivalent biofilm growth were performed according to the guidelines set in Chapter Two. Here, the survival of bacterial populations was quantified using viable cell counting and the cell survival rates of mutant strains were compared to the cell survival rates of the isogenic parental strains. Here, a set of criteria were established and survival in mutant populations was considered significantly different from the wild type population if conditions 1 and 2 or condition 3 were met:

1. There must be at least a 50-fold difference in mean viable cell counts of the mutant versus the wild-type population and this may have occurred at 1 or more tested concentrations of toxic metal species (as described in Chapter Two).
2. The mean of the wild-type population survival, plus or minus one standard deviation, was mutually exclusive of the mean of the mutant population survival, plus or minus one standard deviation (i.e. there must be no overlap between the compared error intervals) (as described in Chapter Two).
3. If sterilization points (i.e. $MBC_{p\text{-}100}$ and $MBC_{b\text{-}100}$ values) could be determined, then there must be at least a 16-fold difference in the median endpoint of the wild type population compared to the endpoint for the mutant population.

7.3 Results

7.3.1 Production of ROS by metal cations and oxyanions

Although it is generally accepted within the field of microbiology that metal ions exert oxidative toxicity on bacteria, this h as not been systematically tested using biochemical assays. In a preliminary set of experiments, the probe NBFhd was used to look for ROS production in *E. coli* cells exposed to bactericidal concentrations of CrO_4^{2-}, Co^{2+}, Cu^{2+}, Ag^{+}, Zn^{2+}, AsO_2^{-}, SeO_3^{2-} and TeO_3^{2-} (Figure 7.1).

In the cases of the metal cations examined, this approach yielded striking, clear results: Cu^{2+} generates ROS during cell exposure, whereas Co^{2+}, Ag^{+} and Zn^{2+} do not. This fits well with previous literature focused on eukaryotic systems (94) as well as with the well known ability of Cu^{2+} to participate in Fenton-type reactions (249). In contrast, the results for the metal oxyanions were not as clear, but might still provide useful information. For example, adding the antioxidant TROLOX (a water soluble analogue of vitamin E) to the reaction mixture protected NBFhd from oxidation by AsO_2^{-}, SeO_3^{2-} and TeO_3^{2-}. It is also interesting to note that *E. coli* biomass protected NBFhd from oxidation by CrO_4^{2-} and SeO_3^{2-}, although the meaning of this latter observation, at least as it pertains to the biochemistry of the toxic oxyanions, is somewhat ambiguous. The most intriguing result occurred for CrO_4^{2-}, as the addition of TROLOX to the mixture increased the oxidation of NBFhd; moreover, this seemed to correspond with the susceptibility data described in the following sections. Overall, these data suggest that all of the metal cations and oxyanions examined in this study participate to different extents in oxidative reactions with *E. coli* biomass.

7.3.2 E. coli biofilm formation

Although it is relatively simple to calibrate the starting cell densities of planktonic cell suspensions, a more thorough approach was used to calibrate biofilm growth. Regardless of the medium used for metal ion exposure, biofilms of all *E. coli* strains were cultivated in LB broth. The means and standard deviations of biofilm cell densities produced by the relevant, different *E. coli* strains grown in this fashion are summarized in Table 7.1. After 24 h incubation, these biofilms were statistically equivalent between the different rows of pegs in the CBD ($0.053 \leq p \leq 0.992$). As an exception, *E. coli* JF420 required 48 h of growth to obtain a starting cell density similar to the other strains; furthermore, only the outer 2 rows of pegs on each side of the device (i.e. rows A and B, G and H) were used for susceptibility testing as the internal regions of the CBD had significantly lower biofilm growth than the outer two rows for this strain (data not shown).

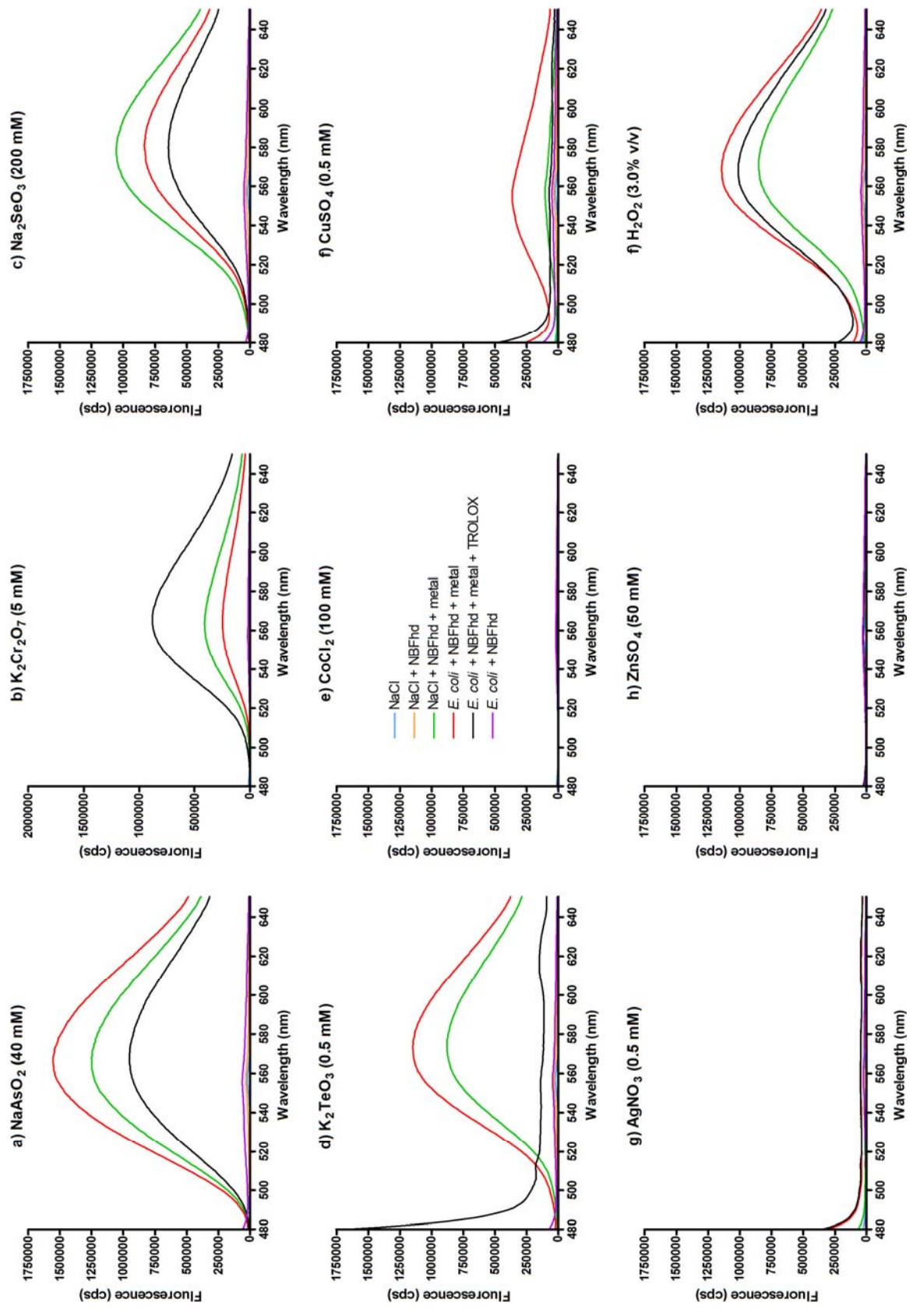
a) NaAsO2 (40 mM)
b) K2Cr2O7 (5 mM)
c) Na2SeO3 (200 mM)
d) K2TeO3 (0.5 mM)
e) CoCl2 (100 mM)
f) CuSO4 (0.5 mM)
f) H2O2 (3.0% v/v)
g) AgNO3 (0.5 mM)
h) ZnSO4 (50 mM)
Fluorescence (cps)
Wavelength (nm)
NaCl
NaCl + NBFhd
NaCl + NBFhd + metal
E. coli + NBFhd + metal
E. coli + NBFhd + metal + TROLOX
E. coli + NBFhd

Figure 7.1. NBFhd assays to detect ROS production during the reaction of *E. coli* K12 BW25113 biomass with toxic metal species. Solutions, which had been incubated with the indicated reagents for 24 h at room temperature, were excited at 468 nm and the fluorescence emission spectrum was measured between 480 and 650 nm. The NBFhd sensor and the antioxidant TROLOX were used at final concentrations of 0.1 mM each. Viable *E. coli* cells were added at a concentration corresponding to a 10-fold dilution of a 1.0 McFarland standard. These results suggest that not all toxic metal species produce ROS during reactions with *E. coli* cell biomass; moreover, the extent to which ROS are produced might be different for each metal that is capable of producing these toxic by-products. Each panel in this figure is a representative example of two independent replicates. Hydrogen peroxide (H_2O_2) has been included as a positive control.

7.3.3 Susceptibility of E. coli thiol-redox mutants to toxic metal ions

A combinatorial experimental approach was taken to look at the susceptibility of biofilms, logarithmic-phase and stationary phase populations of 9 different *E. coli* strains (7 mutant strains and their 2 isogenic parental strains) to 8 different toxic metal species (at 5 different concentrations each plus the associated growth and sterility controls). This initial screening process yielded 1296 combinations of parameters that were subsequently evaluated in quadruplicate. Viable cell counting was used to evaluate the survival of the different *E. coli* strains under these conditions after 4 h of exposure, and these data are presented for CrO_4^{2-}, Co^{2+}, Cu^{2+}, Ag^{+}, Zn^{2+}, AsO_2^{-}, SeO_3^{2-} and TeO_3^{2-}, in periodic order, in Figures 7.2 to 7.9. To identify trends in these sets of survival dynamics, the data were subsequently analyzed using the criteria in section 7.2.6, and the results were grouped by genotype and by the toxic metal to which the cells were exposed. This summary appears in Figure 7.10. It is important to note that the concentration of Co^{2+} used for the susceptibility testing of stationary-phase cells was too low and future assays should examine higher concentrations to complete the trend sets illustrated in Figure 7.10.

Overall, these susceptibility data indicate distinct roles for many genes of the *E. coli* thiol-redox system in the survival of cells exposed to different toxic metal species (Figure 7.10). There are several key trends that emerge from these data. First, as an internal control for this system, two strains bearing different inactivating mutations at the same locus (denoted *marR* or *soxQ*) were tested side-by-side in this system. The criteria set in section 7.2.6 were designed to minimize identification of false positives, and so what were identified as significant differences between the survival of these mutant and wild type populations were not identical under all tested conditions. However, a consistent trend that emerged from this analysis is that *marR* is important for basal levels of survival in *E. coli* populations exposed to toxic metal species. This provides a notable genetic link between the *E. coli* antibiotic and metal toxicity stress responses.

Another trend that emerges from these data is that not all of the genes in the *E. coli* thiol-redox system play a protective role against metal toxicity. In fact, there are five notable exceptions where the opposite is true – i.e. the functional copies of the thiol-redox genes increase the susceptibility of the population to the tested toxic metal species.

Moreover, in two of these cases, these susceptibility data fit with trends observed in the preliminary NBFhd assays. 1) *gor*, *gshA* and *grxA* increase the sensitivity of logarithmic-phase *E. coli* to chromate toxicity and this correlated with the observation that TROLOX increases NBFhd oxidation. 2) *sodAB* increases the sensitivity of *E. coli* to Co^{2+}, Ag^{+} and Zn^{2+}, which correlated with the observation that these three transition metals characteristically do not produce ROS (as least as it can be discerned by NBFhd assays). 3) *gshA* increases the sensitivity of logarithmic-phase planktonic cells and biofilms to TeO_3^{2-}. 4) *trxA* increases the sensitivity of planktonic cell populations to Ag^{+} and Zn^{2+}. 5) *grxA* increases the susceptibility of logarithmic-phase and stationary-phase planktonic cell populations to Ag^{+} and Zn^{2+}, respectively. Collectively, it is in this fashion that the enzymes of the *E. coli* thiol-redox system may be a double-edged sword against the oxidative toxicity of metal ions.

A last trend that emerges from these data is that genes of the *E. coli* thiol-redox system, other than *marR*/*soxQ*, protect populations of planktonic and biofilm cells in different ways. It is striking that in almost all the cases where significant differences in susceptibility could be determined for biofilms that this indicated a protective role for the functional thiol-redox genes. This information has some important implications. Foremost, this suggests that the net activity of the thiol-redox enzymes on the by-products of the reactions between metal ions and biomass may be dependent on the mode of bacterial growth. In other words, the contribution of individual thiol-redox genes to redox homeostasis in planktonic and biofilm cells might be different. Nonetheless, these data provide strong evidence that enzymes for cellular defense against oxidative stress protect biofilms from the distinct chemical toxicities of different metal ions.

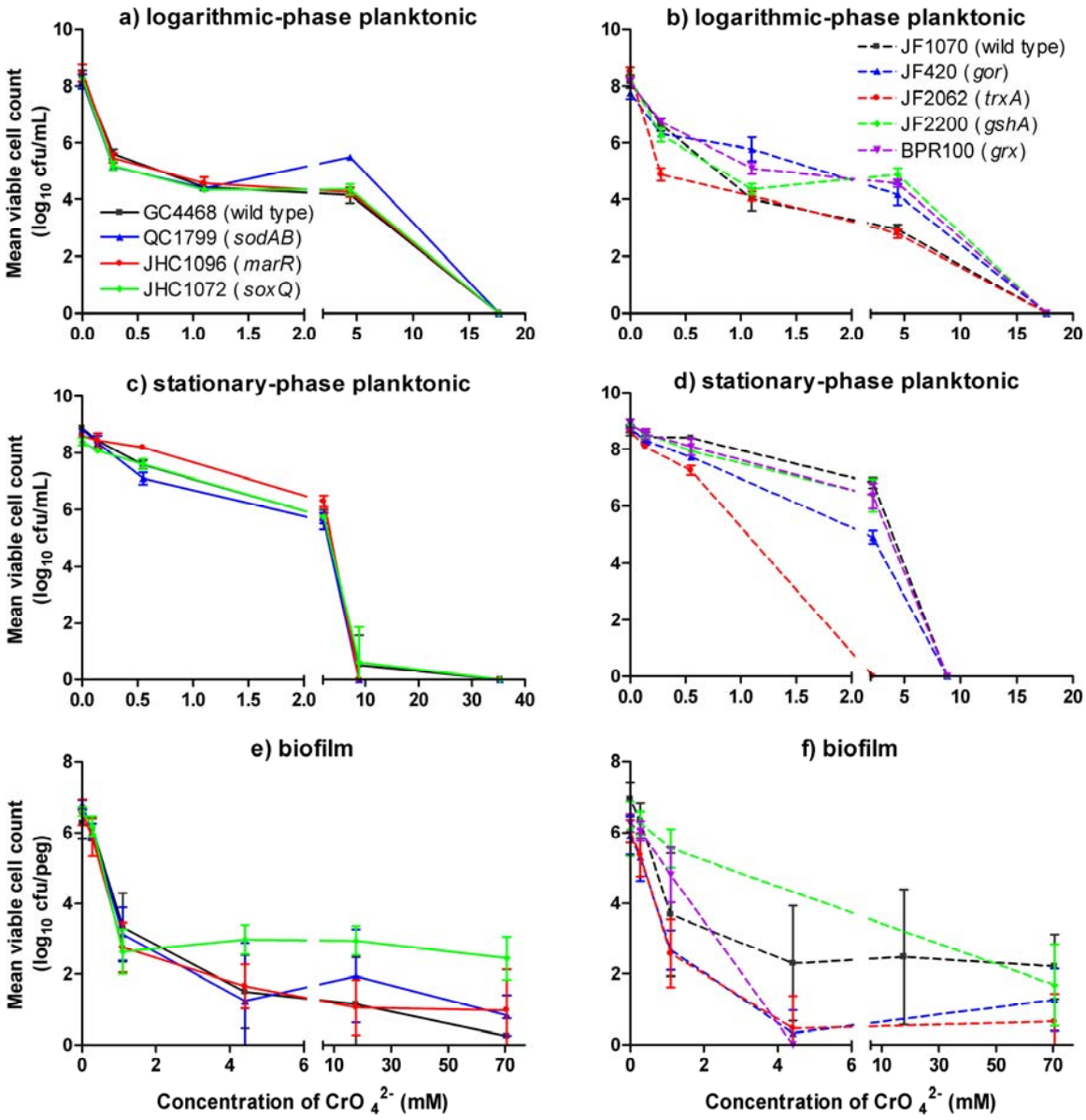

Figure 7.2. Cell survival in biofilm, logarithmic- and stationary-phase planktonic cell populations of *E. coli* thiol-redox mutants exposed to chromate (CrO_4^{2-}). Two different sets of mutants were examined (either in the GC4468 or JF1070 genetic background), and each set is plotted with its isogenic parental strain and mutants. Here, each measurement is the mean and standard deviation of 4 independent replicates of viable cell counts obtained after 4 h of exposure to the metal in LB medium.

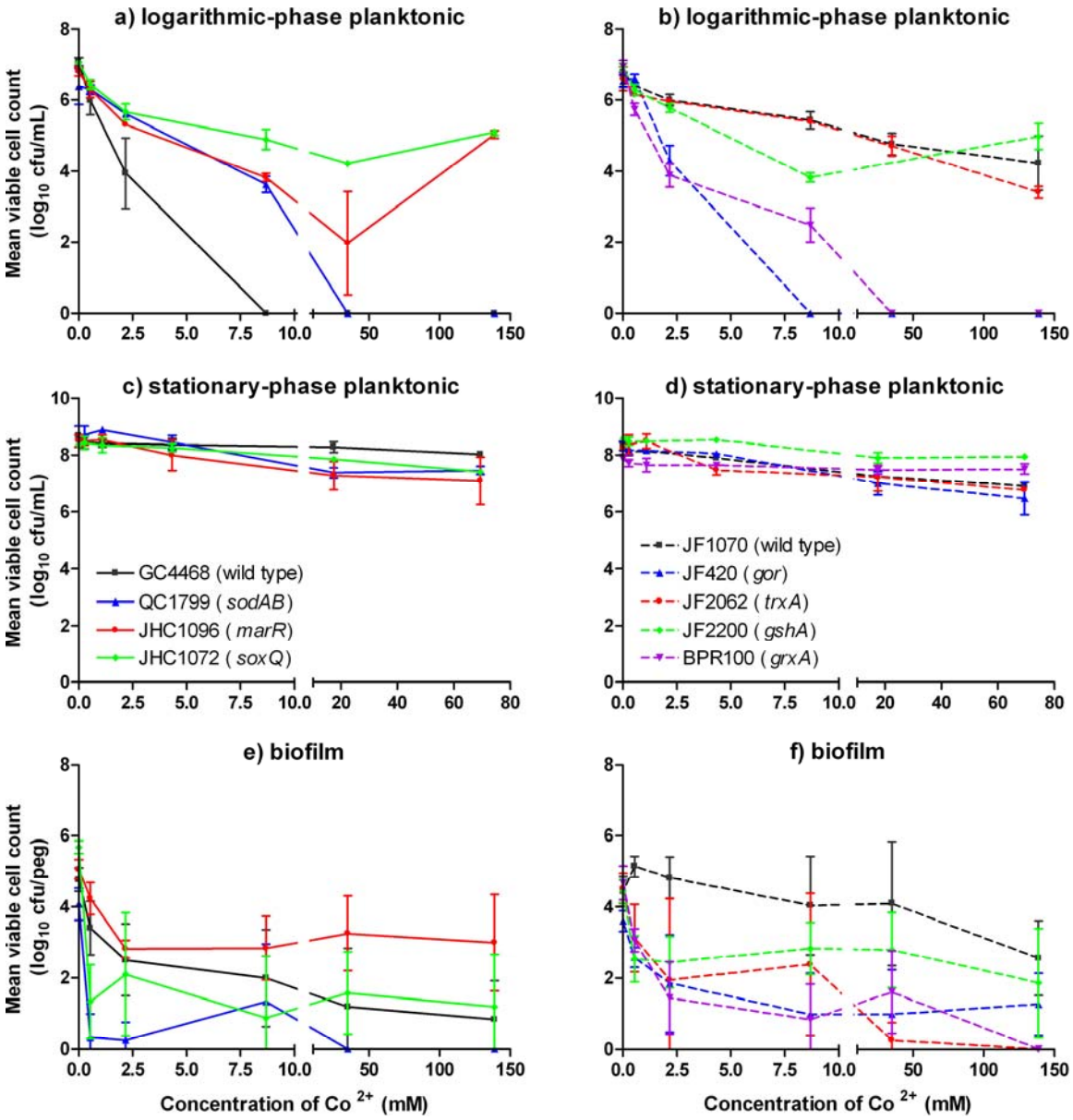

Figure 7.3. Cell survival in biofilm, logarithmic- and stationary-phase planktonic cell populations of *E. coli* thiol-redox mutants exposed to cobalt (Co^{2+}). Two different sets of mutants were examined (either in the GC4468 or JF1070 genetic background), and each set is plotted with its isogenic parental strain and mutants. Here, each measurement is the mean and standard deviation of 4 independent replicates of viable cell counts obtained after 4 h of exposure to the metal in MSVG medium.

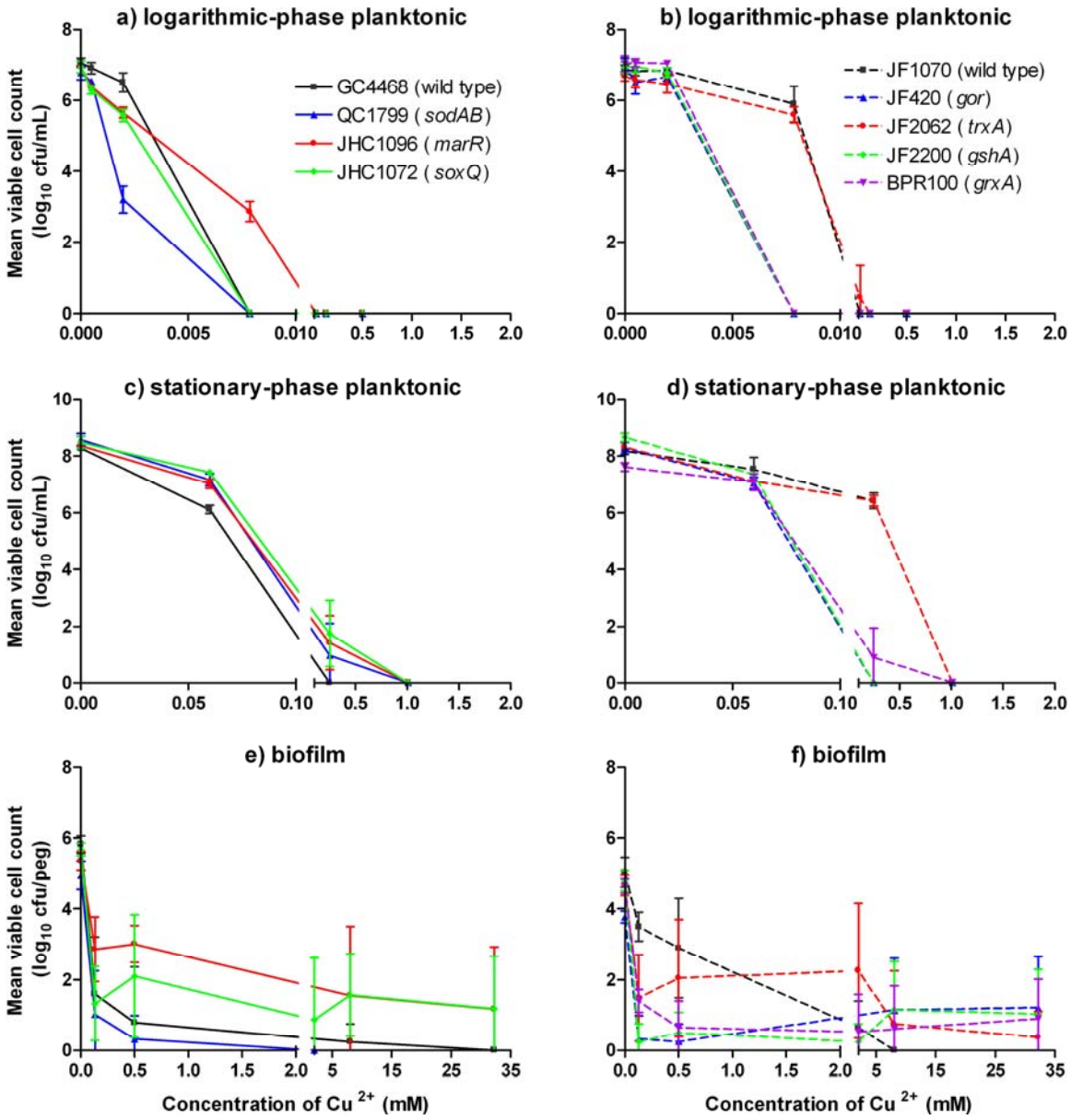

Figure 7.4. Cell survival in biofilm, logarithmic- and stationary-phase planktonic cell populations of *E. coli* thiol-redox mutants exposed to copper (Cu^{2+}). Two different sets of mutants were examined (either in the GC4468 or JF1070 genetic background), and each set is plotted with its isogenic parental strain and mutants. Here, each measurement is the mean and standard deviation of 4 independent replicates of viable cell counts obtained after 4 h of exposure to the metal in MSVG medium.

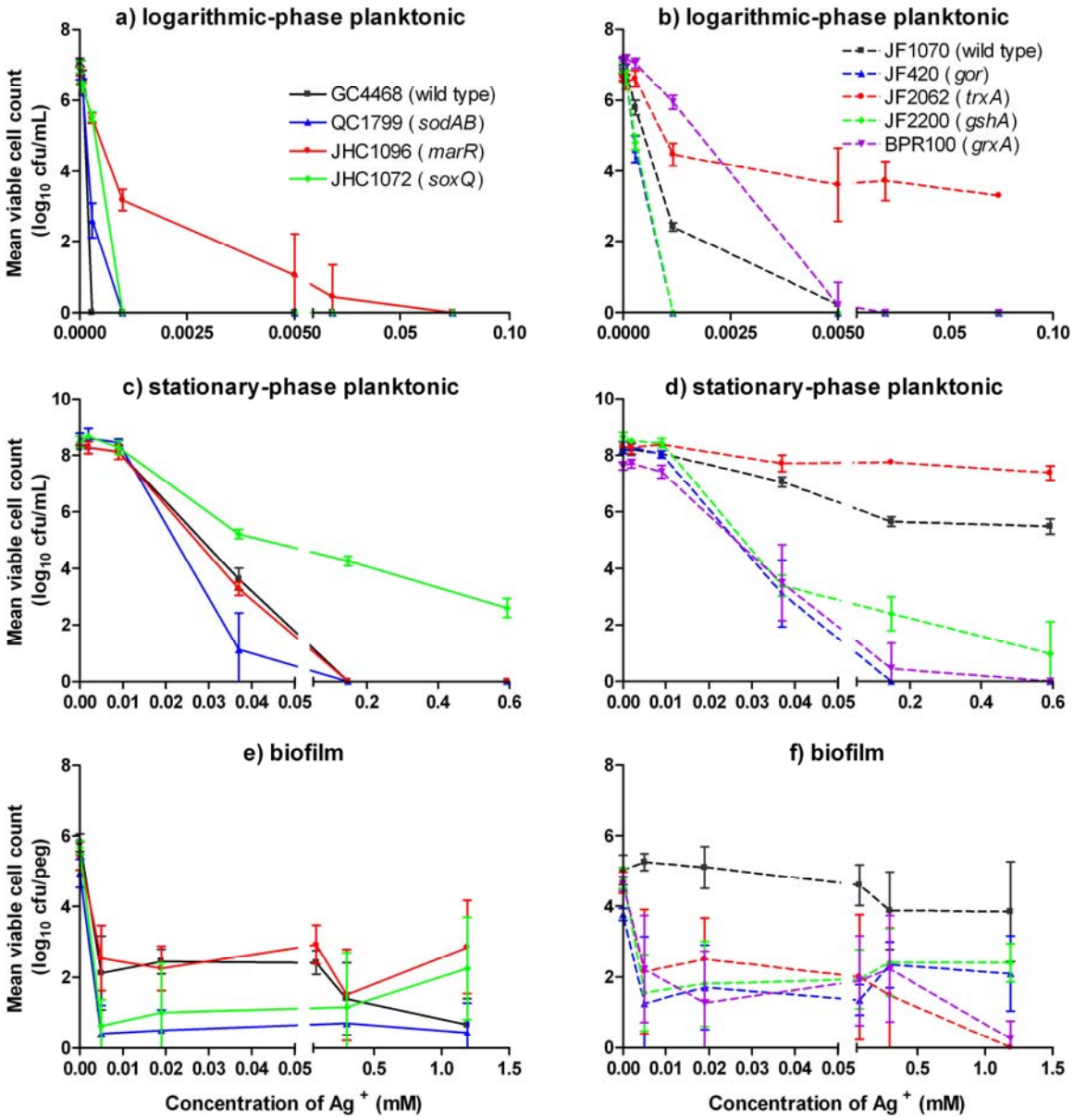

Figure 7.5. Cell survival in biofilm, logarithmic- and stationary-phase planktonic cell populations of *E. coli* thiol-redox mutants exposed to silver (Ag^+). Two different sets of mutants were examined (either in the GC4468 or JF1070 genetic background), and each set is plotted with its isogenic parental strain and mutants. Here, each measurement is the mean and standard deviation of 4 independent replicates of viable cell counts obtained after 4 h of exposure to the metal in MSVG medium.

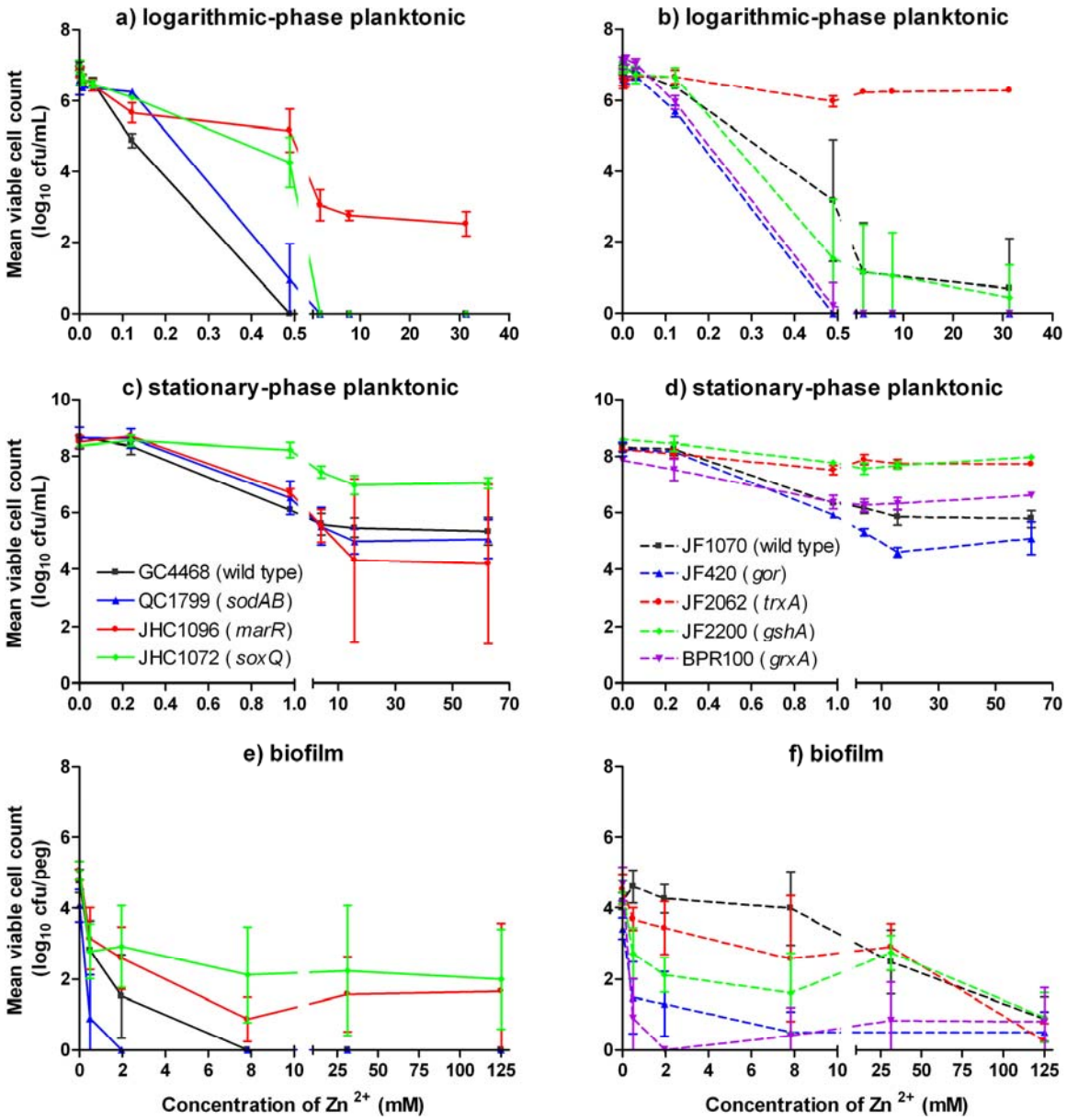

Figure 7.6. Cell survival in biofilm, logarithmic- and stationary-phase planktonic cell populations of *E. coli* thiol-redox mutants exposed to zinc (Zn^{2+}). Two different sets of mutants were examined (either in the GC4468 or JF1070 genetic background), and each set is plotted with its isogenic parental strain and mutants. Here, each measurement is the mean and standard deviation of 4 independent replicates of viable cell counts obtained after 4 h of exposure to the metal in MSVG medium.

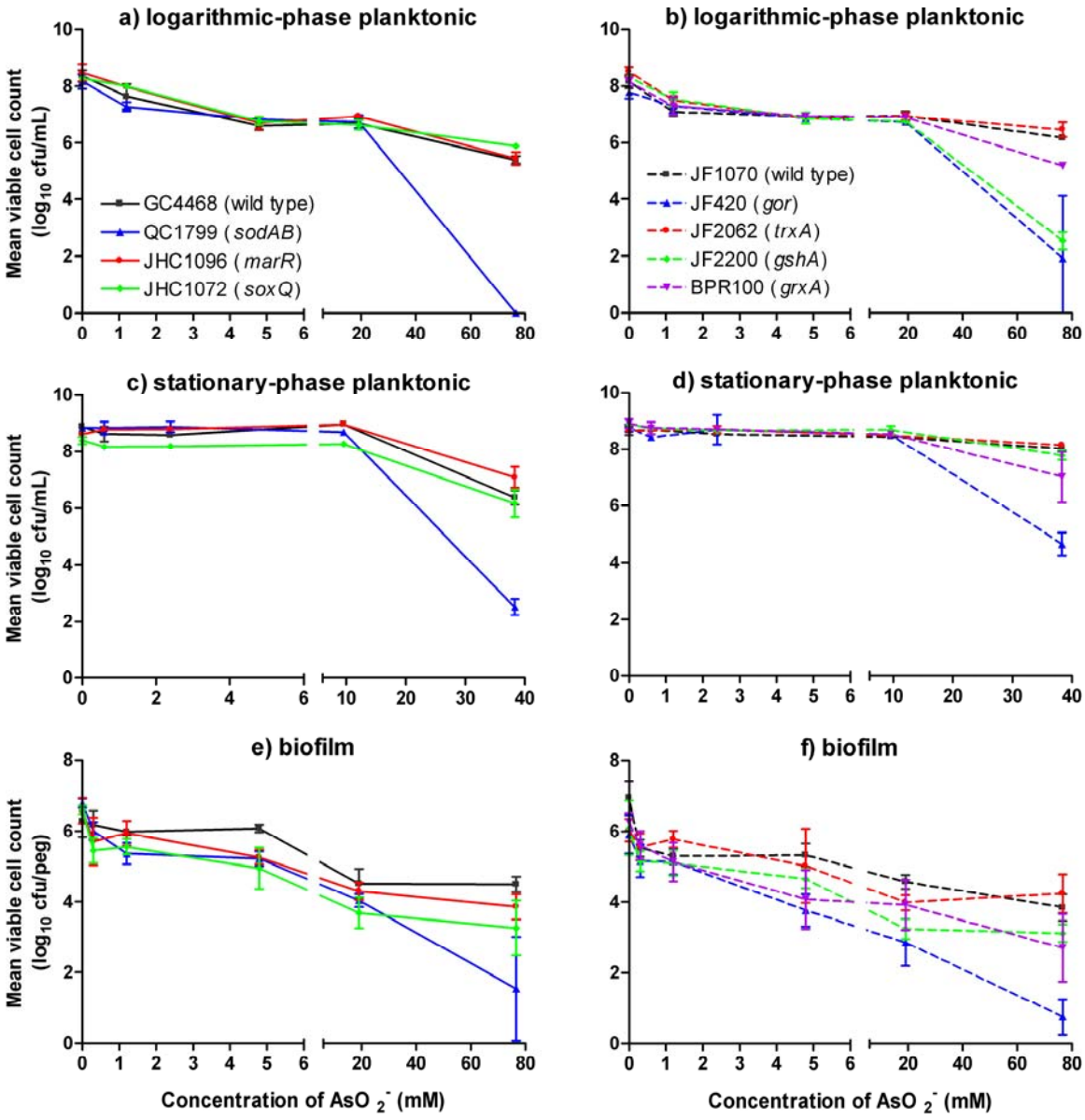

Figure 7.7. Cell survival in biofilm, logarithmic- and stationary-phase planktonic cell populations of *E. coli* thiol-redox mutants exposed to arsenite (AsO_2^-). Two different sets of mutants were examined (either in the GC4468 or JF1070 genetic background), and each set is plotted with its isogenic parental strain and mutants. Here, each measurement is the mean and standard deviation of 4 independent replicates of viable cell counts obtained after 4 h of exposure to the metal in LB medium.

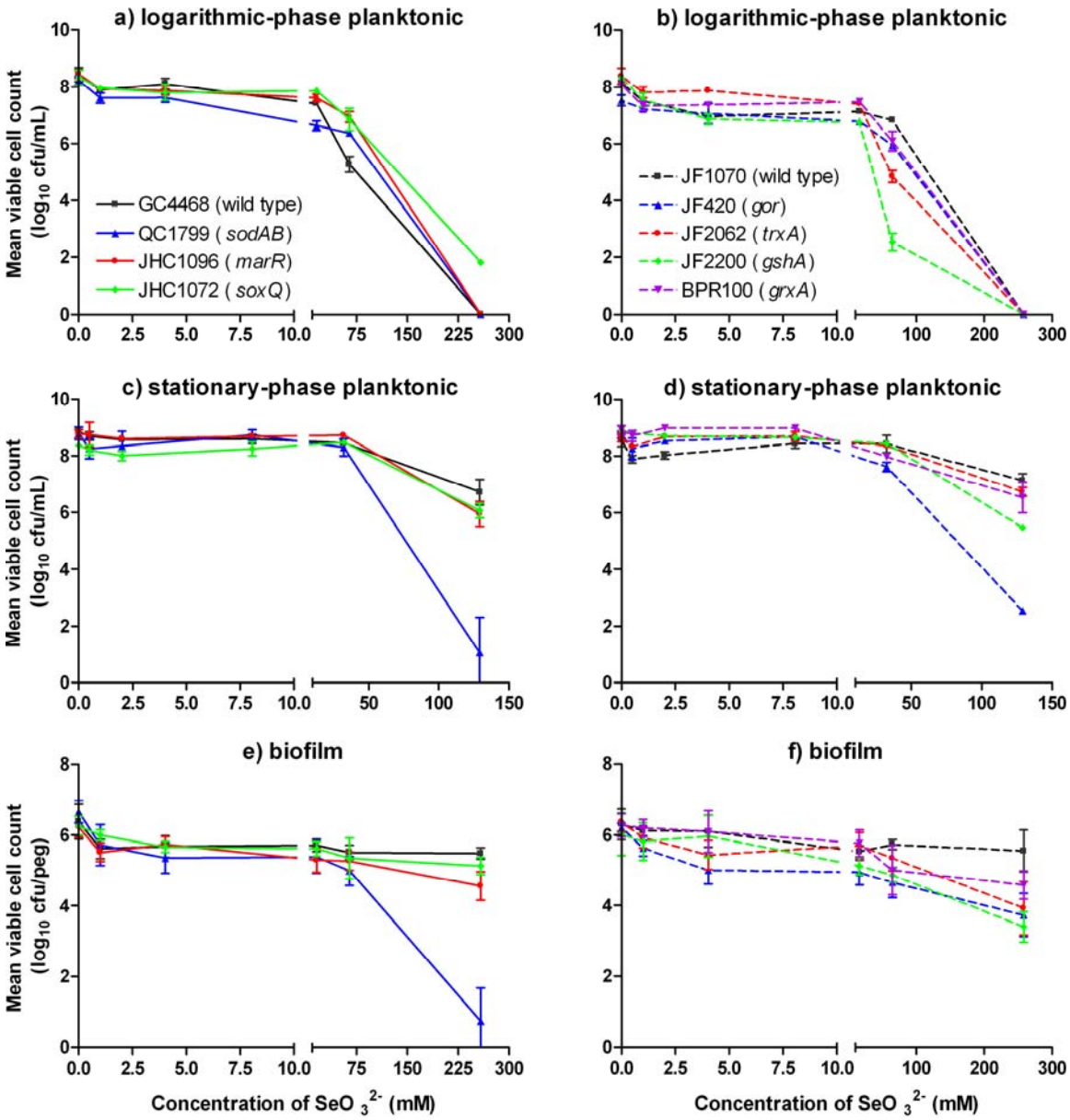

Figure 7.8. Cell survival in biofilm, logarithmic- and stationary-phase planktonic cell populations of *E. coli* thiol-redox mutants exposed to selenite (SeO_3^{2-}). Two different sets of mutants were examined (either in the GC4468 or JF1070 genetic background), and each set is plotted with its isogenic parental strain and mutants. Here, each measurement is the mean and standard deviation of 4 independent replicates of viable cell counts obtained after 4 h of exposure to the metal in LB medium.

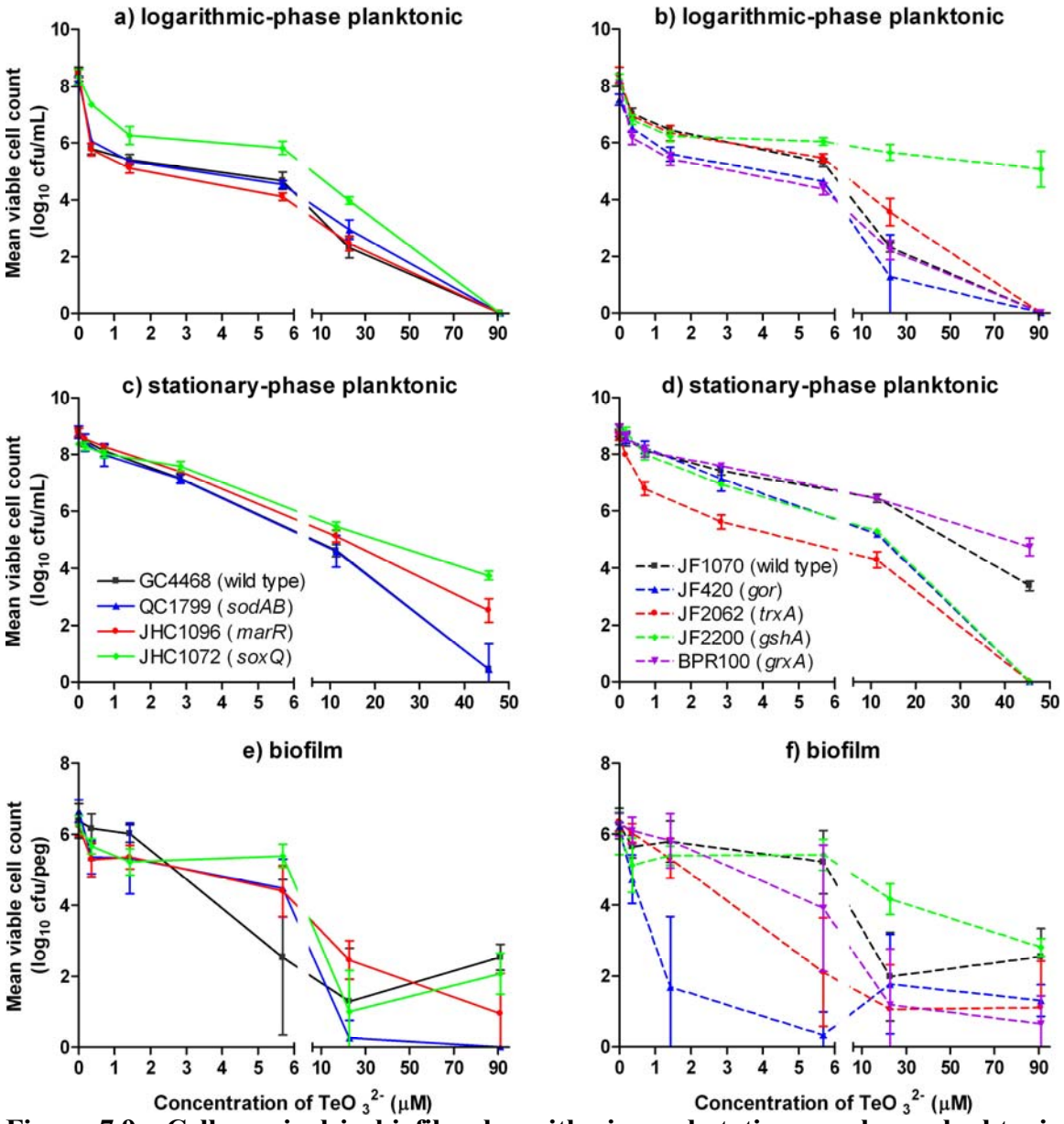

Figure 7.9. Cell survival in biofilm, logarithmic- and stationary-phase planktonic cell populations of *E. coli* thiol-redox mutants exposed to tellurite (TeO_3^{2-}). Two different sets of mutants were examined (either in the GC4468 or JF1070 genetic background), and each set is plotted with its isogenic parental strain and mutants. Here, each measurement is the mean and standard deviation of 4 independent replicates of viable cell counts obtained after 4 h of exposure to the metal in LB medium.

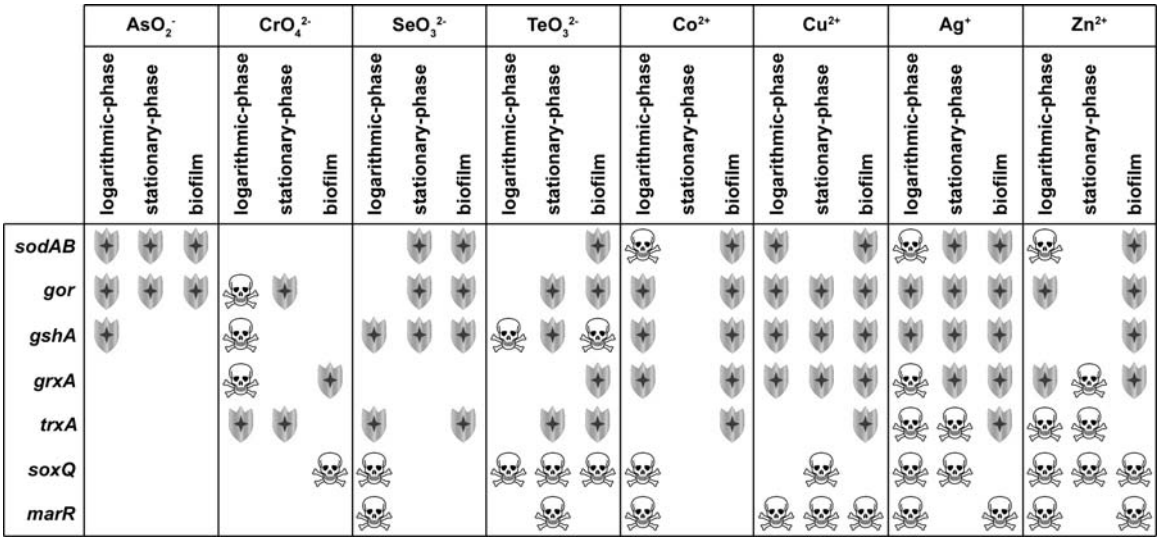

Figure 7.10. Effects of functional genes involved in the thiol-redox system on the survival of *E. coli* populations exposed to toxic metal species. Survival data from susceptibility testing was grouped by gene of interest and by toxic metal, and this was further categorized by bacterial mode of growth. Log-killing data was analyzed using the mean relative log-kill method described in Chapter Two. Here, a shield denotes that a functional copy of the indicated gene enhanced population survival, whereas skull and crossbones indicate that the functional gene decreased population survival. At the time of writing this Thesis, additional susceptibility testing with stationary phase planktonic cells was underway for $CoCl_2$.

7.4 Discussion

There are many sources of oxidative stress and it is likely that these have moulded the evolution of adaptations to aerobic life (94, 191). Aerobic organisms display both constitutive and inducible antioxidant[22] defences against oxidative stress, and this includes the *E. coli* thiol-redox, SoxR, OxyR and MarR systems (94). There are several potential biochemical routes for oxidative metal toxicity (241) and the data in this Chapter indicate that bacterial antioxidant systems have an important and complex role in the defence of cells against toxic metal species. Since thiol-redox systems are a conserved biochemical feature among the kingdoms of life (251), it may be possible to use *E. coli* as a model organism to expand our general understanding of metal toxicology.

At this early experimental stage, it is possible to build a biochemical model out of the known pathways of the *E. coli* redox homeostasis systems (Table 7.1) and to combine this with the comparative, combinatorial susceptibility data generated in this work (Figure 7.10). Using several hypothetical and generalized biochemical routes of metal toxicity discerned from the literature (Figure 1.3), I have integrated these with the known regulation and reactivity of cellular antioxidants in Figure 7.11. Halliwell (93) has proposed that there is no universal 'best' antioxidant; rather, the rank depends on the nature of the oxidative challenge. The redox biochemistry of toxic metal ions is an excellent example of how a single antioxidant may be inadequate to protect cells from all forms of oxidative stress. The data here suggest that certain antioxidants may potentiate the toxicity of certain metal ions – for example GSH and CrO_4^{2-}. Consistent with this idea, there is some evidence from a study using a hepatocyte cell line that suggests the toxicity of CrO_4^{2-} may be reductively activated by GSH (196). Using this thesis work, this biochemical pathway is probably linked directly to the action of glutaredoxins on metal disulfides, which are indirectly reduced by GSH via GorA (Figure 7.11).

In healthy cells, antioxidant systems balance levels of reactive species rather than eliminate them, as there is a metabolic cost associated with generating antioxidants. For

---

[22] An antioxidant may be defined as any substances that delays, prevents or removes oxidative damage to a target molecule.

example, *E. coli* keeps intracellular H_2O_2 levels at approximately 0.2 μM rather than maintaining excess antioxidants (191). Although a common approach in microbiology has been to compare the susceptibility of biofilm, logarithmic-phase and stationary-phase planktonic cells to antimicrobials, the study here has allowed for an additional dimension of comparison – the functional comparison of genes in different modes of bacterial growth. As a caveat, additional statistical testing of pooled viable cell counts will be required to eliminate those genes that are essential for biofilm formation from this comparison. For example, based on the data in Tale 7.2, *gor* may be essential for biofilm growth, and so susceptibility differences may not only be due to the involvement of Gor in metal metabolism. However, biofilms of the other *E. coli* strains seem to have very similar starting cell counts.

Given the data in Figure 7.10, it is reasonable to hypothesize that the overall enzyme activities that maintain *E. coli* thiol-redox balance are different between logarithmic-phase and stationary-phase planktonic cells, and that this is physiologically distinct from cells in biofilm populations. Here, I would propose that biofilm multimetal resistance and tolerance may be linked to these differences. Furthermore, the antibiotic resistance and tolerance of biofilms might be linked to these same changes. This is a bold statement, but this hypothesis fits with the recent discovery that all three major classes of bactericidal antibiotics kill through a common mechanism: an iron-dependent Fenton reaction that generates ROS (138) (Figure 7.11). This change to the redox homeostasis system state might also define distinct subsets of cells in the bacterial population. For example, persister cells show alternate expression of the MarRAB locus when compared to fast-growing planktonic cells (131).

7.5 Conclusions and future directions

The search for chromosomal genetic elements responsible for the reduced susceptibility of biofilms to antimicrobial agents is currently a hot topic of research. Here, I would like to point out some features of the genes in the thiol-redox system that seem to make them a good fit in the search for chromosomal determinants of biofilm resistance and tolerance. First, these genes have a high degree of conservation between

microbial strains and species, which would fit with the observation that the reduced antimicrobial susceptibility of biofilms occurs for the vast majority of microbes examined. Second, the overall function or activity of these genes and their product(s) seems to be different depending of the mode of culture growth (i.e. logarithmic-phase planktonic cell vs. a surface-adherent cell). This does not imply that the level of transcription will be different (although this may be the case). Third, single gene deletions in these systems do not reduce the susceptibility of biofilms to that of logarithmic-phase planktonic cells, which is consistent with the premise that are multiple mechanisms contributing to the resistance and tolerance properties of biofilms. Lastly, inactivation of these genes affects the susceptibility of *E. coli* cells to multiple, as opposed to single, antibacterial agents.

It is also worth mentioning that when testing for hypersensitivity of gene deletion mutants, survival should be quantitatively measured by viable counts (rather than by using MBC endpoints), and this should be done over a range of concentrations. Since biofilm survival dynamics are time-dependent, a less rigorous approach to susceptibility testing might miss a subtle but important phenotype.

Although the data in this Chapter indicate a complex role for the *E. coli* thiol-redox system in defence against toxic metal species, a greater understanding will emerge from continuation of this study. For example, the use of alternate ROS and thiol-specific probes will be invaluable for elucidating the biochemical toxicities of different metal ions. I must also acknowledge that this study has not looked at reactive nitrogen species (RNS) or sulphur radicals, which may also prove to be an important part of metal toxicity. Lastly, transcriptional analysis of genes in the thiol-redox system will yield important information about gene expression of these multimetal resistance and tolerance determinants – regardless of whether the population averaged expression is different in planktonic versus biofilm cells of *E. coli*. That being stated, in conjunction with the rest of the work presented in this Thesis, it would likely be a worthwhile endeavour to build promoter-GFP fusions to look at single cell expression of these genes by CLSM.

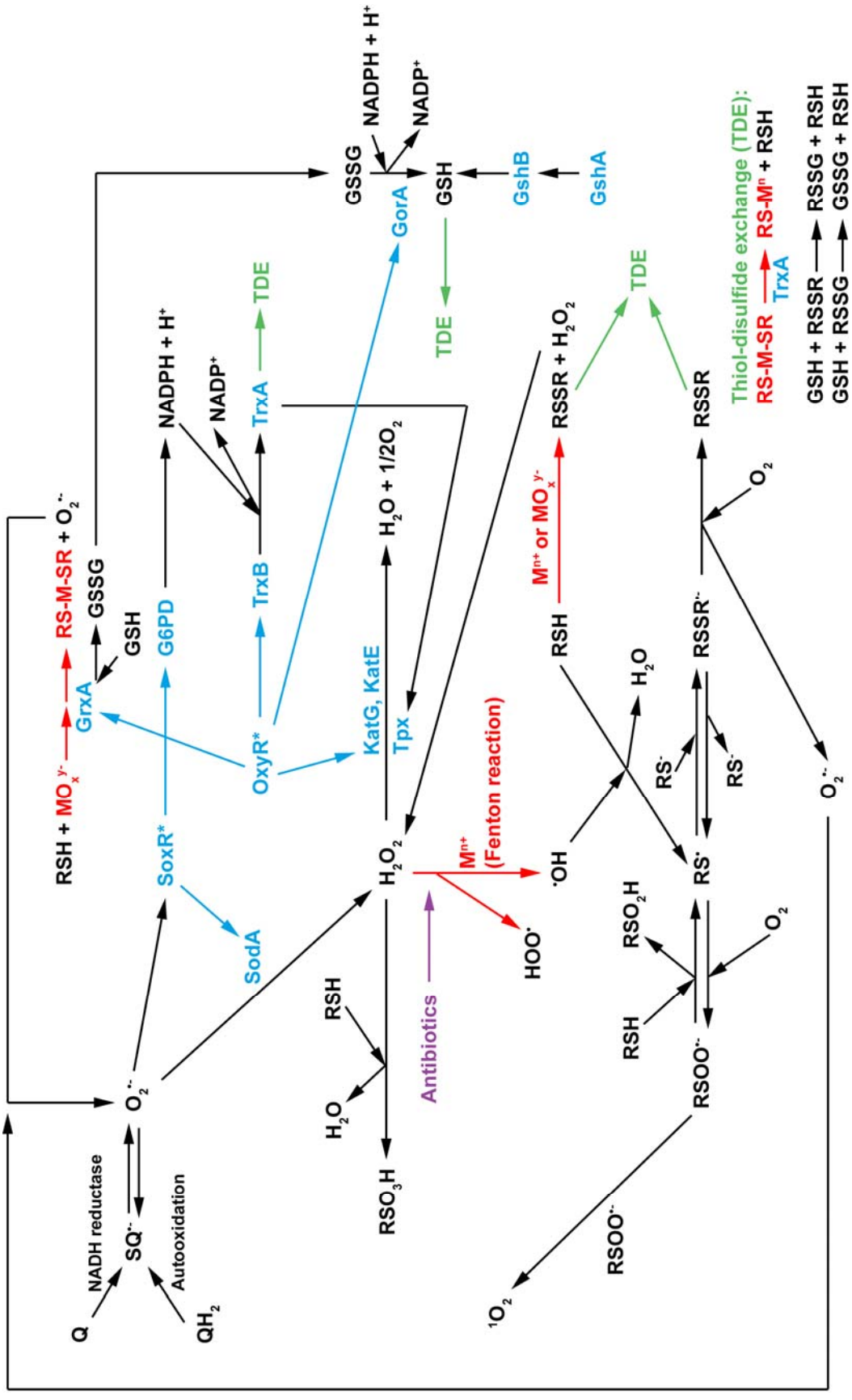
Q
NADH reductase
SQ•-
Autooxidation
QH2
O2•-
SoxR*
SodA
H2O2
H2O
RSH
RSO3H
Antibiotics
Mn+
(Fenton reaction)
HOO•
•OH
H2O
RSH
RS•
RS-
RS-
RSSR•-
RSSR
O2
O2•-
RSH
RSOO•-
O2
RSO2H
RSOO•-
1O2
RSH + MOx y-
RS-M-SR + O2•-
GrxA
GSH
GSSG
G6PD
NADPH + H+
NADP+
TrxB
TrxA
TDE
OxyR*
KatG, KatE
Tpx
H2O + 1/2O2
GorA
TDE
GSSG
NADPH + H+
NADP+
GSH
GshB
GshA
Mn+ or MOx y-
RSH
RSSR + H2O2
TDE
RSSR
O2
Thiol-disulfide exchange (TDE):
RS-M-SR
RS-Mn + RSH
TrxA
GSH + RSSR
RSSG + RSH
GSH + RSSG
GSSG + RSH

Figure 7.11. Hypothetical biochemical routes of oxidative metal toxicity and the repair of damaged cell constituents by the *E. coli* thiol-redox, OxyR and SoxR systems. It is well known that ROS damage biomolecules through reactions with sensitive thiol (RSH) groups (as well as through reactions with other functional groups, which for the sake of simplicity, are not shown here). The well established cycle of ROS toxicity and RSH oxidation is illustrated in black. Certain metal ions may exert oxidative toxicity on cells by autocatalytic production of ROS via Fenton-type chemistry (ex. Fe, Cu), or through many different reactions with RSH and glutathione (GSH). To some extent, all metal ions undergo different and specific reactions with cellular thiols (see Chapter 1 for a discussion). The deleterious reactions of metal ions with cellular biomass are illustrated in red. *E. coli* possesses several homeostatic systems which, based on the data in this chapter, play a role in cellular defence against oxidative metal toxicity. The hypothetical repair routes are illustrated in blue, and a generalized thiol-disulfide exchange mechanism is illustrated in green. In the cases of certain oxyanions, such as with CrO_4^{2-} and TeO_3^{2-}, repair of metal-disulfides by glutaredoxins may lead to an increased production of $O_2^{\bullet-}$, which may account for the decreased toxicity of these oxyanions in *grxA*, *gorA* or *gshA* mutant backgrounds. The recent discovery that bactericidal antibiotics kill cells via Fe-mediated production of ROS may imply that these systems are important for antibiotic resistance and tolerance as well. This pathway is illustrated in purple. Based on the present information, it is unknown how the activities of the illustrated enzymes are different in planktonic versus biofilm cells. However, the data in this Chapter suggest that net changes in these systems for thiol-redox homeostasis may underlie the decreased susceptibility of biofilms to metal ions and potentially to other antimicrobial agents as well.

7.6 Contributions

7.6.1 Author's contributions to this work and personal acknowledgements

I performed about 65% of the experimental work described in this Chapter. In the process of doing this research, I trained 3 undergraduate students (Erin A. Badry, Kimberley M. Sproule and Michelle A. Stan) to assist with susceptibility testing. My sincerest gratitude goes to Dr. Belinda Heyne for synthesizing the probe NBFhd and for providing many useful discussions about reactive oxygen species and the chemistry of metal ions. I would also like to extend thanks to Dr. Michael G. Surette for kindly providing the reporter plasmid pCS26pac. Last of all, I must acknowledge the substantial contribution of Cathy S. Chan, who in the course of helping with the construction of promoter-reporter plasmids has trained me to use many techniques of molecular microbiology.

7.6.2 Relevant publications

At the time of writing this Thesis, the work presented in this Chapter is unpublished.

Chapter Eight: A multifactorial model of multimetal resistance and tolerance in microbial biofilms

8.1 Biofilm growth is a social and multicellular strategy to survive metal toxicity

Biofilm formation might be an intrinsic or induced strategy which microbes might use to survive a toxic flux in metal ions. So how is it that biofilms are less susceptible to metal toxicity than exponentially growing planktonic cell populations? Similar to studies of biofilm antibiotic susceptibility (30, 230), simple time- and dose-dependent killing assays, which were performed as part of this thesis research, show that there are subpopulations of cells in biofilms that die at different rates upon exposure of the entire population to toxic metal ions (59, 97, 105) (Figure 8.1). In this thesis research, I have linked the size of these variant subpopulations to highly conserved chromosomal genetic elements (for example, *E. coli hipA* and *P. aeruginosa gacS*) (59, 97), as well as to previous exposure of the biofilm population to sub-inhibitory concentrations of metal ions (*P. aeruginosa*) (59, 101). Moreover, basal levels of survival in bacterial populations exposed to toxic metal species were linked to a highly conserved set of genes (*sodA*, *sodB*, *grxA*, *trxA*, *gshA*, *gorA* and *marR/soxQ*) responsible for maintaining thiol-disulfide homeostasis in *E. coli* cells, and the data in this thesis suggest that these genes may function differently in planktonic versus biofilm populations.

In this final chapter, I have performed a comprehensive literature review and, in conjunction with my discoveries during this thesis research, I have assembled the known cellular and biochemical processes that may contribute to biofilm multimetal resistance (MMR) and multimetal tolerance (MMT) into a single, qualitative, multifactorial model. As described in the following sections, there are several phenomena that protect biofilm cells from toxic metal species, each of which may be viewed as a single component of a multifactorial model. My assessment of the available evidence suggests that the reduced susceptibility of biofilms to toxic metals is linked to a natural process of phenotypic diversification that is ongoing within the biofilm population. The model that I propose is a conceptual step towards understanding biofilms as a population strategy for survival during exposure to toxic stressors in a diverse range of natural, industrial and

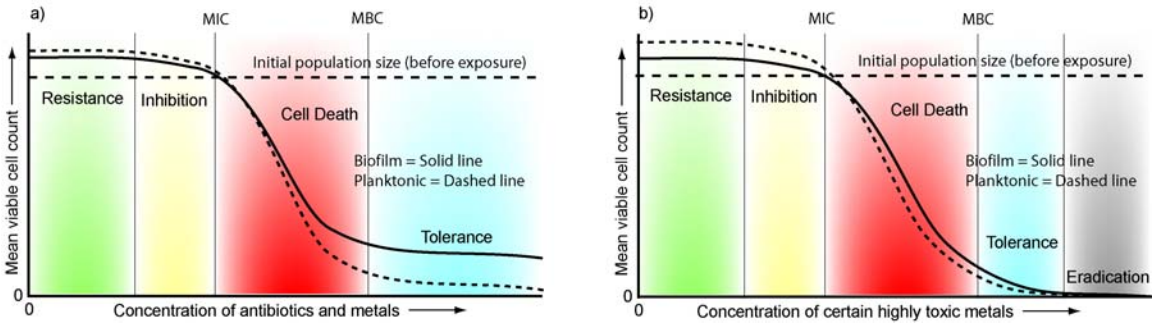

Figure 8.1. Time- and dose-dependent killing of biofilms by metals. Microbial survival in biofilms exposed to toxic metal species suggests that there are different subpopulations of cells in single-species biofilms. (A) In general, both antibiotics and toxic metal species kill biofilm populations in a time- and concentration-dependent fashion. This is observed as biphasic population killing, in which most of the growing population is rapidly killed by a relatively low concentration of the antimicrobial. However, a larger portion of the biofilm population is able to withstand these lethal factors for exposure durations and at concentrations that exceed what is lethal to the corresponding planktonic form (97, 105, 230). The concentration-dependent killing of microbial populations illustrated in (A) is exemplified by a plateau in the activity of the antimicrobial and examples include *P. aerugionsa* ATCC 27853 killing by most antibiotics, Ni or Zn cations for exposure times of up to 1 day (97, 98, 105, 230, 270). These results are also typical of exposure of biofilms to most toxic metal compounds for short exposure times (i.e. only a few hours). In this instance, the surviving subpopulation is comprised of specialized cells that have been termed persisters, which mediate population multidrug and multimetal tolerance (97, 152). (B) However, under certain *in vitro* conditions and with sufficient exposure times, other highly toxic metal species may eradicate 100% of bacterial biofilm populations (97, 98, 104, 105). Examples of this include *E. coli* biofilms exposed to Cr and Te oxyanions (97) for 1 day as well as *P. aeruginosa* biofilms exposed to Cu or Ag cations (105) for 1 day. I must acknowledge that the concentrations of metal ions required to chemically sterilize a culture *in vitro* are for the most part a lot higher than what is found in contaminated environmental milieus, especially when considering biological metal availability given the interaction of metals with minerals, humics or other organics. The trends illustrated in these figures have been

discerned from previous studies by our research group that have used the Calgary Biofilm Device for high-throughput antibiotic and metal susceptibility testing of biofilms (97, 103, 105), all of which have been conducted as part of this thesis research. (This figure has been adapted from Harrison *et al*. (2007) Nature Reviews Microbiology 5:928-938).

clinical settings. So what are the physical, chemical and physiological parameters that, as a result of social interactions between microbes, reduce the susceptibility of biofilm populations to metal toxicity?

8.2 Components of biofilm multimetal resistance and tolerance

8.2.1 Metabolic heterogeneity introduced by population structure

Structured growth establishes metabolite, O_2 and pH gradients in biofilms, which creates chemically distinct microenvironments and results in metabolic heterogeneity among the constituent cells (237). It is possible that this process may explain, in part, the tolerance of bacterial biofilms to metal ions. In principle, cells in anoxic environments may have altered susceptibility to toxic metals due to changes in cell physiology or through altered speciation of the metals, as well as through decreased metabolic ROS production and a likely decrease in metal-catalyzed Fenton-type reactions, which require ROS. However, I will emphasize that mature biofilm structure is likely only one contributing factor that reduces biofilm susceptibility to toxic metals.

Similar to what has been previously described in the literature for biofilm antibiotic susceptibility, cell clusters and layers of adherent cells as well as those biofilms in the early stages of growth possess high levels of resistance and/or tolerance to toxic metal ions relative to planktonic cells. For example, in Chapter Six, biofilms of *C. tropicalis* formed thin layers of cells in microtiter plates as well as on the polystyrene surface of the CBD (101, 103, 147). However, *C. tropicalis* biofilms cultivated in this fashion were highly resistant and/or tolerant to toxic metal species (103, 106, 147). These observations suggest that surface attachment may trigger the physiological transition to a multimetal resistant and/or tolerant state for *Candida* species. Although it was not included on in this thesis, I have made similar observations for the metal susceptibility of *E. coli* biofilms using a series of twin-arginine translocase (*tatABC*) mutants (96).

E. coli mutants bearing inactivating mutations at the *tat* locus are characteristically hypersensitive to detergents as well as to hydrophobic drugs (232). Depending on the growth medium, *E. coli tatABC* mutants may also produce biofilms

that lack complex three-dimensional (3D) organization (96, 125). Biofilms of *E. coli tat* mutants generally retain levels of tolerance to β-lactam antibiotics, Se and Te oxyanions that are similar to or slightly less than that of wild type biofilms. Notably, structurally defective biofilms of the *E. coli tatABC* mutant remain much more drug and metal tolerant than planktonic cells (96). Similarly, a more elegant study by Folkesson *et al*. (75), which used IncF plasmids expressing altered forms of transfer pili to introduce changes in *E. coli* biofilm structure, found that tolerance to colistin, but not ciprofloxacin, was conditional on biofilm structural organization. All together, these data suggest that although structure contributes to multidrug and multimetal tolerance, it is likely not the only reason biofilms have reduced susceptibility to these agents.

As described in Chapter Two, dead cells are frequently ignored components of biofilms that are interspersed at varying ratios with live cells in every microbial population (102). Dead cells are chemically reactive biomasses that provide biosorptive sites that may drive the formation of metal precipitates. Protons extruded across cell membranes might compete with metals for cell-surface binding sites; therefore, metal cations may bind to actively respiring cells in smaller numbers than they bind to dead cells. Dead cells may therefore contribute to pH discontinuities and physiological microenvironments in biofilms that may be responsible for heterogeneous metal accumulation (R.C. Hunter, A. Saxena and T.J. Beveridge, personal communication). In this fashion, dead cells might protect the living from metal toxicity by sequestering or precipitating the reactive metal species.

In summary, microbial biofilms that lack complex 3D structures still have reduced susceptibility to toxic metals as well as to other antimicrobials, indicating that population structure (and the associated metabolic heterogeneity) is one contributing factor to MMR and MMT. As outlined in Chapter One, another set of processes required for structured biofilm growth are the extracellular signalling pathways used by biofilm microorganisms.

8.2.2 Extracellular signalling events affecting biofilm physiology.

There is currently some controversy surrounding the importance of quorum-sensing (QS) in biofilm formation (136, 184); however, there is some evidence to suggest

that the role of QS-systems depends on the nutrients available to bacteria (224) as well as the hydrodynamics of the biofilm environment (117). There is some recent, preliminary evidence linking metal (Ni, As, Cd and Hg) tolerance to biofilm formation and quorum sensing in *Acinetobacter junii* (214). QS is particularly well studied in *P. aeruginosa*, and among many QS-regulated genes that are differentially regulated during biofilm formation, three to note are Mn-cofactored superoxide dismutase (*sodA*), Fe-cofactored superoxide dismutase (*sodB*) and catalase (*katA*) (109). These genes are known to be upregulated during exposure of planktonic *P. aeruginosa* to high concentrations of Cu (249); furthermore, SodA and SodB contribute to basal levels of *E. coli* resistance to Cd, Ni, Co, Cu and Zn toxicity (82, 124) as well as to planktonic *P. aeruginosa* resistance to As (185). As detailed in Chapter Seven, biofilms of *E. coli* strains bearing inactivating mutations in *sodAB*, glutathione oxidoreductase (*gor*), thioredoxin (*trxA*), glutathione synthetase (*gshA*), or glutaredoxin (*grxA*) generally have lower cell survival rates after exposure to metal ions (for example Cr, Co, Zn, Cu, Ag, As, Se or Te) than the corresponding wild-type parental strains. This suggests that cellular defense against oxidative stress protects microbial biofilms from toxic metal species. Therefore, it is reasonable to hypothesize that increased basal levels of these enzymes mediated indirectly by QS systems may contribute to *P. aeruginosa* biofilm MMR or MMT. This may be true in other bacteria as well.

Although there is still debate surrounding the signalling mechanisms involved in the shift of planktonic cells to adherent biofilms, populations of planktonic and biofilm cells metabolize metals in different ways, suggesting that each corresponds to a set of distinct physiological states. I directly examined this early in my PhD research, but I have not included these experiments in this thesis. It is well known that many Gram-negative bacteria, such as *P. aeruginosa*, reduce SeO_3^{2-}, TeO_4^{2-} and TeO_3^{2-} to elemental Se^0 and Te^0, resulting in the formation of orange and gray-black precipitates, respectively (284). Microbial-mediated reduction of these oxyanions occurs in both planktonic and biofilm cultures of *P. aeruginosa* (99). By contrast, although *Staphylococcus aureus* planktonic cells still carry out this reduction, biofilms have lost this capacity; furthermore, the loss of this metabolic pathway is concomitant with an increase in biofilm

susceptibility to these compounds relative to planktonic cells (99). Although *S. aureus* biofilms become more susceptible to these toxic metal species, this example still illustrates that biofilms undergo specific physiological changes that may alter the metal resistance and/or tolerance of the entire population.

To summarize, extracellular signalling events that affect the physiology of biofilm cells contribute to MMR and MMT, and therefore, these signalling systems are another component of our model. One of the other ways signalling events contribute to MMR and MMT is by regulating synthesis of extracellular matrix components (136) that facilitate biosorption.

8.2.3 Metal immobilization by biosorption

Charged particles, including metal ions, may be extracted from a bulk aqueous phase and trapped within a biofilm — a fact that has fueled research into microbial bioremediation of metal-laden industrial effluents (248, 264) and guided the use of biofilms as biosensors for toxic contaminants in rivers (160). This type of metal sorption underlies biomineralization and the microbial lithification[23] process that has orchestrated global biogeochemical cycles for >3.5 billion years (71). The precise chemical composition of a biofilm as well as the metal-speciation state in the bulk solvent versus the biofilm varies with the environment as well as with the genotype(s) of the constituent microorganism(s). Thus, metal-ion sorption varies from organism to organism and from one environment to the next. The chemical interactions involved in biosorption, which include ion exchange, chelation, adsorption and diffusion through cell walls and membranes (264), influence metal-ion mass transfer and consequently may affect biological metal toxicity.

Microbial biofilms are encased in a self-produced, hydrated, viscoelastic extracellular matrix (ECM) that may be composed of DNA, RNA, proteins and chemically modified complex carbohydrates, as well as the monomeric units of each of

---

[23] Lithification is the process in which sediments are gradually converted under pressure into solid sedimentary rock.

these biomolecules (33, 34, 245, 274). Therefore, the biofilm ECM has a polyionic charge derived from the chemical functional groups that are part of these organic compounds, such as carboxylate ($R\text{-}COO^-$), phosphate ($R\text{-}HPO_4^-$), sulphydrl (R-SH), amino ($R\text{-}NH_3^+$), and phenolic ($R\text{-}C_6H_4OH$) groups. Many of these compounds also have hydrogen-bonding potential via hydroxyl (R-OH) groups. The pKa values of these different electrostatic binding sites, which have been characterized from titration data and found to vary from 3 to 11, have been estimated to exceed the number of binding sites present on cell surfaces by 20- to 30-fold (155). In this regard, the matrix may impede the diffusion and equilibration of small molecules (234) as well as metal ions (103, 105, 250) across the biofilm. Furthermore, the pH (123) and redox gradients (198) of biofilms can affect metal-ion speciation and thus certain constituents of the ECM may chelate as well as react with these compounds.

In the field of biofilm research, there has been intense interest in intracellular signalling by the bacterial second messenger bis- (3'–5') cyclic dimeric guanosine monophosphate (c-di-GMP). Recent studies suggest that c-di-GMP is produced nearly ubiquitously in bacterial taxa and that it regulates physiology and many coordinated activities of microbial communities, such as virulence-factor expression and biofilm formation (208). The GGDEF and EAL protein domains (which correspond to diguanylate cyclases and phosphodiesterases, respectively) are responsible for the synthesis and degradation of c-di-GMP, respectively. There is a correlation between antibiotic resistance, phenotypic variation and c-di-GMP signalling (mediated by the EAL-domain protein PvrR) that has been recently established for *P. aeruginosa* PA14(69). Although there are several different proteins in *P. aeruginosa* that mediate c-di-GMP signalling, this second messenger is likely involved in MMR and MMT through regulation of extracellular polymer production, which would likely alter the metal-sorption properties of the ECM.

In this thesis, it was observed time and again that biofilm biomass could entrap metal ions. For example, biofilms of *P. aeruginosa* (Chapter Three), *E. coli* (Chapter Four) and *C. tropicalis* (Chapter Six) all had the capacity to adsorb Cu and Ni. Biofilms of *P. aeruginosa* (data not shown) and *E. coli* (Chapter Four) also trapped and mediated

the biological precipitation Se and Te, although this latter process is likely due to bioaccumulation as opposed to biosorption.

The spatial distributions of Zn in exposed *E. coli* biofilms have been examined using two-photon laser scanning microscopy (2P-LSM) in conjunction with a Zn-binding fluorochrome, 8-hydroxy-5-dimethylsulfoamidoquinolone (119). After 1 hour of exposure, Hu *et al*. (119) identified that Zn was evenly equilibrated across thin (~12 μm) biofilms, but penetrated less than 20 μm into thick (~350 μm) biofilms. More recently, Hu *et al*.(120) have used scanning electrochemical microscopy (SECM) — which uses cyclic voltammetry to determine aqueous labile metal species — to assess the spatial distribution of Cu in *E. coli* biofilms. The authors discovered that after 2 hours of exposure, Cu had penetrated ~150 μm into biofilms and that Cu diffusion kinetics could be mathematically described by a one-dimensional diffusive[24] transport model. The Cu retardation factor was six-fold larger for *E. coli* biofilms than for isotherms calculated for populations of the corresponding planktonic cells.

Other contributors to metal sequestration in biofilms are cell membranes and cell walls, which offer many additional cationic and anionic sites for interactions with metal ions (264). *P. aeruginosa* biofilm cells are capable of binding Fe, Au and La in amounts significantly greater than planktonic cells (148); furthermore, transmission electron microscopy (TEM) of heavy-metal-exposed biofilms shows that this precipitation is restricted to cells in specific regions of the biofilm (148). Other components of biofilm matrices are membrane vesicles, which bind to and sequester the positively charged aminoglycoside antibiotics (218). It is reasonable to hypothesize the membrane vesicles may have a similar role in metal sorption; however, this has not been directly tested.

In summary, the biosorption of metal ions to components of the biofilm, which includes extracellular polymers, cell membranes and cell walls, sequesters these compounds and prevents them from interfering in sensitive metabolic processes. In this regard, cellular and extracellular biomass of biofilm microbes protects cells from transient fluxes in toxic metal species; this protection is proportional to the kinetics of the

biosorption reaction equilibriums, which restrict diffusion and alter biological availability of the toxic metals. It is important to note that colony morphology variants, which are frequently recovered after microbial growth in biofilms (30), produce extracellular polymers of different quantity and character than the original inoculating strain (110, 134) (discussed later in this Chapter). Another component of MMR closely related to biosorption is the sequestration and chemical modification of toxic metal species via reactions with microbial metabolites.

8.2.4 Bioinorganic reactions of metal ions with biofilm metabolites

Microbes produce a diverse array of metabolic end-products, many of which may bind and/or react with metal species to result in the precipitation of bioinorganic metal complexes. A well-known example of this is the co-precipitation of heavy metals such as Cu, Zn, Ni, Cd, Pb and U with sulfide (S^{2-}) produced by biofilms of sulfate-reducing bacteria and archaea (23, 24). Another example is the co-precipitation of metals with carbonates (HCO_3^- and CO_3^{2-}) produced during microbial respiration (71). This results in the deposition of inorganic metal sulfides and metal carbonates, respectively, removing potentially toxic metal species from the aqueous phase. Although the biochemical mechanisms are unknown, biofilms of *Pseudomonas putida* are able to precipitate Mn oxides and oxyhydroxides in soils, sediments and water columns. These compounds have an additional role in regulating the speciation of metals such as Zn, Ni, and Cu in these environmental milieus (253).

Siderophores[25] represent another mechanism by which microbes may interact with metals. The catechol-hydroxyamate siderophore pyoverdine can bind to many kinds of transition metal ions and sequester them, thereby preventing the metals from participating in deleterious chemical reactions which likely require the unbound metal species. *P. aeruginosa* upregulates the transcription of pyoverdine synthetic genes during

---

[24] One-dimensional diffusive transport refers to a mathematical model that describes the density fluctuations in particles undergoing movements that minimize a concentration gradient.
[25] Fe-specific chelators produced by microorganisms under nutrient-limited conditions as part of an Fe acquisition system.

exposure to toxic Cu species (249). The *lasR*/*lasI* QS system, which is involved in biofilm formation and/or development, controls expression of this compound (240); therefore, pyoverdine production by *P. aeruginosa* biofilms may lead to an increased basal level of biofilm resistance to Cu and other transition metal cations. Another example is the chelator pyridine-2,6-bis[monothiocarboxylic acid] (PDTC), which is produced by *P. putida* and *Pseudomonas stutzeri*. PDTC can bind a broad range of metals, including many transition metals, lanthanides and actinides (55). Many toxic metals form insoluble precipitates with PDTC, including toxic Se and Te oxyanions (286). Zawadzka *et al*. (286) have proposed that SeO_3^{2-} may be reduced and bound by PDTC or its hydrolysis product, dipicolinic acid (DPA; also known as pyridine-2,6-bis[carboxylic acid]), resulting in deposition of Se precipitates in the extracellular milieu. Both metal binding and the inorganic reactions of siderophores with metal ions reduce the biological availability of the toxic metal species. These reactions may occur in both biofilms and planktonic cells; however, localized variations in concentrations of these reactants may still drive these chemical reactions to produce heterogeneous metal precipitation in biofilms. Collectively, metal-ion immobilization by biosorption and bioinorganic reactions might permit cells to enter a protected physiological state by giving them time to adapt.

8.2.5 Adaptive responses to metal ions

Studies of planktonic bacterial populations suggest that microbes undergo complex and adaptive physiological changes in response to toxic concentrations of metal species (37, 118, 249). Using the qualitative experimental approach described in Chapter Six, it was discovered that exposure of *C. albicans* and *C. tropicalis* biofilms to certain metal ions changed the pattern of cellular differentiation in the surface-adherent population (that is, the yeast-to-hyphal-cell-type transition may be suppressed or enhanced by metal ions); furthermore, this cell-type shift was concomitant with altered resistance to a subsequent antimicrobial exposure, such as Cu (101).

Szomolay *et al*. (247) have proposed that reaction-diffusion limited penetration of antimicrobials into biofilms may result in low levels of exposure to cells in deep regions

of the biofilm, thereby allowing cells sheltered in this fashion to enter an adapted physiological state that is resistant to the antimicrobial. It is reasonably anticipated that biofilm microbes have an ability to adapt their physiology to survive specific toxic metal exposures; however, the molecular response of biofilm microbes to this kind of stress has not been reported before. Our laboratory and others are currently using transcriptomic and proteomic technologies to elucidate the molecular mechanisms underlying the microbial biofilm response to metal toxicity. This type of response may be viewed as a process of phenotypic diversification that is dependent on the localized concentration of toxic metal species.

Here I will emphasize that restricted diffusion — as mediated by biosorption and bioinorganic reactions of metal ions with biofilm biomass and metabolites — cannot solely account for the reduced susceptibility of biofilms to toxic metal ions. For example, SeO_3^{2-} and TeO_3^{2-} probably have very low binding affinities for the polyanionic biofilm matrix of *E. coli*; yet thin (i.e. 10-20 μm) biofilms of this organism are 310-times more tolerant to the bactericidal action of these compounds relative to planktonic populations (Chapter Four) (97). Similar arguments have previously been made for the fluoroquinolone antibiotic ciprofloxacin, which otherwise quickly penetrates these highly tolerant biofilms (153). Furthermore, the transition metal Ga kills established *P. aeruginosa* biofilm cells in the interior regions of microcolonies before those in the outer layers (128). A similar pattern of killing has been recently reported for colistin, a cyclic cationic antimicrobial peptide, as well as for the anionic detergent sodium dodecyl sulfate (90). It is also interesting to note that cells in *C. tropicalis* biofilms surviving exposure to Co, Se or other antifungals seem to be randomly interspersed in the population (Chapter Six) (103, 106). The spatial patterns of killing deduced from these studies indicate that, although restricted penetration of antimicrobials by biosorption is an important component to reduced biofilm susceptibility to toxic stressors, this phenomenon is not the only mechanism of resistance — otherwise biofilms would always die from the outside in, and not from the inside out. Collectively, the killing kinetics of microbial populations by agents that rapidly penetrate biofilms as well as the spatial patterns of biofilm killing

discussed here indicate that there may be specific cell types with defined physiological states that may withstand the action of antimicrobials, including toxic metal ions.

8.2.6 Persister cells

Microbial biofilms produce persister cells at a frequency that is 10 to 10 000 times greater than that reported for exponentially growing planktonic cell populations (230). At the population level, this specialized cell type mediates MDT, which is observed as biphasic time- and concentration-dependent killing kinetics for biofilms of many organisms, including Gram-positive and Gram-negative bacteria, as well as *C. albicans* (97, 105, 147, 152) (Figure 8.1). As reported in Chapters Three and Four, this subpopulation of specialized cells, which represents approximately 0.1 to 10% of biofilm populations, also mediates time-dependent tolerance to metal cations and oxyanions (97, 105).

Studies using *E. coli* suggest that persister cells are metabolically quiescent and express several genes associated with stress tolerance, including chaperones, the multiple antibiotic resistance (*marRAB*) regulon, and cold-shock proteins (131, 221). There are now several reports that have linked the production of persister cells to chromosomal toxin-antitoxin (TA) loci (152), and although biofilms are thought to produce persister cells at high levels, much of the work done to establish this genetic link has been done with planktonic cell populations. To address this, I have recently initiated a study (in conjunction with W. D. Wade and S. Akiermen) to examine the effect of toxin or antitoxin gene deletion on the antibiotic-mediated killing dynamics of *E. coli* K12 biofilm populations.

Although numerous studies have focused on the *hipBA* operon – which encodes a toxic kinase (HipA) and an antitoxic DNA-binding protein (HipB) that autoregulates expression of *hipBA* (139) – there are few studies that have evaluated the function of other TA modules in bacterial persistence. This might be important, because relative to wild-type *E. coli*, deletion mutants lacking *hipBA* produce a smaller proportion of persister cells in stationary-phase planktonic cell populations as well as in biofilms (131). Using the CBD, I have helped to systematically test and compare the biofilm growth and

antibiotic susceptibility of a series of TA loci mutants – bearing single, markerless deletions at *hipA*, *hipB*, *relE*, *relB*, *chpA*, *chpB*, *yafQ*, *dinJ* or *yoeB* – to the isogenic wild-type strain. In contrast to the well established biphasic concentration-dependent killing dynamics of planktonic and biofilm bacterial populations, our in-depth data suggest that wild-type *E. coli* biofilm populations may have multiple survival phases when exposed to antibiotics (as exemplified by the β-lactam ceftrioxone). Furthermore, susceptibility testing of the mutants has identified that single deletions at any one of the TA loci examined was sufficient to eliminate at least one phase of this drug tolerance. Subsequent rounds of testing with additional antibiotics revealed that the toxins *yafQ* and *yoeB* may also be important for *E. coli* biofilm tolerance to cefazolin and tobramycin. Collectively, these results suggest that *E. coli* biofilm populations may have multiphase tolerance to antibiotic treatments and that TA genes may be linked to these dynamics of cell survival.

With respect to the research presented in this thesis, the *hipA7* allele bears a gain-of-function mutation that results in a 10-fold to 100-fold increase in the proportion of persister cells produced by *E. coli* stationary-phase populations. *E. coli* strains bearing *hipA7* have a 5-fold to 82-fold increased proportion of persister cells in the stationary phase that may survive exposure to TeO_4^{2-}, TeO_3^{2-} and CrO_4^{2-} relative to the isogenic wild-type strain (Chapter Four) (97). Collectively, this evidence suggests that persister cells are a specialized cell type that contribute to MMT and that these cells form at high frequency in biofilms relative to exponentially growing planktonic cells. However, it still is possible to isolate other types of phenotypic variants from biofilm populations, and as persister cells can only explain multidrug and multimetal tolerance, there might be other cell types that mediate biofilm resistance.

8.2.7 Genetic rearrangements, mutations and phenotypic variation

It is frequently possible to recover colony morphology variants from biofilm populations, many of which have altered phenotypic traits relative to the colonizing strain (30, 59). For example, small colony variant (SCV) cells, which are typically superior at forming biofilms and less motile than their progenitors, are often recovered from aged

biofilms of clinical and/or rhizosphere *Pseudomonas* spp. (Chapter Five) (110, 134, 263). In laboratory-grown biofilms of *P. aeruginosa*, *P. chlororaphis* and *P. fluorescens*, SCVs occur at a frequency in the population that is increased by exposure to certain antibiotics and H_2O_2 (59, 69). Intriguingly, certain metal ions also increase the frequency of colony variants recovered from biofilms of these bacterial species, including: Ca^{2+}, Ru^{3+}, Cu^{2+}, Ag^{+}, Ni^{2+}, Pb^{2+} and SeO_3^{2-} (59) (and J. J. Harrison, M. L. Workentine, H. Ceri and R. J. Turner, unpublished data).

Variant formation by *Pseudomonas* spp. may be an important contributor to biofilm metal susceptibility, as the switch to the SCV and other variant phenotypes is correlated with the emergence of multidrug and multimetal resistance and/or tolerance (59, 69). The response of *P. fluorescens* and *P. chlororaphis* biofilms to metal-ion exposure is reasonably anticipated to be highly complex, as it is linked to the formation of multiple colony morphotypes, including the wrinkly-spreader (WS) phenotype in the case of *P. fluorescens* (M.L. Workentine, J. J. Harrison, P. U. Stenroos, H. Ceri and R. J. Turner, unpublished data). This observation gives another connection between metal resistance and intracellular signalling by c-di-GMP, as mutations in proteins bearing GGDEF and EAL domains are known to give rise to the *P. fluorescens* WS phenotype.

As described in Chapter Five, reversion of *P. aeruginosa* SCVs requires the sensor kinase GacS — an SCV strain bearing an inactivating mutation in *gacS* is phenotypically locked and will not revert to a normal phenotype, even after months of serial culture on non-selective media (59). The GacA/GacS two-component system is hierarchically arranged on top of the *Pseudomonas* QS systems and is highly conserved amongst pseudomonads (267). In many rhizosphere and laboratory strains of *Pseudomonas* spp., *gacS* is naturally prone to inactivating mutations (70, 213, 263). Moreover, genotypic variation in *P. fluorescens* is mediated by two site-specific recombinases, XerD and Sss, which seem to introduce mutations into *gacA* and/or *gacS*(162). This would suggest that mutations and/or genetic rearrangements at the *gacA*/*gacS* loci are linked to phenotypic variation, biofilm formation, MDR and MMR. Similarly, Boles *et al.* (30) have also suggested that genetic and phenotypic diversity may be introduced into *P. aeruginosa* biofilm populations and that this is dependent on *recA*. In their study, the phenotypic

variants recovered from biofilms also showed varying levels of resistance to H_2O_2. It is interesting to contrast these findings with the insurance hypothesis (30), in which random mutations or site-specific genetic rearrangements might produce genotypic and phenotypic diversity that ensures population survival, as some phenotypes may survive environmental insults that others may not.

8.3 A model of biofilm multimetal resistance and tolerance

It is possible to bring together these different components of MMR and MMT into a single multifactorial model that may explain the reduced susceptibility of biofilms. A trend that has swept through microbiology is a shift towards viewing biofilm microbes as populations of cells that display complex and coordinated developmental behaviours. Starting from the point at which bacteria adhere to a surface, which might trigger population multidrug and multimetal tolerance through persister-cell formation (59, 147), the natural growth of the microbes at the surface sets in motion the interrelated and ongoing processes of cellular diversification that are linked to MMR and MMT (Figure 8.2). For instance, the formation of phenotypic variants in biofilms might coincide with increased production and altered characteristics of biofilm extracellular polysaccharides, in turn affecting diffusion processes and biosorption of toxic metal species. Similar cascades and relationships may be deduced for the other components summarized in this Chapter. Microbial biofilm populations, therefore, may be poised to survive fluxes in toxic metal species because there are diverse cell types in biofilms that might additionally function to protect each other. I acknowledge that many of the cellular, chemical and biological mechanisms at work in this model may also explain the recalcitrance of biofilms towards multiple, structurally unrelated antibiotics. Despite the complexity of this model, it is limited insofar that it describes populations of single microbial species, and does not consider the vast number of potential interactions involved in natural polymicrobial growth.

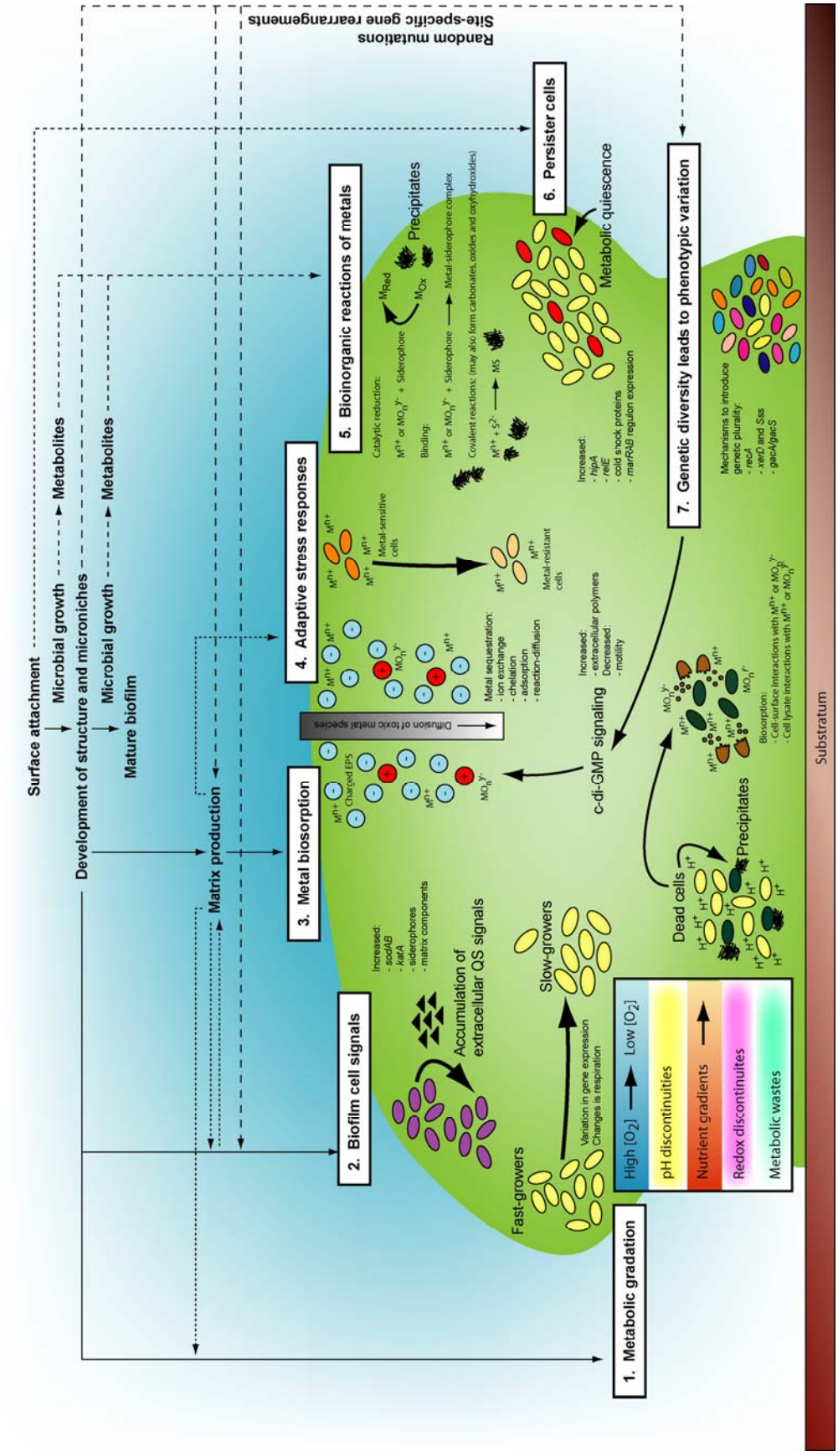
Surface attachment
Microbial growth
Metabolites
Development of structure and microniches
Microbial growth
Metabolites
Mature biofilm
Matrix production
Random mutations
Site-specific gene rearrangements
1. Metabolic gradation
2. Biofilm cell signals
3. Metal biosorption
4. Adaptive stress responses
5. Bioinorganic reactions of metals
6. Persister cells
7. Genetic diversity leads to phenotypic variation
Fast-growers
Slow-growers
Variation in gene expression
Changes is respiration
Accumulation of extracellular QS signals
Increased:
- sodAB
- katA
- siderophores
- matrix components
Charged EPS
Diffusion of toxic metal species
Metal sequestration:
- ion exchange
- chelation
- adsorption
- reaction-diffusion
Metal-sensitive cells
Metal-resistant cells
c-di-GMP signaling
Increased:
- extracellular polymers
Decreased:
- motility
Catalytic reduction:
Binding:
Precipitates
Covalent reactions: (may also form carbonates, oxides and oxyhydroxides)
Increased:
- hipA
- relE
- cold shock proteins
- marRAB regulon expression
Metabolic quiescence
Mechanisms to introduce genetic plurality:
- recA
- xerD and Sss
- gacA/gacS
Dead cells
Precipitates
Biosorption:
- Cell-surface interactions with
- Cell lysate interactions with
High [O2] → Low [O2]
pH discontinuities
Nutrient gradients
Redox discontinuites
Metabolic wastes
Substratum

Figure 8.2. A multifactorial model of multimetal resistance and tolerance in microbial biofilms. In general, the decreased susceptibility of biofilms to toxic metal species may be viewed as an emergent property that arises from several interrelated physiological and chemical parameters. Many of these parameters arise from a natural process of phenotypic diversification that is ongoing during biofilm growth. In this figure, I have overlaid a simplified schematic of biofilm maturation with the many components that contribute to multimetal resistance and tolerance. I propose that biofilm formation is a process that gives rise to multiple cell types — each with a range of expression patterns corresponding to the diversity of biofilm microniches — which positions the population to withstand a diverse range of environmental stressors, including metal toxicity. (This figure has been adapted from Harrison *et al*. (2007) Nature Reviews Microbiology 5:928-938).

8.4 Concluding remarks and future directions

In addition to the components of the multifactorial model described in this Chapter, there may be additional contributors to biofilm multimetal resistance and tolerance, notably humic acids[26], soluble electron carriers[27] and nanowires[28]. There has been no direct examination to link metal resistance in biofilms to extracellular electron transfer or to chelation of toxic metal species by humics; however, since these processes are specialized in changing the speciation and/or biological availability of potentially toxic environmental metals (51, 85), I have included these as a notable future directions for research.

An obstacle facing research into biofilm microbiology is the classical approach to 'omics' technologies, as these techniques inevitably pool protein and nucleic-acid samples from a population of microbes. This ignores any underlying phenotypic heterogeneity and thus the contributions of single cells to population behaviour might remain hidden among an averaged differential expression analysis (4). Future endeavours (including my own) will benefit from separating subpopulations of cells from biofilms before examining the molecular components of the microbes. Breakthrough technologies involving laser-capture microdissection microscopy and high-throughput cell sorting by flow cytometry will catalyse new research into the behaviour of specific biofilm cell types. The next wave of advances into understanding biofilm antimicrobial resistance and tolerance will come from examining the emergent properties of microbial populations based on the concerted behaviours of the individual cells.

---

[26] Humics are colloidal mixtures of substances that are present in soils that arise by the microbial degradation of dead biomass. Humic acids are compositionally undefined, but include hydrophobic bioorganics that self-aggregate and chelate multivalent metal ions.

[27] A soluble electron carrier is a water soluble molecule that shuttles electrons in the microbial respiratory chain by accepting electrons from a donor and transferring them to an acceptor.

[28] Nanowires are electrically conductive pili composed of bundles of individually conductive filaments that are 10–20 nm in diameter.

8.5 Contributions

8.5.1 Relevant publications

I compiled the information in this summary chapter over a period of five years and my multifactorial model of biofilm resistance and tolerance has been published in parts as this concept has evolved. Portions of this final Chapter have been taken from Harrison *et al.* (2005) Recent Research Developments in Microbiology 9:33-55, Harrison *et al*. (2005) American Scientist 93:508-515, Harrison *et al.* (2007) Nature Reviews Microbiology 5:928-938 and Zannoni *et al.* (2008) Advances in Microbial Physiology 53:1-72.

References

1. **Al-Fattani, M. A., and L. J. Douglas.** 2004. Penetration of *Candida* biofilms by antifungal agents. Antimicrobial Agents and Chemotherapy **48:**3291-3297.
2. **Alekshun, M. N., and S. B. Levy.** 1997. Regulation of chromosomally mediated multiple antibiotic resistance: the *mar* regulon. Antimicrobial Agents and Chemotherapy **41:**2067-2075.
3. **Alon, U.** 2007. Network motifs: theory and experimental approaches. Nature Reviews Genetics **8:**450-461.
4. **An, D., and M. R. Parsek.** 2007. The promise and peril of transcriptional profiling in biofilm communities. Current Opinion in Microbiology **10:**292-292.
5. **Anderl, J. N., M. J. Franklin, and P. S. Stewart.** 2000. Role of antibiotic penetration limitation in *Klebsiella pneumoniae* biofilm resistance to ampicillin and ciprofloxacin. Antimicrobial Agents and Chemotherapy **44:**1818-1824.
6. **Anderl, J. N., J. Zahller, F. Roe, and P. S. Stewart.** 2003. Role of nutrient limitation and stationary phase existence in *Klebsiella pneumoniae* biofilm resistance to ampicillin and ciprofloxacin. Antimicrobial Agents and Chemotherapy **47:**1251-1256.
7. **Anderson, C., K. Pederson, and A.-M. Jakobsson.** 2006. Autoradiographic comparisons of radionuclide adsorption between subsurface anaerobic biofilms and granitic host rocks. Geomicrobiology Journal **23:**15-29.
8. **Ariza, R. R., S. P. Cohen, N. Bachhawat, S. B. Levy, and B. Demple.** 1994. Repressor mutations in the *marRAB* operon that activate oxidative stress genes and multiple antibiotic resistance in *Escherichia coli*. Journal of Bacteriology **176:**143-148.
9. **Aslund, F., M. Zheng, J. Beckwith, and G. Storlz.** 1999. Regulation of the OxyR transcription factor by hydrogen peroxide and the cellular thiol-disulfide status. Proceedings of the National Academy of Sciences of the United States of America **96:**6161-6165.
10. **Baba, T., T. Ara, M. Hasegawa, Y. Takai, Y. Okumura, M. Baba, K. A. Kirill, M. Tomita, B. L. Wanner, and H. Mori.** 2006. Construction of

Escherichia coli K-12 in-frame, single-gene knockout mutants: the Keio collection. Molecular Systems Biology **2:**2006.0008.

11. **Baker-Austin, C., M. S. Wright, R. Stepanauskas, and J. V. McArthur.** 2006. Co-selection of antibiotic and metal resistance. Trends in Microbiology **14:**176-182.
12. **Balaban, N. Q., J. Merrin, R. Chait, L. Kowalik, and S. Leibler.** 2004. Bacterial persistence as a phenotypic switch. Science **305:**1622-1625.
13. **Balzer, G. J., and R. J. C. McLean.** 2003. The stringent response genes *relA* and *spoT* are important for *Escherichia coli* biofilms under slow growth conditions. Canadian Journal of Microbiology **48:**675-680.
14. **Barbosa, T. M., and S. B. Levy.** 2000. Differential expression of over 60 chromosomal genes in *Escherichia coli* by consitutive expression of MarA. Journal of Bacteriology **182:**3467-3774.
15. **Battin, T. J., W. T. Sloan, S. Kjelleberg, H. Daims, I. M. Head, T. P. Curtis, and L. Eberl.** 2007. Microbial landscapes: new paths to biofilm research. Nature Reviews Microbiology **5:**76-81.
16. **Beeston, A. L., and M. G. Surette.** 2002. *pfs*-dependent regulation of autoinducer 2 production in *Salmonella enterica* serovar Typhimurium. Journal of Bacteriology **184:**3450-3456.
17. **Beloin, C., and J.-M. Ghigo.** 2005. Finding gene-expression patterns in bacterial biofilms. Trends in Microbiology **13:**16-19.
18. **Beloin, C., J. Valle, P. Latour-Lambert, P. Faure, M. Kzreminski, D. Balestrino, J. Haagensen, S. Molin, G. Prensier, B. Arbeille, and J. M. Ghigo.** 2004. Global impact of mature biofilm lifestyle on *Escherichia coli* K-12 gene expression. Molecular Microbiology **51:**659-674.
19. **Belousov, V. V., A. F. Fradkov, K. A. Lukyanov, D. B. Staroverov, K. S. Shakhbazov, A. V. Terskikh, and S. Lukyanov.** 2006. Genetically encoded fluorescent indicator for intracellular hydrogen peroxide. Nature Methods **3:**281-286.
20. **Berdicevsky, I., D. Lea, D. Marzbach, and S. Yannai.** 1993. Susceptibility of different yeast species to environmental toxic metals. Environmental Pollution **80:**41-44.
21. **Bernas, T., E. K. Asem, J. P. Robinson, P. R. Cook, and J. W. Dobrucki.** 2005. Confocal fluorescence imaging of photosensitized DNA denaturation in cell nuclei. Photochemistry and Photobiology **81:**960-969.
22. **Berridge, M. V., and A. S. Tan.** 1993. Characterization of the cellular reduction of 3-(4,5-dimethylthiazol-2-yl)-2,5-diphenyltetrazolium bromide (MTT): subcellular localization, substrate dependence, and involvement of mitochondrial electron transport in MTT reduction. Archives of Biochemistry and Biophysics **303:**474-482.
23. **Beyenal, H., and Z. Lewandowski.** 2004. Dynamics of lead immobilization in sulfate reducing biofilms. Water Research **38:**2726-2736.
24. **Beyenal, H., R. K. Sani, B. M. Peyton, A. C. Dohnalkova, J. E. Amonette, and Z. Lewandowski.** 2004. Uranium immobilization by sulfate reducing biofilms. Environmental Science and Technology **38:**2067-2074.

25. **Bigger, J. W.** 1944. Treatment of staphylococcal infections with penicillin. Lancet **ii:**497-500.
26. **Bjarnsholt, T., P. Jensen, M. Burmolle, M. Hentzer, J. A. Haagensen, H. P. Hougen, H. Calum, K. Madsen, C. Moser, S. Molin, N. Hoiby, and M. Givskov.** 2005. *Pseudomonas aeruginosa* tolerance to tobramycin, hydrogen peroxide and polymorphonuclear leukocytes is quorum-sensing dependent. Microbiology **151:**373-383.
27. **Bjarnson, J., C. M. Southward, and M. G. Surette.** 2003. Genomic profiling of iron-responsive genes in Salmonella enterica serovar Typhimurium by high-throughput screening of a random promoter library. Journal of Bacteriology **185:**4973-4982.
28. **Black, D. S., B. Irwin, and H. S. Moyed.** 1994. Autoregulation of *hip*, an operon that affects lethality due to inhibition of peptidoglycan or DNA synthesis. Journal of Bacteriology **176:**4081-4091.
29. **Black, D. S., A. J. Kelly, M. J. Mardis, and H. S. Moyed.** 1991. Structure and organization of *hip*, an operon that affects lethality due to inhibition of peptidoglycan or DNA synthesis. Journal of Bacteriology **173:**5732-5739.
30. **Boles, B. B., M. Theondel, and P. K. Singh.** 2004. Self-generated diversity produces "insurance effects" in biofilm communities. Proceedings of the National Academy of Sciences of the United States of America **101:**16630-16635.
31. **Borriello, G., E. Werner, F. Roe, A. M. Kim, G. D. Ehrlich, and P. S. Stewart.** 2004. Oxygen limitation contributes to antibiotic tolerance of *Pseudomonas aeruginosa* in biofilms. Antimicrobial Agents and Chemotherapy **48:**2659-2664.
32. **Borsetti, F., F. Francia, R. J. Turner, and D. Zannoni.** 2007. The thiol:disulfide oxidoreductase DsbB mediates the oxidizing effects of the toxic metalloid tellurite (TeO_3^{2-}) on the plasma membrane redox system of the facultative phototroph *Rhodobacter capsulatus*. Journal of Bacteriology **189:**851-859.
33. **Branda, S. S., F. Chu, D. B. Kearns, R. Losick, and R. Kolter.** 2006. A major protein component of the *Bacillus subtilis* biofilm matrix. Molecular Microbiology **59:**1229-1238.
34. **Branda, S. S., S. Vik, L. Friedman, and R. Kolter.** 2005. Biofilms: the matrix revisited. Trends in Microbiology **13:**20-26.
35. **Brooun, A., S. Liu, and K. Lewis.** 2000. A dose-response study of antibiotic resistance in *Pseudomonas aeruginosa* biofilms. Antimicrobial Agents and Chemotherapy **44:**640-646.
36. **Brown, G. E., A. L. Foster, and J. D. Ostergren.** 2003. Mineral surfaces and bioavailability of heavy metals: A molecular-scale perspective. Proceedings of the National Academy of Sciences of the United States of America **96:**3388-3395.
37. **Brown, S. D., M. R. Thompson, N. C. VerBerkmoes, K. Chourey, M. Shah, J. Zhou, R. L. Hettich, and D. K. Thompson.** 2006. Molecular dynamics of the *Shewanella oneidensis* response to chromate stress. Molecular and Cellular Proteomics **5:**1054-1071.

38. **Bull, C. T., B. Duffy, C. Voisard, G. Defago, C. Keel, and D. Haas.** 2001. Characterization of spontaneous *gacS* and *gacA* regulatory mutations of *Pseudomonas fluorescens* biocontrol strain CHA0. Antonie Van Leeuwenhoek **79:**327-336.
39. **Ceri, H., M. E. Olson, D. W. Morck, D. Storey, R. R. Read, A. G. Buret, and B. Olson.** 2001. The MBEC assay system: Multiple equivalent biofilms for antibiotic and biocide susceptibility testing. Methods in Enzymology **337:**377-384.
40. **Ceri, H., M. E. Olson, C. Stremick, R. R. Read, D. W. Morck, and A. G. Buret.** 1999. The Calgary Biofilm Device: New technology for rapid determination of antibiotic susceptibilities in bacterial biofilms. Journal of Clinical Microbiology **37:**1771-1776.
41. **Cervantes, C., J. Campos-Garcia, S. Devars, F. Gutierrez-Corona, H. Loza-Tavera, J. C. Torres-Guzman, and R. Moreno-Sanchez.** 2001. Interactions of chromium with microogranisms and plants. FEMS Microbiology Reviews **25:**335-347.
42. **Chan, E., and B. Weiss.** 1987. Endonuclease IV of *Escherichia coli* is induced by paraquat. Proceedings of the National Academy of Sciences of the United States of America **84:**3189-3193.
43. **Chancey, S. T., D. W. Wood, E. A. Pierson, and L. S. Pierson III.** 2002. Survival or GacS/GacA mutants of the biological control bacterium *Pseudomonas aureofaciens* 30-84 in the wheat rhizosphere. Applied and Environmental Microbiology **68:**3308-3314.
44. **Chandra, J., D. M. Kuhn, P. K. Mukherjee, L. L. Hoyer, T. McCormick, and M. J. Ghannoum.** 2001. Biofilm formation by the fungal pathogen *Candida albicans*: development, architecture, and drug resistance. Journal of Bacteriology **183:**5385-5394.
45. **Chang, D.-E., D. J. Smalley, and T. Conway.** 2002. Gene expression profiling of *Escherichia coli* growth transitions: an expanded stringent response model. Molecular Microbiology **45:**289-306.
46. **Chang, W. C., G. S. Hsu, S. M. Chiang, and M. C. Su.** 2006. Heavy metal removal from aqueous solution by wasted biomass from a combined AS-biofilm process. Bioresource Technology **97:**1503-1508.
47. **Chasteen, T. G., and R. Bentley.** 2003. Biomethylation of selenium and tellurium: microorganisms and plants. Chemical Reviews **103:**1-25.
48. **Cheng, K. L., K. Ueno, and T. Imamura (ed.).** 1982. CRC handbook of organic analytical reagents. CRC Press, Boca Raton, Fl.
49. **Chin-A-Woeng, T. F., D. van den Broek, B. J. Lugtenberg, and G. V. Bloemberg.** 2005. The *Pseudomonas chlororaphis* PCL1391 sigma regulator psrA represses the production of the antifungal metabolite phenazine-1-carboxamide. Molecular Plant-Microbe Interactions **18:**244-253.
50. **Christensen, S. K., and K. Gerdes.** 2003. Delayed-relaxed response explained by hyperactivation of RelE. Molecular Microbiology **53:**587-597.

51. **Coby, A. J., and F. W. Picardal.** 2006. Influence of sediment components on the immobilization of Zn during microbial Fe-(hydr)oxide reduction. Environmental Science and Technology **40:**3813-3818.
52. **Cole, S. P., J. Harwood, R. Lee, R. She, and D. G. Guiney.** 2004. Characterization of monospecies biofilm formation by *Helicobacter pylori*. Journal of Bacteriology **186:**3124-32.
53. **Compan, I., and D. Touati.** 1993. Interaction of six global transcription regulators in expression of manganese superoxide dismutase in *Escherichia coli* K-12. Journal of Bacteriology **175:**1687-1696.
54. **Correria, F. F., A. D'Onofrio, T. Rejtar, L. Li, B. L. Karger, K. Makarova, E. V. Koonin, and K. Lewis.** 2006. Kinase activity of overexpressed HipA is required for growth arrest and multidrug tolerance in *Escherichia coli*. Journal of Bacteriology **188:**8360-8367.
55. **Cortese, M. S., A. J. Paszczynski, T. A. Lewis, J. L. Sebat, V. Borek, and R. L. Crawford.** 2002. Metal chelating properties of pyridine-2,6-bis(thiocarboxylic acid) produced by *Pseudomonas* spp. and the biological activities of the formed complexes. Biometals **15:**103-120.
56. **Costerton, J. W., P. S. Stewart, and E. P. Greenberg.** 1999. Bacterial biofilms: a common cause of persistent infections. Science **284:**1318-1322.
57. **Cunha, M. V., S. A. Sousa, J. H. Leitão, L. M. Moreira, P. A. Videira, and I. Sá-Correia.** 2004. Studies on the involvement of the exopolysaccharide produced by cystic fibrosis isolates of the *Burkholderia cepacia* complex in biofilm formation and in persistence of respiratory infections. Journal of Clinical Microbiology **42:**3052-3058.
58. **Daims, H., S. Lücker, and M. Wagner.** 2006. *daime*, a novel image analysis program for microbial ecology and biofilm research. Environmental Microbiology **8:**200-213.
59. **Davies, J. A., J. J. Harrison, L. L. R. Marques, G. R. Foglia, C. A. Stremick, D. G. Storey, R. J. Turner, M. E. Olson, and H. Ceri.** 2007. The GacS sensor kinase controls phenotypic reversion of small colony variants isolated from biofilms of *Pseudomonas aeruginosa* PA14. FEMS Microbiology Ecology **59:**32-46.
60. **Davies, J. A., J. J. Harrison, L. L. R. Marques, G. R. Foglia, C. A. Stremick, D. G. Storey, R. J. Turner, M. E. Olson, and H. Ceri.** 2006. The GacS sensor kinase controls phenotypic reversion of small colony variants isolated from biofilms of *Pseudomonas aeruginosa* PA14. FEMS Microbiology Ecology **(in press)**.
61. **de Souza, J. T., M. Mazzola, and J. M. Raaijmakers.** 2003. Conservation of the response regulator gene *gacA* in *Pseudomonas* species. Environmental Microbiology **5:**1328-1340.
62. **De Vries, W., E. Vel, G. J. Reinds, H. Deelstra, J. Klap, E. Leeters, C. Hendriks, M. Kerkvoorden, G. Landmann, J. Herkendall, T. Haussmann, and J. W. Erisman.** 2002. Intensive monitoring of forest ecosystems in Europe 1. Objectives, set-up and evaluation strategy. Forest Ecol Manag **5890:**1-19.

63. **Déziel, E., Y. Comeau, and R. Villemur.** 2001. Initiation of biofilm formation by *Pseudomonas aeruginosa* 57RP correlates with emergence of hyperpiliated and highly adherent phenotypic variants deficient in swimming, swarming and twitching motilities. Journal of Bacteriology **183:**1195-1204.
64. **Diels, L., P. H. Spaans, S. Van Roy, L. Hooyberghs, A. Ryngaert, H. Wouters, E. Walter, J. Winters, L. Macaskie, J. Finlay, B. Pernfuss, H. Woebking, T. Pumpel, and M. Tsezos.** 2003. Heavy metals removal by sand filters inoculated with metal sorbing and precipitating bacteria. Hydrometallurgy **71:**235-241.
65. **Ding, H., and B. Demple.** 1998. Thiol-mediated disassembly and reassembly of [2Fe-2S] clusters in the redox-regulated transcription factor SoxR. Biochemistry **37:**17280-17286.
66. **Diurdjevic, P., and D. Djokic.** 1996. Protein interactions with bivalent tin. 1. Hydrolysis and complexation of tin(II) with glycine. Journal of Inorganic Biochemistry **62:**17-29.
67. **Donlan, R. M., and J. W. Costerton.** 2002. Biofilms: survival mechanisms of clinically relevant microorganisms. Clinical Microbiology Reviews **15:**167-193.
68. **Douglas, J. L.** 2003. *Candida* biofilms and their role in infection. Trends in Microbiology **11:**30-36.
69. **Drenkard, E., and F. M. Ausubel.** 2002. *Pseudomonas* biofilm formation and antibioitic resistance are linked to phenotypic variation. Nature **416:**740-743.
70. **Duffy, B. K., and G. Defago.** 2000. Controlling instability in *gacS-gacA* regulatory genes during inoculant production of *Pseudomonas fluorescens* biocontrol strains. Applied and Environmental Microbiology **66:**3142-3150.
71. **Dupraz, C., and P. T. Visscher.** 2005. Microbial lithification in marine stromatolites and hypersaline mats. Trends in Microbiology **13:**429-438.
72. **Dwyer, M. A., B. Hayete, C. A. Lawrence, and J. J. Colins.** 2007. A common mechanism of cellular death induced by bactericidal antibiotics. Cell **130:**797-810.
73. **Falla, T. J., and I. Chopra.** 1998. Joint tolerance to beta-lactam and fluoroquinolone antibiotics in *Escherichia coli* results from overexpression of *hipA*. Antimicrobial Agents and Chemotherapy **42:**3282-3284.
74. **Falla, T. J., and I. Chopra.** 1999. Stabilization of *Rhizobium* symbiosis plasmids. Microbiology **145:**515-516.
75. **Folkesson, A., J. A. J. Haagensen, C. Zampaloni, C. Sternberg, and S. Molin.** 2008. Biofilm induced tolerance to antimicrobial peptides. PLoS One **3:**1891.
76. **Fothergill, A. W., and D. A. McGough.** 1995. *In vitro* antifungal susceptibility testing of yeasts, p. 5.15.1-5.15.16. *In* H. D. Isenberg and J. Hindler (ed.), Clinical Microbiology Procedures Handbook, vol. 1. ASM Press, Washington.
77. **Foulkes, E. C.** 1998. Biological membranes in toxicology. Taylor & Francis, Philadelphia, PA.
78. **Fridovich, I., and H. M. Hassan.** 1979. Paraquat and the exacerbation of oxygen toxicity. Trends in Biochemical Sciences **4:**113-115.
79. **Friedman, L., and R. Kolter.** 2004. Genes involved in matrix formation in *Pseudomonas aeruginosa* PA14 biofilms. Molecular Microbiology **51:**675-690.

80. **Fux, C. A., J. W. Costerton, P. S. Stewart, and P. Stoodley.** 2005. Survival strategies of infectious biofilms. Trends in Microbiology **13:**34-40.
81. **George, A. M., and S. B. Levy.** 1983. Amplifiable resistance to tetracycline, chloramphenicol, and other antibiotics in *Escherichia coli*: involvement of a non-plasmid-determined efflux of tetracycline. Journal of Bacteriology **155:**531-540.
82. **Geslin, C., J. Llanos, D. Prieur, and C. Jeanthon.** 2001. The manganese and iron superoxide dismutases protect *Escherichia coli* from heavy metal toxicity. Research in Microbiology **152:**901-905.
83. **Gibson, T. J.** 1984. Studies on the Epstein-Barr virus genome. PhD Thesis. University of Cambridge, Cambridge, UK.
84. **Goodman, A. L., B. Kulasekara, A. Rietsch, D. Boyd, R. S. Smith, and S. Lory.** 2004. A signalling network reciprocally regulates genes associated with acute infection and chronic persistence in *Pseudomonas aeruginosa*. Developmental Cell **7:**745-754.
85. **Gorby, Y. A., S. Yanina, J. S. McLean, K. M. Rosso, D. Moyles, A. Dohnalkova, T. J. Beveridge, I. S. Chang, B. H. Kim, K. S. Kim, D. E. Culley, S. B. Reed, M. F. Romine, D. A. Saffarini, E. A. Hill, L. Shi, D. A. Elias, D. W. Kennedy, G. Pinchuk, K. Watanabe, S. Ishii, B. Logan, K. H. Nealson, and J. K. Fredrickson.** 2006. Electrically conductive bacterial nanowires produced by *Shewanella oneidensis* strain MR-1 and other microorganisms. Proceedings of the National Academy of Sciences of the United States of America **103:**11358-11363.
86. **Gottesman, S., and V. Stout.** 1991. Regulation of capsular polysaccharide synthesis in *Escherichia coli* K12. Molecular Microbiology **5:**1599-1606.
87. **Gottofrey, J., K. Borg, and S. Jasmin.** 1988. Effect of postassium ethylxanthate and sodium diethyldithiocarbamate on the accumulation and deposition of nickel in the brown trout (Salmo trutta). Pharmacology and Toxicology **63:**46-51.
88. **Graff, L., G. Muller, and D. Burnel.** 1995. *In vitro* and *in vivo* evaluation of potential aluminum chelators. Veterinary and Human Toxicology **88:**271-292.
89. **Greenberg, J. T., J. H. Chou, P. A. Monach, and B. Demple.** 1991. Activation of oxidative stress genes by mutations at the *soxQ/cfxB/marA* locus of *Escherichia coli*. Journal of Bacteriology **173:**4433-4439.
90. **Haagensen, J. A. J., M. Klausen, R. K. Ernst, S. I. Miller, A. Folkesson, T. Tolker-Nielsen, and S. Molin.** 2007. Differentiation and distribution of colistin- and sodium dodecyl sulfate-tolerant cells in *Pseudomonas aeruginosa* biofilms. Journal of Bacteriology **189:**28-37.
91. **Hagler, A. N., and L. C. Mendocs-Hageler.** 1981. Yeasts from marine and estuarine waters with different levels of pollution in the State of Rio de Janeiro, Brazil. Applied and Environmental Microbiology **416:**173-178.
92. **Hall-Stoodley, L., J. W. Costerton, and P. Stoodley.** 2004. Bacterial biofilms: From the natural environment to infectious diseases. Nature Reviews Microbiology **2:**95-108.
93. **Halliwell, B.** 2007. Biochemistry of oxidative stress. Biochemical Society Transactions **35:**1147-1150.

94. **Halliwell, B., and J. M. C. Gutteridge.** 2007. Free radicals in biology and medicine, 4th ed. Clarendon Press, Oxford.
95. **Hanahan, D.** 1983. Studies on transformation of *Escherichia coli* with plasmids. Journal of Molecular Biology **166:**557-580.
96. **Harrison, J. J., H. Ceri, E. A. Badry, N. J. Roper, K. L. Tomlin, and R. J. Turner.** 2005. Effects of the twin-arginine translocase on the structure and antimicrobial susceptibility of *Escherichia coli* biofilms. Canadian Journal of Microbiology **51:**671-683.
97. **Harrison, J. J., H. Ceri, N. J. Roper, E. A. Badry, K. M. Sproule, and R. J. Turner.** 2005. Persister cells mediate tolerance to metal oxyanions in *Escherichia coli*. Microbiology **151:**3181-3195.
98. **Harrison, J. J., H. Ceri, C. Stremick, and R. J. Turner.** 2004. Biofilm susceptibility to metal toxicity. Environmental Microbiology **6:**1220-1227.
99. **Harrison, J. J., H. Ceri, C. Stremick, and R. J. Turner.** 2004. Differences in biofilm and planktonic cell mediated reduction of metalloid oxyanions. FEMS Microbiology Letters **235:**357-362.
100. **Harrison, J. J., H. Ceri, and R. J. Turner.** 2007. Multimetal resistance and tolerance in microbial biofilms. Nature Reviews Microbiology **5:**928-938.
101. **Harrison, J. J., H. Ceri, J. Yerly, M. Rabiei, Y. Hu, R. Martinuzzi, and R. J. Turner.** 2007. Metal ions may supress or enhance cellular differentiation in *Candida albicans* and *Candida tropicalis* biofilms. Applied and Environmental Microbiology **73:**4940-4949.
102. **Harrison, J. J., H. Ceri, J. Yerly, C. A. Stremick, Y. Hu, R. Martinuzzi, and R. J. Turner.** 2006. The use of microscopy and three-dimensional visualization to evaluate the structure of microbial biofilms cultivated in the Calgary Biofilm Device. Biological Procedures Online **8:**194-215.
103. **Harrison, J. J., M. Rabiei, R. J. Turner, E. A. Badry, K. M. Sproule, and H. Ceri.** 2006. Metal resistance in *Candida* biofilms. FEMS Microbiology Ecology **55:**479-491.
104. **Harrison, J. J., R. J. Turner, and H. Ceri.** 2005. High-throughput metal susceptibility testing of microbial biofilms. BMC Microbiology **5:**53.
105. **Harrison, J. J., R. J. Turner, and H. Ceri.** 2005. Persister cells, the biofilm matrix and tolerance to metal cations in biofilm and planktonic *Pseudomonas aeruginosa*. Environmental Microbiology **7:**981-994.
106. **Harrison, J. J., R. J. Turner, and H. Ceri.** 2007. A subpopulation of Candida albicans and Candida tropicalis biofilm cells are highly tolerant to chelating agents. FEMS Microbiology Letters **272:**172-181.
107. **Harrison, J. J., R. J. Turner, D. A. Joo, M. A. Stan, C. S. Chan, N. D. Allan, H. A. Vrionis, M. E. Olson, and H. Ceri.** 2008. Copper and quaternary ammonium cations exert synergistic bactericidal and anti-biofilm activity against *Pseudomonas aeruginosa*. Antimicrobial Agents and Chemotherapy **(in press)**.
108. **Harrison, J. J., R. J. Turner, L. L. R. Marques, and H. Ceri.** 2005. Biofilms: A new understanding of these microbial communities is driving a revolution that may transform the science of microbiology. American Scientist **93:**508-515.

109. **Hassett, D. J., M. J.F., J. G. Elkins, T. R. McDermott, U. A. Ochsner, S. E. West, C. Huang, J. Fredericks, S. Burnett, P. S. Stewart, G. A. McFeters, L. Passador, and B. H. Iglewski.** 1999. Quorum sensing in *Pseudomonas aeruginosa* controls expression of catalase and superoxide dismutase genes and mediates biofilm susceptibility to hydrogen peroxide. Molecular Microbiology **34:**1082-1093.

110. **Häußler, S.** 2004. Biofilm formation by the small colony variant phenotype of *Pseudomonas aeruginosa*. Environmental Microbiology **6:**546-551.

111. **Häußler, S., I. Ziegler, A. Lottel, F. von Gotz, M. Rohde, D. Wehmhohner, S. Saravanamuthu, B. Tummler, and I. Steinmetz.** 2003. Highly adherent small colony variants of *Pseudomonas aeruginosa* in cystic fibrosis lung infection. Journal of Medical Microbiology **52:**295-301.

112. **Hernandez, L., A. J. Probst, J. L. Probst, and E. Ulrich.** 2003. Heavy metal distribution in some French forest soils: evidence for atmospheric contamination. Science of the Total Environment **312:**195-219.

113. **Heydorn, A., A. T. Nielsen, M. Hentzer, C. Sternberg, M. Givskov, B. K. Ersboll, and S. Molin.** 2000. Quantification of biofilm structures by the novel computer program COMSTAT. Microbiology **146:**2395-2407.

114. **Heyne, B., C. Beddie, and J. C. Scaiano.** 2007. Synthesis and characterization of a new fluorescent probe for reactive oxygen species. Organic and Biomolecular Chemistry **5:**1454-1458.

115. **Hoffman, L. R., D. A. D'Argenio, M. J. MacCoss, Z. Zhang, R. A. Jones, and S. I. Miller.** 2005. Aminoglycoside antibiotics induce bacterial biofilm formation. Nature **436:**1171-1175.

116. **Holm, O., E. Hansen, C. Lassen, F. Stuer-Lauridsen, and J. Kjolholt.** 2002. European Commission DG ENV.E3 - Heavy metals in waste: Final Report ENV.E.3/ETU/2000/0058. COWI Consulting Engineers.

117. **Horswill, A. R., P. Stoodley, P. S. Stewart, and M. R. Parsek.** 2007. The effect of the chemical, biological, and physical environment on quorum sensing in structured microbial communities. Analytical and Bioanalytical Chemistry **387:**371-380.

118. **Hu, P., E. L. Brodie, Y. Suzuki, H. H. McAdams, and G. L. Andersen.** 2005. Whole-genome transcriptional analysis of heavy metal stresses in *Caulobacter crescentus*. Journal of Bacteriology **187:**8437-8449.

119. **Hu, Z., G. Hidalgo, P. L. Houston, A. G. Hay, M. L. Shuler, H. D. Abruña, W. C. Ghiorse, and L. W. Lion.** 2005. Determination of spatial distributions of zinc and active biomass in microbial biofilms by two-photon laser scanning microscopy. Applied and Environmental Microbiology **71:**4014-4021.

120. **Hu, Z., J. Jin, H. D. Abruña, P. L. Houston, A. G. Hay, W. C. Ghiorse, M. L. Shuler, G. Hidalgo, and L. W. Lion.** 2007. Spatial distributions of copper in microbial biofilms by scanning electrochemical micrscopy. Environmental Science and Technology **41:**936-941.

121. **Huang, C., K. D. Xu, G. A. McFeters, and P. S. Stewart.** 1998. Spatial patterns of alkaline phosphatase expression within bacterial colonies and biofilms in

response to phosphate starvation. Applied and Environmental Microbiology **64:**1526-1531.

122. **Huang, G. H., X. Y. Nie, and J. Y. Chen.** 2006. CaMac1, a *Candida albicans* copper ion-sensing transcription factor, promotes filamentous and invasive growth in *Saccharomyces cerevisiae*. Acta Biochimica et Biophysica Sin (Shanghai) **38:**213-217.
123. **Hunter, R. C., and T. J. Beveridge.** 2005. Application of a pH-sensitive fluoroprobe (C-SNARF-4) for pH microenvironment analysis in *Pseudomonas aeruginosa* biofilms. Applied and Environmental Microbiology **71:**2501-2510.
124. **Inoaoka, T., Y. Matsumura, and T. Tsuchido.** 1999. SodA and manganese are essential for resistance to oxidative stress in growing and sporulating cells of *Bacillus subtillis*. Journal of Bacteriology **181:**1939-1943.
125. **Ize, B., I. Porcelli, S. Lucchini, J. C. Hinton, B. C. Berks, and T. Palmer.** 2004. Novel phenotypes of *Escherichia coli tat* mutants revealed by global gene expression and phenotypic analysis. Journal of Biological Chemistry **279:**47543-47554.
126. **Jin, Y., T. Zhang, Y. H. Samaranayake, H. H. P. Fang, H. K. Yip, and L. P. Samaranayake.** 2005. The use of probes and stains for improved assessment of cell viability and extracellular polymeric substances in *Candida albicans* biofilms. Mycopathologia **159:**353-360.
127. **Juhas, M., L. Eberl, and B. Tummler.** 2005. Quorum sensing: the power of cooperation in the world of *Pseudomonas*. Environmental Microbiology **7:**459-471.
128. **Kaneko, Y., M. Theondel, O. Olakanmi, B. E. Britigan, and P. K. Singh.** 2007. The transition metal gallium disrupts *Pseudomonas aeruginosa* iron metabolism and has antimicrobial and antibiofilm activity. Journal of Clinical Investigation **117:**877-888.
129. **Karp, P. D., I. M. Keseler, A. Shearer, M. Latendresse, M. Krummenacker, S. M. Paley, I. Paulsen, J. Collado-Vides, S. Gama-Castro, M. Peralta-Gil, A. Santos-Zavaleta, M. I. Penaloza-Spinola, C. Bonavides-Martinez, and J. Ingraham.** 2007. Multidimensional annotation of the *Escherichia coli* K-12 genome. Nucleic Acids Research **35:**7577-7590.
130. **Keren, I., N. Kaldalu, A. Spoering, and K. Lewis.** 2004. Pesister cells and tolerance to antimicrobials. FEMS Microbiology Letters **230:**13-18.
131. **Keren, I., D. Shah, A. Spoering, N. Kaldalu, and K. Lewis.** 2004. Specialized persister cells and the mechanism of multidrug tolerance in *Escherichia coli*. Journal of Bacteriology **186:**8172-8180.
132. **Kessi, J., and K. W. Hanselmann.** 2004. Similarities between the abiotic reduction of selenite with glutathione and the dissimilatory reaction mediated by *Rhodospirillum rubrum* and *Escherichia coli*. Journal of Biological Chemistry **279:**50662-50669.
133. **King, E. O., M. K. Ward, and D. C. Raney.** 1954. Two simple media for the demonstration of pyocyanin and fluorescein. Journal of Laboratory and Clinical Medicine **44:**301-307.

134. **Kirisitis, M. J., L. Prost, M. Starkey, and M. Parsek.** 2005. Characterization of colony morphology variants isolated from *Pseudomonas aeruginosa* biofilms. Applied and Environmental Microbiology **71:**4809-4821.
135. **Kirisits, M. J., J. J. Margolis, B. L. Purevdorj- Gage, B. Vaughan, D. L. Chopp, P. Stoodley, and M. R. Parsek.** 2007. Influence of the hydrodynamic environment on quorum sensing in *Pseudomonas aeruginosa* biofilms. Journal of Bacteriology **189:**8357-8360.
136. **Kirisits, M. J., and M. R. Parsek.** 2006. Does *Pseudomonas aeruginosa* use intercellular signalling to build biofilm communities? Cellular Microbiology **8:**1841-1849.
137. **Klapper, I., P. Gilbert, B. P. Ayati, J. Dockery, and P. S. Stewart.** 2007. Senescence can explain microbial persistence. Microbiology **153:**3623-3630.
138. **Kohanski, M. A., D. J. Dwyer, B. Hayete, C. A. Lawrence, and J. J. Collins.** 2007. A common mechanism of cellular death induced by bactericidal antibiotics. Cell **130:**797-810.
139. **Korch, S. B., T. A. Henderson, and T. M. Hill.** 2003. Characterization of the *hipA7* allele of *Escherichia coli* and evidence that high persistence is governed by (p)ppGpp synthesis. Molecular Microbiology **50:**1199-1213.
140. **Korch, S. B., and T. M. Hill.** 2006. Ectopic overexpression of wild-type and mutant *hipA* genes in *Escherichia coli*: effects on macromolecular synthesis and persister formation. Journal of Bacteriology **188:**3826-3836.
141. **Kostenko, V., H. Ceri, and R. J. Martinuzzi.** 2007. Increased tolerance of *Staphylococcus aureus* to vancomycin in viscous media. FEMS Immunology and Medical Microbiology **51:**277-288.
142. **Krom, B. P., J. B. Cohen, G. E. McElhaney-Feser, and R. L. Cihlar.** 2007. Optimized candidal biofilm microtiter assay. Journal of Microbiological Methods **(in press)**.
143. **Kuhn, D. M., J. Chandra, P. K. Mukherjee, and M. A. Ghannoum.** 2002. Comparison of biofilms formed by *Candida albicans* and *Candida parapsilosis* on bioprosthetic surfaces. Infection and Immunity **70:**878-888.
144. **Kumamoto, C. A.** 2002. Candida biofilms. Current Opinion in Microbiology **5:**608-611.
145. **Kumon, H., K. Tomochika, T. Matunaga, M. Ogawa, and H. Ohmori.** 1994. A sandwich cup method for the penetration assay of antimicrobial agents through Pseudomonas exopolysaccharides. Microbiology and Immunology **38:**615-619.
146. **Labbate, M., S. Y. Queck, K. S. Koh, S. A. Rice, M. Givskov, and S. Kjelleberg.** 2004. Quorum sensing-controlled biofilm development in *Serratia liquefaciens* MG1. Journal of Bacteriology **186:**692-8.
147. **Lafleur, M. D., C. A. Kumamoto, and K. Lewis.** 2006. *Candida albicans* biofilms produce antifungal tolerant persister cells. Antimicrobial Agents and Chemotherapy **50:**3839-3846.
148. **Langley, S., and T. J. Beveridge.** 1999. Metal binding by *Pseudomonas aeruginosa* PAO1 is influenced by growth of the cells as a biofilm. Canadian Journal of Microbiology **45:**616-622.

149. **Lawrence, J. R., M. R. Chenier, R. Roy, D. Beaumier, N. Fortin, G. D. W. Swerhone, T. R. Neu, and C. W. Greer.** 2004. Microscale and molecular assessment of impacts of nickel, nutrients, and oxygen level on structure and function of river biofilm communities. Applied and Environmental Microbiology **70:**4326-4339.
150. **Lawrence, J. R., G. D. Swerhone, U. Kuhlicke, and T. R. Neu.** 2007. *In situ* evidence for microdomains in the polymer matrix of bacterial microcolonies. Canadian Journal of Microbiology **53:**450-458.
151. **Lewis, K.** 2005. Persister cells and the riddle of biofilm survival. Biochemistry (Moscow) **70:**327-336.
152. **Lewis, K.** 2007. Persister cells, dormancy and infectious disease. Nature Reviews Microbiology **5:**48-56.
153. **Lewis, K.** 2001. Riddle of biofilm resistance. Antimicrobial Agents and Chemotherapy **45:**999-1007.
154. **Li, Y., and Y. Zhang.** 2007. PhoU is a persistence switch involved in persister formation and tolerance to multiple antibiotics and stresses in *Escherichia coli*. Antimicrobial Agents and Chemotherapy **51:**2092-2099.
155. **Liu, H., and H. P. Fang.** 2002. Characterization of electrostatic binding sites of extracellular polymers by linear programming analysis of titration data. Biotechnology and Bioengineering **80:**806-811.
156. **Lloyd-Jones, G., M. Osborne, D. A. Ritchie, P. Strike, J. L. Hobman, N. L. Brown, and D. A. Rouch.** 1994. Accumulation and intracellular fate of tellurite in tellurite resistant *Escherichia coli*: A model for mechanism of resistance. FEMS Microbiology Letters **118:**113-120.
157. **Lohmeier-Vogel, E. M., S. Ung, and R. J. Turner.** 2004. *In vivo* ^{31}P-NMR investigation of tellurite toxicity in *Escherichia coli*. Applied and Environmental Microbiology **70:**7342-7247.
158. **Lopez-Archilla, A. I., A. E. Gonzalez, M. C. Terron, and R. Amils.** 2004. Ecological study of the fungal populations of the acidic Tinto River in southwestern Spain. Canadian Journal of Microbiology **50:**923-934.
159. **Lopez-Archilla, A. L., and I. M. Amils.** 2001. Microbial community composition and ecology of an acidic aquatic environment: the Tinto River, Spain. Microbial Ecology **41:**20-35.
160. **Mages, M., M. Ovari, W. Tumpling, and K. Kropfl.** 2004. Biofilms as bio-indicator for polluted waters? Total reflection X-ray fluorescence analysis of biofilms of the Tisza river (Hungary). Analytical and Bioanalytical Chemistry **378:**1095-1101.
161. **Mah, T. F., B. Pitts, B. Pellock, G. C. Walker, P. S. Stewart, and G. A. O'Toole.** 2003. A genetic basis for *Pseudomonas aeruginosa* biofilm antibiotic resistance. Nature **426:**306-310.
162. **Martinez-Granero, F., S. Capdevila, M. Sánchez-Contreras, M. Martin, and R. Rivilla.** 2005. Two site-specific recombinases are implicated in phenotypic variation and competitive rhizosphere colonization in *Pseudomonas fluorescens*. Microbiology **151:**975-983.

163. **Missy, P., M. C. Lanhers, Y. Grignon, M. Joyeux, and D. Burnel.** 2000. *In vitro* and *in vivo* studies on chelation of manganese. Human and Experimental Toxicology **19:**448-456.
164. **Molin, S., and T. Tolker-Neilsen.** 2003. Gene transfer occurs with enhanced efficiency in biofilms and induces enhanced stabilisation of the biofilm structure. Current Opinion in Biotechnology **14:**255-261.
165. **Moran, L. A., K. G. Scrimgeour, H. R. Horton, R. S. Ochs, and J. D. Rawn.** 1994. Chapter 15: Glycolysis, Biochemistry. Prentice Hall, Upper Saddle River, N.J.
166. **Morck, D. W., K. Lam, S. G. McKay, M. E. Olson, B. Prosser, B. D. Ellis, R. Cleeland, and J. W. Costerton.** 1994. Comparative evaluation of fleroxacin, ampicillin, trimethoprim-sulfamethoxazole, and gentamicin as treatments of catheter associated urinary tract infections in a rabbit model. American Journal of Medicine **94:**23S-30S.
167. **Moyed, H., and S. Broderick.** 1986. Molecular cloning and expression of *hipA*, a gene of *Escherichia coli* K-12 that affects frequency of persistence after inhibition of murein synthesis. Journal of Bacteriology **166:**399-403.
168. **Moyed, H. S., and K. P. Bertrand.** 1983. *hipA*, a newly recognized gene of *Escherichia coli* K-12 that affects frequency of persistence after inhibition of murein synthesis. Journal of Bacteriology **155:**768-775.
169. **Mueller, L. N., J. F. C. de Brouwer, J. S. Almeida, L. J. Stal, and J. B. Xavier.** 2006. Analysis of a marine phototrophic biofilm by confocal laser scanning microscopy using the new image quantification software PHLIP. BMC Ecology **6:**1.
170. **Mukhopadhyay, R., B. P. Rosen, L. T. Phung, and S. Silver.** 2002. Microbial arsenic: from geocycles to genes and enzymes. FEMS Microbiology Reviews **26:**311-325.
171. **Mulvey, M. R., J. Switala, A. Borys, and P. C. Loewen.** 1990. Regulation of transcription of *katE* and *katF* in *Escherichia coli*. Journal of Bacteriology **172:**6713-6720.
172. **Munoz, R., M. T. Alvarez, A. Munoz, E. Terrazas, B. Guieysse, and B. Mattiasson.** 2006. Sequential removal of heavy metal ions and organic pollutants using an algal-bacterial consortium. Chemosphere **63:**903-911.
173. **Nair, S., and S. E. Finkel.** 2004. Dps protects cells against multiple stresses during stationary phase. Journal of Bacteriology **186:**4192-4198.
174. **Nickerson, K. W., A. L. Atkin, and J. M. Hornby.** 2006. Quorum sensing in dimorphic fungi: farnesol and beyond. Applied and Environmental Microbiology **72:**3805-3813.
175. **Nieboer, E., and G. G. Fletcher.** 1996. Chapter 7: Determinants of reactivity in metal toxicology, p. 113-132. *In* L. W. Chang (ed.), Toxicology of metals. CRC Press Incorporated, Boca Raton, FL.
176. **Niederhoffer, E. C., C. M. Naranjo, K. L. Bradley, and J. A. Fee.** 1990. Control of the *Escherichia coli* superoxide dismutatse (*sodA* and *sodB*) genes by the ferric uptake regulation (*fur*) locus. Journal of Bacteriology **172:**1930-1938.

177. **Nies, D. H.** 2003. Efflux-mediated heavy metal resistance in prokaryotes. FEMS Microbiology Reviews **27:**313-339.
178. **Nies, D. H.** 1999. Microbial heavy-metal resistance. Applied Microbiology and Biotechnology **51:**730-750.
179. **O'Toole, G. A., and P. S. Stewart.** 2005. Biofilms strike back: sublethal concentrations of antibiotics increase bacterial drug tolerance by promoting biofilm formation. Nature Biotechnology **23:**1378-1379.
180. **Olson, M. E., H. Ceri, D. W. Morck, A. G. Buret, and R. R. Read.** 2002. Biofilm bacteria: formation and comparative susceptibility to antibiotics. Canadian Journal of Veterinary Research **66:**86-92.
181. **Oremland, R. S., and J. F. Stolz.** 2003. The ecology of arsenic. Science **300:**939-944.
182. **Ovington, L. G.** 2004. The truth about silver. Ostomy/Wound Management **50:**1S-10S.
183. **Parkins, M. D., H. Ceri, and D. G. Storey.** 2001. *Pseudomonas aeruginosa* GacA, a factor in multihost virulence, is also essential for biofilm formation. Molecular Microbiology **40:**1215-1226.
184. **Parsek, M. R., and E. P. Greenberg.** 2005. Sociomicrobiology: the connections between quorum sensing and biofilms. Trends in Microbiology **13:**27-33.
185. **Parvatiyar, K., E. M. Alsabbagh, U. A. Ochsner, M. A. Stegemeyer, A. G. Smulian, S. H. Hwang, C. R. Jackson, T. R. McDermott, and D. J. Hassett.** 2005. Global analysis of cellular factors and responses involved in *Pseudomonas aeruginosa* resistance to arsenite. Journal of Bacteriology **187:**4853-4864.
186. **Pearson, J. P., K. M. Gray, L. Passador, K. D. Tucker, A. Eberhard, B. Iglewski, and E. P. Greenberg.** 1994. Structure of the autoinducer required for the expression of *Pseudomonas aeruginosa* virulence genes. Proceedings of the National Academy of Sciences of the United States of America **91:**197-201.
187. **Pearson, J. P., L. Passador, B. Iglewski, and E. P. Greenberg.** 1995. A second *N*-acyl-homoserine lactone signal produced by *Pseudomonas aeruginosa*. Proceedings of the National Academy of Sciences of the United States of America **92:**1490-1494.
188. **Pedersen, K., S. K. Christensen, and K. Gerdes.** 2002. Rapid induction and reversal of a bacteriostatic condition by controlled expression of toxins and antitoxins. Molecular Microbiology **45:**501-510.
189. **Pederson, K., A. V. Zavialov, M. Y. Pavlov, J. Elf, K. Gerdes, and M. Ehrenberg.** 2003. The bacterial toxin RelE displays codon-specific cleavage of mRNAs in the ribosomal A site. Cell **112:**131-140.
190. **Podgorskii, V. S., T. P. Kasatkina, and O. G. Lozovaia.** 2004. Yeasts - Biosorbents of heavy metals. Mikrobiologicheskii Zhurnal **1:**91-103.
191. **Pomposiello, P. J., and B. Demple.** 2002. Global adjustment of microbial physiology during free radical stress. Advances in Microbial Physiology **46:**319-341.
192. **Pomposiello, P. J., and B. Demple.** 2001. Redox-operated genetic switches: the SoxR and OxyR transcription factors. Trends in Biotechnology **19:**109-114.

193. **Poritsanos, N., C. Selin, W. G. D. Fernando, S. Nakkeeran, and T. R. de Kievit.** 2006. A GacS deficiency does not affect *Pseudomonas chlororaphis* PA23 fitness when growing on canola, in aged batch culture or as a biofilm. Canadian Journal of Microbiology **52:**1177-1188.
194. **Potera, C.** 1998. Forging a link between biofilms and disease. Science **283:**1837-1839.
195. **Potrykus, J., and G. Wegrzyn.** 2004. The ypdI gene codes for a putative lipoprotein involved in the synthesis of colanic acid in Escherichia coli. FEMS Microbiology Letters **235:**265-271.
196. **Pourahmad, J., M. Rabiei, F. Jokar, and P. J. O'Brien.** 2005. A comparison of hepatocyte cytotoxic mechanisms for chromate and arsenite. Toxicology **206:**449-460.
197. **Prieto-Alamo, M.-J., J. Jurado, R. Gallardo-Madueno, F. Monje-Casas, A. Holmgren, and C. Pueyo.** 2000. Transcriptional regulation of glutaredoxin and thioredoxin pathways and related enzymes in response to oxidative stress. Journal of Biological Chemistry **275:**13398-13405.
198. **Pringault, O., E. Epping, R. Guyoneaud, A. Khalili, and M. Kuhl.** 1999. Dynamics of anoxygenic photosynthesis in an experimental green sulphur bacteria biofilm. Environmental Microbiology **1:**295-305.
199. **Purevdorj-Gage, B., W. J. Costerton, and P. Stoodley.** 2005. Phenotypic differentiation and seeding dispersal in non-mucoid and mucoid *Pseudomonas aeruginosa* biofilms. Microbiology **151:**1569-1576.
200. **Radtke, C., W. S. Cook, and A. J. Anderson.** 1994. Factors affecting antagonism of the growth of Phanerochaete chrysosporium by bacteria isolated from soils. Applied Microbiology and Biotechnology **41:**274-280.
201. **Rahme, L. G., E. J. Stevens, J. Wolfort, J. Shao, R. G. Tompkins, and F. M. Ausubel.** 1995. Common virulence factors for bacterial pathogenicity in plants and animals. Science **268:**1899-1902.
202. **Ramage, G., and J. L. Lopez-Ribot.** 2005. Techniques for antifungal susceptibility testing of *Candida albicans* biofilms. Methods in Molecular Medicine **118:**71-79.
203. **Ramage, G., S. P. Saville, P. D. Thomas, and J. L. Lopez-Ribot.** 2005. Candida biofilms: an update. Eukaryotic Cell **4:**633-638.
204. **Rani, S. A., B. Pitts, H. Beyenal, R. A. Veluchamy, Z. Lewandowsky, W. M. Davison, K. Buckingham-Meyer, and P. S. Stewart.** 2007. Spatial patterns of DNA replication, protein synthesis and oxygen concentration within bacterial biofilms reveal diverse physiological states. Journal of Bacteriology **189:**4223-4233.
205. **Rawlings, D. E., and D. B. Johnson.** 2007. The microbiology of biomining: development and optimization of mineral oxidizing microbial consortia. Microbiology **153:**315-324.
206. **Ren, D., L. A. Bedzyk, S. M. Thomas, R. W. Ye, and T. K. Wood.** 2004. Gene expression in *Escherichia coli* biofilms. Applied Microbiology and Biotechnology **64:**515-524.

207. **Roberts, M. E., and P. S. Stewart.** 2005. Modelling protection from antimicrobial agents in biofilms through the formation of persister cells. Microbiology **151:**75-80.
208. **Römling, U., M. Gomelsky, and M. Y. Galperin.** 2005. C-di-GMP: the dawning of a novel bacterial signaling system. Molecular Microbiology **57:**629-639.
209. **Russel, A. D., I. Ahonkhai, and D. T. Rogers.** 1979. Microbiological applications of the inactivation of antibiotics and other antimicrobial agents. Journal of Applied Bacteriology **46:**207-245.
210. **Ryder, C., M. Byrd, and D. J. Wozniak.** 2007. Role of polysaccharides in *Pseudomonas aeruginosa* biofilm development. Current Opinion in Microbiology **10:**644-648.
211. **Sambasivarao, D., H. A. Dawson, G. Zhang, G. Shaw, J. Hu, and J. H. Weiner.** 2001. Investigation of Escherichia coli dimethyl sulfoxide reductase assembly and processing in strains defective for the sec-independent protein translocation system membrane targeting and translocation. Journal of Biological Chemistry **276:**20167-74.
212. **Sambrook, J., and D. W. Russell.** 2001. Molecular cloning: A laboratory manual, 3rd ed. Cold Spring Harbour Lab Press, Melbourne.
213. **Sánchez-Contreras, M., M. Martin, M. Villacieros, F. O'Gara, I. Bonilla, and R. Rivilla.** 2002. Phenotypic selection and phase variation occur during alfalfa root colonization by *Pseudomonas fluorescens* F113. Journal of Bacteriology **184:**1587-1596.
214. **Sarkar, S., and R. Chakraborty.** 2008. Quorum sensing in metal tolerance of *Acinetobacter junii* BB1A is associated with biofilm production. FEMS Microbiology Letters **282:**160-165.
215. **Sauer, K., A. K. Camper, G. D. Ehrlich, J. W. Costerton, and D. G. Davies.** 2002. *Pseudomonas aeruginosa* displays multiple phenotypes during development as a biofilm. Journal of Bacteriology **184:**1140-1154.
216. **Scherrer, R., and H. S. Moyed.** 1988. Conditional impairment of cell division and altered lethality in *hipA* mutants of *Escherichia coli* K-12. Journal of Bacteriology **170:**3321-3326.
217. **Schmidt-Eisenlohr, H., A. Gast, and C. Baron.** 2003. Inactivation of *gacS* does not affect the competitiveness of *Pseudomonas chlororaphis* in the *Arabidopsis thaliana* rhizosphere. Applied and Environmental Microbiology **69**.
218. **Schooling, S. R., and T. J. Beveridge.** 2006. Membrane vesicles: an overlooked component of the matrices of biofilms. Journal of Bacteriology **188:**5945-5957.
219. **Schparyk, Y. S., and V. I. Parpan.** 2004. Heavy metal pollution and forest health in the Ukranian Carpathians. Environmental Pollution **130:**55-63.
220. **Schuster, M., C. P. Lostroh, T. Ogi, and E. P. Greenberg.** 2003. Identification, timing and signal specificity of *Pseudomonas aeruginosa* quorum-controlled genes: a transcriptome analysis. Journal of Bacteriology **185:**2066-2079.
221. **Shah, D., Z. Zhang, A. Khodursky, N. Kaldalu, K. Kurg, and K. Lewis.** 2006. Persisters: a distinct physiological state of *E. coli*. BMC Microbiology **6:**53.
222. **Shen-Orr, S. S., R. Milo, S. Mangan, and U. Alon.** 2002. Network motifs in the transcriptional regulation network of *Escherichia coli*. Nature Genetics **31:**64-68.

223. **Shigeta, M., G. Tanaka, H. Komatsuzawa, M. Sugai, H. Suginaka, and T. Usui.** 1997. Permeation of antimicrobial agents through *Pseudomonas aeruginosa* biofilms: a simple method. Chemotherapy (Tokyo) **43:**340-345.
224. **Shrout, J. D., D. L. Chopp, C. L. Just, M. Hentzer, M. Givskov, and M. R. Parsek.** 2006. The impact of quorum-sensing and swarming motility on *Pseudomonas aeruginosa* biofilm formation is nutritionally conditional. Molecular Microbiology **62:**1264-1277.
225. **Silver, S.** 1998. Genes for all metals - a bacterial view of the Periodic Table: The 1996 Thom Award Lecture. Journal of Industrial Microbiology and Biotechnology **20:**1-12.
226. **Singh, R., D. Paul, and R. Jain.** 2006. Biofilms: implications in bioremediation. Trends in Microbiology **14:**389-397.
227. **Soberón-Chávez, G., and M. Aguirre-Ramírez.** 2005. Is *Pseudomonas aeruginosa* only "sensing quorum"? Critical Reviews in Microbiology **31:**171-182.
228. **Southey-Pillig, C. J., D. G. Davies, and K. Sauer.** 2005. Characterization of temporal protein production in *Pseudomonas aeruginosa* biofilms. Journal of Bacteriology **187:**8114-8126.
229. **Spencer, M., C. M. Ryu, K. Y. Yang, Y. C. Kim, J. W. Kloepper, and A. J. Anderson.** 2003. Induced defence in tobacco by *Pseudomonas chlororaphis* strain O6 involves at least the ethylene pathway. Physiological and Molecular Plant Pathology **63:**27-34.
230. **Spoering, A., and K. Lewis.** 2001. Biofilm and planktonic cells of *Pseudomonas aeruginosa* have similar resistance to killing by antimicrobials. Journal of Bacteriology **183:**6746-6751.
231. **Spoering, A. L., M. Vulic, and K. Lewis.** 2006. GlpD and PlsB participate in persister cell formation in *Escherichia coli*. Journal of Bacteriology **188:**5136-5144.
232. **Stanley, N. R., K. Findlay, B. C. Berks, and T. Palmer.** 2001. *Escherichia coli* strains blocked in Tat-dependent protein export exhibit pleiotropic defects in the cell envelope. Journal of Bacteriology **183:**139-44.
233. **Steinberger, R. E., and P. A. Holden.** 2005. Extracellular DNA in single- and multiple-species unsaturated biofilms. Applied and Environmental Microbiology **71:**5404-5410.
234. **Stewart, P. S.** 2003. Diffusion in biofilms. Journal of Bacteriology **185:**1485-1491.
235. **Stewart, P. S.** 2002. Mechanisms of antibiotic resistance in bacterial biofilms. International Journal of Medical Microbiology **292:**107-113.
236. **Stewart, P. S., and J. W. Costerton.** 2001. The antibiotic resistance of bacteria in biofilms. Lancet **358:**135-138.
237. **Stewart, P. S., and M. J. Franklin.** 2008. Physiological heterogeneity in biofilms. Nature Reviews Microbiology **6:**199-210.
238. **Stewart, P. S., J. Rayner, F. Roe, and W. M. Rees.** 2001. Biofilm penetration and disinfection efficacy of alkaline hypochlorite and chlorosulfamates. Journal of Applied Microbiology **91:**525-532.

239. **Stewart, P. S., F. Roe, J. Rayner, J. G. Elkins, Z. Lewandowski, A. Ochsner, and D. J. Hassett.** 2000. Effect of catalase on hydrogen peroxide penetration into *Pseudmonas aeruginosa* biofilms. Applied and Environmental Microbiology **66:**836-838.
240. **Stintzi, A., K. Evans, J.-M. Meyer, and K. Poole.** 1998. Quorum-sensing and siderophore biosynthesis in *Pseudomonas aeruginosa*: *lasR*/*lasI* mutants exhibit reduced pyoverdine synthesis. FEMS Microbiology Letters **166:**341-345.
241. **Stohs, S. J., and D. Bagchi.** 1995. Oxidative mechanisms in the toxicity of metal ions. Free Radical Biology and Medicine **18:**321-36.
242. **Stoodley, P., K. Sauer, D. G. Davies, and J. W. Costerton.** 2002. Biofilms as complex differentiated communities. Annual Review of Microbiology **56:**187-209.
243. **Sufya, N., D. G. Allison, and P. Gilbert.** 2003. Clonal variation in maximum specific growth rate and susceptibility towards antimicrobials. Journal of Applied Microbiology **95:**1261-1267.
244. **Suihko, M. L., and E. S. Hoekstra.** 1999. Fungi present in some recycled fibre pulps and paperboards. Nordic Pulp and Paper Research Journal **14:**199-203.
245. **Sutherland, I. W.** 2001. Biofilm exopolysaccharides: a strong and sticky framework. Microbiology **147:**3-9.
246. **Sutherland, I. W.** 2001. The biofilm matrix - an immobilized but dynamic microbial environment. Trends in Microbiology **9**.
247. **Szomolay, B., I. Klapper, J. Dockery, and P. S. Stewart.** 2005. Adaptive responses to antimicrobial agents in biofilms. Environmental Microbiology **7:**1186-1191.
248. **Tabak, H. H., P. Lens, E. D. van Hullebusch, and W. Dejonghe.** 2005. Developments in bioremediation of soils and sediments polluted with metals and radionuclides - 1. Microbial processes and mechanisms affecting bioremediation of metal contamination and influencing metal toxicity and transport. Reviews in Environmental Science and Biotechnology **4:**115-156.
249. **Teitzel, G. M., A. Geddie, S. K. De Long, M. J. Kirisits, M. Whiteley, and M. R. Parsek.** 2006. Survival and growth in the presence of elevated copper: transcriptional profiling of copper-stressed *Pseudomonas aeruginosa*. Journal of Bacteriology **188:**7242-7256.
250. **Teitzel, G. M., and M. R. Parsek.** 2003. Heavy metal resistance of biofilm and planktonic *Pseudomonas aeruginosa*. Applied and Environmental Microbiology **69:**2313-2320.
251. **Toledano, M. B., C. Kumar, N. Le Moan, D. Spector, and F. Tacnet.** 2007. The system biology of thiol redox system in *Escherichia coli* and yeast: Differential functions in oxidative stress, iron metabolism and DNA synthesis. FEBS Letters **581:**3598-3607.
252. **Tomlin, K. L., R. J. Malott, G. Ramage, D. G. Storey, P. A. Sokol, and H. Ceri.** 2006. Quorum-sensing mutations affect attachment and stability of *Burkholderia cenocepacia* biofilms. Applied and Environmental Microbiology **71:**5208-5218.

253. **Toner, B., S. Fakra, M. Villalobos, T. Warwick, and G. Sposito.** 2005. Spatially resolved characterization of biogenic manganese oxide production within a bacterial biofilm. Applied and Environmental Microbiology **71:**1300-1310.
254. **Touati, D., M. Jacques, B. Tardat, L. Bouchard, and S. Despied.** 1995. Lethal oxidative damage and mutagenesis are generated by iron in *Δfur* mutants of *Escherichia coli*: Protective role of superoxide dismutase. Journal of Bacteriology **177:**2305-2314.
255. **Tremaroli, V., S. Fedi, and D. Zannoni.** 2007. Evidence for a tellurite-dependent generation of reative oxygen species and absence of a tellurite-mediated adaptive response to oxidative stress in cells of *Pseudomonas pseudoalcaligenes* KF707. Archives of Microbiology **187:**127-135.
256. **Turner, R. J.** 2001. Tellurite toxicity and resistance in Gram-negative bacteria. Recent Research Developments in Microbiology **5:**69-77.
257. **Turner, R. J., Y. Aharonowitz, J. Weiner, and D. E. Taylor.** 2001. Glutathione is a target of tellurite toxicity and is protected by tellurite resistance determinants in *Escherichia coli*. Canadian Journal of Microbiology **47:**33-40.
258. **Turner, R. J., J. Weiner, and D. E. Taylor.** 1998. Selenium metabolism in *Escherichia coli*. BioMetals **11:**223-227.
259. **Turner, R. J., J. Weiner, and D. E. Taylor.** 1999. Tellurite mediated thiol oxidation in *Escherichia coli*. Microbiology **145:**2549-2557.
260. **Turner, R. J., J. Weiner, and D. E. Taylor.** 1992. Use of diethyldithiocarbamate for quantitative determination of tellurite uptake by bacteria. Analytical Biochemistry **204:**3092-3094.
261. **Turner, R. J., J. H. Weiner, and D. E. Taylor.** 1995. The tellurite-resistance determinants tehAtehB and *klaAklaBtelB* have different biochemical requirements. Microbiology **141:**3133-3140.
262. **Valko, M., H. Morris, and M. T. D. Cronin.** 2005. Metals, toxicity and oxidative stress. Current Medicinal Chemistry **12:**1161-1208.
263. **van den Broek, D., G. V. Bloemberg, and B. J. Lugtenberg.** 2005. The role of phenotypic variation in rhizosphere *Pseudomonas* bacteria. Environmental Microbiology **7:**1686-1697.
264. **van Hullebusch, E. D., M. H. Zandvoort, and P. N. L. Lens.** 2003. Metal immobilization by biofilms: Mechanisms and analytical tools. Reviews in Environmental Science and Biotechnology **2:**9-33.
265. **Vásquez-Laslop, N., H. Lee, and A. A. Neyfakh.** 2006. Increased persistence in *Escherichia coli* caused by controlled expression of toxins or other unrelated proteins. Journal of Bacteriology **188:**3494-3497.
266. **Ventre, I., A. L. Goodman, I. Vallet-Gely, P. Vasseur, C. Soscia, S. Molin, S. Bleves, A. Lazdunski, S. Lory, and A. Filloux.** 2006. Multiple sensors control reciprocal expression of Pseudomonas aeruginosa regulatory RNA and virulence genes. Proceedings of the National Academy of Sciences of the United States of America **103:**171-176.
267. **Venturi, V.** 2006. Regulation of quorum sensing in *Pseudomonas*. FEMS Microbiology Reviews **30:**274-291.

268. **Vilchez, R., C. Pozo, M. A. Gomez, B. Rodelas, and J. Gonzalez-Lopez.** 2007. Dominance of sphingomonads in a copper exposed biofilm community for groundwater treatment. Microbiology **153:**325-337.
269. **Wagner, V., D. Bushnell, L. Passador, A. I. Brooks, and B. H. Iglewski.** 2003. Microarray analysis of *Pseudomonas aeruginosa* quorum sensing regulons: effects of growth phase and environment. Journal of Bacteriology **185:**2080-2095.
270. **Walters III, M. C., F. Roe, A. Bugnicourt, M. J. Franklin, and P. S. Stewart.** 2003. Contributions of antibiotic penetration, oxygen limitation, and low metabolic activity to tolerance of *Pseudomonas aeruginosa* biofilms to ciprofloxacin and tobramycin. Antimicrobial Agents and Chemotherapy **47:**317-323.
271. **Welch, R. A., V. Burland, G. Plunkett III, P. Redford, P. Roesch, D. Rasko, E. L. Buckles, S. R. Liou, A. Boutin, J. Hackett, D. Stroud, G. F. Mayhew, D. J. Rose, S. Zhou, D. C. Schwartz, N. T. Perna, H. L. Mobley, M. S. Donnenberg, and F. R. Blattner.** 2002. Extensive mosaic structure revealed by the complete genome sequence of uropathogenic *Escherichia coli*. Proceedings of the National Academy of Sciences of the United States of America **99:**17020-17024.
272. **Wen, Z. T., and R. A. Burne.** 2004. LuxS-mediated signaling in Streptococcus mutans is involved in regulation of acid and oxidative stress tolerance and biofilm formation. Journal of Bacteriology **186:**2682-91.
273. **Werner, E., F. Roe, A. Bugnicourt, M. J. Franklin, A. Heydorn, S. Molin, B. Pitts, and P. S. Stewart.** 2004. Stratified growth in *Pseudomonas aeruginosa* biofilms. Applied and Environmental Microbiology **70:**6188-6196.
274. **Whitchurch, C. B., T. Tolker-Neilsen, P. C. Ragas, and J. S. Mattick.** 2002. Extracellular DNA required for bacterial biofilm formation. Science **295:**1487.
275. **Whiteley, M., M. G. Bangera, R. E. Bumgarner, M. R. Parsek, G. M. Teitzel, S. Lory, and E. P. Greenberg.** 2001. Gene expression in *Pseudomonas aeruginosa* biofilms. Nature **413:**860-864.
276. **Whitfield, C., and I. S. Roberts.** 1999. Structure, assembly and regulation of expression of capsules in *Escherichia coli*. Molecular Microbiology **31:**1307-1319.
277. **Workentine, M. L., J. J. Harrison, P. U. Stenroos, H. Ceri, and R. J. Turner.** 2007. *Pseudomonas fluorescens*' view of the periodic table. Environmental Microbiology **10:**238-250.
278. **Wozniak, D. J., T. O. Wycoff, M. Starkey, R. Keyser, P. Azadi, G. A. O'Toole, and M. R. Parsek.** 2003. Alginate is not a significant component of the extracellular polysaccharide matrix of PA14 and PAO1 *Pseudomonas aeruginosa* biofilms. Proceedings of the National Academy of Sciences of the United States of America **100:**7907-7912.
279. **Wright, M. S., G. L. Peltier, R. Stapanauskas, and J. V. McArthur.** 2006. Bacterial tolerances to metals and antibiotics in metal contaminated and reference streams. FEMS Microbiology Ecology **58:**293-302.
280. **Xu, K. D., G. A. McFeters, and P. S. Stewart.** 2000. Biofilm resistance to antimicrobial agents. Microbiology **146:**547-549.

281. **Xu, K. D., P. S. Stewart, F. Xia, C. Huang, and G. A. McFeters.** 1998. Spatial physiological heterogeneity in *Pseudomonas aeruginosa* biofilm is determined by oxygen availability. Applied and Environmental Microbiology **64:**4035-4039.
282. **Yanisch-Perron, C., J. Vieira, and J. Messing.** 1985. Improved M13 phage cloning vectors and host strains: nucleotide sequences of the M13mp18 and pUC19 vectors. Gene **33:**103-119.
283. **Yarwood, J. M., D. J. Bartels, E. M. Volper, and E. P. Greenberg.** 2004. Quorum sensing in *Staphylococcus aureus* biofilms. Journal of Bacteriology **186:**1838-50.
284. **Zannoni, D., F. Borsetti, J. J. Harrison, and R. J. Turner.** 2007. The bacterial response to the chalcogen metalloids Se and Te. Advances in Microbial Physiology **53:**1-71,312.
285. **Zaslaver, A., A. E. Mayo, R. Rosenberg, P. Bashkin, H. Sberro, M. Tsalyuk, M. G. Surette, and U. Alon.** 2004. Just-in-time transcription program in metabolic pathways. Nature Genetics **36:**486-491.
286. **Zawadzka, A. M., R. L. Crawford, and A. J. Paszczynski.** 2006. Pyridine-2,6-bis(thiocarboxylic acid) produced by *Pseudomonas stutzeri* KC reduces and precipitates selenium and tellurium oxyanions. Applied and Environmental Microbiology **72:**3119-3129.
287. **Zielinski, R., K. Kubinski, E. Stefaniak, and R. Szyszka.** 2001. Heavy metal biosorption from aqueous solution by simple eukaryotic organisms. Folia Histochemica et Cytobiologica **39 Supplement 2:**154-155.
288. **Zolfaghar, I., A. A. Angus, P. J. Kang, A. To, D. J. Evans, and S. M. J. Fleiszig.** 2005. Mutation of *retS*, encoding a putative hybrid two-component regulatory protein in *Pseudomonas aeruginosa*, attenuates multiple virulence mechanisms. Microbes and Infection 7:1305-1316.